

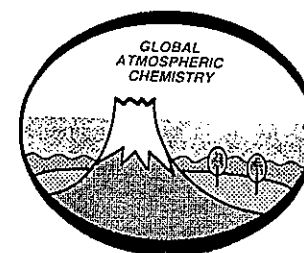
Joint Meeting
on
GLOBAL ATMOSPHERIC CHEMISTRY

Fuji-Yoshida, Japan
5 - 9 September 1994

PROGRAMME
and
COLLECTED ABSTRACTS

8th CACGP Symposium of the IAMAP
Commission on Atmospheric Chemistry
and Global Pollution (CACGP)

2nd Scientific Conference of the
International Global Atmospheric
Chemistry Project (IGAC)



OUTLINE PROGRAMME

Time	5 September Monday	6 September Tuesday	7 September Wednesday	8 September Thursday	9 September Friday
9:00	CONFERENCE OPENING (15 minutes) SESSION 1 Greenhouse Gases	SESSION 1 Cont'd SESSION 2 Tropospheric Ozone	SESSION 2 Cont'd	SESSION 3 Sulphur and Nitrogen	SESSION 4 Cont'd
10:30	COFFEE BREAK				
11:00	SESSION 1 Cont'd	SESSION 2 Cont'd	SESSION 2 Cont'd POSTER REVIEW (II) (30 minutes)	SESSION 3 Cont'd	SESSION 4 Cont'd
12:30	LUNCH		LUNCH (Poster Change)	LUNCH	
14:00	SESSION 1 Cont'd	SESSION 2 Cont'd	EXCURSION	SESSION 3 Cont'd	PANEL DISCUSSION
15:30	TEA BREAK			TEA BREAK	
16:00	SESSION 1 Cont'd POSTER REVIEW (I) (30 minutes)	SESSION 2 Cont'd	EXCURSION	SESSION 4 Aerosol and Cloud Chemistry	
17:30					
18:30	DINNER				
19:30	Open Commission Meeting	POSTER SESSION (I)	POSTER SESSION (II)	BANQUET	

An Opening Reception will be held on Sunday, 4 September at 19:00.

Joint 8th CACGP Symposium/2nd IGAC Conference

Fuji-Yoshida, Japan, 5 - 9 September 1994

PROGRAMME

4 September, Sunday evening 15:00 -

REGISTRATION (15:00 -)
ICE BREAKER (19:00 -)

5 September, Monday morning 09:00 - 10:30

OPENING (9:00 - 9:15)

<Chair: S. A. Penkett>

SESSION-1 Greenhouse Gases

<Chair: R. Prinn>

- 1.01 Distribution and fluxes of greenhouse gases (Overview)
Paul Crutzen
- 1.02 Global gridded emission inventories: current assessment and future prospects
T. E. Graedel
- 1.03 Radiative forcing and climate change due to increased tropospheric ozone concentration
S. Chalita, D. Hauglustaine, H. Le Treut, J. F. Müller and M. Pham
- 1.04 Lifetimes and eigenstates in atmospheric chemistry
Michael J. Prather

5 September, Monday morning 11:00 - 12:30

<Chair: D. Ehalt>

- 1.05 Stable isotopic constraints on the distributions and fluxes of CO₂: a global 3-D GCM study using the NCAR CCM2
David J. Erickson III and Philippe Ciais
- 1.06 The carbon cycle: results of a coupled atmospheric chemical tracer transport model and an ecosystem model
J. Dignon, J. R. Kercher, J. E. Penner and J. J. Walton
- 1.07 Soil C and N cycle feedbacks to elevated CO₂: implications for CO₂, N₂O, and NO exchange
E. Holland, P. Canadell, F. Chapin, N. Chiariello, J. des Rosiers, A. Fredeen, C. Field, B. Hungate, R. Jackson, G. Koch, Y. Luo, H. Mooney, H. Pearson and O. Sala
- 1.08 Spatial distribution of trace gases and particulate matter emissions from biomass burning in diverse tropical ecosystems
Wei Min Hao and Darold E. Ward
- 1.09 The geographic distribution of CO₂ emissions from fossil fuel consumption
Robert J. Andres, Gregg Marland and Inez Fung
- 1.10 Measurements of trace gases in the upper atmosphere using airliner
H. Matsueda, H. Y. Inoue and Y. Sugiyama

5 September, Monday afternoon 14:00 - 15:30

<Chair: P. Fraser>

- 1.11 Possible causes for the decline in the methane growth rate
K. S. Law, S. Bekki and E. Nisbet

- 1.12 Constraints on recent changes in the global methane budget from isotope measurements
M. R. Manning, D. C. Lowe and K. R. Lassey
- 1.13 Atmospheric carbon emission from northern lakes: a factor of global significance
I. P. Semiletov, S. A. Zimov, Yu. V. Voropaev and S. P. Daviodov
- 1.14 Anthropogenic methane emission in Russia
Sh. D. Fridman, A. I. Nakhtin and V. A. Vorobyev
- 1.15 Atmospheric methane and nitrous oxide: sources, sinks and strategies for reducing agricultural emissions
K. Minami
- 1.16 Methane emission from various rice fields in China: an overview
Wang Mingxing and Shangguan Xingjian

5 September, Monday afternoon 16:00 - 17:30 <Chair: K. Smith>

- 1.17 Measurement of nitrous oxide emission from agricultural land using micrometeorological methods
K. J. Hargreaves, F. Wienhold, L. Klemedtsson, J. R. M. Arah, I. Beverland, D. Fowler, B. Galle, D. Griffith, U. Skiba, K. A. Smith and M. Welling
- 1.18 Nitrous oxide emission from biomass burning and its distribution in mainland China
Meiqiu Cao and Ya-Hui Zhuang
- 1.19 The global decrease of carbon monoxide and its causes
M.A.K. Khalil and R.A. Rasmussen
- 1.20 Spectroscopic measurements of the spatial-temporal distribution of the minor gaseous atmospheric constituents (CO, CH₄)
E. I. Grechko and A. V. Dzhola

POSTER REVIEW (I) <Reporter: W. Chameides + T.B.D.>

5 September, Monday evening 19:30 -

OPEN COMMISSION MEETING

6 September, Tuesday morning 09:00 - 10:30 <Chair: H. Singh>

- 1.21 SF₆ a new powerful tracer in the atmosphere
M. Maiss, I. Levin, R. Francey, P. Fraser, R. Langenfels and P. Steele
- 1.22 Global distribution of CO₂ and halogenated hydrocarbons
P. Fabian and R. Borchers
- 1.23 Measurements of HCFCs in the Cape Grim air archive: 1978-1993
D. E. Oram, S. A. Penkett and P. Fraser
- 1.24 Long-term measurements and changing trends of halocarbon concentrations in the atmosphere
Yoshihiro Makide, Limin Chen and Takeshi Tominaga

SESSION-2 Tropospheric Ozone <Chair: S.A. Penkett>

- 2.01 Transport of O₃ and O₃-precursors from anthropogenic sources to the North Atlantic (Overview)
D. D. Parrish, Steven Bertman, James Roberts, R. N. Norton, Michael Trainer and F. C. Fehsenfeld

6 September, Tuesday morning 11:00 - 12:30 <Chair: S.A. Penkett>

- 2.02 A study of vertical and horizontal transport of ozone and ozone precursors using aircraft data from the North Atlantic Regional Experiment
M. Buhr, D. Sueper, M. Trainer, W. Kuster, P. Goldan and F. C. Fehsenfeld
- 2.03 Pacific Exploratory Mission West/Phase B (PEM West B): an overview of preliminary findings
D. D. Davis, S. C. Liu, R. Newell and J. Hoell
- 2.04 Ozone production, transport, and distribution in the western Pacific rim
Gregory R. Carmichael, Yang Zhang, Mahesh Phadnis and Young Sunwoo
- 2.05 Measurements of total reactive nitrogen and ozone in the troposphere over the Pacific Ocean and Japan Sea
S. Kawakami, M. Ieda, M. Koike, H. Nakajima and Y. Kondo
- ~~2.06 Summer time methane hydrocarbon climatology in the Asian Pacific
D. R. Blake and F. S. Rowland~~ CANCEL
- 2.07 Tropospheric ozone measurement at the top of Mt. Fuji
Yukitomo Tsutsumi, Yuji Zaizen and Yukio Makino

6 September, Tuesday afternoon 14:00 - 15:30 <Chair: M. Prather>

- 2.08 The global distribution of tropospheric NO_x and its impact on ozone chemistry
H. Levy II, W. J. Moxim, P. S. Kasibhatla and S. Sillman
- 2.09 The impact of regional ozone pollution on world food production
W. L. Chameides, P. S. Kasibhatla, J. Yienger and H. Levy, II
- 2.10 Global weighted-average concentration and trend for OH based on 15 years of ALE/GAGE CH₃CCl₃ data
R. G. Prinn, R. F. Weiss, B. R. Miller, F. N. Alyea, D. M. Cunnold, D. E. Hartley, P. B. Fraser and P. G. Simmonds
- 2.11 The role of chlorine atoms in determining tropospheric ozone: potential sources from sea salt reactions
B.J. Finlayson-Pitts, R. Vogt, R. Neavyn, J.M. Laux and J.C. Hemminger
- 2.12 A global chemical-transport model using the dynamics provided by the NCAR-CCM2 model
G. P. Brasseur, S. Walters and P. J. Rasch
- 2.13 A three-dimensional study of the global distribution and budget of trace gases in the troposphere
C. Granier, G. Brasseur, J. F. Muller and D. Hauglustaine

6 September, Tuesday afternoon 16:00 - 17:30 <Chair: I. Galbally>

- 2.14 An overview over the IGAC/SAFARI experiment: the role of vegetation fires in the environment of southern Africa
M. O. Andreae and the SAFARI Science Team
- 2.15 Experiment for Regional Sources and Sinks of Oxidants (EXPRESSO)
P. Zimmerman, G. Brasseur, R. Delmas and J. P. Lacaux
- 2.16 Ozone over southern Africa and the Atlantic during the 1992 IGAC/STARE/SAFARI/TRACE-A missions
Anne M. Thompson, Donna P. McNamara, Kenneth E. Pickering, Robert D. Hudson and members of the TRACE-A and SAFARI Science Teams
- 2.17 Atmospheric chemistry of the tropical South Atlantic Ocean: initial results from TRACE-A
Jack Fishman, Anne M. Thompson and the TRACE-A Science Team
- 2.18 Photochemical oxidants in the Venezuelan savanna during the rainy season
Claes de Serves and Alberto Rondón

- 2.19 Tropospheric ozone behavior observed with ozonesondes in Indonesia
Ninong Komala, Slamet Saraspriya and Toshihiro Ogawa

6 September, Tuesday evening 19:30 -

POSTER SESSION (I)

7 September, Wednesday morning 09:00 - 10:30 <Chair: F. Fehsenfeld>

- 2.20 EUROTRAC: a co-ordinated project for tropospheric research
Peter Borrell
- 2.21 On the behaviour of tropospheric ozone in the European Arctic and at Antarctica
P. Taalas, J. Damski, E. Kyrö, M. Ginzburg and V. Tafuri
- 2.22 Airborne measurements and analysis of atmospheric composition over Siberia
G. Inoue, K. Izumi, T. Machida, S. Maksyutov, S. Mitsumoto, Y. Tohjima, Y. Kopylov,
A. Postnov, N. Vinnichenko and V. Khatatov
- 2.23 Variations of lower tropospheric ozone at Syowa Station, Antarctica
S. Aoki and T. Yamanouchi
- 2.24 Distributions and patterns of organic trace gases: Is there evidence for an impact of reactions with chlorine atoms in the troposphere?
J. Rudolph, R. Koppmann and Ch. Plass-Dülmer
- 2.25 Analysis of seven years of continuous observations of peroxyacetyl nitrate (PAN) at the high Arctic station Alert
Jan W. Bottenheim, Leonard A. Barrie and Alain Sirois

7 September, Wednesday morning 11:00 - 12:30 <Chair: G. Brasseur>

- 2.26 Oceanic emissions of non-methane hydrocarbons (NMHC)
W. J. Broadgate, P. S. Liss and S. A. Penkett
- 2.27 The oceanic flux of carbon monoxide to the atmosphere
Timothy S. Bates, Kimberly C. Kelly and James E. Johnson
- 2.28 Acetone in the global troposphere: its possible role as a global source of PAN
H. B. Singh and M. Kanakidou
- 2.29 Net fluxes of nitrogen oxides (NO_x) from a managed tropical savanna
A. Rondón, C. Johansson and E. Sanhueza

POSTER REVIEW (II) <Reporter: B. Huebert + T.B.D.>

September, Wednesday afternoon 14:00 -

EXCURSION

7 September, Wednesday evening 19:30 -

POSTER SESSION (II)

8 September, Thursday morning 09:00 - 10:30 <Chair: R. Duce>

SESSION-3 Sulphur and Nitrogen Cycles

- 3.01 Sulphur and nitrogen cycles: their roles in acidification, with emphasis on the situation in Asia (Overview)
Hajime Akimoto

- 3.02 Interaction between the sulphur and nitrogen cycles in the atmosphere and across the sea surface
P. S. Liss
- 3.03 N mobilization in China and the United States: past, present and future
J. N. Galloway and Zhao Dianwu
- 3.04 Effects of land use changes in NO fluxes from savannah soils
A. Rondón, E. Sanhueza, L. Cárdenas and J. Romero
- 3.05 Soil nitrogen oxide emissions from a fertilized palm plantation in Costa Rica
Micahel Keller

8 September, Thursday morning 11:00 - 12:30 <Chair: H. Akimoto>

- 3.06 A 3D model study of the global sulfur cycle: relative contributions of anthropogenic and biogenic sources
M. Pham, J. F. Müller, G. P. Brasseur, C. Granier and G. Mégie
- 3.07 Simulation of the tropospheric sulfur cycle in a global climate model
J. Feichter, E. Kjellström, H. Rodhe and J. Lelieveld
- 3.08 Aerosol nitrate and sulfate concentrations over the North Atlantic: estimates of anthropogenic contributions
J. M. Prospero, D. L. Savoie, R. Arimoto and R. A. Duce
- 3.09 Quantification of DMS oxidation products in the North Atlantic marine air
S. Rapsomanikis and M. O. Andreae
- 3.10 Sulfur dioxide, dimethyl sulfoxide and dimethyl sulfone formation from dimethyl sulfide oxidation
Alan R. Bandy, Donald C. Thornton and Byron W. Blomquist
- 3.11 Uncertainty and sensitivity analyses of the mechanism of atmospheric oxidation of DMS
J. Hjorth and A. Saltelli

8 September, Thursday afternoon 14:00 - 15:30 <Chair: M. Andreae>

- 3.12 Regional background acidity and chemical composition of precipitation in Thailand
L. Granat, K. Suksomsankh, S. Simachaya, M. Tabucanon and H. Rodhe
- 3.13 Airborne measurements of SO₂ in marine atmosphere between Asian Continent and Japan
S. Hatakeyama, K. Murano, H. Mukai and H. Akimoto
- 3.14 Severe influence of the increasing sulfate aerosols on summer climate of the East China
Xu Qun
- 3.15 Relation in concentration of DMS between surface seawater and air in the temperate North Pacific region
S. Watanabe, H. Yamamoto and S. Tsunogai
- 3.16 The sulfur cycle in the high Arctic summer - an overview of the atmospheric research program of the International Arctic Ocean Expedition 1991 (IAOE-91)
Caroline Leck, E. Keith Bigg, Cecilia Persson, E. Douglas Nilsson, David C. Covert,
Jost Heintzenberg and Alfred Wiedensohler
- 3.17 Ice age Antarctic sulfate revisited
R. J. Delmas

8 September, Thursday afternoon 16:00 - 17:30 <Chair: H. Rodhe>

SESSION-4 Aerosol and Cloud Chemistry

- 4.01 Aerosol and cloud chemistry and their roles in climate regulation (Overview)
Greg Ayers

- 4.02 Vertical profiles and the microphysics, chemistry and optical properties of aerosol in the marine troposphere
A. D. Clarke, J. N. Porter, F. Valero and P. Pilewskie
- 4.03 The seasonal variation in size distribution of aerosol in the Oki Islands, Japan
H. Wakuri, M. Nakao, F. Tanaka, T. Tatano, K. Yamaguchi and H. Hara
- 4.04 Aerosols over the Pacific rim regions of East Asia
M. Yamato, S. Hatakeyama, K. Murano, H. Akimoto, H. Bandow, K. Imai, I. Watanabe, H. Tsuruta, H. Mukai, S. Tanaka, H. Tanaka, Y. Ishizaka and Y. Iwasaka
- 4.05 Anthropogenic impact on number concentrations of cloud processed particles over the North Atlantic
Rita Van Dingenen, Jens Hjorth, Torsten Gröne and Frank Raes

8 September, Thursday evening 19:30 -

BANQUET

9 September, Friday morning 09:00 - 10:30

<Chair: J. Galloway>

- 4.06 The aerosol - wind interrelationship and sea-salt particles over the Southern Ocean
J. L. Gras
- 4.07 Diurnal variation of marine boundary-layer sulfate and MSA: How much DMS is converted to sulfate?
B. Huebert, L. Zhuang, D. Wylie, A. Bandy, B. Blomquist and T. Wade
- 4.08 The relationship between MSA concentrations and temperature in marine (baseline) air at Cape Grim
A. L. Dick, G. P. Ayers, J. Ivey and P. M. Walford
- 4.09 Scales of temporal and spatial variability of sulfate column burdens over the North Atlantic in October and November
C. M. Benkovitz, R. Wagener, S. Nemesure and S. E. Schwartz
- 4.10 Airborne studies of aerosol emissions from savanna fires in southern Africa
M. O. Andreae, T. W. Andreae, P. le Canut, W. Elbert, G. Helas, F. Wienhold, T. Zenker, H. Annegarn, F. Beer, H. Cachier, W. Maenhaut, I. Salma and R. Swap
- 4.11 Ionic, organic components and trace elements in background aerosols in the Amazon basin
P. Artaxo, F. Gerab, M. A. Yamasoe, J. V. Martins, A. H. Miguel, G. P. Ayers and R. Gillet

9 September, Friday morning 11:00 - 12:30

<Chair: G. Ayers>

- 4.12 The role of anthropogenic sulfate in climate change
Catherine C. Chuang, Joyce E. Penner and Karl E. Taylor
- 4.13 The contribution of sulfate aerosol to light scattering over the Pacific Ocean
P. K. Quinn, S. Marshall, V. Kapustin, D. S. Covert and T. S. Bates
- 4.14 Which aerosol particles form cloud droplets?
A. Hallberg, K. J. Noone and J. A. Ogren
- 4.15 On the possible influence of clouds on the nitrogen budget in the remote troposphere
Peter G. Hess, Siri Flokke and Sasha Madronich
- 4.16 On the influence of gas to particle conversion on the modal size distribution of atmosphere particles
H. -C. Hansson, B. Martinsson, B. Svenningsson, E. Swietlicki, A. Wiedensohler and D. Covert
- 4.17 Low molecular weight dicarboxylic acids and related polar compounds in the remote marine rain and aerosol samples from western Pacific
Richard Sempéré and Kimitaka Kawamura

9 September, Friday afternoon 14:00 - 15:30

PANEL DISCUSSION (Topics and Panelists: T.B.A.)

<Chair: T.B.D.>

POSTER SESSION (I)

6 September, Tuesday evening 19:30 -

[Display period: 4 September, Sunday evening - 7 September, Wednesday noon]

- p001 Emission database for global atmospheric research: EDGAR version 2.0
J. G. J. Olivier, A. F. Bouwman, C. W. M. van der Maas and J. J. M. Berdowski
- p002 Source characterization networks, frameworks and major issues
P. Middleton, D. Hopkins and H. Lansford
- p003 Global budgets of CO, CH₄ and O₃
M. G. M. Roemer, A. C. Baart and P. J. H. Builtjes
- p004 1° x 1° global emissions inventory for SO_x and NO_x seasonally resolved into emission sectors and point and area sources
Eva C. Voldner, M. Trevor Scholtz, Keith A. Davidson and Arthur Li
- p005 Global inventories of anthropogenic emissions of SO₂ and NO_x
Carmen M. Benkovitz, Jane Dignon, Jozef Pacyna, Trevor Scholtz, Leonor Tarrasón, Eva Voldner and T. E. Graedel
- p006 Sources and sinks of sulphur and nitrogen: an assessment from a semi-arid industrial area
Anita Saxena, U. C. Kulshrestha, N. Kumar, K. M. Kumari and S. S. Srivastava
- p007 First results of the Bor Forest Island fire experiment Fire Research Campaign Asia-North (FIRESCAN)
FIRESCAN Science Team
- p008 Study on the sources and sinks of trace gases in China
Yang Wen-Xiang
- p009 Spatial distributions of CO₂ over Siberia in a summer season - airborne measurements of greenhouse gases over Siberia -
K. Izumi, T. Machida, S. Maksyutov, Y. Tohjima, S. Mitsumoto, M. Utiyama, G. Inoue, A. Postnov, Y. Kopylov, S. Shmeyer, V. Nikolaev, N. Vinnichenko and V. Khattatov
- p010 Carbon dioxide flux studies in tundra ecosystems in Taymyr Peninsula (Russia)
D. G. Zamolodchikov, D. V. Karelin and S. J. Hastings
- p011 CO₂ budget of coastal Arctic tundra at Barrow in 1993 summer
Yoshinobu Harazono, Mayumi Yoshimoto, Akira Miyata, Walter C. Oechel and George Vouritis
- p012 On the emission and regional budget of greenhouse gases in Hungary
A. Molnár, E. Mészáros and Gy. Kiss
- p013 Effects of ocean stratification on the uptake of greenhouse gases
Hiromasa Ueda, Takashi Karasudani and Kohji Ishii
- p014 Observation of carbon dioxide partial pressure in air and surface sea water in the seas adjacent to Japan
M. Hirota, K. Fushimi, K. Nemoto and A. Murata
- p015 CO₂ trend at the Mt. Cimone (44° 12' N, 10° 42' E) baseline station
T. Colombo, G. Giovanelli and P. Bonasoni
- p016 Sources and sinks of carbon dioxide in Kashmir: a case study
Altaf Hussain Wani and Ya-Hui Zhuang
- p017 Land-use effects on ¹³C-based estimates of tropical carbon sources and sinks
A. R. Townsend, E. A. Holland and E. Veldkamp
- p018 Atmospheric carbon sequestration through agroforestry
Xiaoke Wang and Zongwei Feng
- p019 Russian forests are global sinks of carbon dioxide from atmosphere, current fluxes and influence of climate changes
A. O. Kokorin and I. M. Nazarov
- p020 Analysis of the climate gases CO₂, N₂O and CH₄ by wide bore capillary gas chromatography with single injection of gas sample

- p021 Fluxes of CH₄, N₂O and CO₂ in forest soil influenced by N input and soil acidification
Bishal K. Sitaula, Luo Jiafa and Lars R. Bakken
Bishal K. Sitaula, Lars R. Bakken and Gunnar Abrahamsen
- p022 Control of methane emission from a rice paddy field by water management
K. Yagi, H. Tsuruta, K. Kanda and K. Minami
- p023 Release and retention of methane in rice soils following organic amendments
R. Wassmann, M. C. Alberto, H. U. Neue, R. S. Lantin, J. B. Aduna, K. Bronson, H. Papen,
H. Rennenberg and W. Seiler
- p024 Source strength of methane emission from rice fields and mitigation options
H.U. Neue, R. Wassmann and R.S. Lantin
- p025 Influence of fertilizer and water management on methane emission and production in Chinese rice
fields and possible mitigation options
X. J. Shangguan, M. X. Wang, D. Z. Chen, R. X. Shen, Y. S. Wang, R. Wassmann,
M. Toelg, H. Papen, X. L. Xie and W. D. Wang
- p026 Preliminary study on the relationship between organic acid contents and methane emission rates in
paddy soil in the red earth hilly area of south China
W. D. Wang, X. L. Xie, X. J. Shangguan and M. X. Wang
- p027 Methane emission from rice paddies and the effect of agricultural management
Chen Zong Liang, Shao Ke Sheng, Li Debo, Wang Bujun and Yao Heng
- p028 An estimation of methane emission from rice paddies of China mainland
Yao Heng, Chen Zong Liang and Zhuang Ya-hui
- p029 Flux of methane from rice field in Thailand
W. H. Su and X. Rong
- p030 Micrometeorological measurements of methane flux over agricultural vegetations and an estimation
of methane emission in Tsukuba, Japan
A. Miyata and Y. Harazono
- p031 Upper tropospheric concentration distributions of CH₄, O₃, CO₂ and CO over Siberia: numerical
simulation with a global tracer transport model
G. Inoue, K. Izumi, T. Machida, S. Maksyutov, S. Mitsumoto, Y. Tohjima, Y. Kopylov,
A. Postnov, N. Vinnichenko and V. Khattatov
- p032 Airborne measurement of CH₄ emission from West Siberian lowland
Y. Tohjima, H. Wakita, T. Machida, S. Maksyutov, I. Matsui, G. Inoue, A. Postnov,
Y. Kopylov, V. Nikolaev, N. Vinnichenko and V. Khattatov
- p033 Climate dependence of methane emission from boreal wetlands: a proposed model structure
G. A. Alexandrov
- p034 Water vapor and methane measurements in the troposphere over the Taklimakan desert
Tadao Aoki, Teruo Aoki and Masashi Fukabori
- p035 Local sources and behavior of atmospheric methane in Nagoya, Japan inferred from carbon isotopes
and atmosphere ²²²Rn data
J. Moriizumi, J. Mase, K. Nagamine, T. Iida and Y. Ikebe
- p036 Significance of methane emission from coastal wetlands (mangrove ecosystems) of India
G. R. Purvaja and R. Ramesh
- p037 Tropospheric level of CH₄, CO and O₃ along the longest belt of largest population density
L. S. Hingane
- p038 Continuous automatic measurements of N₂O-, NO-, NO₂- and CH₄-flux rates in a N-supersaturated
temperate coniferous forest in Bavaria
K. Butterbach, R. Gasche and H. Papen
- p039 Nitrous oxide fluxes from a drained organic soil, measured by chamber/GC and chamber/IR
methods
P. Ambus, S. Christensen, H. Clayton, K. A. Smith, J. R. M. Arah, A. Scott, M. Maag,

- A. M. Lind, B. Galle, D. W. T. Griffith and L. Klemetsson
- p040 N₂O emissions from rice paddy fields
H. Tsuruta, K. Yagi, K. Kanda and T. Hirose
- p041 NO and N₂O emissions from fertilized soils in field and laboratory experiments
T. Hirose and H. Tsuruta
- ~~p042 Kinetic isotope fractionation during production and consumption of nitrous oxide
Naohiro Yoshida and Teruki Iwatsuki~~ CANCEL
- p043 The distribution of light halogenated hydrocarbons in the troposphere
R. Koppmann, F. J. Johnen and J. Rudolph
- p044 Seasonal variation of several halocarbons in the Arctic troposphere at Alert, Canada
Y. Yokouchi, L. A. Barrie, D. Toom and H. Akimoto
- p045 Accurate measurements of CFC-114 and halon concentrations in the atmosphere
Limin Chen, Yoshihiro Makide and Takeshi Tominaga
- p046 Atmospheric chemistry of FO₂, CF₃O and FCO_x radicals
Ole J. Nielsen, Thomas Ellermann, Jens Sehested and Knud Sehested
- p047 Reactions of perfluoroalkyl radicals (CF₃ and C₂F₅) with O₂
H. Sato, M. Takeuchi and R. Isaki
- p048 C-C bond cleavage of fully halogenated chlorofluoroethoxy radicals
R. Isaki and H. Sato
- p049 DRS-IR measurement of the surface products on sodium chloride particles exposed to the ambient
air in the Arctic
S. Kutsuna and T. Ibusuki
- p050 Hydrogen chloride release from seaspray: field measurements in clean and polluted air masses in a
tropical area
T. M. Tavares and V. C. Rocha
- p051 Global emissions of organochlorine pesticides
Eva C. Voldner, M. Trevor Scholtz, Keith A. Davidson, Arthur Li and Carol Slama
- p052 Airborne hydrocarbon measurements during the North Atlantic Regional Experiment, 1993
P. Goldan, B. Kuster, F. C. Fehsenfeld and M. Trainer
- p053 The soluble-organic fraction of aerosols as determined in NARE
S. -M. Li, C. M. Banic, W. R. Leitch, P. S. K. Liu, H. A. Wiebe, X. -L. Zhou and Y. -N. Lee
- p054 Airborne and surface formaldehyde and multi-oxygenated carbonyl measurements during the 1993
NARE intensives
Yin-Nan Lee and Xianliang Zhou
- p055 Trace gas measurements over southern Nova Scotia during the 1993 NARE
L. Kleinman, P. Daum, S. Springston, J. Lee, Y. -N. Lee, X. Zhou, R. Leitch, C. Banic,
G. Isaac, I. MacPherson and H. Niki
- p056 Measurements of tropospheric nitrogen oxides in the central North Atlantic region
R. E. Honrath and M. C. Peterson
- p057 Impact of anthropogenic emissions on the North Atlantic atmosphere
Prasad Kasibhatla
- p058 Modeling the role of continental emissions on tropospheric ozone over the North Atlantic Ocean
C. S. Atherton, J. Penner, S. Sillman and J. Walton
- p059 Trajectory modeling of the North Atlantic region
O. Wild, K. S. Law and J. A. Pyle
- p060 Large-scale air mass characteristic observed over the western Pacific during the summertime
E. V. Browell and PEM-West A Science Team
- p061 Ratios of reactive nitrogens over the Pacific during PEM-West A

- p062 M. Koike, Y. Kondo, S. Kawakami, H. B. Singh, H. Ziereis and J. T. Merrill
Reactive nitrogen over the Pacific Ocean during PEM-West A
Y. Kondo, H. Ziereis, M. Koike, S. Kawakami, G. L. Gregory, G. W. Sachse, H. B. Singh,
D. D. Davis and J. T. Merrill
- p063 An Assessment of the photochemical O₃ tendency in the western North Pacific as inferred from
GTE/PEM West(A) observations during fall 1991
D. D. Davis, J. Crawford, G. Chen, J. Bradshaw, S. Sandholm, G. Sachse, B. Anderson,
J. Collins, J. Barrick, E. Browell, D. Blake, S. Rowland, H. Singh, Y. Kondo, B. Heikes,
J. Merrill and R. Talbot
- p064 H₂O₂ and CH₃OOH distributions over the North Pacific
Brian Heikes and Meehye Lee
- p065 Effects of typhoon on semi-global scale mass transport over the northern Pacific Ocean
T. Kitada, T. Yamamoto and Y. Kondo
- p066 Spatial and temporal variability of aerosols over the North Pacific: estimates of anthropogenic
contributions.
J. M. Prospero, D. L. Savoie, R. Arimoto and R. A. Duce
- p067 Aircraft measurements of tropospheric ozone over the western Pacific Ocean
Yukitomo Tsutsumi, Yukio Makino, Miwako Kegami and Yuji Zaizen
- p068 Ozone and aerosol measurements made over the tropical Atlantic during the TRACE-A field
experiment
E. V. Browell, C. F. Butler, M. A. Fenn, W. B. Grant, G. L. Gregory, B. Anderson and
J. Fishman
- p069 Simulation of convective transport of biomass burning emissions over Brazil during TRACE-A:
effects on tropospheric O₃ production
K. E. Pickering, A. M. Thompson, W. -K. Tao and members of the TRACE-A Science Team
- p070 Global measurements of tropospheric CO and CH₄ by MOPITT and their scientific applications
John C. Gille, James R. Drummond, Liwen Pan, Mark D. Smith and Guy Brasseur
- p071 Stratosphere troposphere exchanges and their implication for the tropospheric ozone budget: results
of the European campaigns
G. Ancellet, M. Beekmann, L. Gray and G. Vaughan
- p072 Climatological analysis of free tropospheric ozone in Europe: relationship between ozone variability
meteorological variables and precursor gases
M. Beekmann, G. Ancellet and D. de Muer
- p073 Seasonal patterns of surface ozone measured in a three-year data set at Mt. Cimone
P. Bonasoni, T. Colombo, F. Evangelisti, G. Giovanelli and F. Ravegnani
- p074 Variations of surface ozone at the remote stations in northwestern China
H. Muramatsu
- p075 Yearly cycle of lower tropospheric ozone north of the Arctic circle
Markku Rummukainen and Tuomas Laurila
- p076 Ozone fluxes over farmland and natural vegetation in South Western Australia
S. Chambers, N. J. Clark, J. H. Hacker and S. Venning
- p077 Surface ozone measurements from Baring Head, New Zealand
S. E. Nichol, M. J. Harvey and I. S. Boyd
- p078 Surface and free tropospheric ozone measurements over South Africa
J. Combrink, R. D. Diab, F. Sokolic and E. -G. Brunke
- p079 Boundary layer ozone at Victoria Falls (Zimbabwe): ground level and airborne mixing ratios
Franz X. Meixner
- p080 Status of tropospheric ozone in Delhi
Maneesha Aggarwal and C. K. Varshney

- p081 Monitoring of surface ozone and its precursors at Ahmedabad
Shyam Lal, Manish Naja, P. K. Patra, B. H. Subbaraya and S. Venkataramani
- p082 Seasonal and long term variations in surface ozone at Ahmedabad
Shyam Lal, B. H. Subbaraya and Manish Naja
- p083 A new equatorial ozone sounding campaign: preliminary results
M. Ilyas
- p084 Chemiluminescent sensors for atmosphere monitoring and industry
A. Bryuckanov, I. Zykova and V. Chelibanov
- p085 A global "telescopic" model of chemically active trace constituents: application to the Mauna Loa
Observatory Photochemistry Experiment, I. Model description
Paul Ginoux and Guy Brasseur
- p086 A global "telescopic" model of chemically active trace constituents: application to the Mauna Loa
Observatory photochemistry Experiment, II. Data comparisons
Paul Ginoux, Elliot Atlas, Brian Ridley, Guy Brasseur and MLOPEX II and PEM WEST-A
Science Teams
- p087 Impact of changing natural volatile organic compound emissions on global tropospheric chemistry
Alex Guenther, Guy Brasseur, David Erickson, Sophie Fally and Erwan Favennec
- p088 Atmospheric composition changes due to increased ozone precursor emissions and related radiative
forcings on climate
D. A. Hauglustaine, C. Granier and G. P. Brasseur
- p089 Convective transports of chemical tracers in global transport models driven by analyses from the
forecast centers
Natalie Mahowald, Philip J. Rasch and Ronald G. Prinn
- p090 Generation of emission data for episodes with high temporal and spatial resolution
R. Friedrich
- p091 Photochemical reactions on dust in the troposphere: a three dimensional global model assessment
Frank J. Dentener, Gregory R. Carmichael and Yang Zhang
- p092 Parameterization of bi-directional NH₃ fluxes in the modeling of long range transport of NO_x
A. Sorteberg and Ø. Hov
- p093 Correlations between ozone-NO_x-hydrocarbon chemistry and empirical indicators: NO_y, HCHO,
H₂O₂ and HNO₃
Sanford Sillman
- p094 Regional aspects of the tropospheric ozone budget
P. J. H. Builtjes, M. G. M. Roemer, G. Boersen and P. J. Esser
- p095 The vertical transport, transformation and deposition of air pollutants by convective clouds
Qin Yu, Kong Fanyou and Zhao Chunsheng
- p096 Parameterization of ozone and aerosol particle fluxes
E. Lamaud, J. Fontan, A. Lopez, A. Druilhet, A. Labatut and S. Cieslik
- p097 Sensitivity of the tropospheric composition of different atmospheric regions over the earth surface to
anthropogenic influences
Natalia G. Andronova and Igor L. Karol
- p098 Rate coefficients by parametric equations for modeling purposes
I. Oref and W. C. Gardiner
- p099 Possible impact of ozone column changes on the growth rates of CH₃Br, CH₃Cl and CH₃CCl₃
S. Bekki and K. Law
- p100 On the diffusional uptake of trace gases by polar stratospheric clouds
S. Ghosh and J. A. Pyle

POSTER SESSION (III)

7 September, Wednesday evening 19:30 -

[Display period: 7 September, Wednesday afternoon — 9 September, Friday afternoon]

- p201 Evidence for ozone depletion in clouds
D. Möller, K. Acker and W. Wieprecht
- p202 The effect of clouds on OH and the oxidation of atmospheric trace gases
M.A.K. Khalil and F. Moraes
- p203 H₂O₂, CH₃OOH and CH₂O as primary and secondary pollutants in fire plumes
Meehye Lee, Brian Heikes and Daniel Jacob
- p204 Atmospheric effects of H₂O₂ in South-East China
X. Tang, K. Shao, Q. Sun and M. Wang
- p205 Relationship between peroxide and ozone measured over the equatorial South West Pacific
B. J. Bandy, S. A. Penkett, G. Jenkins, P. Hignett and A. Kaye
- p206 The occurrence of hydroperoxides in mid altitudes of the lower troposphere: measurements at two mountain field sites
W. Junkermann, P. Pietruk and F. Slemr
- p207 Tropospheric aldehydes in remote and urban areas of Japan
M. Ohta and H. Tsuruta
- p208 Atmospheric formic and acetic acids in Venezuela
E. Sanhueza, L. Figueroa and M. Santana
- p209 Kinetics of the oxidation of SO₂, NO₂⁻ and N-S oxides by ozone in aqueous solutions
J. Hahn, G. Lachmann and J.J. Pienaar
- p210 The non-methane hydrocarbon intercomparison experiment
Eric C. Apel and Jack G. Calvert
- p211 Landscape scale emission inventory of individual biogenic organic compounds in three ecosystems in the US
Detlev Helmig, Lee F. Klinger, Alex Guenther, Jim Greenberg and Patric Zimmerman
- p212 Oceanic emissions of light nonmethane hydrocarbons
C. Plass-Duelmer, R. Koppmann, M. Ratte and J. Rudolph
- p213 Laboratory experiments on the origin of C₂-C₃ alkenes in sea water
M. Ratte, O. Bujok, A. Spitz and J. Rudolph
- p214 Airborne measurements of organic trace gas emissions from savanna fires in southern Africa
R. Koppmann, A. Khedim and J. Rudolph
- p215 Light hydrocarbons measured in plumes of savanna fires in South Africa
G. Helas, M. O. Andreae, G. Schebeske, D. Scharffe, S. Manoe, R. Koppmann and J. Rudolph
- p216 Concentrations of C₂-C₅ hydrocarbons over the Baltic Sea and northern Finland
Tuomas Laurila and Hannele Hakola
- p217 Preliminary research on isoprene emission from plant and soil
Lu Chun and Miao Hong
- p218 Terpenic emissions from *Quercus ilex* and *Pinus pinea* at Castelporzlano (Italy)
J. L. Fugit, B. Clément, M. L. Riba, L. Torres, J. Kesselmeier and L. Schaefer
- p219 Hydrocarbons and their derivatives in volcanic gases: origin and composition
V. G. Povarov
- p220 Atmospheric volatile organic compounds containing nitrogen, oxygen, sulfur and halogens: identification, quantitation and sources
Jim Greenberg, Detlev Helmig, Pat Zimmerman and Elliot Atlas
- p221 The effect of water vapour on the ozonolysis of simple alkenes under atmospheric conditions

P. Neeb, O. Horie, S. Limbach, F. Sauer and G. K. Moortgat

- p222 Global distribution of NO_x emissions from lightning
Laura Gallardo
- p223 Measurement and analysis of reactive nitrogen species in the rural troposphere of Southeast United States
D. -S. Kim and V. P. Aneja
- p224 Characterization of nitrogen oxide fluxes from agricultural soils in North Carolina, U.S.A.
Viney P. Aneja, Wayne R. Robarge, Vinod K. Saxena, Benny D. Holbrook, Lee Sullivan, Thomas Moore, T. Pierce and C. Geron
- p225 Vertical distribution of nitric oxide production and consumption in soil cores
J. Rudolph and R. Conrad
- p226 An optimized method for airborne peroxyacetyl nitrate (PAN) measurements
W. Schrimpf, K. P. Müller, F. J. Johnen, K. Lienaerts and J. Rudolph
- p227 Seasonal variation of CO background levels in Venezuela
E. Sanhueza and E. Fernández
- p228 OH radical-initiated photooxidation of isoprene: an estimate of global CO production
Akira Miyoshi, Shiro Hatakeyama, Takashi Imamura and Nobuaki Washida
- p229 Measurement of atmospheric carbon monoxide for environmental impact assessment
A. Ramani
- p230 A possible impact of stratospheric ozone depletion on tropospheric trace gases removed from the atmosphere by hydroxyl
L. N. Yurganov
- p231 Transport, turn-over times and effective sink rates of natural sulfur compounds in the remote Arctic planetary boundary layer during the International Arctic Ocean Expedition 1991 (IAOE-91)
E. D. Nilsson, C. Leck, E. K. Bigg and C. Persson
- p232 Measurements of oceanic and atmospheric dimethylsulfide, sulfur dioxide, biogenic sulfur and sea salt aerosols during the International Arctic Ocean Expedition 1991 (IAOE-91)
Cecilia Persson and Caroline Leck
- p233 Model-calculated particulate sulphate in the Arctic
Trond Iversen and Leonor Tarrason
- p234 Biogenic sulfur and aerosol composition in the Atlantic and Southern Oceans
C. N. Hewitt, B. Davison, R. M. Harrison, M. Schwikowski, U. Baltensperger, C. O'Dowd and M. Smith
- p235 Dimethylsulfide, aerosols and condensation nuclei over the Atlantic Ocean
B. C. Nguyen, J. P. Putaud and N. Mihalopoulos
- p236 Seasonal variations and origin of methanesulfonic acid SO₄²⁻, and SO₂ at two marine and one midcontinental sites in Canada
Shao-Meng Li, L. A. Barrie, D. Toom and H. Dryfhout
- p237 Relative contribution of natural and anthropogenic sources to the aerosol non-sea-salt sulfate at Ny Ålesund, Spitsbergen
W. Maenhaut, G. Ducastel, K. Beyaert and J. E. Hanssen
- p238 Concentrations of aerosol methanesulfonate, non sea-salt sulfate and ammonium at three sites in the Southern Ocean
R. W. Gillett and G. P. Ayers
- p239 Sulfuric acid particles in the wintertime Antarctic atmosphere
Kikuo Okada and Teruo Aoki
- p240 Emission of biogenic sulfur gases from some Chinese and Japanese soils
Z. Yang, K. Kanda, H. Tsuruta and K. Minami

- p241 Transport of anthropogenic sulfur from East Asia to the sea near Japan and its reaction with sea salt particles
Shigeru Tanaka and Hisashi Ishikawa
- p242 An emission of marine biogenic sulfur from enclosed coastal sea and coastal area in Japan to the atmosphere
Shigeru Tanaka, Reiji Tahara and Kenji Matsunaga
- p243 The origin of sulfur dioxide and sulfate in the atmosphere of the North Pacific
Donald C. Thornton, Byron W. Blomquist, Alan R. Bandy and Robert W. Talbot
- p244 A model study on the seasonal variation of MSA to n.s.s. sulfate molar ratio in the marine atmosphere
S. Koga and H. Tanaka
- p245 Production rates, uptake rate constants and compensation concentrations of OCS in various soils
S. Lehmann and R. Conrad
- p246 Formation of COS and methyl thioformate in the oxidation of DMS
I. Barnes, K. H. Becker and J. Patroescu
- p247 Aqueous-phase oxidation of S(IV) by CH₃OOH at pH 1-2
H. Hara, S. Nakasato and S. Hatakeyama
- p248 ESR studies of the peroxide oxidation of aqueous sulphite
W. G. Filby and W. H. Kalus
- ~~p249 Surface measurements of sulfate aerosol in Alaska
W. C. Munn and A. V. Polissar~~ CANCEL
- p250 Stomatal absorption of sulphur dioxide by pine needles
T. Vesala, K. Hämeri, T. Ahonen, M. Kulmala, P. Aalto and P. Hari
- p251 The study of sulphur dioxide pollution
S. Madhuri
- p252 Sulphur in the Siberian atmosphere
A. Ryaboshapko, S. Gromov and S. Paramonov
- p253 Modeling the global dynamics of soot and sulphate aerosol
W. F. Cooke, F. Raes and J. J. N. Wilson
- p254 Tropospheric aerosols — their characteristics of radiative and climate effects
Yang Jianliang and Wang Mingxing
- p255 Physio-chemical measurement to investigate regional cloud-climate feedback mechanisms
V. K. Saxena, J. D. Grovenstein and K. L. Burns
- p256 Chemical composition of aerosols on a transect from the Sahara to the Gulf of Guinea and the influence on the element concentrations in rain water
L. Herrmann, K. Stahr and A. Bationo
- p257 Effects of aerosols from biomass burning: a model study
Joyce E. Penner, Catherine Liou, Charles R. Molenkamp, John J. Walton, Ingrid Schult and Hélène Cachier
- p258 Regional aerosol composition in the eastern Transvaal, South Africa, and impact of biomass burning
W. Maenhaut, I. Salma, J. Cafmeyer, H. J. Annegarn and M. O. Andreae
- p259 Large scale aircraft measurements of biomass burning aerosols in the Amazon basin
F. Gerab, P. Artaxo and A. Setzer
- p260 Trace elements and ionic components in aerosols from direct emissions from biomass burning in the Amazon basin
M. A. Yamasoe, P. Artaxo, A. H. Miguel and A. G. Allen
- p261 Aerosol size distribution and water content measurements during MAGE/ASTEX
Y. Kim, H. Sievering, J. Boatman, D. Wellman and A. Pszeny
- ~~p262 Aerosol iron input and open ocean productivity
Neil W. Tindale and Collaborators~~ CANCEL
- p263 Mineral-particle chemistry and size distributions in remote marine aerosols
J. R. Anderson and P. R. Buseck
- p264 Aerosol dynamics in the equatorial Pacific
Antony D. Clarke
- p265 New ways of looking at atmospheric trace element data
R. Arimoto, R. A. Duce, K. A. Rahn and T. M. Church
- p266 Aircraft measurement of aerosol concentration and size-distribution over the western Pacific Ocean
Y. Zaizen, M. Ikegami, Y. Tsutsumi, Y. Makino and K. Okada
- p267 Large-scale transport of chemical elements in aerosols over the east coast of Asia
A. N. Medvedev, M. Uematsu, G. M. Kolesov and V. V. Anikiev
- p268 Numerical modeling of transformation of Kosa (yellow sand) in polluted air over China
P. C. S. Lee and T. Kitada
- p269 Marine and urban aerosols observed by an aircraft
M. Yamato, H. Tanaka, K. Ohta and K. Matsumoto
- p270 Asian yellow dust particles observed in Japan
M. Yamato, H. Tanaka, Y. Ishizaka, K. Arao, Y. Iwasaka and M. Nagatani
- p271 Sea-salt component on Asian dust-storm particles
N. Niimura, K. Okada, X.-B. Fan, K. Kai, K. Arao and G. -Y. Shi
- p272 Deposition and inflow sources of non-seasalts sulfate in Shimane Prefecture, Japan
M. Nakao, F. Tanaka, K. Yamaguchi, T. Tatano, H. Wakuri, H. Mukai and H. Hara
- p273 Gobi dust storms and forestation in China
Farn Parungo
- p274 Scavenging processes of particles by using natural radionuclide
M. Uematsu
- p275 Variation of tropospheric aerosol extinction profile and optical thickness over Tsukuba, Japan observed by the NIES lidar
Yasuhiro Sasano, Tamio Takamura and Tadahiro Hayasaka
- p276 The distribution of aerosols as function of altitude in the atmosphere
R. Jaenicke and V. Dreiling
- p277 Sedimentation and subsequent deposition of the Mt. Pinatubo aerosol over Antarctica
V. K. Saxena and John Anderson
- p278 Stratospheric aerosol lidar measurements from Mount Pinatubo at Camaguey, Cuba
Juan Carlos Antuña
- p279 Precipitation chemistry in India: dusty atmosphere and alkaline rain
L. T. Khemani, G. A. Momin, P. D. Safai, L. Granat and H. Rodhe
- p280 Estimates of CCN spectra from hygroscopic growth factors and aerosol particle size distributions
B. Svenningsson and H.-C. Hansson
- p281 Potential acid-reducing capacity of aerosol particles and its dependence on particle size over northern China
Y. Gao, R. A. Duce, R. Arimoto and M. Y. Zhou
- p282 Research into the chemical content of aerosols and gases in the atmosphere over the North Atlantic, Baltic, Mediterranean and Black Seas
V. I. Medinets
- p283 High abundance of oxalic, malonic and succinic acids in the remote marine aerosol samples
Kimitaka Kawamura and Futoshi Sakaguchi
- p284 Seasonal changes of dicarboxylic acids and related polar compounds in the Arctic aerosol samples

- K. Kawamura, H. Kasukabe and L. A. Barrie
- p285 Interactions between aerosol particles, cloud droplets and ice crystals at the high-alpine site Jungfraujoch
M. Schwikowski, U. Baltensperger and H. W. Gäggeler
- p286 Historical and future trends of lead and cadmium air concentrations and total depositions over Europe
J. Alcamo, L. Bozó, J. Bartnicki and J. M. Pacyna
- p287 Chemical composition of small particles and annual behaviour of ozone concentrations in the Eastern Highlands of Zimbabwe, Africa
W. Kosmus, R. Wippel and S. B. Jonnalagadda
- p288 Size distributed chemical composition of CCN at Cape Grim
J. Caíney, G. Ayers and M. Hooper
- p289 The chemistry and size distribution of aerosol measured at Baring Head, New Zealand
M. J. Harvey, I. S. Boyd, D. J. Wylie, A. G. Allen and A. L. Dick
- p290 Physicochemical properties of Arctic aerosols
M. Yamato, H. Tanaka, K. Tsuboki, R. Kimura, T. Endou, Y. Asuma, A. Yamashita, H. Toritani, M. Calvez and R. Gillis
- p291 Wet deposition in remote regions: implications for environmental processes
J. N. Galloway, W. C. Keene and G. E. Likens
- p292 The model simulations on the amount of soluble mass during cloud droplet formation
M. Kulmala, P. Korhonen, T. Vesala and S. Clegg
- p293 A model calculation of sulfate and nitrate deposition in Japan
N. Katatani, Y. Sasaki, N. Murao, S. Okamoto and K. Kobayashi
- p294 Increase of radiation dose due to acid precipitation
K. Okamoto and S. Tanimoto
- p295 Influence of the growth mechanism of a snow particle on its acidification
T. Takahashi, T. Endoh, K. Muramoto, T. Nakagawa and I. Noguchi
- p296 Relationship between the atmospheric particulate fraction and the ionic content of precipitation
H. Casado, D. Encinas and J. P. Lacaux
- p297 S and N wet deposition at two rural sites of the western Maracaibo Lake Basin, Venezuela
J. Morales, C. Bifano and A. Escalona
- p298 Assessment of the sulphur and nitrogen wet deposition and rain acidity over the central Caribbean region: evidence for natural fluctuations and anthropogenic perturbations
C. M. López Cabrera
- p299 A 90-year precipitation chemistry record from the Chongce ice cap in West Kunlun Mountains, China
Kumiko Goto-Azuma, Masayoshi Nakawo and Han Jiankang
- p300 Acid deposition of sulfur in Asia
Richard Amdt and Gregory R. Carmichael
- p301 Rainwater composition and acidity at the Hong Kong BAPMoN site, Yuen Ng Fan
G. P. Ayers and K. K. Yeung
- p302 On acid precipitation of Shanghai
Zhang Chao
- p303 The acidification of atmospheric aerosol related to relative humidity and its contribution to the acid precipitation
Yang Jianliang and Wang Mingxing
- p304 Variation of sulphate and nitrate concentration in precipitation in Jakarta Indonesia and their roles in acidification: 1983-1992
Nurlaini and Mahmud

- p305 Washout of alkaline components during the convective showers at Pune, India
Medha S. Naik, G. A. Momin, P. S. P. Rao, P. D. Safai, A. G. Pillai and L. T. Khemani
- p306 Chemical composition of wet and dry deposition at Delhi, North India
R. K. Kapoor, S. Tiwari and R. N. Chatterjee
- p307 Acid rain analysis
P. Suneetha
- p308 Some observations from the statistical analyses of major ion concentrations in precipitation in an industrial-coastal environment
A. Narayana Swamy

1.02

Global Gridded Emissions Inventories: Current Assessment and Future Prospects

T.E. Graedel
AT&T Bell Laboratories
Murray Hill, NJ USA

Global gridded emissions inventories have traditionally been prepared by computer modelers with specific research goals and specific models in mind. The Global Emissions Inventory Activity, a component of IGAC, has the task of generating such inventories for all species of interest and for general use. The first of these inventories became available during 1994. This presentation will discuss both common and distinct features of those new inventories and present a tentative schedule for the availability of other new inventories over the next several years.

1.03

Radiative forcing and climate change due to increased tropospheric ozone concentrations

S. CHALITA¹, D. HAUGLUSTAINE¹, H. LE TREUT², J.F. MULLER³ AND
M. PHAM¹

¹Service d'Aéronomie du CNRS, Université de Paris VI, Paris, France

²Laboratoire de Météorologie Dynamique du CNRS, ENS, Paris, France

³Institut d'Aéronomie Spatiale de Belgique, Bruxelles, Belgique

Recent work shows that changes in both tropospheric and stratospheric ozone may have a significant impact on climate. In the troposphere, ozone is produced by complex chemical reactions involving many trace gases such as NO_x , CO , CH_4 and other hydrocarbons, which have both natural and anthropogenic sources. Tropospheric ozone concentrations have been calculated by the 3D Chemistry-Transport Model IMAGES (Intermediate Model for the Annual and Global Evolution of Species) for preindustrial and industrial conditions. In this study, we realise long pluriannual experiments with these calculated global tropospheric ozone fields, which are introduced in the General Circulation Model of the Laboratoire de Météorologie Dynamique, to determine the radiative forcing and climatic impact due to ozone changes since pre-industrial times. These results are compared to those resulting from other greenhouse gases (i.e., CO_2 , CH_4 , N_2O , $CFCs$) enhanced concentrations.

1.04

Lifetimes and Eigenstates in Atmospheric Chemistry

Michael J. Prather,
Earth System Science, UC Irvine, California, USA

The time scales and mode of the atmosphere's response to chemical perturbations are described by the eigenvalues and eigenvectors, respectively, of the system. When the cycles of different trace species are coupled (i.e., non-linear), a change to one species excites a coupled perturbation that decays with a characteristic time scale different from the inverse loss frequencies of any individual species. A study of the eigenstates of a simplified CH₄-CO-OH system shows that the longest time constant (smallest eigenvalue) always exceeds the lifetime defined by the steady-state loss frequency for CH₄, the longest lived gas. This eigenvalue, or response time, for a CH₄ perturbation can be diagnosed from the OH-CH₄ coupling that has been reported for global models, specifically the OH decrease per CH₄ increase. The ratio of response to lifetime can also be diagnosed by how close we are to a chemically unstable troposphere, i.e., how much production of OH exceeds that minimum needed to oxidize just the global emissions of CH₄, CO, and other hydrocarbons and species. The response time applies even to infinitesimal perturbations and to chemical systems that are not in steady-state. This formalism is extended to a simplified atmospheric chemistry model with transport and is compared with results from the global three-dimensional chemical transport models.

1.05

Stable isotopic constraints on the distributions and fluxes of CO₂:
A global 3-D GCM study using the NCAR CCM2

David J. Erickson III and Philippe Ciais¹
Theoretical Studies and Modeling Section, Atmospheric Chemistry Division,
National Center for Atmospheric Research, Boulder, CO 80307-3000

¹Also at: Laboratoire de Modelisation du Climat et de l'Environnement, Saclay, France

We describe global, 3-D numerical simulations of the distributions and fluxes of ¹³CO₂ and ¹²CO₂ in the Earth system. An atmospheric general circulation model, the NCAR CCM2 is used to transport a variety of chemical species using a semi-Lagrangian approach at a 15 minute time step. The spatial resolution of the model is 2.8° x 2.8° latitude-longitude in the horizontal with 18 vertical levels. The ¹³CO₂ fluxes implied to be due to atmospheric exchange with the ocean, soil respiration and the terrestrial biosphere are used to influence the separate isotopic tracers in the model. Global source estimates associated with biomass burning and the combustion of fossil fuels are also included so as to account for the time transient in the atmospheric CO₂ isotopic record. A detailed comparison between model output and the observational record in terms of both ¹³CO₂ and ¹²CO₂ will be assessed. Analyses of particular interest include the latitudinal gradient of ¹³CO₂, the site-specific seasonal cycle of ¹³CO₂ and the interannual variability and rate of change of ¹³CO₂. An off-line version of the transport model is also forced with the identical surface chemical boundary fluxes at an effective time step of 12 hours. A comparison of the off-line and on-line simulations will be presented. The off-line approach decreases the computational requirements of the model substantially and allows for the inclusion of a large variety of chemical species in addition to CO₂.

1.06

The Carbon Cycle: Results of a Coupled Atmospheric Chemical
Tracer Transport Model and an Ecosystem Model*

J. Dignon, J.R. Kercher, J.E. Penner and J.J. Walton
Lawrence Livermore National Laboratory
P.O. Box 808, L-262, Livermore, CA 94551 USA

Human activities have created large anthropogenic emissions of greenhouse gases, particularly carbon dioxide from fossil fuel burning and deforestation. Much of the carbon emitted into the atmosphere is taken up by the oceans; however, balancing the contemporary carbon budget requires a large "missing sink," possibly located in the terrestrial biosphere. We are developing a global scale ecosystem model with a resolution of 1x1 which represents water, carbon, and nitrogen dynamics as a set of ordinary, coupled nonlinear differential equations in order to study the ability of present-day ecosystem models to explain this missing sink. The initial version of this model, called TERRA, has been coupled to our 3-dimensional atmospheric chemical tracer model, called GRANTOUR. The two models are used to simulate the seasonal carbon cycle for a pre-industrial and present-day vegetation cover. Predicted concentrations of atmospheric CO₂ are compared to the atmospheric record at the NOAA GMCC stations. Preliminary results using potential vegetation show that the seasonal amplitude of the average monthly net ecosystem production has both a maximum of >100 gC m⁻² month⁻¹ and minimum of <20 gC m⁻² month⁻¹ occurring in the tropics. Amplitude values in the northern mid-latitudes range from roughly 40 to 75 gC m⁻² month⁻¹. At the meeting, results of the pre-industrial and present-day simulations will be discussed.

*This work was performed under the auspices of the U.S. Department of Energy by the Lawrence Livermore National Laboratory under Contract No. W-7405-Eng-48.

1.07

Soil C and N Cycle Feedbacks to Elevated CO₂: Implications for CO₂, N₂O, and NO
Exchange

¹E. Holland, ²P. Canadell, ²F. Chapin, ³N. Chiariello, ⁴J. des Rosiers, ³A. Fredeen,
³C. Field, ²B. Hungate, ⁴R. Jackson, ⁴G. Koch, ³Y. Luo, ⁴H. Mooney, ⁴H. Pearson,
⁴O. Sala

¹National Center for Atmospheric Research, Boulder, Colorado; ²University of California,
Berkeley, California; ³Carnegie Institute of Washington and ⁴Stanford University,
Stanford, California, USA

Increasing atmospheric CO₂ can alter carbon exchanges with terrestrial ecosystems, causing feedbacks to atmospheric CO₂. The terrestrial response to elevated CO₂ can vary dramatically with changes in resources such as water or nitrogen. We have conducted an integrated experimental and modeling study of the response of two California annual grasslands to elevated CO₂. Using open-top chamber, microecosystems and growth chambers, we have measured system-level responses to elevated CO₂ following experimental manipulations of resource availability. In this presentation, we focus on feedbacks in soil carbon and nitrogen cycles that could affect exchanges of CO₂ and other trace gases between terrestrial systems and the atmosphere. We found that elevated CO₂ increased photosynthesis, microbial biomass, and soil respiration, but also increased C/N ratios in litter, causing a decrease in nitrogen availability. Nitrogen limitation in turn constrained the ecosystem's ability to take up and store carbon. This feedback affects trace gas exchanges by causing a release of "excess carbon" through respiration and a decrease in N₂O, and possibly NO, fluxes due to the decrease in available nitrogen.

1.08

Spatial Distribution of Trace Gases and Particulate Matter Emissions from Biomass Burning in Diverse Tropical Ecosystems

Wei Min Hao and Darold E. Ward

Intermountain Fire Sciences Laboratory, USDA Forest Service, Missoula, Montana, USA

Substantial research has been carried out to determine the amount of CO₂, CO, CH₄, non-methane hydrocarbons, and particulate matter emitted from biomass fires in tropical forests and savannas. The field research has been conducted in the Amazon rain forest, Brazilian cerrado, South African arid savanna, and humid savanna in Zambia since 1989. The emissions of these gases and particulate matter are compared under different combustion conditions for a variety of vegetation. Linear relationships are developed to relate the emission factors of different trace gases and particulate matter to the combustion efficiency. The results are extrapolated to estimate the spatial distribution of these gases and particulate matter emitted from biomass burning in tropical Africa, America, and Asia with 1° latitude x 1° longitude resolution. The spatial distribution is derived from the emission factors, the aboveground biomass density, and the area cleared annually due to deforestation, shifting cultivation, and savanna burning. The results are critical for modelling tropospheric chemistry, assessing the impact of biomass burning on global climate, and developing strategies for reducing emissions of trace gases and particulate matter.

1.09

The Geographic Distribution of CO₂ Emissions from Fossil Fuel Consumption

Robert J. Andres¹, Gregg Marland¹ and Inez Fung²

¹ Environmental Sciences Division, Oak Ridge National Laboratory, Box 2008, Oak Ridge, TN 37831-6335 USA

² National Aeronautics and Space Administration, Goddard Space Flight Center Institute for Space Studies, 2880 Broadway, New York, NY 10025 USA, Currently at: School of Earth and Ocean Sciences, Univ. of Victoria, Box 1700, Victoria BC V8W 2Y2 CANADA

Emissions of CO₂ from fossil fuel consumption and cement manufacture have been estimated on a 1° latitude by 1° longitude (1x1) grid. Maps for 1950, 1960, 1970, 1980 and 1990 were created from national estimates of CO₂ emissions and 1x1 maps of political units and human population density. The estimates show continual growth over most of the world with increased growth in major urban areas. A southerly shift in the distribution is due largely to rapid growth in emissions from Asia. Using a linear extrapolation of recent trends and a projection based on the goals of the Framework Convention, 2 scenarios for the distribution of emissions in 2020 are included.

1.10

Measurements of trace gases in the upper atmosphere using airliner

H. Matsueda, H.Y. Inoue and *Y. Sugiyama
Geochemical Research Division, MRI, Japan
*Engineering Development, JAL, Japan

Airliner is suitable for frequently observing the temporal and spatial distributions of the trace gases in the upper atmosphere over a long period of time. Since 1991, we have been developing an automatic flask sampling system for Boeing 747 through a co-operative program supported by the JAL foundation, JAL, Ministry of Transport in Japan and Meteorological Agency of Japan. This system was developed to collect sample air into twelve titanium flasks of Automatic Sampling Equipment (ASE-1,2) using a metal bellows pump. Since our sampling system was tested under severe conditions, it could be utilized as airborne equipment on board Boeing 747's operating in the world. Since April 1993, monthly sampling between Cairns in Australia and Narita in Japan has been continuously performed using the ASE-1,2 installed in JAL airliner. After the sampling flight, the ASE-1,2 was returned to MRI to measure carbon dioxide (CO₂) and methane (CH₄) concentrations of the sampled air collected at 10-12 km altitude. A significant change in concentrations of both the CO₂ and CH₄ was found at the Intertropical Convergence Zone (ITCZ). In October, lowest CO₂ and highest CH₄ concentrations were observed between 10°N and 20°N, where ITCZ was located in the western Pacific region. These results indicated that CO₂ and CH₄ in the surface air was largely transported upward by active convection processes. Seasonal variations of CO₂ and CH₄ were found in the upper atmosphere, but the amplitude and cycle of their variations depended on the latitude.

1.11

Possible Causes for the Decline in the Methane Growth Rate

K.S. Law¹, S. Bekki¹ and E. Nisbet²

¹Center for Atmospheric Science, Cambridge, U.K.

²Dept. of Geology, Royal Holloway and Bedford College, London, U.K.

Analysis of CH₄ observations over the past decade has shown a dramatic slow down in the growth rate of CH₄ in recent years and particularly in the northern hemisphere during 1992 (Steele et al, 1992; Dlugokencky et al, 1994). In this study, a 2-D photochemical model of the atmosphere is used to investigate reasons for the slowing CH₄ trend. The recent decline coincided with a large reduction in the global ozone which may have enhanced OH and thereby led to increased loss of CH₄ in the troposphere. The possible relationship between changes in the growth rate of methane in the troposphere and the observed changes in column ozone is examined. Trends in anthropogenic emissions of CH₄ from coal and gas sources are estimated for the period 1981 to 1992. This includes substantial reductions in the emissions from gas pipelines which are likely to have occurred in the former Soviet Union. The impact of these changes on the CH₄ growth rate is assessed. The results show that both the decline in anthropogenic emissions of CH₄ and the impact of a reduced ozone column can make a major contribution to the slowing CH₄ trend.

1.12

Constraints on Recent Changes in the
Global Methane Budget from Isotope Measurements

M.R. Manning, D.C. Lowe and K.R. Lassey

NIWA Climate Division, Lower Hutt, New Zealand

Measurements of atmospheric CH₄ concentration have shown a decrease in its growth rate to near zero over the period 1989 - 1993 (Dlugokencky et al, 1993). Measurements of the ¹³C/¹²C isotope ratio in CH₄ in the Southern Hemisphere over this period show a seasonal cycle, out of phase with that of concentration, and a recent trend towards isotopically lighter values (Lowe et al, 1994). Here we consider how source scenario runs from the GISS model (Fung et al, 1991) can simulate the isotopic data. This leads to additional constraints on CH₄ sources and sinks and their recent changes. Simulation of the seasonal cycle of δ¹³C requires a larger kinetic isotope effect in the atmospheric oxidation of CH₄ than found in laboratory studies and a seasonal influx of isotopically heavy methane (δ¹³C > -25‰) into the Southern Hemisphere, consistent with simpler model analyses (Lassey et al, 1993). Reduced CH₄ growth rate is due to a reduction in isotopically heavy sources such as biomass burning and fossil fuel production, but distinguishing between changes in these source types is difficult with the data currently available. The model results are used to suggest additional isotopic measurement sites.

1.13

Atmospheric carbon emission from northern lakes: a factor
of global significance

I.P.Semiletov, S.A.Zimov, Yu.V.Voropaev and S.P.Davidov
Pacific Oceanological Institute and North Eastern Science
Station, FEB, Academy of Sciences, Russia

Northern ecosystems contain up to 455 Gt of C in the soil active layer (SAL) and the upper levels of the permafrost, or up to 60% of the 750 Gt C contained currently in the atmosphere as CO₂. Taking into account that CH₄ atmospheric content is about 0.5% of CO₂, liberation of less than 1% of buried C in CH₄ form is enough to double the modern CH₄ atmospheric burden. Due to aerobic predominant conditions in the SAL, main part of available C is oxidized and emitted to atmosphere as CO₂. Deeper buried C is become available for microorganisms only by way of the lake evolution. Anaerobic lake sediments and underlaid melted permafrost produce CH₄ all-year-roundly. Our all-year-round measurement of CH₄ emission from thermokarst lakes in North Asia are correlated with the δ¹³C-CH₄ measurement of Quay et al (1991) and one shows that northern lakes play an important role in the global methane cycle in the present and past. It is also shown that the northern CH₄ emission might influence on global changes in air content of other greenhouse species via the thermokarst evolution. Also, initial results show that CO₂ flux from northern lakes to the atmosphere is only 3d source of CO₂ after the SAL and Arctic Ocean.

1.14

ANTHROPOGENIC METHANE EMISSION IN RUSSIA

Sh.D. Fridman, A.I. Nakhutin, V.A. Vorobyev
Institute of Global Climate and Ecology
under Russian Academy of Science and Roshydromet, Russia

Total anthropogenic emission of methane in Russia was estimated as 16,3 Mt/year in 1993, basing on available emission factors and national economy statistics data.

Differing from World emission structure oil and natural gas production and transportation plays the major role (>50% of total emission) for Russia.

Analyses of emission structure and trend demonstrates decrease of 8% for the period 1990-1993 due to the economical crisis in spite of slow rise of emissions from natural gas production and landfills.

1.15

Atmospheric methane and nitrous oxide: Sources, sinks
and strategies for reducing agricultural emissions

K. Minami

Division of Environmental Planning, NIAES, Japan

Methane and nitrous oxide play an important role in photochemical reactions of the troposphere and stratosphere. Change in their concentrations exerts a strong influence on the atmospheric chemistry. The concentration of atmospheric methane and nitrous oxide increases by about 1.0 and 0.3 % per year, respectively, and accounts for almost over 25% of the radiative force added to the atmosphere. Methane and nitrous oxide are released to the atmosphere from various natural and anthropogenic sources. Although several global methane and nitrous oxide budgets have been estimated (for example IPCC), the values of individual sources and sinks are still highly uncertain and very tentative.

I review first the global methane and nitrous oxide budgets estimated by IPCC, IGBP and others. Then, I introduce mainly methane production, oxidation and emission from rice paddies, and nitrous oxide emission from fertilized soils. Finally, I discuss plans and possibilities on how to reduce methane and nitrous oxide emission from rice paddies and fertilized soils, and show some examples in detail.

1.16

Methane emission from various rice fields in China : An overview

Wang Mingxing and Shangguan Xingjian

Institute of Atmospheric Physics, Chinese Academy of Sciences, 100029 Beijing, PR. China

Until 1993, the methane emission rates from Chinese rice fields have already been recorded in all the five typical rice growing areas, which are South China Region, Central China Region, Southwest China Region, Middle and Lower Course of Changjiang River Region and North China Region. The total emission from Chinese rice fields can be estimated $11-14 \text{ TgCH}_4\text{yr}^{-1}$ which is rather small as we expected before. Great spatial variation has been obviously observed, which could be coupledly caused by climate and water regimes, soil type, rice variety, and various agricultural practice (e.g. cropping system, the way of fertilizer application and water management), while the effect of the above individual factor is not yet well understood. As seen from the data available, it can not simply be explained by the organic carbon content of the soil and annual mean temperature, but is well related to the amount of organic fertilizer applied. The temporal variation of emission rate varies from fields to fields and sometimes seasons to seasons: The major factors explaining the seasonal variation (long-term) of methane emission rate could be temperature variation, cropping system (rice-rice, wheat or other crop-rice, single rice), status of rice growing, all of which can affect the seasonal trend of methane production and transport efficiency. The reason for diurnal variation (short-term) is relatively simple, which is mainly the variation of methane transport efficiency from the soil further caused by the variation of air temperature. The application of organic manure almost always enhanced methane emission while the effects of various mineral fertilizers were rather contradictory. The proper use of fermented fertilizer instead of fresh organic manure, scientific water management (e.g. ridge rice, frequent drainage) instead of permanent flooding were approved to be able to reduce methane emission. The transport separation measurement in Hunan Province show that the role of rice plant in emitting methane was changing greatly and depended on the status of rice growing. The seasonal average percent (about 55% for early rice, and ca. 75% for late rice) was much lower than estimated before.

1.17 Measurement of Nitrous Oxide Emission from Agricultural Land using Micrometeorological Methods

K.J. Hargreaves¹, P. Wienhold², L. Klemedtsson³, J.R.M. Arah⁴, I. Beverland⁵, D. Fowler¹, B. Galle³, D. Griffith⁶, U. Skiba¹, K.A. Smith⁴ and M. Welling².
ITE Edinburgh, UK¹, MPI Mainz, Germany², IVL Gothenburg, Sweden³, SAC Edinburgh, UK⁴, IERM, University of Edinburgh, UK⁵ and University of Wollongong, Australia⁶.

The spatial variability of the N_2O flux in soil makes the extrapolation to the field scale very difficult using conventional chamber techniques ($< 1\text{m}^2$). Micrometeorological techniques, which integrate N_2O fluxes over areas of 0.1 to 1 km^2 were therefore developed and compared in a large field campaign. Micrometeorological measurements of N_2O emission from an organic soil were made over a 10 day period at Lammefjord, Denmark. Flux-gradient and relaxed eddy accumulation techniques were applied using two Tunable Diode Laser spectrometers (TDL's), a Fourier Transform Infra-Red spectrometer (FTIR) and a gas chromatograph (GC). Eddy correlation measurements were also made using the two TDL's. Over the 10 day campaign approximately 5 days of continuous fluxes by the different methods were obtained. Fluxes determined by eddy correlation, using the TDL's, were in excellent agreement, showing a mean flux of $290 \mu\text{g N m}^{-2} \text{ h}^{-1}$ over an area cropped with carrots. At the same time flux-gradient techniques measured fluxes over wheat stubble. The mean flux was $148 \mu\text{g N m}^{-2} \text{ h}^{-1}$.

1.18

Nitrous Oxide Emission from Biomass Burning and Its Distribution in Mainland China*

Mei-qiu Cao and Ya-hui Zhuang

Research Center for Eco-environmental Sciences,
Academia Sinica

PO Box 2871, Beijing, 100085, China

The emission factors of nitrous oxide during the combustion of rice straw, wheat stalk and maize stalk have been determined in an experimental combustion facility. The experimental errors in the determination of nitrous oxide concentration by gas chromatography and in the sampling procedure have been discussed. Necessary measures have been taken to ensure the quality of analytical results. The emission factors thus determined for rice straw, wheat stalk and maize stalk are 84.4, 132 and 27.3 g/ton , respectively.

The distribution of nitrous oxide emission from biomass burning in mainland China has been estimated, and the results have been presented as an $1^0 \times 1^0$ grid map. The biomass formation in mainland China were calculated from the annual cereal production in the counties and regions.

*Supported by the Chinese National Natural Science Foundation.

1.19

The Global Decrease of Carbon Monoxide and Its Causes

M.A.K.Khalil and R.A.Rasmussen

Global Change Research Center and Department of Environmental Science &
Eng. Oregon Graduate Institute, P.O.Box 91,000, Portland, Oregon 97291 USA

Global measurements show that atmospheric CO increased during the early part of the 1980s at about $1\%/\text{yr}$ ¹. Between 1987 and the present, global concentrations have declined rapidly at about $-1.4 \pm 0.9\%/\text{yr}$ in the northern hemisphere and $-5.2 \pm 0.7\%/\text{yr}$ in the southern hemisphere². Decreases can occur if the sources decline, if the sinks increase, or by a combination of these two processes. Both possibilities may be contributing to the current trends. Increased uv can lead to a decrease of CO in regions where most of the CO does not come from the oxidation of CH_4 and other hydrocarbons and over regions where significant ozone depletion has occurred (middle and high latitudes). Based on current data, it seems that some of the decreasing trends in the northern hemisphere may be explained by OH increase, but most probably comes from a slowdown in emissions. In the southern hemisphere, however, it appears that the decreasing trends are probably due to a reduction of biomass burning in the tropics and not due to changes in OH. The slowdown of biomass burning may be permanent or temporary and may be driven by climatic events.

References and Acknowledgements: 1. Khalil & Rasmussen, *Nature* 332, 242-245 (1988). 2. Khalil & Rasmussen, Global Decrease of Atmospheric Carbon Monoxide, *Nature* (submitted, August 1993). Supported by grants from NSF, DOE, Biospherics Research Co., and the Andarz Co. Samples at some sites collected by NOAA/CMDL staff.

1.20 Spectroscopic measurements of the spatial-temporal distribution of the minor gaseous atmospheric constituents (CO, CH₄)

E.I. Grechko and A.V. Dzhola

Institute of Atmospheric Physics, Russian Academy of Sciences, Moscow, Russia

First evidences of atmospheric CO and CH₄ increase were obtained by spectroscopic technique (Rinsland and Levine, 1985; Dianov-Klokov et al., 1989). The abundant collection of data were accumulated in field measurements in different regions of the former USSR and in the Arctic, Antarctic and Oceanic regions by the Institute of Atmospheric Physics. Spectroscopic technique based on absorption of the solar radiation was applied. Regular observations were carried out at Zvenigorod scientific station near Moscow (56°N, 37°E) in 1970-1993. Before 1983 CO was increasing for all seasons (1.4% per year), since 1983 winter trend is equal to 1% per year, summer-autumn trend equals to 0%. The total trend of CH₄ in Zvenigorod for 1974-1993 is 0.5% per year.

1.21 SF₆ a new powerful tracer in the atmosphere

M. Maiss¹, I. Levin¹, R. Francey², P. Fraser², R. Langenfelds² and P. Steele²

¹ Inst. f. Umweltphysik, Univ. Heidelberg, Germany; ² Div. of Atm. Res., CSIRO, Australia

High precision long-term observations of the assumed solely anthropogenic trace gas sulphur hexafluoride (SF₆) at four background monitoring stations are presented: Cape Grim, Australia (1978-94); Neumayer Station, Antarctica (1986-94); Alert, Canada (1993-94) and Izaña, Canary Islands (1991-94). These world-wide observations considerably extend a first data set published by Maiss and Levin [GRL, in press]. SF₆ has increased by two orders of magnitude since 1970 from 0.03 to 3 pptv with a recent increase rate of 8 % yr⁻¹. This is due to a growing industrial production and emission combined with an atmospheric lifetime of probably more than 3000 years [Ravishankara et al., 1993]. The concentration in the northern hemisphere is persistently higher if compared to the southern hemisphere due to a predominant release of SF₆ in the northern hemisphere. Meridional profiles confirm this significant north-south gradient from which an interhemispheric exchange time of 1.1-1.4 years can be calculated. The greenhouse effect of SF₆ on a per molecule basis is likely to be one of the highest of any atmospheric trace gas [Rinsland et al., 1990], but due to the present low atmospheric concentration (≈10⁻² of CFC) its climatic impact is only of minor relevance today [Ko et al., 1993]. However, here we will show that the development of SF₆ in both hemispheres is an extremely powerful tool for modelling investigations in the atmosphere and the hydrosphere. SF₆ is an ideal tracer to quantify mixing processes in the troposphere and between troposphere and stratosphere. Moreover, the atmospheric input function can be used for dating of deep ocean water and firn air. Especially in the atmosphere SF₆ is a promising alternative to ⁸⁵Krypton as it is easier to measure and more regular in emission.

1.22

Global distribution of CO₂ and halogenated hydrocarbons

P. Fabian, University of Munich and R. Borchers, Max-Planck-Institut für Aeronomie, Germany

In-situ measurements of CO₂ and various halocarbons, most of which being efficient greenhouse gases, were carried out at tropical (17°N), midlatitude (44°N) and high latitude regions (69°N). Cryogenically collected whole-air samples were analysed by GC and GC-MS as well as infrared absorption techniques.

Average vertical profiles, growth rates and budgets covering the time periods given in brackets will be presented for CO₂ (1979-1993), CCl₃F and CCl₂F₂ (1977-1993) as well as CCl₄, CClF₃, CF₄, CCl₂F-CClF₂, CClF₂-CClF₂, CClF₂-CF₃, CF₃-CF₃, CH₃Cl, CHClF₂, CH₃-CCL₃, CBrClF₂, CBF₃ (1980-1993) and CH₃Br (1992-93).

1.23

Measurements of HCFCs in the Cape Grim Air Archive : 1978-1993

D.E. Oram, S.A. Penkett University of East Anglia, Norwich, U.K.
P. Fraser CSIRO, Aspendale, Australia.

In response to concern over stratospheric ozone depletion and global warming, the Montreal Protocol calls for a ban on the production of a number of chlorine-containing compounds, including the chlorofluorocarbons (CFCs). Hydrochlorofluorocarbons (HCFCs) have been proposed as replacement compounds since they have shorter atmospheric lifetimes, due to their reaction in the troposphere with OH radicals, and therefore lower ozone depletion potentials. The major HCFC, HCFC-22, has been in use for many years and several studies have determined its atmospheric concentration and distribution. The highly-sensitive GC-MS instrument at UEA has the capability of detecting a number of other HCFCs, including HCFC-142b (CH₃CF₂Cl), HCFC-141b (CH₃CFCl₂) and HCFC-123 (CF₃CHCl₂), in the background atmosphere. The Cape Grim Air Archive consists of around 50 samples of clean background air collected over the period 1978-1993 at Cape Grim, Tasmania (41°S). These samples have been analysed for CFCs and HCFCs at UEA during the summer of 1993. Trends in the major CFCs follow expected patterns with evidence for declining emissions in recent years. HCFC-142b and HCFC-141b have been detected in all samples back to 1978, and show rapidly increasing concentrations since the late 1980s. Using a well proven global 2-D model, the measurements have been used to estimate global emissions of these new potential greenhouse gases.

1.24

Long-Term Measurements and Changing Trends of
Halocarbon Concentrations in the Atmosphere

Yoshihiro MAKIDE, Limin CHEN, and Takeshi TOMINAGA
The University of Tokyo, Tokyo, Japan

Chlorofluorocarbons (CFCs), chlorocarbons, and halons with extremely long lifetimes are responsible not only for stratospheric ozone depletion but also for global warming. The ozone depletion induced by the halocarbons may also affect the global warming. We initiated very accurate measurements of trace halocarbons in the atmosphere as early as in 1979 in order to clarify their distributions and trends in the Northern and Southern Hemispheres, and also their vertical profiles in the stratosphere.

The averaged atmospheric concentrations of CFC-12 (CCl_2F_2) and CFC-11 (CCl_3F) in the mid-latitude Northern Hemisphere observed in Hokkaido, Japan, and in the Southern Hemisphere observed at Syowa Station in Antarctica had been increasing by about 4% a year, and CFC-113 ($\text{CCl}_2\text{FCClF}_2$) by 10-20% a year over the decade up to 1990. However, since then, their increasing trends in the Northern Hemisphere have been slowing down to 0-2% a year, which are reasonably corresponding to the international regulation of emissions according to the Montreal Protocol on Substances that Deplete the Ozone Layer. Methylchloroform (CH_3CCl_3) which is decomposed in the troposphere with OH radicals showed much smaller increasing rate, and has been rather decreasing recently.

Although our measurement data of atmospheric concentrations of CFC-113, carbon tetrachloride (CCl_4), and methylchloroform based on our originally developed standards had shown apparently different values (such as 30%) from the ALE/GAGE data, the gaps have been reduced by the revision of ALE/GAGE calibration.

2.01

Transport of O_3 and O_3 -Precursors from Anthropogenic Sources to the North Atlantic

D.D. Parrish, Steven Bertman, James Roberts, R. N. Norton,
Michael Trainer, and F.C. Fehsenfeld
U.S. Department of Commerce, Aeronomy Laboratory, Boulder, Colorado USA

The North Atlantic Regional Experiment (NARE), an activity of IGAC, is aimed at investigating the sources for ozone over the North Atlantic and the processes responsible for that ozone. The goals and research activities of NARE will be briefly outlined.

Correlation of simultaneously measured O_3 and CO at sites in the North Atlantic region as a function of season that were carried out as part of the NARE research have provided the basis for estimating the amount of O_3 that is produced photochemically from anthropogenic pollution in North America and transported to the North Atlantic. The measured relations between the concentrations of O_3 and CO indicate that the amount O_3 produced from anthropogenic sources is greater than that reaching the lower troposphere in this region from the stratosphere. This conclusion supports the contention that ozone derived from anthropogenic pollution has a hemisphere wide effect at northern temperate latitudes. These studies will be described and their results will be discussed.

In addition, during the summer of 1993, measurements of O_3 along with NO_x and NO_y along with a suite of photochemically active trace compounds were made during the summer of 1993 in the Maritime Provinces of Canada as part of the NARE 1993 Summer Intensive. The relation between O_3 and these reactive nitrogen species, and the relation of reactive nitrogen oxide species to other O_3 -precursor compounds will be used: 1) to assess our current understanding of the photochemistry; 2) to estimate the potential for additional ozone production in the air masses transported into the North Atlantic; and 3) to provide evidence that the production of O_3 is NO_x limited.

2.02

A study of vertical and horizontal transport of ozone and ozone precursors using aircraft data from the North Atlantic Regional Experiment.

M. Buhr, D. Sueper, M. Trainer, W. Kuster, P. Goldan, and F.C. Fehsenfeld
U.S. Department of Commerce, Aeronomy Laboratory, Boulder, Colorado USA

Measurements of O_3 , NO_y , NO, CO, C_2 - C_5 hydrocarbons, and a variety of other chemical and physical parameters were collected aboard the NCAR KingAir in 16 flights off the northeastern coast of the U.S. during August, 1993, as part of the North Atlantic Regional Experiment (NARE). Evidence for the vertical and horizontal transport of O_3 and its precursors found in these measurements will be examined using a combination of bivariate and multivariate data analysis methods, including Principal Component Analysis (PCA). The relationships observed between ozone and its precursors, both in general and as a function of the air mass types identified with PCA, will be examined in terms of air mass origin and photochemical age. Particular attention will be paid to the effect of clouds and convective transport on the spatial distribution of ozone. A brief discussion of the measurement methods used will be included.

2.03

Pacific Exploratory Mission West/Phase B(PEMWestB):
An Overview of Preliminary Findings

D.D. Davis
School of Earth and Atmospheric Science, Georgia Institute of Technology, Atlanta,
GA 30332
S.C. Liu
Aeronomy Laboratory/NOAA, 325 Broadway, Boulder, CO 80303
R. Newell
Mass. Institute of Technology, Rm 54-1854, Cambridge, MA 02139
J. Hoell
Langley Research Center, Mail Stop 483, Hampton, VA 23665-5225
PEMWest(B) Science Team

The Pacific Ocean is the only major region in the Northern Hemisphere that is relatively free from direct anthropogenic influence. In remote regions of the northern Pacific and in most of the southern Pacific, it should be possible to study the biogeochemical cycles of carbon, nitrogen, ozone, and sulfur in an environment almost unperturbed by anthropogenic activities. On the other hand, there is little doubt that long-range transport of air pollutants from Asia and, to a lesser extent, North America is beginning to have a significant impact on the atmosphere over a large part of the Pacific. Thus, the Pacific Basin also offers an excellent opportunity to study the anthropogenic impact on the atmospheric cycles of nitrogen, carbon, sulfur, and ozone. In this context, the PEMWest program has as its primary and secondary scientific objectives: (A) To investigate the atmospheric chemistry of O_3 and its precursors (NO_x , CO, CH_4 , and NMHC's) over the western Pacific, and to examine the natural budgets of these species and the impact of anthropogenic sources. (B) To investigate some important aspects of the atmospheric sulfur cycle over the western Pacific with emphasis on the identification of the relative importance of continental and oceanic sources. The first mission in the NASA sponsored PEM series, PEMWest(A) was conducted during the northern hemisphere fall time period of September and October of 1991, at which time the outflow from the Asian Continent was weak. The second phase of this program (i.e., 1994) will be conducted, for the most part, over the same general geographical location but during the early spring at which time the outflow from Asia into the Pacific basin should be near its maximum. As part of the IGAC/APARE program, PEMWest(B) will encompass both ground-based sampling as well as a major airborne component (NASA's DC-8). To be discussed are the preliminary scientific findings of this new field initiative and how these findings compare and contrast with those of PEMWest(A).

2.04

Ozone Production, Transport, and Distribution
in the Western Pacific Rim

Gregory R. Carmichael, Yang Zhang, Mahesh Phadnis and Young Sunwoo
The University of Iowa
Department of Chemical and Biochemical Engineering
Center for Global and Regional Environmental Research
Iowa City, IA 52242 USA

The characteristics of tropospheric ozone production and transport in the middle to lower latitudes of East Asia are being studied. In this paper ozone data from surface observations, satellite and ozonesondes are analyzed and discussed. The surface data includes information from the background ozone monitoring network of Japan and the southern island site of Cheju in South Korea. The seasonal behavior shows a spring peak and summer minimum for most of the sites with characteristics dependent on site elevation, local meteorology, and proximity to anthropogenic sources. Satellite-derived residual ozone shows a similar seasonal cycle. Both surface and residual ozone show a trend with increasing values over the past decade.

The mechanisms of transport, chemical transformation and removal of ozone and other trace gas species are studied using a detailed three-dimensional tropospheric trace gas model (i.e., the STEM-II model). The characteristics of the photochemical oxidant cycle and the effects of pollutant long-range transport on the distribution of ozone in this region are discussed. Estimates of the fluxes from the Pacific Rim to the background troposphere are also presented. Finally, interactions between the photochemical oxidant cycle and springtime dust storms are also discussed.

2.05

Measurements of Total Reactive Nitrogen and Ozone in the Troposphere
over the Pacific Ocean and Japan Sea

S. Kawakami, M. Ieda, M. Koike, H. Nakajima, Y. Kondo
(Solar Terrestrial Environment Lab., Nagoya University)

Measurements of total reactive nitrogen (NO_y) and Ozone (O_3) are presented from three aircraft flights made over the Pacific Ocean and the Japan Sea in the winter and autumn of 1993 at altitudes between 0.3 km and 6 km. Two flights were made on Jan. 20 and Feb. 13 over the Pacific Ocean between $28^\circ N$ and $35^\circ N$. One flight was made on Nov. 3 over the Japan Sea between $35^\circ N$ and $40^\circ N$. NO_y was catalytically converted to NO on the heated A_U surface, and NO was subsequently detected by NO/O_3 chemiluminescence. NO_y was about 200~300 pptv in the 2~4 km region on both Feb. 13 and Nov. 3. However NO_y mixing ratios at altitudes below 1.5 km were different between these days; about 1.1 ppbv, 2 ppbv, respectively. O_3 mixing ratios were also different at altitudes below 1.5 km. O_3 was about 58 ppbv on Feb. 13 and was 70 ppbv on Nov. 3. NO_y increased from about 400 pptv to 800 pptv with altitudes between 5 and 6 km on Nov. 3. NO_y above 1.5 km was constant of about 200 pptv on Feb. 13. The maximum NO_y and O_3 were found below 1.5 km during the three flights. The correlation of O_3 with NO_y below 1.5 km suggests that emissions of NO_y originated from the Asian continent associated with the photochemical production of O_3 occurred near the surface of the continent.

2.07

Tropospheric Ozone Measurement at The Top of Mt. Fuji

Yukitomo Tsutsumi, Yuji Zaizen and Yukio Makino
Meteorological Research Institute, 1-1 Nagamine, Tsukuba, Ibaraki, 305 Japan

Mt. Fuji ($35^\circ 21' N, 138^\circ 44' E$) is not only the highest mountain in Japan whose height is 3776m in the middle troposphere but also an isolated and dormant konide volcano whose summit has an only 800m in diameter. These conditions suit the background measurement of tropospheric ozone. Since the August of 1992, ozone concentration has been measured at the top of Mt. Fuji to make clear the background feature of tropospheric ozone in the East Asia.

During one year observation, the diurnal amplitude shows quite small variation throughout the year. At the top of Mt. Fuji, it appears to be little affected by the mountain and valley winds. The maximum concentration of monthly mean ozone at Mt. Fuji was 60.0 ppbv in May and the minimum was 32.1 ppbv in August. Summertime day-to-day variations are highly variable and sometimes marked very low concentration around 20 ppbv. This is attributed to the horizontal advection of ozone poor air in the troposphere. In wintertime, the deviation of ozone concentration is small. High steep peaks higher than 80 ppbv were frequently observed in spring. These peaks have different patterns from surface ozone at Tsukuba ($36^\circ 03' N, 140^\circ 08' E$).

2.08

The Global Distribution of Tropospheric NO_x and its Impact on Ozone Chemistry

H. Levy II and W. J. Moxim
 Geophysical Fluid Dynamics Laboratory/NOAA, Princeton, New Jersey, 08542, USA
 P.S. Kasibhatla
 EAS, Georgia Institute of Technology, Atlanta, Georgia, 30332, USA
 S. Sillman
 AOSS, University of Michigan, Ann Arbor, Michigan, 48109-2143, USA

The GFDL Global Chemical Transport Model [GCTM], with the six known sources of tropospheric NO_x and an off-line chemistry for 3 transported reactive nitrogen surrogates, "NO_x", "HNO₃" and "PAN", [Kasibhatla et al., 1993; Levy et al., 1994], is used to determine the global distribution of tropospheric NO_x. The resulting NO_x fields are shown to be in harmony with available observations. The simulated 3-D monthly mean NO_x fields, along with specified 3-D fields of T and water and 2-D fields of hydrocarbons, carbon monoxide, and ozone, are then used as input for a comprehensive photochemical model [Sillman, 1991], which calculates 3-D maps of ozone net chemical production and destruction. While net ozone chemical production is found to occur over much of the Northern Hemispheric troposphere, its rate varies greatly with season, latitude and altitude. With the exception of the tropical and subtropical South Atlantic, most of the Southern Hemisphere experiences net ozone chemical destruction. Both seasonal and regional variations in NO_x and the net ozone chemistry are discussed.

2.09

The Impact of Regional Ozone Pollution on World Food Production

W.L. Chameides and P.S. Kasibhatla
 School of Earth and Atmospheric Sciences
 Georgia Institute of Technology
 Atlanta, Georgia 30332

J. Yienger, and H. Levy, II
 Geophysical Fluid Dynamics Laboratory
 Princeton University
 Princeton, New Jersey 08542

Three regions of the northern mid-latitudes presently dominate global industrial and agricultural productivity. While covering only 23% of the earth's continents, these regions (referred to as Continental-Scale Metro-Agro-Plexes) account for most of the world's commercial energy consumption, fertilizer usage, food-crop production, and food exports. These regions also account for more than half of world's atmospheric nitrogen oxide emissions and as a result are prone to ground-level O₃ pollution during the summer months. On the basis of a global simulation of atmospheric reactive nitrogen (NO_y), we estimate that about 10-30% of the world's food crops may be grown in parts of these regions where O₃ pollution may reduce crop yields. Exposure to yield-reducing O₃ pollution may triple by the year 2025 if rising anthropogenic NO_x emissions are not abated. The impact upon world food production and the economic costs of compensations for this impact may be significant.

2.10

Global weighted-average concentration and trend for OH based on 15 years of ALE/GAGE CH₃CCl₃ data.

R.G. Prinn (Massachusetts Institute of Technology, Cambridge, MA),
 R.F. Weiss & B.R. Miller (Scripps Institution of Oceanography, La Jolla, CA),
 F.N. Alyea, D.M. Cunnold, and D.E. Hartley
 (Georgia Institute of Technology, Atlanta, GA),
 P.B. Fraser (CSIRO, Australia), and P.G. Simmonds (Bristol University, UK)

Reactions with OH comprise the major loss mechanism for many environmentally important trace gases including CH₃CCl₃, CH₄, hydrochlorofluorocarbons, CO, and CH₃Br. Real-time *in situ* measurements of CH₃CCl₃ have been made continuously since 1978 at the globally distributed ALE/GAGE/AGAGE stations. Using optimal estimation inverse techniques, these data are utilized together with recent estimates of industrial CH₃CCl₃ emissions, and new absolute calibrations for this gas, to provide quantitative estimates of the magnitude and trend in the CH₃CCl₃ lifetime. Recent kinetic data, and estimates of oceanic and other non-OH-related removal rates, are then used to provide estimates of the weighted-average global OH concentration and trend. We present these new results, and from them provide estimates of the lifetimes of CH₄, key hydrochlorofluorocarbons, and CH₃Br due to their reaction with OH.

2.11

The Role of Chlorine Atoms in Determining Tropospheric Ozone: Potential Sources from Sea Salt Reactions

B. J. Finlayson-Pitts,^a R. Vogt,^a R. Neavyn,^a J. M. Laux,^b and J. C. Hemminger^b
^aDepartment of Chemistry, California State University Fullerton, Fullerton, CA, 92634; ^b
 Department of Chemistry, University of California, Irvine, CA, 92717, U.S.A.

Chlorine atoms, if produced in the troposphere in significant quantities, may play a key role in the formation and fate of ozone either by a direct reaction or alternatively, by generating O₃ via reactions with organics and NO_x. Hence atomic chlorine may potentially impact global chemistry, and since ozone is a greenhouse gas, possibly play a role in the radiation balance as well. While sea salt particle reactions may generate photochemically active chlorine atom precursors, relatively little is known about the kinetics and mechanisms of such reactions. We report here laboratory studies of the kinetics and mechanisms of the reactions of NaCl, the major component of sea salt particles, with NO₂, N₂O₅ and HNO₃ using the techniques of diffuse reflectance Fourier transform infrared spectrometry (DRIFTS), a Knudsen cell and X-ray photoelectron spectroscopy. The reaction of NO₂ is shown to be too slow to be significant under typical tropospheric conditions, while that of N₂O₅ to form the photolabile nitryl chloride (ClNO₂) may equal and possibly exceed that of HNO₃ to form HCl. The effects of water on the surface chemistry will also be described and shown to provide an explanation for field observations of almost complete replacement of chloride by nitrate in some sea salt particles.

2.12

A Global Chemical-Transport Model Using the Dynamics
provided by the NCAR-CCM2 Model

G.P. Brasseur, S. Walters and P.J. Rasch

National Center for Atmospheric Research, Boulder, CO, USA

A chemical model describing key chemical and photochemical processes in the troposphere (and stratosphere) is coupled to a transport model at T42 resolution (2.8 degrees in longitude and latitude) to describe the formation and fate of approximately 25 chemical trace constituents between the surface and the level of 5 mbar. Advection is simulated by a semi-lagrangian transport scheme driven by winds produced by the NCAR Community Climate Model (version 2). Boundary layer and convective exchanges are parameterized. Surface emissions and deposition velocities are either specified or calculated as a function of the model meteorology (temperature, precipitation, solar flux, etc.).

The paper presents global distributions of several key constituents which will be compared to available observations. The focus will be on nitrogen compounds (NO_x, HNO₃, PAN) and their relations with the ozone budget. The relative effects of chemistry, transport and wash-out processes on the distribution of these compounds will be discussed. The role of dynamical fluctuations at the resolution captured by the model will be analyzed.

2.13

A Three-dimensional Study of the Global Distribution
and Budget of Trace Gases in the Troposphere

C. Granier¹, G. Brasseur¹, J.F. Muller² and D. Hauglustaine³

¹ National Center for Atmospheric Research, Boulder, CO, USA

² Belgian Institute for Space Aeronomy, Brussels, Belgium

³ Service d'Aéronomie CNRS, Paris, France

A global three-dimensional chemical-transport model of the troposphere has been used to study the production and destruction processes of key tropospheric chemical species. This model, called IMAGES (Intermediate Model for the Annual and Global Evolution of Species) has been used to simulate the three-dimensional behavior and seasonal evolution of a relatively large number of trace constituents, and to estimate their global budgets. The changes in the global budgets and lifetimes of tropospheric species and in the oxidizing capacity of the atmosphere in response to changes in the surface (anthropogenic and biogenic) emissions of trace constituents will be evaluated. The impact of these changes on the radiative forcing of climate will be discussed, with a particular emphasis on the impact of the tropospheric ozone increase in the Northern hemisphere since the preindustrial period.

2.14

An Overview Over the IGAC/SAFARI Experiment: The Role of Vegetation Fires
in the Environment of Southern Africa

M.O. Andreae and the SAFARI Science Team

Max Planck Institute for Chemistry, P.O. Box 3060, D-55020 Mainz, Germany

Recent studies demonstrate that pyrogenic emissions affect regional ozone concentrations and the oxidative characteristics of the tropical atmosphere. Fire also has both short- and long-term effects on trace gas emissions from affected ecosystems which, for instance in the case of CO₂ and N₂O, may be more significant than their immediate release during the fire. Burning alters the long-term dynamics of the cycling and storage of elements within terrestrial ecosystems, thereby altering their significance as sources or sinks of various trace gases. Finally, deposition of pyrogenic compounds on pristine tropical ecosystems may affect their composition and dynamics.

The first large, coordinated program being conducted under IGAC/BIBEX is the Southern Tropical Atlantic Regional Experiment (STARE), an aircraft and ground-based measurement program to investigate the role of fire in the atmospheric and terrestrial environment of the region from South America to Africa. The sources of trace gases, their atmospheric transport, and the chemical processes in the atmosphere which lead to elevated levels of O₃, CO, and other trace gases over the southern Atlantic, as well as the role of fire in the savanna ecosystems have been investigated. During the 1992 fire season, SAFARI-92 (Southern Africa Fire/Atmosphere Research Initiative), the African component of STARE, took place successfully. Some measurement sites remain in operation to investigate the seasonal and longer term trends in the distribution of pyrogenic emissions and ecosystem behavior. A follow-up experiment (SAFARI-94) will take place during the wet season to establish the atmospheric background in the absence of fires. An overview over the concept and results from these experiments will be presented.

2.15

EXPeriment for REgional Sources and Sinks of Oxidants (EXPRESSO)

P. Zimmerman and G. Brasseur

Atmospheric Chemistry Division, National Center for Atmospheric Research, USA

R. Delmas and J.P. Lacaux

Laboratoire D'Aerologie, Université Paul Sabatier, France

Tropical biomes are the most dynamic, yet most poorly understood on Earth. Tropical forests are being cleared at a rate of ~1% per year. Biomass burning, ubiquitous in African savanna, exerts a dominant influence on ecology and atmospheric chemistry. Biogenic fluxes of reactive or radiatively active trace gases are concentrated in tropical land areas and are strongly influenced by land use change and biomass burning. Future human population increase is projected to be higher in tropical areas than in any other region and will accelerate changes in land use. The interplay of global change, climate change, biogeochemical processes, population increases and resource limitations are likely to effect more people in the tropics than anywhere else.

Plans for an international experiment, EXPRESSO, to investigate tropical biogeochemistry will be presented and discussed in relation to the goals of various IGAC programs. The goals of EXPRESSO are: 1) to better quantify the exchange fluxes of reactive trace gases and aerosols between the biosphere and the atmosphere in the tropics; 2) to analyze chemical interactions between the savanna and the tropical forest; 3) to isolate the roles of photochemical and meteorological processes; 4) to characterize the effects of ecological processes on trace gas fluxes; 5) to assess the impact of these tropical processes and land use change on the global atmosphere.

2.16 OZONE OVER SOUTHERN AFRICA AND THE ATLANTIC DURING THE 1992 IGAC/STARE/SAFARI/TRACE-A MISSIONS

Anne M. Thompson,¹ Donna P. McNamara,¹ Kenneth E. Pickering,¹
Robert D. Hudson² and Members of the TRACE-A and SAFARI Science Teams

Characteristics of total and tropospheric O₃ in southern Africa and the adjacent Atlantic Ocean during the IGAC/STARE/TRACE-A/SAFARI-92 (International Global Atmospheric Chemistry/South Tropical Atlantic Regional Experiment/Southern African Fire Atmospheric Research Initiative/Global Tropospheric Experiment/Transport and Atmospheric Chemistry near the Equator - Atlantic) field experiments have been studied using a variety of data sources: 1) Nimbus 7/TOMS, for total ozone and for tropospheric ozone column by a new technique; 2) total ozone instruments at Okaukuejo (Namibia) and Irene (Pretoria); 3) Ozonesondes at Ascension, Brazzaville, Okaukuejo, and Irene; 4) SAFARI aircraft O₃ measurements at Victoria Falls; DC-3 flights over South Africa, Namibia, Botswana, and Zimbabwe; at the Kruger Park controlled burn site; coastal Namibian flights. 5) the DC-8 in-situ O₃ sampler and uv-DIAL instruments.

Trajectory analysis and AVHRR fire count data show the likely contribution of biomass burning to high ozone events, although large-scale dynamics may also play a role over the Atlantic. Concentrations of O₃ precursors (NO_x, hydrocarbons, CO) near active fires are used in a photochemical model to calculate rates of O₃ photochemical formation.

¹ Address: NASA/Goddard/916, Greenbelt, MD 20771, USA; ² Dept. Meteorology, University of Maryland, College Park, MD 20742 USA

2.17 Atmospheric Chemistry of the Tropical South Atlantic Ocean: Initial Results from TRACE-A

Jack Fishman
NASA Langley Research Center, Hampton, Virginia, U.S.A.

Anne M. Thompson
NASA Goddard Space Flight Center, Greenbelt, Maryland, U.S.A.

and the TRACE-A Science Team

The IGAC-sponsored Transport and Atmospheric Chemistry near the Equator--Atlantic (TRACE-A) field experiment was conducted in September-October, 1992, to investigate the chemistry over the tropical South Atlantic Ocean which is characterized by unusually high concentrations of tropospheric ozone initially identified from analyses of satellite observations. A suite of chemical and meteorological measurements were obtained aboard NASA's DC-8 "Flying Laboratory" and other ground stations to provide an understanding of the complex chemistry and dynamics in this heretofore unstudied region of the world. Experiments were designed to identify how much of this ozone was produced *in situ*, how much had been transported from Brazil and southern Africa, and how much may have been recently transported from the stratosphere.

2.18

Photochemical oxidants in the Venezuelan savanna during the rainy season

Claes de Serves¹ and Alberto Rondón²
1. Department of Meteorology, MISU, Sweden
2. IVIC, Atmospheric Chemistry Laboratory, Venezuela

Formaldehyde, peroxides (H₂O₂+organic peroxides), O₃, and NO, NO₂ were measured together with the photolysis rate of NO₂ and total actinic flux, during the wet season, September 1993, at a remote Venezuelan savanna site. These measurements constitute a part of the ASTROS (Atmospheric Studies in the TROPical Savanna) campaign, a joint Venezuelan, German, and Swedish field experiment, to further characterize the remote tropical savanna atmosphere, to investigate the formation of organic acids, and to examine photochemical processes.

Preliminary results from the campaign shows a pronounced diurnal variation for peroxides, formaldehyde, and O₃. The peroxide concentration reached an afternoon maximum concentration of ~2.5 ppbv which decreased drastically at sunset to about 0.1 ppbv during the night. At sunrise there was again a sharp increase. Formaldehyde had maximum concentrations at 1-2 ppbv and a night time low of less than 0.5 ppbv. Ozone fluctuated from 22 ppbv around noon to less than 2 ppbv at nights. NO_x values were also very low, NO and NO₂ mean concentrations were 0.1 ppbv (<0.025-0.7 ppbv) and 0.4 ppbv (<0.1-3.0 ppbv), respectively. Boundary layer conditions, photochemical and dry deposition processes will be put into perspective to explain these diurnal variations. The photostationary state (NO-NO₂-O₃) will be further discussed.

2.19

Tropospheric Ozone Behavior Observed with Ozonesondes in Indonesia

Ninong Komala, Slamet Saraspriya
Atmospheric Research and Development Center, LAPAN, Bandung, Indonesia
and

Toshihiro Ogawa
Graduate School of Science, University of Tokyo, Tokyo, Japan

We analyzed ozonesonde data obtained at Watukosek (73°4'S, 112°38'E), Indonesia during the period between November 1992 and December 1993. The ozonesonde data were verified for surface ozone concentration using a Dasibi ozone monitor. The integrated amount of tropospheric ozone indicates the largest value in September and the smallest in March, ranging from 20 to 43 milli-atm-cm. The average profile shows that the partial pressure of tropospheric ozone is relatively high near the ground surface, gradually decreases with altitude and reaches the minimum near the tropopause. Enhanced layers were sometimes found at a pressure level around 400 hPa (~7 km).

2.20

EUROTRAC: a co-ordinated project for tropospheric research

Peter Borrell

EUROTRAC ISS, Fraunhofer Institute (IFU), Garmisch-Partenkirchen

EUROTRAC, the European co-ordinated research project within the EUREKA initiative, addresses three major scientific problems in tropospheric research:

- the formation of photo-oxidants;
- acid precipitation;
- biosphere-atmosphere exchange of trace substances.

The project has achieved a remarkable success since its start in 1989 in bringing together international groups of scientists to work on problems directly related to the transport and chemical transformation of trace substances in the troposphere.

The contribution will outline the organisation of the project and illustrate in a pictorial fashion some of the more significant results obtained by the 250 research groups involved within the 14 subprojects.

The newly formed Application Project, which is intended to extract and interpret the results so that they can be used by policy makers, will also be described as will proposed future project to follow EUROTRAC in 1996.

2.21

On the behaviour of tropospheric ozone in the European Arctic and at Antarctica

P. Taalas, J. Damski and E. Kyrö
Finnish Meteorological Institute, Finland

M. Ginzburg and V. Tafuri
Servicio Meteorológico Nacional, Argentina

Regular ozone soundings have been performed in Northern Finland, Sodankylä (67 °N) and at Antarctic Peninsula, Marambio (64 °S) since late 1988. Both stations are using Vaisala ground unit and ECC-sondes. The NO_x/HC emissions in the European Arctic are fairly low, but the area is lying in the downstream of other European and US emissions. Antarctica may be considered as more natural area with no major influences of man-made NO_x/HC compounds. The long- and short-term variability of tropospheric ozone at high latitudes of both hemispheres during 1988-93 has been studied. The tropospheric ozone content is fairly equal at both hemispheres during midwinter. Large interhemispheric differences are seen after the photochemical activation in spring. In the Arctic the partial pressures of ozone are 2-3 times higher than at Antarctica during spring and summer. The photochemical activation leads to a loss of ozone at Antarctica due to low NO_x concentration of the background air. Special anomalies related to chemical and dynamical factors have been analysed. 3-dimensional trajectories based on the ECMWF global analysis fields and local sounding observations of humidity, temperature, wind speed and direction have been used for the interpretation.

2.22

AIRBORNE MEASUREMENTS AND ANALYSIS OF ATMOSPHERIC COMPOSITION OVER SIBERIA.

G. Inoue, K. Izumi, T. Machida, S. Maksyutov, S. Mitsumoto¹, Y. Tohjima²,
Y. Kopylov, A. Postnov, N. Vinnichenko and V. Khattatov³

¹National Institute for Environmental Studies, Tsukuba, Japan

²Faculty of Science, Tokyo University, Tokyo, Japan

³Central Aerological Observatory, Dolgoprudny, Russia

Because of scarcity of direct measurements of greenhouse gas concentrations and their emission rates over Siberia, it was difficult to constrain emission and sink estimates for that area by observational data. Airborne observations of ozone, methane, carbon dioxide performed over Siberia in 1992-1993 provided first mid-tropospheric composition data available for that area. In 1993 several large scale dynamic events were observed which transport air masses up from the surface layer and down from stratosphere. Those large scale vertical transport events are related to the interface between low and high pressure systems. CO and H₂ concentrations, measured with a gas chromatography system, are affected by sink processes at the stratosphere (CO) and the land surface (H₂). Stratospheric ozone intrusion event was observed and simulated with a global tracer transport model. Stratospheric air characterized with low humidity and high ozone concentration was observed in many occasions. Multiple vertical concentration profile observations were obtained which are useful for estimation of vertical mixing and the surface source/sink rates.

2.23

Variations of lower tropospheric ozone at Syowa Station, Antarctica

S. Aoki and T. Yamanouchi
National Institute of Polar Research, Japan

Continuous measurement of the lower tropospheric ozone have been made at Syowa Station, Antarctica since February 1988. The diurnal variation of the lower tropospheric ozone was observable only for the austral spring and the variation could not be seen in the other seasons. The average amplitude of the diurnal variation reached a maximum value of about 2 ppb at most on September and October. The maximum and minimum concentrations of the diurnal variations appeared before sun rise and afternoon, respectively. The daily mean ozone concentrations showed a clear seasonal cycle with maximum concentration in winter and minimum concentration in summer and the mean amplitude of about 20 ppb. Minimum concentrations of the seasonal cycle were almost the same for each year but maximum concentrations were variable from year to year; higher concentrations appeared in 1988 and 1990 and lower concentrations appeared in 1989, 1991 and 1992. These variations might be ascribed to changes of atmospheric circulation in the Antarctic. It was found that extremely low values of lower tropospheric ozone with periods of a few days appeared sporadically between August and October every year. The ozone destruction phenomenon should be related to the photochemical process of the antarctic atmosphere.

2.24

Distributions and patterns of organic trace gases: is there evidence for an impact of reactions with chlorine atoms in the troposphere?

J. Rudolph, R. Koppmann and Ch. Plass - Dülmer
Institut für Atmosphärische Chemie, Forschungszentrum Jülich, 52425 Jülich, Germany

Presently there are speculations that reactions with Cl atoms may significantly contribute to the turnover of organic compounds in the marine atmosphere. One of the arguments is based on changes in the pattern of nonmethane hydrocarbon concentrations in the remote troposphere which cannot be explained by reactions with OH radicals only. We made several series of measurements of a broad range of organic trace gases during a ship cruise in the Mediterranean Sea and the North Atlantic. These data are analyzed for Cl reaction induced changes in the concentration patterns. No significant evidence for a Cl reaction induced removal of organic trace gases could be found.

Another possibility to look for the impact of Cl atoms on the removal of organic trace gases in the troposphere is to study the budgets of compounds which react with Cl atoms much faster than with OH radicals. The rate constants for the ethane and tetrachloro ethene reaction with Cl are by more than a factor of 200 higher than those with OH radicals. From several series of measurements in the remote troposphere we derived an estimate of their tropospheric concentration distributions and seasonal cycles. Together with OH fields from model calculations we can calculate their tropospheric removal by OH radicals. Within the uncertainties the calculated removal agrees with the known emissions of these substances. In spite of the substantial uncertainties of these budgets, the relatively high reactivity of these substances towards Cl atoms allows to estimate upper limits for the average tropospheric Cl atom concentration.

2.25

ANALYSIS OF SEVEN YEARS OF CONTINUOUS OBSERVATIONS OF PEROXYACETYL NITRATE (PAN) AT THE HIGH ARCTIC STATION ALERT

Jan W. Bottenheim, Leonard A. Barrie and Alain Sirois
Atmospheric Environment Service, Downsview, Ontario, Canada

Substantial buildup of pollutants from anthropogenic origin occurs during the winter in the arctic troposphere. For the case of nitrogen oxides (NO_y) it has been documented that PAN is the main constituent, with spring maxima as high as 600 pptv. An arctic reservoir of ozone precursors (NO_y and hydrocarbons) might make an important contribution to the spring maximum of ozone in the northern hemispheric troposphere. To evaluate the magnitude of the arctic NO_y reservoir a program of continuous observations of PAN at the Canadian high Arctic station Alert was initiated in late 1986, and we report on the results to date. Long term and seasonal trends are investigated, and covariances with other chemical data explored. It is found that PAN is highly correlated with sulphate aerosol in contrast to nitrate aerosol or ozone. Using multivariate statistics it is confirmed that most PAN originates from anthropogenic sources in mid latitude regions. The question whether this arctic PAN has an impact on mid latitude regions is addressed by comparing incidental observations at rural sites in Canada during the late winter/early spring with the Alert data.

2.26

Oceanic Emissions of Non-Methane Hydrocarbons (NMHC)

W.J. Broadgate, P.S. Liss and S.A. Penkett
University of East Anglia, Norwich, NR4 7TJ, U.K.

NMHC influence the oxidising capacity of the troposphere via reaction with O_3 and NO_3 and OH radicals. The oceanic source of NMHC is potentially a significant proportion of natural global emissions due to the large surface area of the ocean. Recent measurements suggest that the ocean is supersaturated in NMHC with respect to the atmosphere. However measurements of emissions are poorly documented and there is little spatial and temporal resolution with considerable variability in concentrations. In this study measurements of C_2 - C_8 NMHC were carried out in seawater and the atmosphere from the Southern Ocean (50°S - 70°S ; 53° - 88°W) during a cruise on the *RRS Discovery* in November/December 1992. In contrast to this, emissions of NMHC from the North Sea are shown over a full seasonal cycle.

2.27

The Oceanic Flux of Carbon Monoxide to the Atmosphere

Timothy S. Bates, Kimberly C. Kelly and James E. Johnson
NOAA, Pacific Marine Environmental Laboratory, Seattle, WA, USA

Carbon monoxide (CO) is photochemically produced in the surface ocean and emitted to the atmosphere. To assess the magnitude of this ocean-atmosphere flux, eight cruises were conducted by PMEL throughout the Pacific Ocean from 1987-1993. During this seven year period over 7000 CO measurements were made in surface seawater and the overlying atmosphere. These data will be used to reassess the seasonal, regional and global oceanic CO flux to the atmosphere.

2.28

Acetone in the global troposphere: Its possible role as a global source of PAN

H. B. Singh¹ and M. Kanakidou²

1. NASA Ames Research Center, Moffett Field, CA 94035, USA

2. Centre des Faibles Radioactivites, F-91198 Gif sur Yvette Cedex, France

Oxygenated hydrocarbons are thought to be important components of the atmosphere but, with the exception of formaldehyde, very little about their distribution and fate is known. Aircraft measurements of acetone (CH_3COCH_3), PAN ($\text{CH}_3\text{CO}_3\text{NO}_2$) and other organic species (e. g. acetaldehyde, methanol and ethanol) have been performed over the Pacific, the southern Atlantic, and the subarctic atmospheres. Sampled areas extended from 0 to 12 km altitude over latitudes of 70°N to 40°S. All measurements are based on real time in-situ analysis of cryogenically preconcentrated air samples. Substantial concentrations of these oxygenated species (10-2000 ppt) have been observed at all altitudes and geographical locations in the troposphere. Important sources include, emissions from biomass burning, plant and vegetation, secondary oxidation of primary nonmethane hydrocarbons, and man-made emissions. Direct measurements within smoke plumes have been used to estimate the biomass burning source. Photochemistry studies are used to suggest that acetone could provide a major source of peroxyacetyl radicals in the atmosphere and play an important role in sequestering reactive nitrogen. Model calculations show that acetone photolysis contributes significantly to PAN formation in the middle and upper troposphere.

2.29

NET FLUXES OF NITROGEN OXIDES (NO_x) FROM A MANAGED TROPICAL SAVANNA.

A. Rondón¹, C. Johansson² and E. Sanhueza¹.

1. IVIC, Atmospheric Chemistry Lab., Apartado 21827, Caracas 1020-A, Venezuela.
2. Department of Meteorology, Stockholm University, S-106 91 Stockholm, Sweden.

Nitrogen oxides are important in the photochemistry of the tropical atmosphere. Some efforts have been made to evaluate the strength of soils as source of nitrogen oxides in this region. However, much less is known about the dry deposition of these oxides to soil and vegetation. In this study, net fluxes of nitrogen oxides ($\text{NO}_x = \text{NO} + \text{NO}_2$) and ozone were measured in a grassland savanna site in Venezuela using the aerodynamic method. Simultaneous measurements of NO , NO_2 , O_3 , water vapor, wind speed and temperature were made at four different heights above the surface, at the edge of a grassland area with ~ 200 m of fetch. NO emissions were also measured using a closed chamber technique. The rate of emission of NO strongly depends on the soil moisture, ranging from 0.1 to 15 $\text{ng N m}^{-2} \text{ s}^{-1}$. NO fluxes derived from the aerodynamic and chamber methods are compared. From the emission of NO and the dry deposition of NO_2 , a small net flux of NO_x to the atmosphere is calculated for this savanna ecosystem.

3.02

Interaction between the sulphur and nitrogen cycles in the atmosphere and across the sea surface

P.S. Liss

School of Environmental Sciences, University of East Anglia, Norwich, U.K.

The reduced forms of the elements sulphur (largely dimethyl sulphide-DMS) and nitrogen (NH_3 and methylamines) play important roles in controlling the acidity and climatology of the atmosphere. The cycling of these elements between the oceans and atmosphere has previously often been studied element by element. However, recent work (Liss and Galloway, 1993, In: *Interactions of C, N, P and S Biogeochemical Cycles and Global Change*, Ed. R. Wollast et al., Springer, Berlin, 259-281) has shown that there is considerable evidence for interaction between the cycles. For example, in atmospheric aerosol and rain samples collected away from terrestrial sources, nitrogen and sulphur occur in a molar ratio which generally ranges between 1:1 and 2:1, and further this is approximately the ratio with which the precursor compounds (DMS and NH_3) are emitted from seawater. This implies a rather tight linkage of the elements between the ocean and atmosphere, without the need to invoke land sources. In this presentation the evidence for such coupling between the sulphur and nitrogen cycles will be assessed and possible reasons for it discussed.

3.03

N Mobilization in China and the United States: Past, Present and Future

J. N. Galloway
Environmental Sciences Department
University of Virginia
Charlottesville VA, United States

Zhao Dianwu
Eco-Environmental Sciences Center
Academia Sinica
Beijing, China

Globally, the anthropogenic processes of combustion, fertilizer production and legume cultivation convert nitrogen from unreactive N_2 to reactive N species [e.g., NO_x , NH_3] at about 150 Tg N yr^{-1} compared to the natural biological fixation rate of 140 Tg N yr^{-1} . The amount of N fixed by human activities has grown with time because of increases in population and level of development. This paper tracks the time course of N mobilization for two countries, China and the United States from 1950 to 1990 and makes a prediction for 2020.

In 1950, the most significant process mobilizing N in both countries was combustion of fossil fuels in the USA [about 4 Tg N]. In 1990 it was fertilizer consumption in China [about 18 Tg N]; the second largest rate was fertilizer consumption in the US [about 8 Tg N]. By 2020, it is predicted that fertilizer consumption in China will grow to >50 Tg N, far exceeding other sources of reactive N in both countries.

More than 50% of the N mobilized by human activities is emitted to the atmosphere, resulting in extensive dispersal within and downwind of both countries. In addition, much of the anthropogenic N accumulates in the environment. This increasing reservoir of reactive N contributes to regional and global environmental change [e.g., oxidizing capacity of the atmosphere, ecosystem productivity, acid deposition, greenhouse effect].

3.04

Effects of land use changes in NO fluxes from savannah soils

A. Rondón, E. Sanhueza, L. Cárdenas and J. Romero
Atm. Chem Lab., IVIC, Caracas, Venezuela

NO fluxes were measured from natural and managed savannah grasslands, and cultivated soils in Venezuela. Measurements were made using a closed chamber technique and a chemiluminescence analyzer. No significant differences were observed from natural and managed savannah grassland; soil emissions strongly depend on soil nitrate and moisture, and very weakly on soil ammonium and temperature. Higher emissions were observed from cultivated soils; soil plowing increases surface area and transport within the soil promoting NO emissions to the atmosphere. Very different emissions were observed in two different years. During the period May-July 1991 the average emission from cultivated soils was 50 ngN/m²s (~6 times higher than non cultivated soils), whereas during the same period in 1992 the average emission was only ~1 ngN/m²s (~4 times higher than the uncultivated grassland); the main cause of the difference between this two growing seasons was due to the fact that 1992 was a very rainy year and the gravimetric soil moisture was most of the time >12%, conditions where NO emissions are strongly inhibited from these soils.

3.05

Soil Nitrogen Oxide Emissions From a Fertilized Palm Plantation in Costa Rica

Michael Keller
USDA Forest Service, Rio Piedras, Puerto Rico

Previous studies estimate that nitrogen fertilizer additions to agricultural soils lead to emissions of about 1 Tg of N₂O-N annually. However, published studies concentrate on temperate zone agriculture mainly in North America and Europe. Our work in the Atlantic Lowlands of Costa Rica, suggests that N₂O emissions from tropical agriculture may greatly exceed their temperate zone counterparts. We used chamber techniques to measure field fluxes of N₂O and NO emissions. Semi-permanent sampling sites were located on sandy loam and clay textured soils supporting a crop of peach-palm (*Bactris gasipaes*) grown for palm heart. Ammonium nitrate fertilizer (200 kg-N ha⁻¹ yr⁻¹) was manually broadcast in 6 bimonthly applications. We sampled emissions over a one-year period from several sites at a range of time scales. We found large emissions associated with fertilization events. Soil-atmosphere fluxes generally peaked within the first week following fertilizer additions. Peak emissions for N₂O and NO exceeded 250 and 50 ng-N cm⁻² h⁻¹ respectively. NO emissions generally remained above background levels for approximately a week following fertilization. N₂O emissions remained elevated for periods approaching one month. In several cases, the combination of large emissions and long periods of elevated flux result in calculated yields of N₂O from added fertilizer N of greater than 10%. Similarities between this site and others suggests that large nitrogen oxide emissions may be common at tropical agricultural sites.

3.06

A 3D model study of the global sulfur cycle : relative contributions of anthropogenic and biogenic sources

M. Pham¹, J.F Müller², G. P. Brasseur³, C. Granier³ and G. Mégie¹

¹ Service d'Aéronomie, Paris, FRANCE

² Institut d'Aéronomie Spatiale, Bruzelles, BELGIUM

³ National Center for Atmospheric Research, Boulder, U.S.A

Sulfur compounds play a major role in the atmosphere. Besides their direct impact on the environment, they influence the budget of both tropospheric and stratospheric ozone and have an impact on the climate through the formation of aerosols and the backscattering of solar radiation. Eight sulfur compounds (DMS, SO₂, SO₄²⁻, COS, DMSO, MSA, H₂S and CS₂) have been investigated in the 3D tropospheric chemistry-transport model IMAGES (Intermediate Model for the Annual and Global Evolution of Species). Results for preindustrial and industrial cases will be presented in terms of sulfur deposition, global sulfate aerosol distribution, and climate forcing. Comparisons with measurements show a broad consistency between model concentrations and observations. The calculations show an increase of more than two orders of magnitude for sulfur dioxide concentrations in some parts of the northern hemisphere since preindustrial times. Distributions for biogenic compounds have also been modified because of the changes in the oxidizing capacity of the atmosphere. Over the most polluted areas moreover, the increase in sulfates deposition has reached a factor of 30.

3.07 Simulation of the Tropospheric Sulfur Cycle in a Global Climate Model

J. Feichter

Max-Planck-Institute for Meteorology, Hamburg, Germany.

E. Kjellström and H. Rodhe

Department of Meteorology, Stockholm University, Sweden.

J. Lelieveld

Department of Air Quality, Agricultural University of Wageningen, Netherland.

The tropospheric part of the atmospheric sulfur cycle has been simulated in a global, three-dimensional GCM (Hamburg climate model ECHAM). The principal goal of modeling the sulfate aerosols as a function of precursor concentrations by means of a climate model is to get a better understanding of the sensitivity of the climate system due to changes in the aerosol distribution. The model calculates on-line with the meteorology the emission, transport, chemistry and deposition processes for the three sulfur compounds: Dimethylsulfide (DMS), sulfur dioxide (SO₂) and sulfate. The chemistry part considers the gas-phase reactions of DMS and SO₂ with the OH-radical and aqueous-phase reactions in liquid water clouds -the liquid water of clouds is a prognostic variable of the model- with H₂O₂ and O₃. In-cloud and below-cloud scavenging is parameterized using the model calculated precipitation rates. The scheme was evaluated by comparison of calculated and observed concentrations of sulfur species in the atmosphere and in precipitation. The approach used for the parameterization of chemistry and wet scavenging and some results of the comparison with observations will be presented. A comparison is also made with previous simulations using a simpler, climatological, model (MOGUNTIA).

3.08

Aerosol nitrate and sulfate concentrations over the North Atlantic: estimates of anthropogenic contributions.

J.M. Prospero¹, D.L. Savoie¹, R. Arimoto², R.A. Duce³,

¹University of Miami, Miami, FL, ²University of Rhode Island, Narragansett, RI
³Texas A & M University, College Station, TX

Aerosol nss-SO₄⁼ and NO₃⁻ have been continuously measured over the North Atlantic from 1989 as a part of the Atmosphere/Ocean Chemistry Experiment (AEROCE). Measurements are made in the marine boundary layer at Barbados, Bermuda and Mace Head, Ireland; and in the free troposphere at Tenerife, Canary Islands. The annual mean concentrations for 1989-1993 at these stations are, respectively (in µg m⁻³): NO₃⁻ - 0.53, 1.06, 1.49, and 0.77; nss-SO₄⁼ - 0.78, 2.19, 2.03 and 0.92. Mean NO₃⁻ concentrations are 5-17 times higher than those measured in the remote central South Pacific; nss-SO₄⁼ values are 2-7 times higher. Based on the concentration of MSA (a surrogate for oceanic DMS) and Sb (a tracer for pollution) we estimate that anthropogenic sources account for 50% of the total nss-SO₄⁼ at Barbados, 70% at Bermuda, and 85-90% at Mace Head. Our measured concentrations of nss-SO₄⁼ aerosols equal or exceed those used in models (Charlson et al., 1992; Langner and Rodhe, 1991) that suggest that anthropogenic aerosols have a significant cooling effect on climate in the Northern Hemisphere.

3.09

Quantification of DMS oxidation products in the North Atlantic marine air.

S. Rapsomanikis and M. O. Andreae

Biogeochemistry Department, Max Planck Institute of Chemistry,
P.O. Box 3060, 55020 Mainz, Germany.

Dimethyl sulphide (DMS) is ubiquitous in the marine environment and is the main sulphur compound that is emitted to the atmosphere from the oceans. In the remote and unpolluted areas, it is the main source of methane sulphonic acid (MSA) and non sea sulphate (NSS). These two oxidation products of DMS, contribute to marine aerosol number concentrations and may play a role in new cloud formation and hence global cloud albedo. Indirectly, DMS may affect the earth's climate leading to a climatic cooling [Charlson et al., 1987]. However, a number of questions remain unanswered about the quantification of the cycle that leads to cloud condensation nuclei. For example, given an atmospheric DMS concentration, in clean marine air, the proportion that is converted to SO₂, MSA and NSS, condensation nuclei (CN) and cloud condensation nuclei (CCN) needs to be quantified.

We utilise the research station at the west coast of Ireland, Mace Head, where "clean marine air" originates from the North Atlantic, at certain times of the year and with westerly winds. All the above parameters are measured together with a number of meteorological parameters. Results of the long term sampling will be presented.

3.10

Sulfur Dioxide, Dimethyl Sulfoxide and Dimethyl Sulfone
Formation from Dimethyl Sulfide Oxidation

Alan R. Bandy, Donald C. Thornton and Byron W. Blomquist
Chemistry Department
Drexel University
Philadelphia, PA 19104

A study of the chemistry of atmospheric dimethyl sulfide was conducted on the island of Kirabati (Christmas Island). Measurements of sulfur dioxide, dimethyl sulfide, dimethylsulfoxide, and dimethyl sulfone were made with a frequency of one sample per 15 minutes to obtain highly resolved diurnal variations. Measurements of non-sea salt sulfate and methane sulfonate (Barry Huebert, University of Hawaii) and studies of condensation nuclei (Tony Clarke, University of Hawaii) are reported in companion papers. This paper will discuss the efficiency of the formation of sulfur dioxide, dimethyl sulfoxide and dimethylsulfone from the oxidation of dimethyl sulfide. Also discussed will be the rate of loss of these species to aerosol and the ocean surface.

3.11

Uncertainty and sensitivity analyses of the mechanism of atmospheric oxidation
of DMS

J. Hjorth and A. Saltelli

Commission of the European Communities, Environment Institute, JRC, Ispra, Italy

The main oxidation pathway for DMS in the atmosphere is generally believed to be initiated by the reaction with the OH radical. Based on the available experimental studies of the reactions involved in this oxidation process and the hypotheses about the main reaction pathways that have been presented in the literature, a chemical reaction scheme has been set up. An uncertainty and sensitivity analysis of the kinetic model represented by this reaction scheme has then been carried out to identify the uncertainties (on reaction rate constants as well as concentrations of chemical species) that most significantly contribute to the overall uncertainty on selected output parameters of the model. This analysis thus serves to help identifying the parameters which it would be most relevant to study in order to reach an adequate understanding of the atmospheric chemistry of DMS.

The rate constants and concentrations of trace gases involved in the model have been assigned uncertainty ranges reflecting the level of our present knowledge about them. Particular emphasis has been put on an analysis of the various possible pathways to formation of H₂SO₄ and SO₂ including the possibility of a direct pathway from DMS to H₂SO₄, not involving SO₂ as an intermediate.

3.12

Regional background acidity and chemical composition of precipitation in Thailand

L. Granat¹, K. Suksomsankh², S. Simachaya², M. Tabucanon² and H. Rodhe¹

¹Department of Meteorology, Stockholm University, Sweden

²Environmental Research and Training Center, Bangkok, Thailand (ERTC)

In a joint Thai-Swedish project within the framework of the IGAC/DEBITS/CAAP project, precipitation has been collected for chemical analysis on a daily basis since mid 1991 at two sites in the countryside in Thailand. The quality assurance plan includes investigation of the effect of different sampling equipment (including wet-only collectors), sampling time and stability of samples collected in tropical conditions. Consistent results, not biased by local conditions, have been obtained.

The data show striking day-to-day fluctuations, reflecting changes in transport direction and an inhomogenous atmosphere. Mean concentrations are similar at the two stations but correlation between daily samples is low as can be expected for a distance of 500 km. A seasonal variation could not yet be significantly determined. The best correlation between components is found for NH₄ - SO₄ and mutually between Na, Mg and Ca. Absence of correlation between Ca and SO₄ suggests that SO₄ is not soil derived. The samples are generally slightly acidic (H⁺:10 µeq/l) which, stoichiometrically, can be explained as an imbalance between acidifying components in modest to low concentration (SO₄: 20, NO₃:8 µeq/l) and neutralizing components in somewhat lower concentration (NH₄:11 and "alkaline dust" including K:2, Mg:3 and Ca:10 µeq/l). Additional (dry) deposition can be inferred from aerosol and gas phase measurements at one of the sites. Preliminary model calculations of the dispersion and deposition of sulfur compounds in the S-E Asia region will also be presented and compared to the observed data.

3.13

Airborne Measurements of SO₂ in Marine Atmosphere between Asian Continent and Japan

S. Hatakeyama, K. Murano, H. Mukai, and H. Akimoto †

Division of Global Environment, National Institute for Environmental Studies

† Research Center for Advanced Science and Technology, The University of Tokyo

East Asian area is one of the biggest region in the world of the anthropogenic emission of NO_x and SO₂. On account of population growth and rapid development of industrial activity, this area is anticipated to become the largest source area of NO_x and SO₂ in the world in the 21st century. In order to avoid such a situation, it is necessary to analyze the present status of air pollution over East Asian and Western Pacific region, to evaluate the amount of anthropogenic emissions, to predict accurately the future situation by use of computer models, and to apply these results to work out a countermeasure. For this purpose we have started aircraft observation of atmospheric pollutants named IGAC/APARE/PEACAMPOT Survey from 1991. In November 8-12, 1992 we surveyed over East China Sea as well as Sea of Japan at 4 altitudes and observed a high concentration of SO₂ over Sea of Japan between Korea and Oki islands, Japan. Results of 1994 March survey mission will also be presented.

3.14

Severe influence of the increasing sulfate aerosols on summer climate of the east China

Xu Qun

Jiangsu Meteorological Institute, Nanjing 210008, China

Summer climate of the east China has experienced a notable change since 1980, the high summer monsoon rainy belt has moved abnormally southward with persistent droughts occurring in the north China and more floods in the mid-lower Yangtze through recent 14 years (1980-1993), which is actually an unique phenomenon since AD 950. This change may be caused by a significant downward trend of solar radiation in China, the total downward ranges of the direct solar radiation and global radiation of clear skies in China (data of 9 stations) for recent thirty winters (1959-1988) have reached to 20.9% and 12.7% respectively. A dominant role of this reduction in S has been played by the large amounts of discharged SO₂, which had reached to 202×10⁵t in year 1992 mainly occurred in the industrialized east China with area of about 39×10⁵km² only, it means the annual mean column burden of SO₄ in the east China has reached to 21mg/m². Hence this source of anthropogenic sulfate aerosols may be the largest of our globe. We should take vigilance to the fact that this high concentration of sulfate aerosols will still increase at an annual rate of 5% resulting severe influence on our summer climate not only in the east China, but of global scale.

3.15

Relation in concentration of DMS between surface seawater and air in the temperate North Pacific region

S. WATANABE, H. YAMAMOTO and S. TSUNOGAI

Department of Chemistry, Faculty of Fisheries, Hokkaido University, Hakodate 041, JAPAN

The concentrations of DMS in the surface seawater and in the air were measured at the same time during a cruise across the North Pacific around 40°N in August 1988. Those in the surface seawater ranged widely from 44 to 542 ngS/l (n=37) with a mean value of 189 ngS/l and those in the air ranged more widely from 4 to 694 ngS/m³ (n=23) with a mean value of 176 ngS/m³. The relation in the concentration between the surface seawater and the air, however, was fairly well. The linear correlation was analyzed with a simple model introducing an assumption that the atmospheric DMS released from sea surface was oxidized with a first order photochemical reaction induced by OH radicals in the air. The rate constant for the oxidation or the turnover time of the atmospheric DMS were obtained to be 1.4 × 10⁻⁵ sec⁻¹ or 1.0 day with an uncertainty of 50% or more.

3.16

The sulfur cycle in the high Arctic summer - An overview of the Atmospheric Research Program of the International Arctic Ocean Expedition 1991 (IAOE-91).

Caroline Leck, E. Keith Bigg, Cecilia Persson, E. Douglas Nilsson, David C. Covert, Jost Heintzenberg, and Alfred Wiedensohler.
Department of Meteorology, Stockholm University, Sweden

The remote marine boundary layer of the summer Arctic provides a unique environment for interdisciplinary studies aimed at quantifying the chemical and physical processes that control the evolution and properties of the aerosol relevant to radiation fluxes and forcing of climate. The summer high Arctic not only provides an opportunity to determine the chemical, physical and optical properties of the natural aerosol system, but also establish a background against which to quantify any anthropogenic perturbation.

Measurements during IAOE-91 showed a seasonal variation with highest values for all gas-aerosol parameters in August and lowest values in October. The seasonal variations are consistent with previous studies in the Southern Hemisphere. The interchange of air between the surface mixed layer and the stable cloud layer, related to low level jets, dominated the short-duration (~1 hour) changes in sub micron aerosol number concentration and thus had a strong influence on the chemical and physical processes that control the properties of the aerosol. This mixing process deserves more attention in future work. Overall, non-linear relationships were found between atmospheric DMS (dimethyl sulfide) and CN/CCN (cloud nuclei/cloud condensation nuclei). However, the relation was linear for a relatively narrow range of low DMS concentrations. This paper will give an overview of the essential findings related to the formation, growth and fate of the DMS-derived aerosol particles produced within the Arctic region.

3.17

Ice age Antarctic sulfate revisited

R.J. Delmas
Laboratoire de Glaciologie et Géophysique de l'Environnement, CNRS, France

Atmospheric sulfate particles play a specific and significant role in the troposphere as cloud condensation nuclei. However, the link between marine sulfate (derived mostly from gaseous dimethylsulfide, DMS, produced by marine biogenic activity) and the climate is still not very well understood and modelled.

The Vostok ice core has documented decisively the atmospheric sulfate and MSA (methanesulfonic acid) concentrations at high southern latitudes over the last ice age. It was concluded from the data that the source of biogenic sulfur was more intense in glacial than in interglacial climatic conditions (Legrand et al., 1988). On this basis, speculations have been made about the interplay between atmospheric sulfate and global climate.

In this paper, an alternative interpretation of the Vostok sulfate and MSA profiles is proposed which leads to the conclusion that the strength of the marine DMS source, as estimated from ice data, probably did not change significantly during the studied period of time. The SO_4 and MSA variations that were observed can be better explained by atmospheric chemistry processes rather than by marine productivity changes.

4.02

Vertical profiles and the microphysics, chemistry and optical properties of aerosol in the marine troposphere

A. D. Clarke, J. N. Porter, F. Valero and P. Pilewskie
Department of Oceanography, University of Hawaii, Hawaii
NASA Ames Research Center, California

The potential climatic effects (radiative forcing) by aerosol as well as their influence upon the retrieval of radiances observed from satellite are topics of current and related interest (Penner et al., 1993). The relative influence of anthropogenic and natural sulfates, windblown dusts, sea-salt etc. upon column optical properties are important to understand if progress is to be made in resolving uncertainties associated with these effects. We have utilized a variety of rapid and size-resolved aerosol measurements and thermal volatility in order to characterize these properties in marine regions. These data and the resultant equilibrium size change in response to changes in relative humidity are used to establish closure between observed aerosol properties and measured radiative effects. Vertical profiles over both the Atlantic and Pacific Oceans will be presented to illustrate and characterize the aerosol properties and their diverse contributions to aerosol optical extinction in these regions.

4.03

The seasonal variation in size distribution of aerosol in the Oki Islands, Japan

H. Wakuri, M. Nakao, F. Tanaka, T. Tatano, K. Yamaguchi
Shimane Prefectural Institute of Public Health and Environmental Science, Japan
and H. Hara
The Institute of Public Health, Japan

The particle-size distribution and the concentration of major ionic components were measured in the Oki Islands located in Japan Sea, ca. 60 km north of the prefectural capital, in order to elucidate the seasonal variation of the distribution and concentration levels. Aerosol samples were collected by using an 8-staged Andersen impactor during the following periods covering the four seasons: Jan. 18 - Feb. 8, 1991 (winter), Sept. 3 - 23, 1991 (fall), Mar. 30 - Apr. 27, 1992 (spring) and June 30 - Aug. 4, 1993 (summer). The distribution showed commonly reported bimodal nature with a minimum at 1 - 2 μm in the four cases. Non-seasalt sulfate and ammonium ions comprised a predominant portion of fine particles (20 - 50 %, 4 - 14 for mass) whereas coarse particles consisted of sodium and chloride ions (5 - 23, 6 - 36). Non-seasalt sulfate concentration was suppressed in summer (1.8 $\mu\text{g}\cdot\text{m}^{-3}$) compared with those for the other seasons: 4.6, 4.5 and 3.9 $\mu\text{g}\cdot\text{m}^{-3}$ for spring, fall and winter, respectively. These concentration levels were discussed in term of meteorology.

4.04

Aerosols over the Pacific Rim regions of East Asia

M. Yamato¹, S. Hatakeyama², K. Murano², H. Akimoto³, H. Bandow⁴,
K. Imai¹, I. Watanabe⁵, H. Tsuruta⁶, H. Mukai², S. Tanaka⁷,
H. Tanaka⁸, Y. Ishizaka⁹, and Y. Iwasaka⁹

¹Gunma University, ²National Institute for Environmental Studies,
³University of Tokyo, ⁴University of Osaka Prefecture, ⁵The Institute
of Public Health, ⁶National Institute of Agro-Environmental Sciences,
⁷Keio University, ⁸Nagoya University, Japan

Free tropospheric and boundary layer aerosols over the East China Sea, Yellow Sea and Japan Sea have been examined by aircrafts in the PEACAMPOT field campaign in October 1991 and November 1992 under the IGAC-APARE program. Particles were analyzed by vapor-deposited thin-film techniques in conjunction with electron microscope. H₂SO₄ particles were predominant in the unpolluted free troposphere. Mineral dust particles and black carbon (BC) particles were frequently transported from Asian continent via free troposphere. In the marine boundary layer at 0.5 km altitude, ammoniated sulfate particles are internally mixed with nitrate (NO₃⁻). The presence of nitrate in the marine boundary layer is well correlated with high NO_x mixing ratio measured by Hatakeyama and Bandow (1993). They seem to be transported from Asian industrial and urban regions.

4.05 Anthropogenic impact on number concentrations of cloud processed particles over the North-Atlantic

Rita Van Dingenen, Jens Hjorth, Torsten Gröne and Frank Raes
Commission of the European Communities, JRC Environment Institute, Ispra, Italy

The pronounced minimum round particle diameter 0.1 µm in the number size distribution (i.e. between nuclei mode and accumulation mode) of remote marine aerosol has been explained by Hoppel (1990) as due to cloud processing of those particles that are larger than the critical size for cloud nucleation. Hence, identifying the accumulation mode (AM) with cloud processed particles, their properties can be studied relatively easily with size-discriminating instruments.

We investigated correlations between the number concentration in the AM on the one hand and tracers for biogenic (methanesulphonate [MSA], dimethylsulphide [DMS]) and anthropogenic (black carbon) activity on the other hand, during a cruise between Halifax and the Moroccan coast and back in September - October 1992. Our analysis shows that the AM concentration is much better correlated with black carbon and with non-sea-salt sulphate than with MSA. No correlation was obtained between AM concentration and DMS in sea water and in the air. This suggests that long range transport of anthropogenic pollution, coming from Europe and the American continent, has affected cloud condensation nuclei populations over the North Atlantic.

4.06

The aerosol - wind inter-relationship and sea-salt particles over the Southern Ocean

J.L. Gras
Division of Atmospheric Research, CSIRO, Australia.

Covariance between methanesulphonate (MSA) and cloud condensation nucleus (CCN) concentrations in seasonally averaged data was reported for Cape Grim by Ayers and Gras (1991). This showed a linear relationship within a limited range of MSA concentrations but a relatively important CCN offset that is observed when MSA concentrations approach zero. A similar relationship exists between dimethylsulphide (DMS) and CCN concentrations. Wind generated sea-salt is a probable major source for these "offset" particles and this component needs to be understood to determine the full climatic importance of remote marine particles. Indeed, Latham and Smith (1990) have proposed that such wind-produced CCN may play a more important climatic role than previously recognised. The relationships between wind-strength CN, CCN and size-resolved aerosol concentrations have been examined in Southern Ocean air at Cape Grim (41 °S) and Macquarie Island (54 °S). These show the presence of a systematic signal that can be attributed to wind-produced sea-salt particles. However, this work also shows a complexity of the relationships between aerosol components and meteorology that reinforces the need for caution in simple predictions of climate change effects.

4.07

Diurnal variation of marine boundary-layer sulfate and MSA:
How much DMS is converted to sulfate?

B. Huebert, L. Zhuang, and D. Wylie
Department of Oceanography, University of Hawaii, Honolulu, HI 96822 USA

A. Bandy, B. Blomquist, and T. Wade
Department of Chemistry, Drexel University, Philadelphia, PA 19104 USA

Modeling the climatic importance of changes in DMS emissions requires an estimate of the fraction of DMS which is ultimately oxidized to non-sea salt sulfate (NSS). Many existing models assume a high efficiency conversion of DMS to SO₂, followed by competition between SO₂ dry deposition and both homogeneous and heterogeneous oxidation pathways to sulfate. The UH group measured the diurnal variation of NSS and MSA during July and August of 1994 at Christmas Island (2°N, 157°W), while the Drexel group measured DMS, SO₂, DMSO, and DMSO₂. A. Clarke measured aerosol properties vs size. We also used MOUDI impactors to observe the chemical size distribution and a sonic anemometer to estimate resistances to dry deposition. From the diurnal variations and estimates of dry deposition fluxes, we will make inferences about conversion efficiencies.

4.08

The relationship between MSA concentrations and temperature in marine (baseline) air at Cape Grim

A.L. Dick¹, G.P. Ayers², J. Ivey³ and P.M. Walford¹

¹ Cape Grim Baseline Air Pollution Station, Smithton, Tasmania, Australia

² Division of Atmospheric Research, CSIRO, Aspendale, Australia

³ Australian Government Analytical Laboratories, Kingston, Tasmania, Australia

If the postulated feedback mechanism by which marine biological activity might control tropospheric temperature does operate, then a relationship should exist between sea-surface temperature and emissions of reduced sulphur gases such as DMS (dimethyl sulphide) from marine organisms. Concentrations of aerosol MSA (methane sulphonate), a major oxidation product of DMS, have been measured at Cape Grim (41°S, 145°E) since 1978. This quantity may be used as a surrogate measure of DMS emissions. A continuous detailed record of air temperature at the site allows the separation of marine air temperatures from the 'baseline' sector, considered to be a proxy for sea-surface temperature in the region, from the overall averages which include all wind directions. After removal of the mean seasonal cycle for both variables, residual MSA concentrations are compared with the baseline air temperature 'anomalies' to test for correlation. An attempt is also made to examine other factors which might influence the relationship, such as wind speed, rainfall amount and air mass trajectories.

4.09 Scales of Temporal and Spatial Variability of Sulfate Column Burdens over the North Atlantic in October and November, 1986

C.M. Benkovitz, R. Wagener, S. Nemesure and S.E. Schwartz
Environmental Chemistry Division, Brookhaven National Laboratory, Upton, NY, USA

Anthropogenic sulfate aerosol is thought to enhance clear-sky and cloud albedo and thus influence climate (Twomey et al., 1984, 1977; Charlson et al., 1992). Indications of the enhancement of cloud albedo have been obtained using satellite data averaged monthly or annually over regions with extent of several thousand kilometers (Kim and Cess, 1993; Han et al., 1994). Here we report studies of the scales of temporal and spatial variability of the sulfate column burdens over an area of the central North Atlantic well away from anthropogenic sources during October and November, 1986 using an Eulerian transport and transformation model with fine temporal (6-h) and spatial (1.125°) resolution, driven by observation-derived meteorology. The 1/e-folding time characterizing the temporal variability averages 13 hours, with 95% of the values being 25 hours or less. Likewise, the characteristic distance of spatial autocorrelation for this region is short; the average is 1600 km, with 10th percentile value of 400 km and 90th percentile value of 1700 km. These results demonstrate the need for fine temporal and spatial resolution in the analysis of satellite data to discern influences of anthropogenic sulfate.

4.10

Airborne studies of aerosol emissions from savanna fires in southern Africa

M.O. Andreae, T.W. Andreae, P. le Canut, W. Elbert, G. Helas, F. Wienhold and T. Zenker
(Max Planck Institute for Chemistry, P.O. Box 3060, D-55020 Mainz, Germany)
H. Annegarn, F. Beer (University of Witwatersrand, Johannesburg, South Africa)
H. Cachier (University of Paris VII, Paris, France)
W. Maenhaut, I. Salma (University of Gent, Belgium)
R. Swap (University of Virginia, Charlottesville, Va, USA)

The emission of smoke aerosols from savanna fires was investigated during the SAFARI-92 experiment in southern Africa (South Africa, Namibia, Botswana, Zimbabwe, Zambia, Swaziland and Angola). The background aerosol over this region in the absence of fires was studied during the wet-season experiment SA'ARI-94. Particle number and volume distributions as a function of size were determined with a laser-optical particle counter, the black carbon content of the aerosol with a reflectance aethalometer. For the determination of its chemical composition, we collected aerosol on quartz glass filters and on stacked filter units, consisting of a prefilter for particles larger than ca. 1 µm and a Teflon second filter for the submicron fraction, and on cascade impactors. The samples were analyzed for soluble ionic components, organic carbon, and for trace elements.

We determined the emission ratios for aerosols (relative to CO₂ and CO) from fires in savanna, forest, and agricultural ecosystems by airborne sampling of fire plumes close to prescribed and incidental fires. We investigated the regional and large-scale distribution of pyrogenic and background aerosols on survey missions of several days duration through the entire study area, and on several shorter flights. In spite of an intensive drought, which had reduced the biomass available for burning in 1992, we found high levels of aerosols throughout southern Africa. Our results suggest that pyrogenic emissions had a pronounced influence on the chemical and optical properties of the troposphere in southern Africa during the study period.

4.11 Ionic, organic components and trace elements in background aerosols in the Amazon basin

P. Artaxo(*), F. Gerab(*), M.A. Yamasoe(*), J. V. Martins(*), A.H. Miguel (**), G. P. Ayers(***) , R. Gillet(***)
(*) Instituto de Física, (**) Instituto de Química, Universidade de São Paulo, Brazil,
(***) Division of Atmospheric Research, CSIRO, Australia.

Background atmospheric aerosol particles composition in the Amazon basin was studied in three sampling stations. Aerosols were collected continuously since July 1991 in three background stations in Cuiaba, Alta Floresta and Serra do Navio sampling sites. The natural biogenic as well as the anthropogenic biomass burning component was measured. Ion chromatography was used to measure K⁺, NH₄⁺, NO₃⁻, PO₄⁻, Cl⁻, SO₄⁻, Na⁺, Mg⁺, Ca⁺⁺, CH₃COO⁻, HCOO⁻ and C₂O₄⁻. Trace elements (Al, Si, P, S, Cl, K, Ca, Ti, V, Cr, Mn, Fe, Ni, Cu, Zn, Sr, Se, Zr, and Br) were measured by the PIXE technique. Soot carbon was determined using a reflectance technique. Fine and coarse aerosol mass concentration was also measured. Size distribution was measured using a MOUDI cascade impactor. More than 200 fine and coarse mode aerosol samples were collected for each sampling site. Multivariate statistical analysis differentiate three main aerosol components: The natural primary biogenic, the biomass burning and the soils dust component. For two of the sites there is a clear difference between the natural primary biogenic and the biomass burning components. Long range transport of biomass burning aerosol can be observed for the Serra do Navio sampling site.

4.12

The Role of Anthropogenic Sulfate in Climate Change*

Catherine C. Chuang, Joyce E. Penner, and Karl E. Taylor
Lawrence Livermore National Laboratory, U.S.A.

Anthropogenic sulfur emissions dominate over natural emissions by a factor of 2 on a global average. Photochemical reactions of these emitted sulfur compounds lead to a large increase in the concentration of sulfate over and around industrialized regions. Sulfate can scatter solar radiation, thereby, directly changing the planetary radiation budget. For the indirect effect, sulfate-containing aerosols modify the microphysics of clouds by acting as cloud condensation nuclei and enhancing the cloud reflectivity.

We couple a climate model with a 3-D global chemistry model to investigate the forcing by anthropogenic sulfate. The mass concentration of sulfate from fossil fuel combustion and biomass burning is calculated in the chemistry model and provided to the climate model where it affects the shortwave radiation. We also investigate the indirect effect, with cloud nucleation parameterized in terms of local aerosol number, sulfate mass concentration, and updraft velocity. Simulations show that the range of annual average anthropogenic sulfate forcing is between 0 and -5 W m^{-2} . We estimate that current concentrations of anthropogenic sulfate have direct and indirect effects that may be comparable in magnitude and at least locally will tend to mask the warming effects of increased greenhouse gases. Sensitivity tests to quantify uncertainties will be performed in a future study.

* Work performed under the auspices of the U.S. Department of Energy by the Lawrence Livermore National Laboratory under contract No. W-7405-Eng-48.

4.13

The Contribution of Sulfate Aerosol to Light Scattering Over the Pacific Ocean

P.K. Quinn, S. Marshall, V. Kapustin, D.S. Covert, and T.S. Bates
NOAA/Pacific Marine Environmental Laboratory, USA

The clear-sky climate forcing due to the backscattering of solar radiation by tropospheric aerosol is a function of the aerosol mass concentration, number size distribution, chemical composition, and particle shape. To assess the spatial and temporal variability of these parameters over the Central Pacific Ocean, measurements were made during two cruises along 140°W between 54°N and 70°S . The first cruise took place during the Austral fall of 1993 and the second during the Austral summer of 1993. Measurements were made of the number size distribution from 0.02 to $9.6 \mu\text{m}$, mass size distributions of non-seasalt sulfate, ammonium, and sodium from 0.08 to $4 \mu\text{m}$, and light scattering at 0.449 and $0.690 \mu\text{m}$. During the first cruise, aerosol scattering at $0.690 \mu\text{m}$ dominated that at $0.449 \mu\text{m}$ between 50°S and 10°N . Between 10°N and 40°N , however, scattering at $0.449 \mu\text{m}$ was greater than at $0.690 \mu\text{m}$. This difference was due to a changing chemical composition and number concentration as a function of size. A lower accumulation mode number concentration occurred in the southern hemisphere accompanied by a higher coarse mode number concentration. To determine seasonal variability, these data will be compared to those obtained during the second cruise. In addition, the results of a Mie calculation applied to the measured mass and number size distributions will be presented to indicate the contribution of non-seasalt sulfate and seasalt to light scattering and hemispheric backscattering.

4.14

Which Aerosol Particles Form Cloud Droplets?

A. Hallberg, K.J. Noone^a, J.A. Ogren^b
Department of Meteorology, Stockholm University, S-106 91 Stockholm (Sweden)

Ground-based simultaneous measurements of cloud droplet residual particles and interstitial particles in ambient clouds have allowed us to characterise these particles in terms of their physical and chemical nature. The size dependent partitioning of aerosol particles between interstitial air and cloud droplets was studied as a function of time. The partitioning curve was s-shaped with a plateau at larger particle sizes that did not reach unity. A small variation over several hours of the partitioning curve within a cloud event was observed. At particle sizes smaller than ca. $0.2 \mu\text{m}$ diameter a small fraction ($<10\%$) of the total number of particles at each size were found as residual particles indicating that only a "favoured few" of these particles formed cloud droplets. Among the residual particles however, 75% of the particles were smaller than $0.25 \mu\text{m}$ diameter. So, even though a small fraction of these particles formed cloud droplets they dominate the number of cloud droplets. Concurrent measurement showed that a substantial fraction of hygroscopic particles of the same size as those that formed cloud droplets remained in the interstitial air. Hypotheses are discussed as to why only a few hygroscopic particles formed cloud droplets, while many other hygroscopic particles of the same size did not.

Present affiliation:

^aCenter for Atmospheric Chemistry Studies, Graduate School of Oceanography, Narragansett, RI 02882-1197 (USA)

^bNOAA/CMDL/R/E/CG, 325 Broadway, Boulder, CO 80303-3328 (USA)

4.15

On the Possible Influence of Clouds on the Nitrogen Budget in the Remote Troposphere

Peter G. Hess, Siri Flocke, and Sasha Madronich

Atmospheric Chemistry Division,
National Center for Atmospheric Research, Boulder, CO USA

In this study we examine evidence for the influence of cloud processing on the nitrogen budget in the remote subtropical middle troposphere. The ratio of HNO_3 to NO_x has been measured at 3.4 km on the island of Hawaii from 2 May 1988 to 3 June 1988 as part of the Mauna Loa Observatory Photochemistry Experiment (MLOPEX). Clear sky model studies of the photochemical budget of nitrogen species indicate the ratio of HNO_3 to NO_x should be about 6 times larger than observed. To test the hypothesis that cloud processing may be an important sink for HNO_3 we have coupled backward trajectories from the Mauna Loa Observatory with cloud data from ISCCP (International Satellite Cloud Climatology Project). The length of time since the trajectory was last subjected to probable cloud processing is correlated with the ratio of HNO_3 to NO_x observed at Mauna Loa. The data suggest that nearly all trajectories have encountered clouds within a five-day period. The ratio of HNO_3 to NO_x tends to be high when the parcel trajectory has not recently encountered clouds. Low ratios are correlated with recent episodes of possible cloud processing.

- 4.16 On the influence of gas to particle conversion on the modal size distribution of atmospheric particles.

HC Hansson^{1,2}, B. Martinsson¹, B. Svenningsson¹, E. Swietlicki¹
A. Wiedensohler³ and D. Covert⁴

¹Department of Nuclear Physics, University of Lund, Lund, Sweden

²Department of Meteorology, University of Stockholm, Stockholm, Sweden

³Institute of Tropospheric Research, Leipzig, Germany

⁴Department of Atmospheric Sciences, University of Washington, Seattle, USA

Atmospheric particle number distributions with high size resolution obtained with Differential Mobility Analyzers (DMA) has started to appear in literature. We also have obtained numerous particle size distributions in several extensive field campaigns in Europe. Close examination of this data shows consistently that the number size distribution is actually comprised of two, approximately log normal, modes in the accumulation size range, i.e. with geometric mean diameters between 40 and 200 nm. Very recent measurements down to 3 nm show that at times a third mode of ultrafine particles less than 25 nm in diameter exists simultaneously with the two larger modes. We will present available measurements and give indices for particle growth mechanisms that support the hypothesis that the observed size distribution is the result of a combination of uptake from gas phase, liquid phase chemistry (in both the aerosol phase and the droplet phase) and particle scavenging by clouds. If this hypothesis can be supported, it allows us to estimate the mass transfer from gas phase to condensed phase through liquid phase chemistry both in and outside clouds directly from particle size measurements.

- 4.17 Low molecular weight dicarboxylic acids and related polar compounds in the remote marine rain and aerosol samples from western Pacific

Richard Sempéré^{1,2} and Kimitaka Kawamura¹

¹Department of Chemistry, Faculty of Science, Tokyo Metropolitan University, Tokyo, Japan and ²Laboratoire de Microbiologie Marine, CNRS, Marseille, France

Wet precipitation and aerosol samples collected from the remote marine areas (Pacific Ocean), were studied for the molecular distribution of C₂-C₁₀ α, ω-dicarboxylic acids, C₂-C₁₀ ω-oxocarboxylic acids, pyruvic acid and C₂-C₃ α-dicarbonyls by capillary gas chromatography (GC) and GC-mass spectrometry. Wet samples were also analyzed for dissolved organic carbon (DOC), whereas aerosol samples were studied for total carbon (TC), total nitrogen (TN) and water soluble organic carbon (WSOC). Total diacid concentration range was 36-958 μg L⁻¹ for the rain and 7.1-605 ng m⁻³ for aerosol samples. These values were lower than those observed for the urban area of Tokyo. Diacid carbon accounted for up to 5 % of TC and 15 % of WSOC in the remote aerosol samples. Rainwater analyses showed that diacid carbon comprised 0.12-0.71 % of rainwater DOC. Both rain and aerosol samples showed that the smallest diacid (oxalic acid, C₂) was the most abundant and comprised roughly 50 % of the total diacids.

p001

Emission Database for Global Atmospheric Research: EDGAR Version 2.0

J.G.J. Olivier¹, A.F. Bouwman¹, C.W.M. van der Maas¹ and J.J.M. Berdowski²

¹National Institute of Public Health and Environmental Protection (RIVM), Bilthoven

²Netherlands Organization for Applied Scientific Research (TNO), Delft

Atmospheric chemistry and climate modellers require gridded global emissions data as input into their models. Also, scenario models such as RIVM's climate assessment model IMAGE require underlying data - on grid or by region - as input in their scenario models. To meet this urgent need a global emissions source database called EDGAR has been developed by TNO and RIVM in order to estimate on a regional and on a grid basis base year emissions of greenhouse gases (CO₂, CH₄, N₂O, CO, NO_x, non-methane VOCs, SO_x), of NH₃, and of ozone depleting compounds (halocarbons) for all major known sources, both biogenic and anthropogenic. Version 2.0 comprises a complete and consistent set of data required to estimate the total source strength in 1990 of the various gases at an 1° x 1° resolution (altitude resolution of 1 km), as agreed upon in the Global Emissions Inventory Activity (GEIA) of the International Atmospheric Chemistry Programme (IGAC). The data comprise separately activity levels and emission factors for major source categories; and allocation functions, such as demographic data, land use distributions, point sources; etc. Due attention is paid to flexibility regarding the disaggregation of sources, spatial and temporal resolution and species. The objective and methodology chosen for the construction of the database as well as the type and data collected will be presented. Examples of inventories for one compound as well as for a specific source category will be presented.

p002

Source Characterization: Networks, Frameworks and Major Issues

P. Middleton, D. Hopkins and H. Lansford

Assessment/Communication Team, ASRC, SUNYA, USA

Development of emissions inventories for regional and global studies benefits from co-operative networking among inventory developers and modelers, development of flexible frameworks for evaluating and modifying data bases, and continued responsiveness to major issues and uncertainties in source characterizations. Some recent advances in these areas are discussed. An update is presented of the networking activities of the Global Emissions Inventory Activity (GEIA) Data Management and Information Exchange Center, with a focus on the development of intercomparison strategies for basic data bases, such as population, that are used in many of the GEIA inventories. The extension of geographic information systems, currently being used for regional inventories such as those for the Southern Oxidant Study in the United States, to the development of more flexible frameworks for global-scale inventories also is discussed. Finally, the importance to regional and global climate and related air quality assessments of characterizing aerosol emissions by particle composition and size is illustrated by analysis from the regional Denver Air Quality Modeling Study in the United States.

p003

Global Budgets of CO, CH₄ and O₃M.G.M. Roemer, A.C. Baart and P.J.H. Builtjes
TNO Environmental Sciences, The Netherlands

A global two-dimensional model of the troposphere has been used to calculate regional and global distributions of CO (carbon monoxide), CH₄ (methane) and O₃ (ozone). The emissions in the model stem from the EDGAR/GELA emission database. Calculated concentrations are compared with measurements from global networks and satellite observations and agree in general reasonably good with the observations. Calculations are performed to identify the sensitivity of CO, CH₄ and O₃ distributions with respect to changes in ground level and high altitude emissions, the parametrization of deep convection, an increase of UV radiation in the upper and middle troposphere and to some changes in the chemistry.

The model indicates that in the current global tropospheric ozone budget stratospheric influx and net ozone production are of about equal importance, the sum of them balanced by the loss through dry deposition. The net chemical ozone production is the small difference between two large terms: ozone production and ozone destruction. Major sources regions of net chemical production are the lowest layers of the northern midlatitudes and to a lesser extent the upper troposphere. The most important sink region is the equatorial middle troposphere. Calculations with pre-industrial emissions (anthropogenic emissions almost negligible) not only show much lower ozone concentrations, especially at northern midlatitudes, but also that at that time the troposphere might have acted as a small photochemical sink to ozone.

p004

1°x1° Global Emissions Inventory for SO_x and NO_x
Seasonally Resolved into Emission Sectors and Point and Area SourcesEva C. Voldner¹, M. Trevor Scholtz², Keith A. Davidson² and Arthur Li¹.

An anthropogenic global emissions inventory with both seasonal and sector distribution on two emission height levels (0 - 100m and > 100m) has been prepared for emissions of SO₂, SO₄, NO and NO₂. The two height levels are based on the effective height of emission after allowing for an expected plume rise. The inventory has global coverage on a 1° x 1° latitude/longitude grid and is for the base year 1985 where data for this year are available. For SO_x and NO_x, several national, regional and global data sets were used in compiling the global inventory with seasonal and sectoral resolution. The 0 - 100m emissions are resolved into mobile, non-mobile and minor point sources, while upper level emissions are provided separately for power plants, smelters and other major point sources. Not all of the available data sets used have the required two-level, sectoral breakdown; in these instances, the unresolved portions of the emissions are provided as gridded unclassified totals. In total, 76% and 67% respectively, of the global total sulphur and nitrogen, have been disaggregated into the above classes. The remaining unclassified emissions are expected to be mainly at low level but will likely include some emissions into the >100m level.

1) Environment Canada, Toronto, Ontario, Canada
2) ORTECH, Mississauga, Ontario, Canada

p005

Global Inventories of Anthropogenic Emissions of SO₂ and NO_xCarmen M. Benkovitz¹, Jane Dignon², Jozef Pacyna³, Trevor Scholtz⁴,
Lionor Tarrasón⁵, Eva Voldner⁶ and T.E. Graedel⁷

¹Brookhaven National Laboratory, Upton, NY 11973, USA; ²Lawrence Livermore National Laboratory; ³Norwegian Institute for Air Research; ⁴ORTECH International; ⁵Norwegian Meteorological Institute; ⁶Atmospheric Environment Service, ⁷AT&T Bell Laboratories.

One of the most important scientific tools used in the assessment of atmospheric chemistry, air quality, and climatic conditions of the past, present, and future is mathematical models of transport and transformations in the atmosphere. These models rely on inventories of emissions constructed on appropriate temporal and spatial scales, and including the required species. Under the Global Emissions Inventory Activity (GEIA) an international project has assembled annual global inventories of anthropogenic emissions of SO₂ and NO_x with 1° horizontal resolution for base year 1985. The data were derived from regional inventories for the United States, Canada, Europe, Asia, South Africa and Australia, and from the global inventories of Spiro et al. (1992) and Dignon (1992). Analyses of the resulting data will be presented.

p006

Sources and Sinks of S, N: Assessments from a Semi-Arid Industrial Area

A. Saxena, U.C. Kulshrestha, N. Kumar, K.M. Kumari and S.S. Srivastava

Department of Chemistry, Faculty of Science,
Dayalbagh Educational Institute, Agra 282 005, India

Reactant (SO₂, NO_x) and product (SO₄, NO₃, HNO₃) species were measured as functions of phase (gas, aerosol, wet and dry deposition) and particle size at Agra, a semi-arid industrial area in India. Mean levels of SO₂, NO_x were 7.7, 24.9 μg m⁻³ respectively; mean atmospheric SO₄, NO₃ were 10.2, 6.3 μg m⁻³ respectively. SO₄ levels were equal to values reported from highly industrialized cities in Europe, China but the presence of 42% of SO₄ in the coarse fraction of size-segregated samples suggested its origin from soil or oxidation of SO₂ on soil surfaces. Relations between ambient SO₂, SO₄ indicated that SO₂ conversion is favoured by the alkaline nature of the aerosol. The relation is best described by $y = ax^b$, ($y = \%$ of sulphate in total S (SO₄ + SO₂), $x =$ concentration of total S in air). Correlations between NO_x and each of HNO₃, NO_{3p} indicated that NO_{3p} is also contributed by crustal sources and formed by the reaction of HNO₃ on soil surfaces. Using a local source inventory, emission and removal rates by wet and dry deposition were evaluated. For S, sources and sinks roughly balanced, the background of S being mainly natural with anthropogenic sources exerting only a small influence. The sink of NO_x was smaller than its source; this imbalance may partially be explained by defining the horizontal and vertical dimensions of the area over which the N cycle would be considered closed.

p007

First results of the Bor Forest Island Fire Experiment
Fire Research Campaign Asia-North (FIRESCAN)

FIRESCAN Science Team
c/o Johann G. Goldammer, Biogeochemistry Department
Max Planck Institute for Chemistry, Mainz, Germany

In 1993 a conference on Fire in Ecosystems of Boreal Eurasia and a subsequent Fire Research Campaign Asia-North (FIRESCAN) were organized *in tandem* in Krasnoyarsk Region, Central Siberia. The aim of the conference was to compile, discuss and publish the state of knowledge on fire in boreal ecosystems, particularly in Eurasia. The research campaign was designed to investigate hypotheses developed by the International Boreal Forest Research Association (IBFRA), Stand Replacement Fire Working Group. These hypotheses are related to quantitatively understanding boreal ecosystems, the role of fire in boreal ecosystems, and modeling and predicting forest dynamics. The involvement of atmospheric scientists through the structures of the International Global Atmospheric Chemistry (IGAC) Programme, a core project of the International Geosphere-Biosphere Programme (IGBP) gave additional insights into aspects of fire emissions and atmospheric chemistry. On 6 July 1993 an experimental high-intensity stand replacement fire was set in a light *taiga* coniferous forest dominated by a *Pinus silvestris* and a lichen-dominated ground cover (*Cladonia* sp.), on Bor Forest Island, Krasnoyarsk Region. First results of describing fire characteristics and ecological and atmospheric chemical impacts of the fire are given. The medium- to long-term objectives of follow-up research and implications for fire research strategies are discussed.

p008

Study on the Sources and Sinks of Trace Gases in China

Yang Wen-Xiang
(Research Center for Eco-Environmental Sciences,
Academia Sinica, Beijing, China. 100085)

Abstract

In the past five decade years, the rate of increasing of trace gases in the atmosphere grew so rapidly. Some serious environmental problems, we are faced today, always relate with the trace gases in air. It is important to study the sources and sinks of trace gases in China.

The emission of CO₂, CH₄, N₂O, CF₄, C₂F₆, NO_x in China are estimated. At the present time, the emission of CO₂ is believed to occur from fossil fuel consumption, cement production and deforestation. Two kind of methods were used for estimating the emission of CO₂. And it was 654.4 TgC in 1990.

Rice paddy is one of the important sources for methane. China is the largest rice production country in Asian. The area of rice paddy is about one fourth of the cultivated area in China. Dr. Wang M.X. estimated that the emission of methane from rice paddy would be about 23 TgCH₄ in China. The other sources of methane are believed to occur from livestock, fossil fuel combustion, biomass burning, coal mine, oil and natural gases leakage etc.. The total emission of methane was estimated to be 45 TgC in China.

The emission fluxes of nitrous oxide from different kinds of eco-environmental system are studied. The amount of N₂O emission from fossil fuel burning, biomass burning, fertilizer used and from farmland soil is about 0.018 TgN₂O-N in China.

The significant known anthropogenic sources for CF₄ (CFC-14) and C₂F₆ (CFC-116) is primary aluminium smelting. The emission of CF₄ and C₂F₆ from aluminium production factories are estimated to be 1540 ton of CF₄ and 192.5 ton of C₂F₆ in China in 1991.

The sinks of some trace gases are studied. The photolysis and photooxidation of DMS, HCFC-22, HFC-134a, CFC-12 and N₂O have been investigated. The reaction rates of some trace gases with OH are measured by using discharge flow resonance fluorescence method. The chemical processes for the sinks of trace gases are suggested.

p009

Spatial distributions of CO₂ over Siberia in a summer season
--Airborne measurements of greenhouse gases over Siberia--

K. Izumi¹, T. Machida¹, S. Maksyutov¹, Y. Tohjima², S. Mitsumoto¹,
M. Utiyama¹, G. Inoue¹, A. Postnov³, Y. Kopylov³, S. Shmeter³, V. Nikolaev³,
N. Vinnichenko³ and V. Khattatov³

¹National Institute for Environmental Studies, Japan. ²Laboratory for Earthquake Chemistry, Faculty of Science, Tokyo University, Japan. ³Central Aerological Observatory, Russian Federation.

Horizontal distributions of CO₂ were obtained in July of 1992 and 1993 during transit flights (about 7000m), which traversed the Continent of Eurasia along a latitude of 60deg.N (Moscow to Yakutsk) and along a longitude of 130 deg.E (Sendai to Tiksi). CO₂ concentration was found to be predominantly affected by large scale motion of air masses such as a high or low pressure system. Vertical profiles were also measured in taking off and landing. They showed interesting features, which reflected the nature of Siberian vegetation: CO₂ concentration was rather uniform, being about 355ppm, over the northern part of Siberia, in which the activity of vegetation is quite low. On the other hand, over the area, where Taiga forests are developed, the concentration was low near the ground surface and concentration difference between the free troposphere and the mixed layer was large, exceeding 10ppm.

p010 Carbon dioxide flux studies in tundra ecosystems in Taymyr Peninsula (Russia)

D.G. Zamolodchikov
Center for Ecology and Productivity of Forests, RAS, Russia
D.V. Karelin
Biological Department, Moscow State University, Russia
S.J. Hastings
Biological Department, San Diego State University, USA

In July 1993 we did field measurements of carbon dioxide flux in Taymyr Peninsula most representative tundra ecosystems on a peak of seasonal productivity. All diurnal measurements were made using a portable infra-red gas analyzer Li-Cor 6250 and chamber method for determining carbon flux. The investigations were carried out at four sites along a 450 km latitudinal transect including: south shrub tundra (70 51N, 89 54E), limit between south and typical subarctic tundra (71 26N, 89 14E), typical tundra (72 17N, 85 45E) and limit between typical and arctic tundra (73 15N, 90 36E). Data show, that south tundra ecosystems had a positive net ecosystem carbon flux (0.252 to 0.688 gC/m² per day), while typical tundra - negative flux (-0.049 to -0.313 gC/m² per day). The biggest values of carbon flux into atmosphere were found in arctic tundra (1.899 gC /m² per day), in spite of the fact that the time of measurements was close to peak seasonal productivity. Analysis of the carbon flux data shows a strong correlation with climatic (soil temperature, thaw depth) and vegetation (fractions phytomass and cover) characteristics resulting in regression equations with low residual sum of squares (10-30%).

p011

CO₂ budget of coastal Arctic tundra at Barrow in 1993 summerYoshinobu HARAZONO*, Mayumi Yoshimoto*, Akira Miyata*,
Walter C. Oechel** and George Vouritis**

* National Institute of Agro-Environmental Science, Tsukuba, 305 Japan

** Dept. of Biology, San Diego State Univ., San Diego CA, USA

There are large carbon stocks at northern ecosystems (tundra and boreal forests), which seemed to affect the event of global warming, because there is considerable uncertainty whether this northern ecosystem will act as a CO₂ sink or not. In this study, CO₂ flux was measured using aerodynamic method and eddy correlation method over an Arctic tundra near Barrow (71°17'42"N, 156°41'10"E), Alaska. The results were examined comparing with that of IBP in 1970's obtained by the same aerodynamic method. The measurement was carried out at two sites (polygonized moist tundra and wet tundra) from June 8 to August 25, 1993, which covered almost full of growing active period of the vegetation. Diurnal CO₂ flux at polygonized tundra in 1993 was approximately 1/5 of that at vegetation in the temperate zone. Total budget at polygonized tundra was small efflux (upward) during the period, while that at wet tundra was downward. As the soil temperature was lower at wet tundra, the paddy condition at wet tundra seemed to decrease the decomposition rate of soil organic matter and the water surface seemed to prevent to diffuse CO₂ to the atmosphere. In 1970's CO₂ budget at the same polygonized site was downward and the tundra acted as CO₂ sink, while today it has changed to a source, major reason was thought as the atmospheric warming (about 2 °C higher) and drying of tundra eventually.

p012

On the emission and regional budget of greenhouse gases in Hungary

A. Molnár, E. Mészáros and Gy. Kiss

University of Veszprém, H-8201 Veszprém P.O.B. 158, Hungary

Hungarian sources and sinks of atmospheric carbon dioxide, methane and nitrous oxide are estimated for the time period between 1988-1992. The total strength of CO₂-C emission for 1988 is in the range of 92-102 Tgyr⁻¹. This range is somewhat lower for 1992 (87-97 TgCyr⁻¹) owing to economic changes in the country. Thus, the anthropogenic release decreased between 1988 and 1992 from 21 to 16 TgCyr⁻¹. Since the vegetation removes annually from the air over the country a carbon mass of 57 Tg, our region is a net carbon source, even if anthropogenic effects are neglected. The total methane release of the country lies between 0.4-0.6 TgCyr⁻¹ with some decrease in the time period mentioned. The emission is controlled by anthropogenic sources like solid waste treatment, natural gas production and distribution as well as animal husbandry. Preliminary data show that CH₄ concentration in Hungary is near 1.9 ppm. Taking into account this concentration as well as a tropopause height of 12000 m and a rate constant of $5 \times 10^{-15} \text{ cm}^3 \text{ molecule}^{-1} \text{ s}^{-1}$ for the reaction with OH radicals ($5 \times 10^5 \text{ cm}^{-3}$), a chemical removal of 0.1 TgCyr⁻¹ can be calculated for the tropospheric air above the country. The comparison of this figure with the methane emission range indicates that the atmospheric box above the country is also a source of carbon in reduced form. Finally, the emission of nitrous oxide is 0.017 TgNyr⁻¹ for 1988, while the corresponding figure for 1992 is 0.014 TgNyr⁻¹. Calculations show that the nitrous oxide emission is determined mostly by the use of fertilizers.

p013

Effects of ocean stratification on the uptake of greenhouse gases

Hiromasa Ueda, Takashi Karasudani, Kohji Ishi-i

Research Institute for Applied Mechanics, Kyushu University, Japan

Uptake of greenhouse gases into the ocean is caused by liquid-side turbulence just beneath the air-sea interface, which is induced both by wind over the sea and by buoyancy on the liquid side. However, the ocean uptake of CO₂ estimated hitherto have been taken into account the wind-induced turbulence only (e.g., Liss and Merlivat, 1986). A laboratory experiment and theoretical modelling are made for the effects of buoyancy and reveals their large contribution on the ocean uptake. At first, exchange coefficient due to convection beneath the free surface is shown to be twice as large as that in convection over a solid wall, while it is decreased drastically by stable stratification. Secondly, contribution of oceanic convection in the middle and high latitudes gives rise a larger absorption rate of CO₂, e.g., that in the East China Sea attains to the effect of an wind of $3-5 \text{ m s}^{-1}$ over the sea, while stable stratification in tropical oceans gives a smaller desorption rate from the ocean. These facts suggest the neglect of buoyancy effects leads to a significant underestimation of the ocean uptake of CO₂ and other greenhouse gases and pollutants.

p014

Observation of carbon dioxide partial pressure in air and surface sea water in the seas adjacent to Japan

M. HIROTA, K. FUSHIMI, K. NEMOTO and A. MURATA

Marine Department, Japan Meteorological Agency, Japan

To understand the role of ocean as the source and sink of the atmospheric CO₂, the JMA started operational observations of pCO₂ in both air over the sea and surface sea water in the seas adjacent to Japan and in the western North Pacific in 1989.

The observation is done four times a year in the seas adjacent to Japan. The observation along the fixed line off Boso peninsula shows that this region was a sink of the atmospheric CO₂ all the year. However, there was a large seasonal variation (about 60ppm) in pCO₂ in surface sea water. The maximum and minimum were observed in October and June, respectively. This seasonal variation was parallel with that of the SST, and opposite to that of the atmospheric pCO₂. The results will be discussed in relation to other oceanographic/meteorological data.

p015

CO₂ trend at the Mt. Cimone (44°12' N, 10°42' E) baseline stationT. Colombo¹, G. Giovannelli² and P. Bonasoni²¹Italian Meteorological Service, via delle Ville 100, 41029 Sestola (Mo), Italy.²CNR - FISBAT Institute, via Gobetti 101, 40127 Bologna, Italy.

The trend of atmospheric CO₂ measured since 1979 at the Mt. Cimone station (44°12' N, 10°42' E, 2165 m a.s.l.) is reported and discussed. Mt. Cimone, a baseline mountain station in Italy's north-central Apennines, is part of the WMO Background Air Pollution Monitoring Network (BAPMoN).

The atmospheric CO₂ concentration is known to be influenced by global phenomena. Thus, the present paper thus also discusses the effects that the violent eruptions of the Mount St. Helen (1980), El Chichon (1982) and Mt. Pinatubo (1991) volcanoes, together with the "El Nino" phenomenon, have had on the CO₂ trend registered at Mt. Cimone. Eruptions of this nature generate volcanic clouds in the stratosphere that diminish the amount of solar radiation reaching the surface of the ocean and the earth and, hence, tend to cool the earth-atmosphere system as well as directly influence ocean surface temperature, which in turn plays a determinant role in the CO₂ sink-source process.

p016

Sources and Sinks of Carbon Dioxide in Kashmir: A Case Study

Altat Hussain Wani¹ and Ya-Hui Zhuang²¹Asian Institute of Technology, G.P.O. Box 2754, Bangkok 10501, THAILAND²Lawrence Berkeley Lab., University of California at Berkeley, CA 94720, USA

An attempt has been made to estimate the CO₂ budget of Kashmir valley, India. The study delineates and assesses the CO₂ emission patterns from different anthropogenic sources and net primary productivity of the vegetation which serves as a principal sink for these emissions. Fluxes considered include fossil- and domestic- fuel combustion, limestone processing as well as changes in the carbon stores in forests, and their relative contribution towards the total annual emissions. From the emission inventory, domestic sector ranks first with its contribution of about 2 million tons, followed by transport and industrial sectors, in the total annual CO₂ emissions of 2.79 million tons. The estimates indicate that these CO₂ emissions are currently accumulating in terrestrial ecosystem, mainly in the form of forest biomass, and if the current accumulation of carbon by the forests is subtracted from the direct emissions resulting from fossil fuel combustion and other sources, the net contribution of CO₂ is zero. Based on these results the region is altogether internally CO₂ neutral, with a significant potential to confront the global CO₂ buildup by checking the trans-boundary releases, in addition to sequestration of local emissions.

p017

Land-use effects on ¹³C-based estimates of tropical carbon sources and sinksA.R. Townsend¹, E.A. Holland¹, and E. Veldkamp²¹NCAR, Boulder, CO; ²La Selva Biological Station, Costa Rica

Carbon-13 measurements of atmospheric CO₂ and atmospheric transport models can help resolve terrestrial and oceanic sources and sinks in the global carbon cycle. Such models specify the isotopic fractionation associated with exchanges of carbon between the terrestrial biosphere, the atmosphere, and the ocean. For example, photosynthesis discriminates strongly against ¹³CO₂, and decomposition of soil organic carbon formed decades ago, when the atmosphere contained more ¹³C than at present, can cause respiration to be enriched in ¹³C relative to newly fixed plant carbon. Modeled estimates of this "biospheric disequilibrium" are ~1‰ in boreal and tundra biomes, and accounting for the disequilibrium in a tracer model can change the partitioning of carbon sources and sinks between land and ocean by more than 1 Gt.

A second "biospheric disequilibrium" arises from tropical land-use changes. The widespread conversion of C₃ forests to C₄ pastures and croplands causes a sudden change in the ¹³C fractionation in photosynthesis by typically 10-13‰. The isotopic change in soil carbon lags far behind because of the decadal to millennial time scales of soil organic matter turnover, and CO₂ respired will be much lighter in ¹³C than photosynthesis for decades. Using the Century Model and data on land-use, we show that the ¹³C disequilibrium between respiration and photosynthesis due to land conversion in the tropics could significantly alter inverse model estimates of tropical carbon sources and sinks. The modeled estimates are supported by measurements of ¹³C in respiration and recently fixed plant carbon taken from several field studies.

p018

Atmospheric Carbon Sequestration through Agroforestry

Xiaoke Wang and Zongwei Feng

Research Center for Eco-Environmental Sciences

Academia Sinica, PO Box 2871, Beijing 100085, China

Two types of agroforestry systems, namely, the tree-belt type with poplar growing along the boundaries of crop field grid cells and the interspersing type with paulownia-crop mixed plantation, have been demonstrated in Fengqiu County, Henan Province, for the study on atmospheric carbon sequestration. Both types of agroforestry systems gave a higher crop productivity, total biomass, productivity and carbon sequestration rate, as compared with the conventional agricultural systems. The trees in the crop fields play a three-fold role, i.e., (i) they provide timber which is a long-lived carbon pool, (ii) they furnish firewood which can substitute fossil fuel and thus reduce the net carbon release into the atmosphere, and (iii) they promote the crop yield by reducing the detrimental impact of the local dry and hot wind during the growing season.

According to our estimation, the existing agroforestry systems in China, comprising of 2 million ha. of crop-tree mixed plantation and 1 million ha. of farmland shelterbelt, can sequester about 1.2 million tons of carbon annually, which is 0.16% of the total carbon release from fossil fuel combustion and cement production.

p019

Russian forests are global sinks of carbon dioxide from atmosphere, current fluxes and influence of climate changes.

A. O. Kokorin and I. M. Nazarov
Institute of Global Climate and Ecology, Moscow, RUSSIA

The boreal forests and forest's soils are giant carbon reservoir: in Russia they contain more than 250 Pg-C. CO₂ uptake by Russian Taiga forests can be increased significantly in warming - up to 15 percents per 1°C. However the warming increases the decomposition rate and CO₂ emission too. These processes are studied by long-scale model of CO₂ exchange in atmosphere - forests system. It is very important to use primary meteorological data for different Russia regions and primary data on forests' age distribution and fires. The total CO₂ exchange between Russian forests and the atmosphere are equal to 3 Pg-C/yr. There is net sequestration and CO₂ uptake of 0.2 Pg-C/yr, which is caused by 1) increase of CO₂ in atmosphere and a little warming in summer in some parts of Siberia (40%) and 2) unequilibrium forests' age distribution (60%). Calculations based on climate scenarios show that the uptake will be increased rapidly, up to 0.4 and 0.7 Pg-C/yr by 2020 and 2040 yrs., that is significant in global scale.

p020

Analysis of the climate gases CO₂, N₂O and CH₄ by wide bore capillary gas chromatography with single injection of gas sample

Bishal K. Sitaula, Luo Jiafa and Lars R Bakken
Agricultural University of Norway, 1432 Aas- NLH, Norway

A gas chromatographic method is described which gives sensitive and rapid (3.3 min) measurement of the three greenhouse gases CO₂, CH₄ and N₂O. A wide bore capillary column operated at optimal conditions gave sufficient separation to allow a switch of the column flow between two detector systems (TCD and FID in series, and ECD) during the chromatogram, thus all three gases could be analyzed with a single sample injection. Application of a peristaltic pump allowed gas samples to be transferred directly from gas sampling vials, through a drying agent [(Mg)ClO₄]₂ and into the injection loop (0.5 ml). Back flushing of the injection system (pump and drying agent) with He between each injection ensured minimal carry over between samples (< 0.6 %). Experiences with storage of gas samples in vials with butyl rubber septa are described. The best result is obtained by a minimization of storage. Thus, there is a need for a rapid analysis systems, such as we have attempted to achieve with the present GC system.

p021

Fluxes of CH₄, N₂O and CO₂ in forest soil influenced by N input and soil acidification

Bishal K. Sitaula, Lars R Bakken and Gunnar Abrahamsen
Agricultural University of Norway, 1432 Aas- NLH, Norway

Effects of N inputs and soil acidification on fluxes of CH₄, N₂O and CO₂ was studied in soil from 100-year-old Scots pine forest of Norway. N fertilization [30 kg (Medium) and 90 kg (High) N ha⁻¹ y⁻¹] increased N₂O emission by a factor of 1.2 to 6 times with medium N and 4 to 7 times with high N treatments. Soil acidification (irrigation with artificial rain with pH 3, pH 4 and pH 5.5) with most acidic "rain" (pH 3) resulted in decreased N₂O and CO₂ fluxes and increased CH₄ uptake in soil. The estimated fertilizer derived N₂O-N emission during summer period was 94 and 93 mg d⁻¹ kg⁻¹ of added NH₄NO₃-N for medium and high N respectively. High nitrogen input decreased CO₂ concentration by 10-60% and CO₂ fluxes 12-16% compared to medium N treatments. Soil CO₂ concentration were significantly lower (2-12 times) in the most acidic treatment compared to pH 4 and pH 5.5 treatments. The significant reduction in CH₄ uptake and increase in N₂O release due to input of nitrogen demonstrates the potential double green house effects of nitrogen deposition. The effect of rain acidity for decreased N₂O and CO₂ release and increased CH₄ uptake in soil seems to be pronounced only with extreme or most acidic "rain" (pH 3). Hence, the usual ambient rain acidity of pH 4.2 - pH 4.9 is only likely to have minor effects on these gas fluxes in soil.

p022

Control of methane emission from a rice paddy field by water management

K. Yagi, H. Tsuruta, K. Kanda, and K. Minami
National Institute of Agro-Environmental Sciences, Tsukuba, JAPAN

Effect of different water management on methane emission from a Japanese rice paddy field to the atmosphere was studied by using an automated sampling and analyzing system for three cultivation periods. The flux data were collected every one hour by this system. The test site was divided into two plots. The plots were flooded from May to August with or without short-time draining practices. Effects of drainage on methane emission were significant. Large methane fluxes were observed immediately after drainage, following the rapid decrease of the fluxes. After re-flooding, the drained plot kept emitting significantly lower amount of methane than the continuously flooded plot. Soil redox potential (Eh) was increased by the draining practices, suggesting a decrease in methane production rates in paddy soil. The effects on the increase in soil Eh and the decrease in the emission depend on the length of the drainage. The total amounts of methane emitted to the atmosphere were reduced to 55-58% by the short-term draining practices compared with the continuously flooded management. These results indicate that water management practices can be applied as a possible mitigation technique for methane emission from rice paddy fields.

Release and retention of methane in rice soils
following organic amendments

R. Wassmann^{1,2}, M.C. Alberto¹, H.U. Neue¹, R.S. Lantin¹, J.B. Aduna¹,
K. Bronson¹, H. Papen², H. Rennenberg², and W. Seiler²
¹International Rice Research Institute, Los Baños, Philippines; ²Fraunhofer
Institute for Atmosph. Environm. Research, Garmisch-Partenkirchen, Germany

The effect of organic amendments on the methane budget of rice fields was investigated by (1) recording the flux rates of methane emission and ebullition (release of gas bubbles) as well as (2) by determining the amount of gaseous and dissolved methane in the soil. Incorporation of organic material, i.e. rice straw and green manure, generally increased methane emission and ebullition, especially subsequent to incorporation. During the latter stages of the growing season, emission and ebullition rates were generally high irrespective of the type of N-source added.

The seasonal patterns of methane flux rates correlated with the variation of methane pools retained in the soil. As a consequence of the incorporation of organic material, high methane concentrations in the soil solution and an immediate build up of gaseous methane reservoirs in the soil were observed. In the absence of organic amendments, the development of pools of gaseous methane was restricted to the latter stage of the growing season.

These findings provide evidence that the incorporated methanogenic substrates were dissipating during the first half of the vegetation period, while methane production based on recently produced substrate gradually increased.

Source strength of methane emission from ricefields and mitigation options.

H.U. Neue¹, R. Wassmann^{1,2}, and R.S. Lantin¹

¹International Rice Research Institute (IRRI), Los Baños, Philippines
²Fraunhofer-Institute for Atmospheric Environmental Research (FhG),
Garmisch-Partenkirchen, Federal Republic of Germany

Recent progress made in understanding factors and processes that control methane emission from ricefields has opened up various options to mitigate emissions. The large uncertainties of regional and global CH₄ emissions (annually 20 to 100 Tg) remain because respective mechanistic models and geographic information systems are lacking. Rice production has to increase by 70% within the next 30 years. This will increase CH₄ emission if feasible mitigation technologies won't become available. Generally, higher yields mean higher plant biomass which results in higher CH₄ fluxes. New rice cultivars with a higher harvest index and less but only productive tillers per unit area have the potential to lower CH₄ fluxes. Midseason aeration periods and field drying before harvest reduce emission but could increase N₂O emission. Sulfate containing fertilizer lower CH₄ emission while any addition of easily degradable carbon increases it. Changes of rice cultivars and water management will probably have no trade off in productivity. Less use of easily degradable organic inputs may take place with increased use of mineral fertilizer. Reducing CH₄ emission while increasing production of irrigated rice is feasible. Raising the low production of rainfed rice will probably increase CH₄ emission.

Influence of fertilizer and water management on methane emission and
production in Chinese rice fields and possible mitigation options

X.J. Shangguan M.X. Wang D.Z. Chen R.X. Shen Y.S. Wang
Institute of Atmospheric Physics, Chinese Academy of Sciences, Beijing 100029, China
R. Wassmann M. Toelg H. Papen
Fraunhofer Institute for Atmospheric Environmental Research, Germany
X.L. Xie W.D. Wang
Changsha Institute for Agricultural Modernization, Academia Sinica, Changsha, China

CH₄ emission and production rates were recorded in Hunan Province, central region of China, in the years of 1991-1992. The fertilizer treatments were based on identical doses of nitrogen, but with different ratio of organic/mineral fertilizer. The locally used combination of organic and mineral fertilizers yielded seasonal average of 8.0-50.1 mgCH₄m⁻²h⁻¹. The averages for pure mineral fertilizers were rather lower whereas the exclusive use of unfermented organic manure made the highest emission. The effect of residues derived from biogas generators was up to its treatment before applied as manure (airdried or wet). The seasonal averages of CH₄ production rates of the combined and organic treatment did not differ by means of statistics and varied from 57 to 114 mgCH₄m⁻²h⁻¹, while significantly lower in the plot with pure chemicals. The rather low efficiency of carbon transformation to CH₄ was observed in the field with pre-fermented organic manure. Average CH₄ emission in deep water covered field was relatively low in early rice but relatively high in late rice compared to the other three plots. Constant moisture field always yielded the lowest emission, and CH₄ emission rate was almost identical in the fields received normal water cover and 3-day frequent drainage. The averages of CH₄ production rates during both early and late season decreased with the decreasing of water level. The main CH₄ producing area was in the upper part of soil (3-7 cm), in the fields with better water supply, while in deeper soil (9-13 cm) with not enough flooding water. After the soil moisture lowered down to certain extent (26%-31%), CH₄ emission went almost to zero, even after the fields reflooded, it did not resume in a very long time. The combination of fermented organic manure plus mineral fertilizers with a suitable timetable frequent drainage can be one option to reduce CH₄ emission. The lag phase between the time of reflooding and resuming of emission should be especially studied.

Preliminary study on the relationship between organic acid contents
and methane emission rates in paddy soil in the red earth hilly area of
south China

W.D. Wang and X.L. Xie
Changsha Institute of Agricultural Modernization, Academia Sinica, Changsha, China
X.J. Shangguan and M.X. Wang
Institute of Atmospheric Physics, Academia Sinica, Beijing, China

At Taoyuan County, Hunan Province of P.R. China (28°55' N, 110°30' E), the measurements of organic acid contents in the paddy soil and methane emission were carried out by spectrophotometry and gas chromatography respectively. It was observed that the temporal variation tendencies of organic acid content in the soil were uniform for all the fertilizer treatment fields. Regression analysis shows that a very obvious correlation between organic acid content in the soil and methane emission rates could be found (0.980 and 0.860 respectively) for the plots received fully organic manure and locally used fertilizer (organic plus mineral); for pure mineral fertilizer and fermented fertilizer (sludges from biogas pits) treatment fields, the correlation was very poor (0.350 and 0.021 respectively). The correlation coefficient between organic acid contents and methane emission rate in all the four plots was 0.87. For the four water management plots, the temporal variation tendencies of organic acid content in the soil were also uniform, so were those of CH₄ emission rate from three water treatment plots except constant moisture plot. Regression analysis shows that except for constant moisture plot, CH₄ emission rates correlated quite well with organic acid contents with correlation coefficients as 0.99, 0.91, 0.71 respectively for the other three plots received deep water cover (~8cm), 3-day frequent drainage, normal water cover (~3cm). A close relationship was found between all CH₄ emission rates and all organic acid contents in the four water management field (R=0.97). The determinations of organic acid and methane production rates at different depth of the soil were also carried out by spectrophotometry and head-space gas chromatography respectively, which show that the vertical distribution of organic acid contents in paddy soil was roughly consistent with that of methane production rates.

p027

Methane Emission from Rice Paddies and the Effect of Agricultural Management

Chen Zong Liang¹, Shao Ke Sheng², Li Debo³, Wang Bujun⁴ and Yao Heng¹¹Department of Atmosphere Environment, Chinese Research Academy of Environmental Sciences, Beijing 100012²Center of Environmental Sciences, Peking University, Beijing 100087³Nanjing Research Institute of Environmental Sciences, Nanjing 210042⁴Crop Breeding and Cultivation Institute, Chinese Academy of Agricultural Sciences, Beijing 100081

During three year experiment(1990-1992), the methane emission rates from three testing sites in Beijing and Nanjing area had been measured, studies concentrated on the effect of agricultural management on the methane emission from rice paddies. The observing results indicated that seasonal and daily methane emission pattern are very complicated. They varied with the physical and chemical properties of paddy soil, agricultural management and climatic condition. In our study the maximum emission rate usually appeared in the afternoon and affected by soil temperature. Meanwhile a basically bi-mode pattern of seasonal variation with the highest peaks appeared about in the tillering stage and reproductive stage. Under common field management, the determined results of methane emission rate in Beijing area were 17.5, 20.4 and 15.0mg/hr.m² for the rice after wheat in 1990, 1991 and 1992, 10.0 and 8.5mg/hr.m² for spring rice in 1991 and 1992 respectively. In Nanjing area, they 10.8mg/hr.m² for the normal organic fertilizer application in 1990, and 19.8 mg/hr.m² for winter flooded paddy in 1992. Intermittent irrigation was found both to decrease methane emission and increase rice yield. Ridge cultivation in the southern area is favorable to reduce methane emission from winter flooded rice paddies. Dry seeded cultivation in Beijing obviously reduced the methane emission also. Application of organic fertilizer enhanced the methane emission. Reasonable application of some kinds of chemical fertilizer may reduce the amount of methane emitted from rice paddies.

p028 An Estimation of Methane Emission from Rice Paddies of China Mainland

Yao Heng, Zhuang Ya-hui and Chen Zong Liang

Department of Atmosphere Environment, Chinese Research Academy of Environmental Sciences, Beijing 100012, P.R.China

Methane emission from rice paddies of China mainland was estimated using three methods. The first technique we used was based on the methane emission rates obtained in Beijing, Nanjing, Hangzhou, and Tuzu by local research groups. Regional classification of rice cropping area and a land-use data base identifying rice-farming regimes were used for this estimation. The second and third method were based on the Neue's assumptions that methane emission from rice paddies is proportional to the land net primary production and rice grain production. Through these techniques total methane emission was calculated between 15.7 and 27.3 Tg/Yr. A one degree diagram describing methane emission from rice paddies in each cropping regions was presented. Further improvement on method for estimation of methane emission from rice field was also discussed in this paper.

p029

Flux of Methane from Rice Field in Thailand

W.H. Su^{1,2} and X. Rong¹

¹Environmental Engineering Program
School of Environment, Resources and Development
Asian Institute of Technology
G.P.O. Box 2754, Bangkok 10501, Thailand

²Research Center for Eco-Environmental Sciences
Chinese Academy of Sciences
P.O.Box 2871, Beijing, 100085, PRC

The agriculture sector contributes more than 90 percent of total methane emission in Thailand, most of which comes from paddy field. Measurement of CH₄ flux have been performed in the paddy field, Pathumthani, Thailand, by using a closed chamber technique with gas collector. Gas samples were analyzed by gas-chromatography instrument with FID detector. The flux data shows variations with the rice ages, water and soil temperature, and also exists diurnal variation of flux. It is shown that there are some differences between CH₄ flux figures for gas samples collected in different environments of rice growth and the differences are so large as in several times. These problems are discussed on basis of mechanism and modelling work. Comparison of data from this study and other works are made and discussed. Annual emission rate of methane from rice paddy field is estimated.

p030 Micrometeorological measurements of methane flux over agricultural vegetations and an estimation of methane emission in Tsukuba, Japan

A. Miyata and Y. Harazono

National Institute of Agro-Environmental Sciences, Japan

Methane fluxes over a paddy field and a grassland were measured by gradient method. Concentration gradients of methane over each canopy were measured continuously with NDIR(Non-Dispersive Infrared Analyzer) and gas diffusion velocities were evaluated from wind profiles. Over the paddy field under continuous flooding and with no application of organic fertilizers, obvious gradients of methane corresponding to its emission from the paddy were observed all day. The methane flux showed the diurnal variations with the maximum in the afternoon, which was closely related to changes in soil temperature. The daily emission ranged from 80 to 210 mgm⁻²day⁻¹. Over the grassland, which was managed with no contamination of fertilizers, significant downward gradients of methane were observed under strongly stable atmospheric conditions. This indicated methane was absorbed at the grassland surface. Under the circumstance, a proportional relation was observed between the gradients of methane and those of CO₂ at night. By using the relation, the nocturnal methane flux over the grassland was estimated at four orders of magnitude smaller than the respiration rate.

Nocturnal methane flux on a tract of land of several kilometers was assessed using a simple one-dimensional model from the concentration buildup observed at a height of 25 m under stable conditions. It showed a considerable emission of methane out of the ground even in winter when paddy fields were dormant as a methane source. This suggests the methane budget on the similar scale is regulated by natural sources as well as paddy fields or anthropogenic sources.

p031

UPPER TROPOSPHERIC CONCENTRATION DISTRIBUTIONS OF CH₄, O₃, CO₂, CO OVER SIBERIA: NUMERICAL SIMULATION WITH A GLOBAL TRACER TRANSPORT MODEL.

G. Inoue, K. Izumi, T. Machida, S. Maksyutov, S. Mitsumoto¹, Y. Tohjima², Y. Kopylov, A. Postnov, N. Vinnichenko and V. Khattatov³

¹National Institute for Environmental Studies, Tsukuba, Japan

²Faculty of Science, Tokyo University, Tokyo, Japan

³Central Aerological Observatory, Dolgoprudny, Russia

Airborne observations of ozone, methane, carbon dioxide and carbon monoxide were performed over Siberia in 1993. Analysis of large scale concentration distributions revealed existence of several spatial scales which are characterized with different correlations between tracers. A data filtering technique is proposed to select between different air mass which is based on correlation between different tracer concentrations in order to derive averaged longitudinal and latitudinal profiles. Global tracer transport model was applied to the simulation of large scale CH₄, O₃, CO₂, CO concentration distributions over the area of the measurements. Model was driven by the observed winds and reproduces the observed weather patterns and corresponding concentration variations. The model simulations of tropospheric (about 400 mbar) concentration distributions could explain qualitatively the concentration variations caused by the large scale air motions such as stratospheric folding and upward transport from lower troposphere.

p032

Airborne measurement of CH₄ emission from West Siberian Lowland

Y. Tohjima¹, H. Wakita¹, T. Machida², S. Maksyutov², I. Matsui², G. Inoue², A. Postnov³, Y. Kopylov³, V. Nikolaev³, N. Vinnichenko³ and V. Khattatov³

¹Laboratory for Earthquake Chemistry, The University of Tokyo, Japan

²National Institute of Environmental Studies, Japan

³Central Aerological Observatory, Russia

In July, 1993, we carried out *in situ* airborne measurements of CH₄ concentration over the West Siberian Lowland, where vast wetlands are distributed. After non-methane hydrocarbons in sample air were removed by oxidation on Pt catalyst, CH₄ was continuously detected by a flame ionization detector (FID). An aircraft (Ilusin-18) equipped with systems for measuring trace gases traversed over about 100 km area of wetlands at several different altitudes sequentially; most of the flights were at 150 m, 500 m and 1000 m above ground level. The flight observations in three different wetland areas showed high CH₄ concentration in the lower troposphere near the ground surface. The daily variations in the spatial distribution of CH₄ over wetlands revealed that the CH₄ emitted from the wetlands was transported to the overlying atmosphere with the growth of the mixed layer. From the vertical profiles of average CH₄ concentration, we estimate the spatially averaged CH₄ fluxes over the studied areas. This result confirms the importance of the West Siberian Lowland as a source of global atmospheric CH₄ budget.

p033

Climate dependence of methane emission from boreal wetlands: a proposed model structure

G. A. Alexandrov

Institute of Atmospheric Physics,
Russian Academy of Sciences, Russia

A number of global scale estimates and site scale field observations were made to evaluate the role of boreal wetlands as a source of methane. But a reliable prediction of climate feedback (increase of methane flux due to global warming) from boreal wetlands is hardly to be drawn yet. One part of the problem is wide scatter of flux values measured in the field, another part is the difference of ways by which the global scale estimates can be drawn. Toward resolving the dilemma, a regional model (compatible with some of global carbon cycle models) of methane production in taiga landscapes is proposed.

p034

Water vapor and methane measurements in the troposphere over the Taklimakan Desert

Tadao Aoki, Teruo Aoki and Masashi Fukabori

Meteorological Research Institute Tsukuba, Ibaraki 305, Japan

A ground-based instrument has been developed to remotely measure the vertical profile of trace gases in the troposphere, where the absorption lines of trace gases are selected by a very narrow band pass filter and scanned with a tunable etalon. Measurements were made with the resolution of about 0.05 cm⁻¹ for the absorption line of water vapor at 6541 cm⁻¹ and that of methane at 5972 cm⁻¹. From the experiments in Tsukuba in Japan it has been found that the accuracy of column amount of the retrieved water vapor is a few percent, which is much better than those of current satellite observations.

Using this instrument measurements have been made for the water vapor and methane at two sites of Taklimakan Desert; Hotan in October 1992 and Qira in October 1993. Diurnal variations of the total column amounts of these gases are discussed.

p035

Local sources and behavior of atmospheric methane in Nagoya, Japan,
inferred from carbon isotopes and atmospheric ^{222}Rn data

J.Moriizumi, J.Mase, K.Nagamine, T.Iida and Y.Ikebe
School of Engineering, Nagoya University, Nagoya, Japan

To clarify the sources and behavior of atmospheric methane, we monitored the concentration of atmospheric methane in Nagoya and measured its carbon isotopic composition. The concentration fluctuated diurnally, and we collected air samples of various concentrations for isotope analysis. Trace amount of methane in the sample was separated from the other components and enriched with active carbon at -196°C . The enriched methane purified with a gas chromatograph and combusted to prepare for isotope analyses. There was a weak inverse correlation between the ^{14}C content and the concentration of methane in the samples. The correlation suggests that fossil methane of little ^{14}C content contributes to the diurnal variation. We also monitored the concentration of atmospheric ^{222}Rn , which is one of trace components in the atmosphere, and we compared the concentration of the ^{222}Rn with that of methane. They were similar in diurnal fluctuation. Radon-222 is a radioactive and inert gas, and it is released from the ground to the atmosphere. Meteorological factors such as stability of the atmosphere cause its diurnal variation. A numerical simulation shows that the ^{222}Rn which contributes to the diurnal variation is mainly originated from local area within several ten kilometers. For the similarity of diurnal variation between methane and ^{222}Rn concentrations in the atmosphere, the fossil methane is released from the same local area that the ^{222}Rn which contributes to the diurnal variation is released.

p036

Significance of methane emission from coastal wetlands
(mangrove ecosystems) of India

G.R. Purvaja and R.Ramesh[®]
Centre for Water Resources, Anna University, Madras, India
[®] presently at: Department of Earth and Planetary Sciences, Harvard University,
Cambridge, MA, U.S.A.

Methane is produced mainly by anaerobic bacterial methanogenesis, which occurs in wetlands, paddy fields, ruminant digestive systems, land fill sites etc. Emissions from wetlands are the largest natural source of methane (about 115 Tg/year-based on recent global budget) to the atmosphere. Wetlands, consisting primarily of mangroves in sub-tropical and tropical regions, typically occupy low-wave energy protected coastlines in bays, estuaries and lagoons. Mangroves represent the dominant soft-bottom plant communities of the marine terrestrial transition zone and are both major source and sink for various trace gases like methane. The chemistry of this ecosystem is strongly affected by natural and anthropogenic processes and a variety of greenhouse gases are released to the atmosphere through the sediment-water interface of the mangroves. The adverse changes due to anthropogenic or human driven activities such as sewage discharge, oil pollution and agricultural runoff in the emission of methane have been determined spatially and temporally from three different mangrove ecosystems of south India.

To refine estimates of source from the natural wetlands and to understand the processes leading to the production and emission of methane from the mangroves, year round field measurements have been carried out, adopting the Closed Chamber Technique and analyzed using a Gas Chromatograph with Flame Ionization Detector. Properties of soil and water influencing the emission and absorption of methane are also discussed. Estimates of methane emission from the Indian mangroves to the atmosphere assume special significance due to their enormous nature to emit methane. From the present investigation, lowest methane emission was recorded at the site influenced by oil pollution, due to suppression of gaseous exchange from the sediment to the atmosphere, while peak and highly erratic emission rates were observed at the site severely affected by domestic effluent discharges. The data obtained from the year round survey was extrapolated to project a minimum-maximum range using precalculated extent of mangroves along the Indian sub-continent to determine their contribution of methane to the global atmosphere. The present study indicates about 11 to 51 Tg CH_4 per year is contributed by the major mangrove ecosystems of India. Attempts have also been made to predict the impact of natural and anthropogenic forcing on the chemical composition of the atmosphere.

p037

Tropospheric level of CH_4 , CO and O_3 along the longest
belt of largest population density

By

L.S. Hingane
Indian Institute of Tropical Meteorology, Pune-411008, INDIA

A B S T R A C T

In the light of increasing worldwide mixing ratio of ozone precursor gases like methane (CH_4), carbon monoxide (CO), the tropospheric level of ozone has been assessed over a region which remained some what unnoticed by the researchers but should be considered important as far as the biogenic activities are concerned. This region which lies along the foot of the Himalayas in Asia constitutes 1% of the world's land area and supports 10% of its human population as well as 9% of herbivorous animal population. The production of CH_4 by enteric fermentation of herbivorous animals and paddy fields and that of CO and NO_2 from burning of biomass and fossil fuel, over the region has been estimated. The values obtained from this estimation are used to define the lower boundary conditions in a one-dimensional (1-D) photochemical dynamical model which is employed to examine the tropospheric level of ozone during winter (as residence time of air during this season is relatively more). It is, within the limitations of 1-D model, clearly seen that the emission of enormous amount of CH_4 and CO at the surface are escalating the tropospheric level of O_3 . Observational values also give the same indications.

p038 CONTINUOUS AUTOMATIC MEASUREMENTS OF N_2O -, NO -, NO_2 -, AND
 CH_4 -FLUX RATES IN A N-SUPERSATURATED TEMPERATE CONIFEROUS
FOREST IN BAVARIA

K. Butterbach, R. Gasche, and H. Papen
Fraunhofer Institute for Atmospheric Environmental Research,
D-82467 Garmisch-Partenkirchen, Germany

In an effort to establish a broader data base for the estimation of the contribution of temperate coniferous forest soils to the global and regional budgets of N_2O , complete annual cycles of N_2O emission rates are determined by use of fully automated measuring system in a N-supersaturated coniferous forest in Bavaria (The "Höglwald"). Since NO_x is involved in the formation of tropospheric O_3 , which itself is a greenhouse gas, NO and NO_2 flux rates are also measured continuously using a completely automated measuring system. In order to estimate the sink strength of this N-supersaturated forest ecosystem for atmospheric CH_4 , complete annual cycles of flux rates of this radiatively important trace gas are also followed. Furthermore, the impact of liming of the acid soils on the flux rates of these trace gases is studied. The design of the completely automated measuring systems as well as first results obtained during autumn, winter, and spring 1993/1994 will be presented.

p039

Nitrous oxide fluxes from a drained organic soil, measured by chamber/GC and chamber/IR methods

P. Ambus and S. Christensen (Department of Population Biology, University of Copenhagen, Denmark); H. Clayton, K.A. Smith, J.R.M. Arah and A. Scott (SAC, Edinburgh, UK); M. Maag and A.M. Lind (Soils and Crop Research, Foulum, Denmark); B. Galle, D.W.T. Griffith and L. Klemetsson (IVL, Gothenburg, Sweden)

During a two-week field campaign in August 1993 several chamber methods were used to measure N_2O fluxes from an organic soil in land reclaimed by drainage. The site is characterised by high fluxes arising from denitrification at ca 75 cm-105 cm depth. Arrays of closed chambers (<1 m² in size) were employed, together with both automated and manual GC systems, to characterise the spatial and temporal variations in the flux. Ultra-large (>60 m²) chambers were also used, together with long-path IR systems. Fluxes were of the order of 50-100 g N_2O -N ha⁻¹ d⁻¹; good agreement was obtained between the different chamber methods, and between chamber and micrometeorological methods (described in another poster presentation: *Therrien et al.*)

p040

N_2O emissions from rice paddy fields

H. Tsuruta, K. Yagi, K. Kanda, and T. Hirose
National Institute of Agro-Environmental Sciences, Japan

It is well known that rice paddy fields are one of the major sources of atmospheric CH_4 . N_2O flux, however, was not measured from paddy fields, although paddy soils after water drainage for harvest are a possible source of atmospheric N_2O . We have initiated to measure N_2O flux from a Japanese paddy field since August 1992 by a closed chamber method, in addition to fluxes of CH_4 and CO_2 . The vertical profiles of these gases in the soil have been also measured. In the no flooding period, from August or September to coming April, when the soil was under reduced conditions, N_2O and CO_2 were emitted, while the emission of CH_4 stopped. During 2-3 months after the water drainage, N_2O and CO_2 fluxes were higher with the decomposition of organic matter, and the uptake of CH_4 to the soil was observed. In winter and spring, the emissions of N_2O and CO_2 were much lower than in autumn due to the lower soil temperature. No detectable emission or absorption of N_2O was not found during a flooding period from May to August in 1993. These results demonstrate that rice paddy fields are also one of the sources of atmospheric N_2O , and the N_2O emission rate from rice paddy fields is expected to be higher in the tropical region where soil temperature is much higher than in the mid-latitude region.

p041

NO and N_2O emissions from fertilized soils
in field and laboratory experiments

T. Hirose and H. Tsuruta
National Institute of Agro-Environmental Sciences, Japan

NO is emitted to the atmosphere from natural and fertilized soils as well as N_2O . The production processes and the factors controlling the emission of NO , however, have not been made clear compared with N_2O . We have carried out the field measurement of NO and N_2O fluxes from fertilized soils with the application of nitrogen fertilizer to volcanic ash soils. The flux measurement confirmed the results of our previous measurements that NO flux was larger than N_2O flux, and temporal change of the ratio of NO -N to N_2O -N was observed. The measurement on the vertical profiles of the NO and N_2O concentrations in soil atmosphere showed that the depth of the highest concentration was different. A few data from the measurement in a paddy field after water drainage, however, showed NO flux was lower than N_2O flux. Focussing on the factors controlling the temporal change of the ratio of NO flux to N_2O flux, an incubation experiment is being performed.

p043

The Distribution of Light Halogenated Hydrocarbons in the Troposphere

R. Koppmann, F.J. Johnen, and J. Rudolph
Institut für Atmosphärische Chemie, Forschungszentrum Jülich, 52425 Jülich, Germany

Halogenated hydrocarbons of different atmospheric lifetimes and similar source distributions can be used as tracers for urban and industrial emissions and long range transport. During the cruise ANT VIII/1 of the German research vessel *Polarstern* in August/September 1989 the distributions of the atmospheric concentrations of light halogenated hydrocarbons (CH_3Cl , CH_2Cl_2 , C_2HCl_3 and C_2Cl_4) were measured over the Atlantic between 45°N and 30°S by in-situ gas chromatography. The methylchloride distribution was uniform with an average mixing ratios of 532 ± 8 and 550 ± 12 ppt in the Northern and Southern Hemisphere, respectively. Dichloromethane increased linearly between the ITCZ and 45°N with average mixing ratio of 36 ± 6 ppt and was almost constant in the Southern Hemisphere with 18 ± 1 ppt on average. Tetrachloroethene mixing ratios were between less than 1 ppt and 10 ppt in the Northern Hemisphere and always below 3 ppt in the Southern Hemisphere. Similar to dichloromethane tetrachloroethene was constant in the Southern Hemisphere and increased north of the equator linearly towards more northern latitudes. This is compatible with the predominantly industrial origin of these compounds. Trichloroethene varied between 0.3 ppt and about 15 ppt in the Northern Hemisphere with an average of 3 ± 1 ppt and was generally lower than 1 ppt in the Southern Hemisphere. These findings agree with the results obtained during the STRATOZ III aircraft campaign in 1984. In general, for the halocarbons, except CH_3Cl , the north-south gradients are similar. Due to the relatively long atmospheric lifetimes only small vertical gradients were found.

p044

Seasonal variation of several halocarbons in the Arctic troposphere at Alert, Canada

Y. Yokouchi¹, L. A. Barrie², D. Toom² and H. Akimoto³¹National Institute for Environmental Studies, Japan, ²Atmospheric Environment Service, Canada, ³Research Center for Advanced Science and Technology, Tokyo Univ., Japan

Recent studies (Barrie et al., 1988; McConnel, 1992) have shown the importance of halogens in the Arctic tropospheric ozone chemistry. Volatile halocarbons are possible sources of the halogens (Cl, Br and I) through their chemical reaction. However, very limited data are available for their seasonal change in the Arctic area. Therefore, we conducted weekly measurements of trichloroethylene (C₂HCl₃), tetrachloroethylene (C₂Cl₄), dibromomethane(CH₂Br₂) and dibromochloromethane(CHBr₂Cl) as well as bromoform(CHBr₃), through January, 1992 - September 1993. All the compounds except for CH₂Br₂ showed significant seasonal variation. The concentration of C₂HCl₃ was around 6 ppt in December - February, and rapidly decreased to as low as 0.1 ppt during March-April when the surface-ozone depletion occurred. C₂Cl₄ showed less seasonal variation in the range of 3 - 12 ppt. The difference in their decrease ratio in the summertime was almost consistent with the difference in their reactivity with OH radicals. The concentration of CHBr₃ (0.3 - 3.5 ppt) was approximately one-third of the values at Point Barrow, Alaska reported by Ciceron et al.(1988), although its seasonal trend was similar to each other. CHBr₂Cl and CH₂Br₂ which are likely to be natural-origin, did not exceed 1 ppt.

p045

Accurate Measurements of CFC-114 and Halon Concentrations in the Atmosphere

Limin CHEN, Yoshihiro MAKIDE, and Takeshi TOMINAGA
The University of Tokyo, Tokyo, Japan

Among the chlorofluorocarbons and halons which have been internationally regulated according to the 1987 original Montreal Protocol and the following revisions, reliable atmospheric measurement data and the distributions of CFC-114 (CClF₂CClF₂), Halon-1301 (CBrF₃) and Halon-1211 (CBrClF₂) were not reported because of their extremely low concentrations, some interferences in the analysis, and difficulties in preparation of pptv (10⁻¹² v/v) level calibration standards. We have established an accurate measurement system and the analytical procedure for CFC-114 and Halon concentrations in the atmosphere.

Atmospheric samples collected in Hokkaido or at Syowa Station in Antarctica and stored in our laboratory from 1986 were analyzed. Sample aliquots in canisters were preconcentrated and analyzed by electron-capture gas chromatography (ECGC). While the halon and CFC-114 peaks are usually overlapped with other halocarbons and ECD-sensitive isomer CFC-114a (CCl₂FCF₃), respectively, the complete separation of these compounds were attained with the double column system or with a special column for isomer separation. Vertical distributions of CFC-114 and halons up to the mid-stratosphere were also obtained by analyzing the stratospheric samples collected with a balloon-borne liquid-helium cryogenic sampler. The annual increasing rates of these compounds in the troposphere have been slowing down since 1990 while they are still larger than other major CFCs (such as CFC-11 or CFC-12). Even after the complete phase out of these compounds, it will need a long time before the concentrations begin to decrease due to their extremely long atmospheric lifetimes.

p046 ATMOSPHERIC CHEMISTRY OF FO₂, CF₃O and FCO_x RADICALSOle J. Nielsen, Thomas Ellermann, Jens Sehested and Knud Sehested
CRS, ES&T Dept, Risø National Laboratory, DK-4000 Roskilde, Denmark

The atmospheric chemistry of FO₂, CF₃O and FCO_x radicals have been studied using pulse radiolysis combined with UV absorption spectroscopy. Upper limits for the rate constants of the reaction of the FO₂ radical with O₃, CH₄, and CO were determined to be <3.4x10⁻¹⁶, <4.1x10⁻¹⁵, and <5.1x10⁻¹⁶ cm³molecule⁻¹s⁻¹, respectively. The rate constants for the reactions of FO₂ radicals with NO and NO₂ were measured to be (1.47±0.08)x10⁻¹² and (1.05±0.15)x10⁻¹³ cm³molecule⁻¹s⁻¹, respectively. From computer modelling of experimental absorption transients at 254 nm and 276 nm, upper limits of the rate constants for the reaction of CF₃O₂ and CF₃O radicals with ozone were determined as <0.5x10⁻¹⁴ and <1x10⁻¹³ cm³molecule⁻¹s⁻¹. UV spectra of FCO and FC(O)O₂ radicals were measured over the ranges 265-275 and 220-290 nm, respectively. The decay of UV absorption was used to study the kinetics of the self reactions of FCO and FC(O)O₂ radicals. Observed self reaction rate constants were (1.1±0.2)x10⁻¹¹ and (6.0±0.7)x10⁻¹² cm³molecule⁻¹s⁻¹. A rate constant, (1.2±0.2)x10⁻¹² cm³molecule⁻¹s⁻¹, was derived for the addition reaction FCO + O₂ → FC(O)O₂ in 1000 mbar of SF₆ diluent. Rate constants for the reactions of FCO, FC(O)O, and FC(O)O₂ radicals with NO were determined to be (1.0±0.2)x10⁻¹², (1.3±0.7)x10⁻¹⁰, and (2.5±0.8)x10⁻¹¹, cm³molecule⁻¹s⁻¹, respectively. An upper limit of <6 x 10⁻¹⁴ cm³molecule⁻¹s⁻¹ was measured for the reaction of FC(O)O radicals with O₃. Results are discussed with respect to the atmospheric chemistry and potential ozone depletion of HFCs.

p047

Reactions of Perfluoroalkyl Radicals (CF₃ and C₂F₅) with O₂H. Sato, M. Takeuchi, and R. Isaki
Department of Chemistry, Faculty of Science,
Science University of Tokyo, Japan

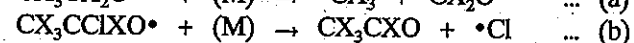
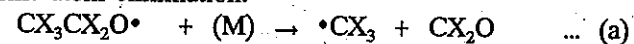
Hydrofluorocarbons (HFCs) have been used already as alternatives to fully halogenated chlorofluorocarbons (CFCs), because HFCs are less stable in the atmosphere than CFCs and thus have greatly reduced global warming potentials. It is necessary to understand their degradation mechanisms in the atmosphere in order to assess the lifetimes of HFCs and secondary pollution by their degradation products. CF₃ and C₂F₅ radicals are formed during the tropospheric degradation reactions of HFC-134a (CH₂FCF₃), HFC-125 (CHF₂CF₃), and 5FP (C₂F₅CH₂OH). Therefore, the reactions of these perfluoroalkyl radicals with O₂ have been studied by using FT-IR. To generate CF₃ and C₂F₅, the H abstraction reactions of CHF₃ and CHF₂CF₃ and the photodissociation reactions of CF₃I and CF₃CF₂I were performed. These fluoroalkyl radicals reacted with O₂ to form the peroxy radicals, and finally to form CF₃COF, CF₂O, and CF₃OOOCF₃ as the major products. The effect of the O₂ partial pressure on the yields of these degradation products was also investigated to evaluate the F abstraction reaction by O₂. The possible atmospheric significance of these degradation products is discussed.

C-C Bond Cleavage of Fully Halogenated Chlorofluoroethoxy Radicals

R. Isaki and H. Sato

Department of Chemistry, Faculty of Science,
Science University of Tokyo, Japan

Many investigations about the degradation mechanisms and products of hydrochlorofluorocarbons (HCFCs) and hydrofluorocarbons (HFCs) under atmospheric conditions have been reported already. In those degradations, the fully halogenated chlorofluoroethoxy radicals can react by two main pathways; (a) unimolecular decomposition by C-C Bond Cleavage, and (b) unimolecular decomposition by chlorine atom elimination.



The branching ratios of these pathways (1) and (2) about $\text{CX}_3\text{CCl}_2\text{O}$, CX_3CClFO , and $\text{CX}_3\text{CF}_2\text{O}$ ($\text{X}=\text{F}, \text{Cl}$) have been studied by using FT-IR. These haloethoxy radicals were formed by the Cl atom-initiated oxidation reactions of CHX_2CX_3 . CX_3CXO and CX_2O , the degradation products, were determined from the FT-IR spectra in order to obtain the branching ratios. The branching ratios are found to be correlated to the differences in the heats of decomposition reaction, $\Delta H_{(a)} - \Delta H_{(b)}$, which are obtained by the group additivity method (Benson, 1976) or the ab initio calculations.

p049 DRS-IR measurement of the surface products on sodium chloride particles exposed to the ambient air in the Arctic

S. Kutsuna and T. Ibusuki

National Institute for Resources and Environment, MITI, Japan

The role of heterogeneous reactions on sea salts in the formation of nitrous acid (HONO) in the Arctic during polar sunrise was studied. A diffuse reflection type FTIR spectrometer was used to measure surface products on sodium chloride (NaCl) particles exposed to the ambient air at Alert, North West Territories, Canada (82.5°N, 62.3°W). The IR absorption bands due to nitrite ion (NO_2^-) on NaCl were observed in both winter and spring, while the intensity in winter was greater. In winter a heterogeneous reaction of dinitrogen pentoxide (N_2O_5) on NaCl is probably the major formation pathway of NO_2^- on NaCl, by considering the accumulation rates of NO_2^- owing to several nitrogen species in our laboratory and their atmospheric concentrations at Alert. The formation of NO_2^- in spring may imply other heterogeneous reactions involving some gaseous reactants other than N_2O_5 .

HYDROGEN CHLORIDE RELEASE FROM SEASPRAY: FIELD MEASUREMENTS IN CLEAN AND POLLUTED AIR MASSES IN A TROPICAL AREA

Tavares, T.M. and Rocha, V.C.
Chemistry Institute, Federal University of Bahia, Brazil

Hydrogen chloride represents a chlorine reservoir, specially in winter low temperature stratospheric clouds over the arctic regions. One of the largest source of HCl in the atmosphere is the seaspray as a result of its release due to adsorption of SO_2 and/or H_2SO_4 , NO_2 and/or HNO_3 and other gaseous species from the atmosphere. Its most important removal process in the troposphere is reaction with NH_3 and wet deposition (washout or closed incorporation followed by rainout).

Field measurements in the coastal area around 12°37'S and 38°W have been made simultaneously for 24h sampling for gaseous NH_3 and SO_2 using denuders tubes, for gaseous HCl and HNO_3 and fine particulated NH_4NO_3 and H_2SO_4 with a thermodenuder system and for anions and Na^+ in particulates fractionated by size with a six stage Berner impactor. Determination were carried out by ion chromatography for anions, flame photometry for sodium ion, spectrophotometry with pararosaniline for SO_2 and with indophend blue for NH_4^+ .

Concentrations of gaseous HCl and of Cl^- in seaspray particles ranged respectively from 0.51 to 1.9 (average 0.98) and from 5.2 to 11 $\mu\text{g}/\text{m}^3$ in clean air masses from the Atlantic and from 0.075 to 1.5 and from 0.7 to 6.5 in same air masses enriched by industrial pollution. Taking sea salt production as 1,000 Tg/yr and HCl/ Cl^- ratio of 1/5 obtained for these tropical conditions, annual production of HCl from seaspray would be 100 Tg/yr. Chloride deficit in particles were higher than accounted by levels of NO_3^- and SO_4^{2-} present, indicating adsorption of other species onto seaspray particles. HCl plus NH_4Cl levels did not account for all the chloride deficit in the marine particles.

Global Emissions of Organochlorine Pesticides

Eva C. Voldner¹, M. Trevor Scholtz²,

Keith A. Davidson², Arthur Li¹ and Carol Slama²

Estimation of pesticide emissions to the atmosphere are essential input to global scale models for the transport, transformation and deposition of organochlorines. Such models are important tools for determining the historical and future trends of the impacts of pesticides on sensitive areas. The trends in emissions are also important for understanding and predicting the response times of various components of the ecosystem to changes in the atmospheric loadings of these air toxics. Estimates of emissions for areas of heavy pesticide use, worldwide, have been made for several pesticides of concern such as DDT, lindane, toxaphene and atrazine using a numerical air-surface exchange model. The model simulates the movement of pesticides in soils and their volatilization from the surface and canopy to the atmosphere following application to agricultural lands and crops. The emissions are dependent on pesticide application practices and use rate, as well as meteorology, soil properties and the physical/chemical properties of the pesticides. In preparing the inventory, pesticide use data and model input data characteristic of each area were used in the air-surface exchange model.

1) Environment Canada, Downsview, Ontario, Canada.

2) Ortech, Mississauga, Ontario, Canada

p052

Airborne Hydrocarbon Measurements During The North Atlantic Regional Experiment,
1993

P. Goldan, B. Kuster, F.C. Fehsenfeld and M. Trainer
U.S. Dept. of Commerce, Aeronomy Laboratory, Boulder, Colorado USA
H. Niki
York University, Chemistry Dept., Toronto, Ontario, CANADA

An automated gas chromatograph, capable of immediate analysis of whole air samples for the light alkane, alkene and alkyne hydrocarbons from ethane to pentane, was flown aboard an aircraft based in Portland, Maine, USA during August 1993 as part of the North Atlantic Regional Experiment (NARE). Samples were acquired and analyzed every 15 minutes allowing the determination of vertical distributions from central Massachusetts USA (72°W) to Sable Island, Nova Scotia, Canada (60°W). Samples acquired during low level over flights of ground based measuring sites and during paired flights with other aircraft in the NARE program provided hydrocarbon measurements for comparison with other data sets. The use of these data to better understand the spatial distribution of anthropogenic ozone precursors in the North Atlantic region and as corroboration of other anthropogenic tracer measurements will be presented.

p053

The Soluble-Organic Fraction of Aerosols as Determined in NARE

S.-M. Li, C.M. Banic, W.R. Leitch, P.S.K. Liu, H.A. Wiebe
Atmospheric Environment Service, Downsview, Ontario, M3H 5T4, Canada

X.-L. Zhou, and Y.-N. Lee
Brookhaven National Laboratory, Upton, New York, 11973, USA

During a five week period in August and September, 1993, aerosol chemical and physical measurements were made near the coast in southern Nova Scotia, Canada as part of the North Atlantic Regional Experiment (NARE). Aerosol samples were collected on teflon filters both at a coastal ground site at Chebogue Point (37 filters of approximately 3 hour duration each) and within a 100 km radius at altitudes up to 5 km with the Canadian Institute for Aerospace Research De Havilland Twin Otter aircraft (39 filters of 30 minutes to 1 hour each). During filter collection, dry aerosol size distributions were measured continuously at the surface and aloft using Particle Measuring System-PCASP-100X light scattering probes. Total small aerosol concentrations were determined with a TSI 3025 Ultrafine Condensation Particle Counter and at surface with a TSI 7610 CN counter. The CCN concentrations at 0.3% supersaturation were measured at the surface with a DH Associates MI CCN counter. The filter samples were analyzed for inorganic ions including SO_4^- , NO_3^- , Cl^- , NH_4^+ , Na^+ , K^+ , Ca^{++} , Mg^{++} and for water soluble organic species including formate, acetate, propionate, pyruvate, oxalate, glyoxylate, pyruvate, methanesulfonate, formaldehyde, and glycoaldehyde. This paper investigates the relationship between the inorganic and organic species. It will also assess (1) the abundance of the organic species compared with the water soluble mass and compared with the total mass determined by the PCASP probes, and (2) the efficiency of these species as CCN.

p054

Airborne and Surface Formaldehyde and Multi-Oxygenated Carbonyl Measurements
During the 1993 NARE Intensives

Yin-Nan Lee and Xianliang Zhou
Environmental Chemistry Division, Brookhaven National Laboratory, Upton, NY
U. S. A.

Formaldehyde (Fa) and multi-oxygenated carbonyls, including glycoaldehyde (Ga), glyoxal (Gly), methylglyoxal (Mgl), glyoxylic acid (Gl-A) and pyruvic acid (Py-A), were measured both on the ground at a coastal site (7-min integrated every 30 min) and aloft, up to 5 km, on board a Canadian NRC Twin Otter (5-min integrated, continuous) in southern Nova Scotia, Canada, during the 1993 NARE summer intensive. The concentrations of Fa on the ground and aloft ranged up to ~3 ppb and ~4 ppb, respectively. The multi-oxygenated carbonyls exhibited concentrations in decreasing order: $\text{Gl-A} > \text{Ga} \sim \text{Mgl} \sim \text{Gly} > \text{Py-A}$, and on occasions surface concentration of Gl-A approached that of Fa. While the photochemical reaction products Fa, Ga, Gly, and Mgl correlated strongly, Gl-A, Py-A and an unknown soluble carbonyl, which were also well correlated, displayed a distinct diurnal pattern decoupled from the photochemical signatures, suggesting possible local biogenic sources for the latter group. The vertical distribution of formaldehyde and its relation with that of ozone and accumulation mode particle concentrations permitted assessment of the relative importance of photochemical production and transport in governing ozone in both boundary layer and free troposphere. In the shallow marine inversion layer, Fa showed markedly reduced concentrations with respect to O_3 , indicating that deposition to surface water is an important loss process for Fa. The relationships of the carbonyls with hydrocarbon precursors and the contributions of the carbonyls to free radical, O_3 and CO budgets in this geographical region will be discussed.

p055 Trace Gas Measurements over Southern Nova Scotia during the 1993 NARE

L. Kleinman, P. Daum, S. Springston, J. Lee, Y.-N. Lee, and X. Zhou
Brookhaven National Laboratory, Upton, NY, USA
R. Leitch, C. Banic, and G. Isaac
Atmospheric Environment Service, Downsview, Ontario, Canada
I. MacPherson
Institute for Aerospace Research, Ottawa, Canada
H. Niki
York University, North York, Ontario, Canada

As part of the summer 1993 NARE intensive, the Canadian National Research Council Twin Otter was used to measure the concentration of O_3 and O_3 precursors in a series of more than 40 vertical profiles over the NOAA surface site in Chebogue, Nova Scotia. Under conditions of southwest flow this location is downwind of plumes from major eastern US cities. Elevated concentrations of O_3 (up to 120 ppb) and other pollutants (CO , VOC's, NO_x , SO_2 and aerosol particles) were observed in distinct layers at altitudes between 500 and 3000 m. Correlations between pollutants are similar to that observed in continental locations. We will present an overview of these trace gas measurements focusing on concentrations as a function of altitude, dew point, and photochemical age as determined by the ratios of light hydrocarbons. Evidence will be presented for an anthropogenic influence on O_3 , even in dry layers at high altitude.

p056

Measurements of Tropospheric Nitrogen Oxides in the Central North Atlantic Region

R. E. Honrath and M. C. Peterson
Dept. of Civil and Environmental Engineering
Michigan Technological University, U. S. A.

We report the results of measurements of NO_y (total reactive nitrogen) and NO made at a site in the Azores Islands during August 1993 (27.35°W, 38.73°N, elevation 1 km). These measurements were made during the summer intensive of NARE (North Atlantic Regional Experiment), with the aim of investigating the extent of impacts of anthropogenic emissions (primarily North American) on the photochemistry of the mid-North Atlantic troposphere. Air sampled at the site was frequently characteristic of the marine boundary layer (MBL) in that region of the North Atlantic; however, free tropospheric air was observed following passage of cold fronts. NO_y mixing ratios ranged from below 100 pptv to >1 ppbv, with the higher levels reflecting periods when the site was influenced by island sources and, on at least one occasion, free-tropospheric air unaffected by local emissions. The extent to which evidence of anthropogenic impacts on tropospheric composition was observed will be discussed using these measurements, in conjunction with observations of a number of other species made at the site by collaborating investigators and the results of back-trajectory analyses.

p057

Impact of anthropogenic emissions on the North Atlantic atmosphere

Prasad Kasibhatla, Georgia Institute of Technology, Atlanta, Georgia, U.S.A

The 11-level GFDL global chemical transport model (GCTM) has been used to assess the impact of anthropogenic and natural sources on the global NO_x distribution. The GCTM, which has a horizontal resolution of ~265 km, is driven using meteorological data from a GFDL general circulation model. NO_x , HNO_3 , and PAN are explicitly treated in the GCTM as transported species, with their chemical interconversion rates specified from off-line calculations. NO_x sources specified surface-based fossil fuel combustion emissions (21 tg N year^{-1}), biomass burning emissions (8.5 tg N year^{-1}), biogenic emissions (5.6 tg N year^{-1}), production in lightning discharges (3 tg N year^{-1}), production in the stratosphere (0.65 tg N year^{-1}), and sub-sonic aircraft emissions (0.45 tg N year^{-1}). The model is currently being extended to include a more complete on-line tropospheric chemistry module, in order to study the factors governing the distribution of tropospheric ozone and of its precursors. Analysis presented here will focus on detailed comparisons of model results with measurements taken during the NARE 1993 field campaign over the north-western Atlantic Ocean. The mechanisms governing the spatial and temporal variability in model results will be elucidated, and concurrent analysis of observations, using tools such as trajectory box model calculations, will be performed to shed light on the factors regulating the export of anthropogenic emissions to the North Atlantic atmosphere. Such a study can be used to test our understanding of the chemical system in this region, as well as to interpret the spatially- and temporally-limited measurements in terms of a broader basin-scale and seasonal context.

p058

Modeling the Role of Continental Emissions on Tropospheric Ozone Over the North Atlantic Ocean*

C.S. Atherton, J. Penner, S. Sillman[†], and J. Walton,
Global Climate Research Division
Lawrence Livermore National Laboratory
P.O. Box 808, L-262, Livermore, CA 94551 USA

[†]Department of Atmospheric and Oceanic Science, University of Michigan,
Ann Arbor, MI 48109-2143 USA

Man's activities may significantly affect the concentrations of a number of chemically and radiatively important tropospheric gases, including O_3 , OH, PAN, and NO_x . We have developed a global, three-dimensional, chemistry-transport-deposition model of the troposphere (GRANTOUR) which includes the oxidation cycles of CO, CH_4 , and non-methane hydrocarbons (NMHCs). The model predicts the concentrations of 76 species, including O_3 , OH, PAN, NO, NO_2 , HNO_3 , CO, isoprene, and other NMHCs. Here we investigate the role of North American emissions on ozone levels over the North Atlantic Ocean and adjacent regions. Model simulations are conducted using the IGAC emission databases for anthropogenic NO_x and biogenic hydrocarbons, as well as CO, NMHCs, and other NO_x sources. We examine a base case and two scenarios in which emissions over the North American continent are significantly reduced to assess the effect of North American emissions on the North Atlantic and nearby regions. To assess its validity, model results from the base case simulations are compared to data from the NARE campaigns.

*This work was performed under the auspices of the U.S. Department of Energy by the Lawrence Livermore National Laboratory under Contract No. W-7405-Eng-48.

p059

Trajectory Modelling of the North Atlantic Region

O. Wild, K.S. Law and J.A. Pyle
Centre for Atmospheric Science, Cambridge, U.K.

Measurements taken over the Azores and Tenerife by the Meteorological Research Flight during the OCTA Campaign in August 1993 indicate the possibility of long-range transport of pollutants from North America to the western coast of the Atlantic. To test this hypothesis, analysed wind fields are used to perform a trajectory analysis for the region of Izaña, Tenerife, to determine the sources of air masses for the period of August. These 3-D back trajectories are used to define a climatology for the period. A photochemical trajectory model is run along a number of representative trajectories to determine the sensitivity of the chemistry to the meteorological conditions. The sensitivity of the chemistry to a range of realistic initial chemical conditions is also investigated. These runs are then used to assess the importance of North America as a source of pollution for the western coast of the Atlantic. The relative contributions of photochemically aged air from Europe and North America to the composition of the air at the site is also examined.

Large-Scale Air Mass Characteristics Observed Over the Western Pacific During the Summertime

E. V. Browell¹ and PEM-West A Science Team

¹NASA Langley Research Center, Hampton, Virginia, U.S.A.

Remote and in situ measurements of gases and aerosols were made with airborne instrumentation to investigate the sources and sinks of tropospheric gases and aerosols over the western Pacific during the NASA Global Tropospheric Experiment (GTE)/Pacific Exploratory Mission-West conducted in September-October 1991 (PEM-West A). At low latitudes, the airflow was generally from the east, and the air had low O₃ and low aerosol loading. The O₃ was less than 10 ppbv near the surface to less than 30 ppbv in the middle to upper troposphere. In the mid and high latitude regions, the air flow was mostly westerly, and the background O₃ was generally less than 55 ppbv. On 60% of the PEM-West flights, O₃ was observed to exceed these levels in regions that were determined to be associated with stratospheric intrusions. In convective outflows from typhoons, near-surface air with low O₃ (<25 ppbv) was transported into the upper troposphere (>10 km). Several cases of continental plumes from Asia were observed over the Pacific during westerly flow conditions. These plumes were found in the lower troposphere with O₃ levels in the 60-80 ppbv range and with enhanced aerosol scattering. The frequency of observation of these air mass types and their average chemical composition are discussed in this paper.

Ratios of Reactive Nitrogens over the Pacific during PEM-West A

M. Koike¹, Y. Kondo¹, S. Kawakami¹, H. B. Singh², H. Ziereis³, and J. T. Merrill⁴

1. Solar Terrestrial Environment Laboratory, Nagoya University, 3-13 Honohara, Toyokawa, Aichi, 442 Japan
2. NASA Ames Research Center, Moffett Field, CA 94035
3. German Aerospace Research Establishments (DLR), 82230 Wessling, Germany
4. Center for Atmospheric Chemistry Studies, Graduate School of Oceanography, University of Rhode Island, Narragansett, RI 02882

Measurements of total reactive odd nitrogen (NO_y) and known individual odd nitrogen species were made over the Pacific Ocean in September and October 1991 during the NASA Global Tropospheric Experiment, Pacific Exploratory Mission - West A (GTE/PEM-West A). The ratios between active nitrogen (NO_x), peroxyacetyl nitrate (PAN), and NO_y have been investigated in these data. The NO_x/NO_y ratios in the continental air showed a C-shaped vertical profile, while they generally increased with altitude in the oceanic and tropical air. In the middle troposphere, the NO_x/NO_y ratios were similar in continental, oceanic, and tropical air. The PAN/NO_y ratios in the continental air were systematically higher than those in the oceanic and tropical air. The observed features show that the influence of the anthropogenic emissions on both the continental and the oceanic air. The high latitude air is characterized by low NO_x/NO_y ratios and high PAN/NO_x ratios probably due to the low atmospheric temperatures.

Reactive Nitrogen over the Pacific Ocean during PEM-West A

Y. Kondo,¹ H. Ziereis,² M. Koike,¹ S. Kawakami,¹ G. L. Gregory,³ G. W. Sachse,³ H. B. Singh,⁴ D. D. Davis,⁵ and J. T. Merrill⁶

- 1 Solar Terrestrial Environment Laboratory, Nagoya University, Toyokawa, Japan
- 2 German Aerospace Research Establishments (DLR), Wessling, Germany
- 3 NASA Langley Research Center, Hampton, Virginia
4. NASA Ames Research Center, Moffett Field, California
- 5 School of Earth and Atmospheric Sciences, Georgia Institute of Technology, Atlanta
- 6 Center for Atmospheric Chemistry Studies, Graduate School of Oceanography, University of Rhode Island, Narragansett,

Aircraft measurements of NO and NO_y were carried out during NASA's PEM-West-A. Measurements were made over the Pacific Ocean, predominantly over the western Pacific Ocean in September and October 1991. The NO, calculated NO_x, and NO_y mixing ratios in the continental air are significantly higher than in the maritime air. In maritime air, NO increased with altitude. In continental air, NO and NO_x mixing ratios showed a C-shaped profile. NO_y didn't show an apparent altitude dependence neither in maritime nor in continental air. The lowest values of NO, NO_x, NO_y, PAN, and O₃ were observed in tropical airmasses throughout the whole altitude region. PAN, O₃, CO, CH₄, and C₂H₆ data have been used to study the budget of the reactive nitrogen over the Pacific Ocean. These data suggest that photochemical production of O₃ from precursor species over the continent is important for the O₃ budget.

An Assessment of the Photochemical O₃ Tendency in the Western North Pacific as Inferred from GTE/PEMWest(A) Observations during Fall 1991

D. D. Davis, J. Crawford, G. Chen, J. Bradshaw, and S. Sandholm
School of Earth and Atmospheric Sciences, Georgia Institute of Technology, Atlanta, GA 30332

G. Sachse, B. Anderson, J. Collins, J. Barrick, and E. Browell
NASA Langley Research Center, Hampton, VA 22331

D. Blake and S. Rowland
Dept of Chemistry, University of California at Irvine, Irvine, CA 92717

H. Singh
NASA Ames Research Center, Moffett Field, CA 94035

Y. Kondo
Nagoya University, 3-13 Honohara, Toyokawa, Aichi, Japan 442

B. Heikes and J. Merrill
University of Rhode Island, Narragansett, RI 02882-1197

R. Talbot
University of New Hampshire, Durham, NH 03824

Based on the results from nearly a thousand independent observations, photochemical box modelling calculations have been used to explore the photochemical ozone tendency of the western Pacific during the fall season of 1991. By filtering the observations according to a fixed zenith angle range (e.g. 30°-55°), meaningful latitudinal and altitudinal trends were assessed for model estimated values for the ozone tendency, P(O₃). The bulk of these data fell into two large geographical zones having distinctively different chemical characteristics. The first of these zones has been labelled the North Pacific Rim region and the second the tropical western North Pacific corridor. The first zone covered the latitude range of 45° to 18°N, the second from 18° to 0°N. With the exception of a small sub-set of data collected in the polluted marine boundary layer near the coast of Japan and China, the altitudinal trend in P(O₃) tended to be out of phase with other critical photochemical parameters such as OH. For example, with the exception of the coastal data, P(O₃) was on average negative at all latitudes for altitudes less than 6 km. However, for the latitude range 18-42° N and altitudes above 6 km, P(O₃) was nearly always positive. Between 0-18° N and above 6 km, P(O₃) was found to be much lower in magnitude and to oscillate between negative and positive values. In general, therefore, the calculated value of P(O₃) was shown to have increasing positive values with increasing latitude and altitude. Correlations with other photochemical species/parameters revealed that the mixing ratio for NO was the single most important factor controlling the sign and magnitude of P(O₃). To be discussed are the detailed chemical processes controlling P(O₃) as a function of altitude and latitude, the nature of the NO_x source at high altitudes, and the photochemical O₃ budget for the western North Pacific.

H₂O₂ and CH₃OOH Distributions Over the North Pacific

Brian Heikes and Meehye Lee
GSO/CACS, University of Rhode Island, RI, USA

In an exploration of tropospheric net-ozone production and sulfur oxidation over the western North Pacific Ocean, H₂O₂ and CH₃OOH were measured using a coil-collector HPLC-analysis method. The measurements were made during the NASA/GTE PEM-West-A mission and were part of the IGAC/APARE program. The airborne study was conducted in Sept. and Oct. of 1991 and extended from 0.3 to 12.5 km and from 0 to 60 N Latitude. Results show a latitudinal gradient in both peroxides at all altitudes; e.g., between 3 and 5 km H₂O₂ median values decrease from 1700 to 500 pptv in going from 0-15 N to 45-60 N, and the corresponding decrease in CH₃OOH was 1100 to 200 pptv. Concentration maxima are observed in both species at altitudes of 2 to 3 km with H₂O₂ concentrations below 1 km lower by 30%, 10% for CH₃OOH, and by a factor of 10 for both above 9 km. The H₂O₂ to CH₃OOH ratio increased with altitude and latitude with ratios <1 in the tropical surface layer and >2 at mid-latitude high altitude. Highest peroxide concentrations were encountered over the Celebes Sea in air which was impacted by aged biomass fire and urban pollutants. CH₃OOH was below the level of detection in stratospheric air. H₂O₂ exceeded SO₂ 95% of the time, with the exceptions generally above 9 km. Above 3 km, O₃ increases with decreasing H₂O₂ and CH₃OOH. Below 3 km, the O₃-CH₃OOH trend is the same but O₃ increases with increasing H₂O₂.

Effects of Typhoon on Semi-Global Scale Mass Transport over the Northern Pacific Ocean

T. Kitada¹, T. Yamamoto¹ and Y. Kondo²

¹Dept. Ecological Eng., Toyohashi Univ. of Tech., Toyohashi 441, Japan

²STE Lab., Nagoya University, Toyokawa 442, Japan

During the months of August to October, typhoon, i.e. a tropical cyclone born over equatorial Pacific ocean, frequently reaches to the mid-latitude Japan area. Strong winds in association with the typhoon should largely contribute to the mass transport into both upper troposphere and remote Northern Pacific of anthropogenic pollutants discharged over East Asia. In this study, a 3-D Eulerian transport/chemistry model in spherical coordinate, with 22 advected species and 90 chemical reactions, is developed and used to simulate spatial distributions of trace chemical species over east Asia and the north-western Pacific ocean for the latter half of September in 1991. The simulations were performed by using the Global Analysis Data for 3D meteorological fields by the Japan Meteorological Agency and anthropogenic emission sources in East Asia. The results are compared with PEM-WBST(A) data, and analyzed, for instance, in terms of upward mass fluxes due to the typhoon and effects of precipitation on concentration-distributions.

Spatial and temporal variability of aerosols over the North Pacific: estimates of anthropogenic contributions.

J.M. Prospero¹, D.L. Savoie¹, R. Arimoto², R.A. Duce³,

¹University of Miami, Miami, FL, ²University of Rhode Island, Narragansett, RI
³Texas A & M University, College Station, TX

Aerosol measurements have been made almost continuously in a network of stations in the central North Pacific beginning in the early 1980's as a part of the SEAREX program. In 1991 the network was augmented in the western Pacific in conjunction with the NASA Pacific Exploratory Mission - West (PEM-West). At all sites weekly filter samples are collected (daily during intensives) and subsequently analyzed for a variety of species: nss-SO₄⁼ and NO₃⁻; selected trace metals (including Sb, Al, V and Se) that provide information on source regions and source type; and methanesulfonate (MSA) which is used as a surrogate for oceanic DMS. There is evidence of substantial anthropogenic impacts at all sites in the North Pacific. At the western Pacific sites (Hong-Kong, Taiwan, Okinawa and Cheju, Korea) the mean concentrations of NO₃⁻ (1.9-5.1 μg m⁻³) and non-sea-salt SO₄⁼ (4.2-9.3 μg m⁻³) are among the highest that we have observed in any ocean region in the world; they are about an order of magnitude higher than those at the three central Pacific locations (Shemya, Midway and Oahu) where the means are 0.22-0.35 μg m⁻³ for NO₃⁻; 0.37-0.53 μg m⁻³ for nss SO₄⁼. At the central Pacific sites, oceanic DMS (based on MSA) contributed over half of the nss-SO₄⁼; in contrast, at the western Pacific sites oceanic DMS contributed less than 5-10% of the nss-SO₄⁼.

Aircraft measurements of tropospheric ozone over the western Pacific Ocean

Yukitomo Tsutsumi, Yukio Makino, Miwako Ikegami and Yuji Zaizen
Meteorological Research Institute, 1-1 Nagamine, Tsukuba, Ibaraki, 305 Japan

We made an aircraft observation of tropospheric ozone between Japan and Philippine in January 1993. The round-trip flights ranged between 4.2 km to 4.6 km altitude were made over Okinawa islands in Japan, Luzon island, Cebu island, and Mindanao island in Philippine (from 34.5° N to 4.65° N) along the longitude of 125° ± 5°E.

The weather condition on the southbound flight route to Davao was fine except over Okinawa where covered with nimbostratus below the aircraft. The high ozone mixing ratio about 50 ppbv and low water vapor mixing ratio were observed from Osaka to Cebu except over Okinawa marked a few ppbv lower ozone level and higher water vapor mixing ratio. The weather condition of local flight over Davao (~4.65° N) was rainy and water vapor mixing ratio was high and ozone mixing ratio was very low (about 20 ppbv). The ozone mixing ratio of transition area between fine and rainy condition (about 10 - 8° N on south bound and 10 - 14° N on north bound) was variable.

The ozone mixing ratio changed from 55 ppbv to 30 ppbv across the boundary at 24° N. Isentropic back trajectory analysis of air parcels starting from several points on the flight route was made. It appears that the ozone decrease around 24° N was attributed to the difference of the trajectory paths. The air parcels around 21° N came from south part of China, on the other hand those around 25° N came from Pacific Ocean.

The results of the Pacific Atmosphere Chemistry Experiment from Australia to Japan will be also reported.

p068

Ozone and Aerosol Measurements Made Over the Tropical Atlantic During the TRACE-A Field Experiment

E. V. Browell, C. F. Butler, M. A. Fenn, W. B. Grant,
G. L. Gregory, B. Anderson, and J. Fishman
NASA Langley Research Center, Hampton, Virginia, U.S.A.

Large-scale distributions of O₃ and aerosols in the troposphere were obtained over the tropical Atlantic with remote and in situ airborne instrumentation during the NASA GTE/TRACE-A (Global Tropospheric Experiment/Transport and Atmospheric Chemistry near the Equator - Atlantic) field experiment conducted in September-October 1992. Gases from extensive fires in Brazil were transported by convective storms into the upper troposphere where O₃ was photochemically produced and advected eastward over the Atlantic. In central Africa, the fires were widespread, and in the absence of convective storms, the fire plumes were advected westward at low altitudes (below ~6 km) over the Atlantic. There was a positive correlation between O₃ and aerosols found in plumes that were not involved in convection. High O₃ (>75 ppbv) was observed in the low-altitude plumes, and in the upper troposphere, O₃ often exceeded 100 ppbv with low aerosol loading. The remote and in situ measurements of O₃ and aerosol distributions have been used to determine the relative contribution of various processes on the buildup of high O₃ over the tropical southern Atlantic.

p069

Simulation of Convective Transport of Biomass Burning Emissions over Brazil During TRACE-A: Effects on Tropospheric O₃ Production

K. E. Pickering¹, A. M. Thompson¹, and W.-K. Tao¹ and
Members of the TRACE-A Science Team

A major outbreak of deep convection occurred during the Brazilian component of the TRACE-A experiment, which took place in the latter part of the 1992 cerrado burning season. We have used the nonhydrostatic version of the NCAR/Penn State Mesoscale Model (MM5) to simulate the sequence of convective storms that occurred over the region during a two-day period. An associated tracer advection/diffusion model was used to transport burning-related species (e.g., CO) with lifetimes considerably longer than the simulation length. We compared the simulated CO fields with regional CO measurements taken from the NASA DC-8. Meteorological profiles from MM5 were used to initialize a cloud-resolving model (Goddard Cumulus Ensemble Model). We used the cloud-scale model to simulate the specific cloud system from which upper level outflow containing greatly enhanced CO, NMHCs, and NO_x was sampled at 9 to 11.5 km with the DC-8. Profiles of ozone precursor gases before and after redistribution by the cloud were used in a 1-D photochemical model to estimate the perturbation to ozone production in the cloud outflow layer.

¹ Address: NASA/Goddard Space Flight Center, Greenbelt, Maryland USA

p070

Global measurements of tropospheric CO and CH₄ by MOPITT and their scientific applications

John C. Gille,* James R. Drummond,+ Liwen Pan,* Mark D. Smith* and Guy Brasseur*
*National Center for Atmospheric Research, Boulder, CO, USA
+University of Toronto, Toronto, Canada

The Measurement of Pollutants in the Troposphere (MOPITT) experiment will fly on the AM Platform of the NASA's Earth Observing System (EOS), measuring upwelling radiances from which the vertical distribution of CO, and the total column amount of CH₄ can be determined over the globe. We briefly describe the retrieval methods, and show results of data simulations which indicate that a precision of 10% or better can be obtained for CO, and about 1% for column CH₄, for realistic instrument parameters. Plans for ground-based and aircraft tests will be described, and preliminary results presented.

Such data will be very useful in aiding the understanding of tropospheric chemistry, and improving tropospheric chemical models. A possible way to use such data in models will be described, and preliminary results of some experiments will be presented.

p071

Stratosphere Troposphere Exchanges and their implication for the tropospheric ozone budget: results of the European campaigns

G. Ancellet¹, M. Beekmann¹, L. Gray², G. Vaughan³
Service d'Aéronomie, Paris, France
Rutherford Appleton Laboratory, Chilton, U.K.
University of Wales, Aberystwyth, U.K.

During the last four years, several studies were conducted in Europe to improve the knowledge of the Stratosphere Troposphere Exchanges (STE) on tropospheric ozone budget by climatological studies using ozone records in Europe and meteorological analysis, and by coordinated campaigns in Europe to assess the respective impact of tropopause foldings and cut-off lows. The climatological studies includes an estimate of the seasonal and altitudinal variability of the ozone to potential vorticity ratio, and a comparison of the ozone variability for air masses with a recent stratospheric origin compared to the variability of the tropospheric background. During the European campaigns, wind profiles, ozone profiles, and tropopause structure were measured at several stations in Europe. These data were interpreted by the means of ECMWF analysis to compute potential vorticity fields and air mass trajectories. Modelling studies were performed using a 3D tracer model including transport and radiative processes. The estimated transport by tropopause folds is smaller by at least a factor of two than earlier studies. Impact of cut-off low dissipation show for some cases no contribution to STE, while another other case exhibits a contribution similar to the transfer by a tropopause fold. Modelling studies were able to reproduce the observed evolution of a cut-off low.

p072

Climatological analysis of free tropospheric ozone in Europe: relationship between ozone variability, meteorological variables, and precursor gases.

M. Beekmann¹, G. Ancellet¹, D. de Muer²

¹Service d'Aéronomie, Paris, France

²Institut Royal de Météorologie, Bruxelles, Belgique

Ozone profiles were measured at several stations in Europe during the last 10 years. Part of this work was done in the frame of the Tropospheric Ozone Network, which includes also a network of more than 15 ground-based stations to monitor ozone precursor gases. The work presented here includes the analysis of ozone vertical profiles performed at two of these stations (the French Observatoire de Haute Provence (OHP), 44°N, 6°E, and the Belgium Uccle station, 51°N, 2°E). To assess the impact of transport processes on the observed ozone variability in the free troposphere, potential vorticity (PV) was used as a criteria for impact of stratospheric input in the troposphere, and air mass trajectories were used to classify the ozone profiles according to different source regions. Preliminary work shows that the impact of stratospheric input is rather large on the observed ozone variability (correlation of 50% between PV and O₃), but that the overall contribution to tropospheric ozone should remain rather small (15 ± 10 ppb). Results on the impact of source regions is currently analysed and will be presented. The contribution of photochemical production or destruction from precursor gases will be assessed from a Lagrangian model using air mass trajectories calculated with the ECMWF analysis, and a gas phase chemical module. The initialization of the Lagrangian model will use either precursor climatology from larger scale model output or in-situ measurements from existing aircraft campaigns.

p073 Seasonal patterns of surface ozone measured in a three-year data set at Mt. Cimone

P. Bonasoni¹, T. Colombo², F. Evangelisti¹, G. Giovanelli¹ and F. Ravagnani¹

¹CNR - FISBAT Institute, via Gobetti 101, 40127 Bologna, Italy.

²Italian Meteorological Service, via delle Ville 100, 41029 Sestola (Mo), Italy.

Troposphere ozone concentration has been monitored since March 1991 at the Mt. Cimone Observatory (44°12' N, 10°42' E, 2165 m asl), a mid-latitude mountain site far from sources of anthropogenic pollution. It shows that the progressive diminution registered in data is also found in the total-column measurements recorded at the nearby Dobson station at Sestola. This surface ozone decrease can be correlated to the UV radiation increase resulting from the drop in stratospheric ozone recorded over Europe in the last few years and/or to the diminished flux of stratospheric ozone. In this connection the present study reports and discusses a seasonal analysis of the UVB radiation monitored at Sestola since 1992. Tropospheric ozone evinces a distinct seasonal variation marked by a maximum in spring and summer and a minimum in winter. The measurement site is marked by a seasonal reverse diurnal variation over the summer months, when the Observatory finds itself at times above and at times below the local planetary boundary layer (LPBL). During this period, horizontal transport phenomena of air masses rich in photochemical ozone produced in the Po valley, source of anthropic pollution, can occur. Because Mt. Cimone is situated in a cyclogenic area, which is a fairly common situation in the Mediterranean Basin, stratospheric intrusions, which are usually associated with cut-off lows or slanting dry air, have also been registered.

p074

Variations of surface ozone at the remote stations in northwestern China

H. Muramatsu

Disaster Prevention Research Institute

Kyoto University, Gokasho, Uji, Kyoto 611, Japan

The daily maximum mixing ratios of the surface ozone at Zhangye and desert stations are lower than at Uji and show the maximum in July, the same month at Uji. The maximum in seasonal variation at Uji is determined by photochemical effects in summer, while at northwestern China it is determined by the transport from the free troposphere.

Synoptic scale disturbances lead to high correlation between ozone mixing ratios at northwestern China and Uji in winter, induced by the enhanced vertical transport of ozone. In summer correlation is low because of the photochemical effects at Uji.

Hourly mean ozone at desert in winter increases with wind speed and approaches three different extreme values of ozone in the specific time of a day, except the day overlaid by the ridge in upper layer when only one extreme is recognized. These extreme values of ozone originate from the degree of the coupling between the surface and the free troposphere. The daily maximum of the surface ozone decreases below the ridge in the upper layer due to the decrease in the ozone in the free troposphere.

p075

Yearly cycle of lower tropospheric ozone north of the arctic circle

Markku Rummukainen and Tuomas Laurila

Finnish Meteorological Institute, Finland

Tropospheric ozone is a climate gas affecting radiation transfer in the UV, as well as longer wavelengths of the spectrum. High levels of ozone in the Arctic boundary layer are also detrimental to boreal forests. Tropospheric ozone budget is largely regulated by long-range transport, vertical exchange with the stratosphere and local chemistry. The relative, as well as absolute, importance of these is dependent on the geographical location and the altitude. In order to elucidate the relationships between these three factors in the European Arctic, we have analysed two years of surface ozone data from three measurement sites north of the arctic circle in northern Finland. The southernmost station, Oulanka (66.3°N), represents a continental, boreal forest site, while the northernmost one, Sammaltunturi (68°N), is a mountain site with a more oceanic character. At the third site, Sodankylä (67.4°N), regular ozone sonde launches have provided information also on the vertical distribution of ozone and vertical exchange processes. A trajectory climatology has been obtained for mapping the pattern of advection of polluted air from Middle Europe and the Kola peninsula, as well as cleaner air from the Arctic Ocean.

p076

Ozone Fluxes over Farmland and Natural Vegetation
in South Western Australia:

S. Chambers, N.J. Clark, J.H. Hacker and S. Venning

Flinders Institute of Atmospheric and Marine Sciences
Flinders University, Adelaide, South Australia

A vermin-proof fence running SE to NW in the SW of Western Australia forms a boundary between wheat lands and natural vegetation which is visible on a continental scale AVHRR image of Australia; it is well removed from coastal influences and major topographic features. Fluxes of sensible heat, water vapour and trace gases have been measured by the eddy correlation method over natural and agricultural areas using detectors mounted on a Grob 109B motorised glider. Ozone deposition velocities were measured by coumarin dye, and luminol chemiluminescence-based methods with the two systems mounted in series in the same sample stream. Each method is temperature and humidity sensitive to varying degrees. Deposition velocities corrected for these interferences are presented for summer, autumn and winter/spring conditions when agricultural growth varies from senescence to vigorous.

p077

Surface ozone measurements from Baring Head, New Zealand

S.E. Nichol, M.J. Harvey, and I.S. Boyd
National Institute of Water & Atmospheric Research Ltd., Lower Hutt, New Zealand

Surface ozone measurements were made at Baring Head (41°S, 175°E) in 1991 and 1992 using a Dasibi UV ozone monitor. Air for these measurements was drawn from 5 metres above the ground through a dedicated teflon tube. The measurements show a strong seasonal cycle with a winter maximum and a summer minimum. The monthly mean surface ozone values for the winter months are typically around 30 ppbv, and the means for the summer months are close to 15 ppbv. The maximum and minimum hourly values observed during the year are 35 ppbv and 6 ppbv respectively. A diurnal cycle is evident throughout the year, with a maximum occurring at 3 p.m. local time and a minimum occurring at 9 a.m. local time. The amplitude of the diurnal cycle is about 2.5 ppbv. The highest ozone values are generally obtained during baseline conditions (i.e. southerly winds greater than 10 knots). Comparisons made with surface ozone data from the Australian Baseline Station at Cape Grim (41°S, 145°E) show a similar seasonal cycle.

p078

SURFACE AND FREE TROPOSPHERIC OZONE MEASUREMENTS OVER SOUTH AFRICA

J. Combrink, Diab, R.D., Sokolic, F. and Brunke, E-G*

Department of Geographical and Environmental Sciences,
University of Natal, King George V Ave, Durban, 4001
* EMATEK, CSIR, P O Box 320, Stellenbosch, 7599

An account of the diurnal, daily and seasonal behaviour of surface and free tropospheric ozone is provided for South Africa. Continuous surface ozone measurements, from Cape Point and the Eastern Transvaal highveld, vertical ozone profiles at Irene (Pretoria) and TOMS (Total Ozone Mapping Spectrometer) total column ozone data have been investigated. Cape Point is representative of a background monitoring station which is remote from pollution impacts, whereas the Eastern Transvaal Highveld (ETH) and Irene are situated in an area of intense urban and industrial activity. At Cape Point the surface ozone diurnal cycle is small, the seasonal cycle shows a winter maximum and a summer minimum. In contrast, the ETH stations show a spring maximum in surface ozone with evidence of a summer enhancement. Comparison with Cape Point data suggests that photochemical ozone production accounts for about 50% of the background value. Seasonal variation in total ozone is consistent over South Africa, indicating a cycle which is independent of varying surface or tropospheric ozone concentrations.

p079

Boundary layer ozone at Victoria Falls (Zimbabwe):
Ground level and airborne mixing ratios

Franz X. Meixner
Max Planck Institute for Chemistry, Biogeochemistry Department, Mainz, Germany

During the IGAC-BIBEX experiment SAFARI'92 (Southern African Fire-Atmospheric Research Initiative) ground level monitoring of ozone, CO₂ and meteorological parameters was performed at Victoria Falls (Zimbabwe), end of the dry season (September/October 1992). These measurements were completed by gradient surface flux measurements and some 20 aircraft ascents extending over the daylight local mixed layer (1000 - 4500m a.s.l.). Surface O₃ mixing ratios generally show strong regular diurnal variations which may be due to the combined action of chemistry, downward mixing from the free troposphere, and dry deposition. Furthermore, the influence of local and regional biomass burning on mean O₃ levels is demonstrated. Attempt is made to establish surface O₃ fluxes by the CBL (Convective Boundary Layer) budget method which integrates over scales of some ten to hundred km².

p080

Status of Tropospheric Ozone in Delhi

Maneesha Aggarwal and C.K. Varshney
School of Environmental Sciences, JNU, New Delhi -
110 067, India

Systematic measurements of ground level ozone in the urban environment of Delhi were carried out at different sites synoptically during 1989 - 1991. Ozone levels exhibited wide temporal and seasonal variation. On many occasions ozone level exceeded the 1-h maximum ozone permissible limit of $120 \mu\text{g m}^{-3}$ set by WHO (1976) and USEPA (1979). Vertical ozone measurement were carried out at ground level and at a height of 23 m, 51 m, 117 m and 155 m synoptically at four different sites in winter, spring and summer during 1989-90. Considerable vertical ozone variation was recorded at all sites. At any given time O_3 levels were lowest close to the ground and invariably increased with increasing distance from the ground. In general the ground level ozone concentration in the State of Delhi varied from $20 - 275 \mu\text{g m}^{-3}$. Rapid growth in population, automobile traffic and industrialization seems to be primarily responsible for tropospheric ozone build up which is likely to escalate further on account of growing anthropogenic emissions from a variety of mobile and stationary sources.

p081

MONITORING OF SURFACE OZONE AND ITS
PRECURSORS AT AHMEDABAD

Shyam Lal, Manish Naja, P.K. Patra, B.H. Subbaraya
and S. Venkataramani

Physical Research Laboratory, Ahmedabad 380 009, India

ABSTRACT - Measurements of ozone, carbon monoxide, methane and NO_x have been made in different months each time for three days continuously at Ahmedabad. The measuring site is located on the western edge of the city which has a population of about 3.5 million. Surface ozone data show a systematic noon maximum while CO and NO_x data show morning and evening increase in the concentrations. Methane does not show any appreciable diurnal variability during summer months, however, in winter it increases in night periods. All these species show very high values in winter months during night hours. The wind data show that during night period the direction of the wind is from the city side. High levels of ozone are also observed during winter months suggesting higher production of ozone due to photo-oxidation of ozone precursors during this period.

p082

Seasonal and longterm variations in surface ozone at Ahmedabad

Shyam Lal, B. H. Subbaraya and Manish Naja

Physical Research Laboratory, Ahmedabad 380009, India

Abstract - Surface ozone at Ahmedabad is being monitored regularly since November 1991 using a UV absorption based microprocessor controlled analyser. The data collected at 15 minutes interval show diurnal, day to day and seasonal variations. Ozone is maximum in the noon hours and low during night hours. However, the minimum in ozone concentration is reached in the morning some time after the sun rise. The noon, night and morning values show considerable variability with season. The highest concentration is reached during winter months, in particular in January, when the average monthly noon values exceed 55 ppbv and the night time values around 20 ppbv. Ozone concentrations are low in summer months with noon time maximum around 30 ppbv and night time minimum around 15 ppbv. However, the lowest ozone concentrations are observed in the monsoon months of August and September.

The present data is compared with the measurements made in 1954/55 at this place itself. The present ozone values are found to be larger by a factor of 2 to 2.5 during the winter months.

p083

A New Equatorial Ozone Sounding Campaign: Preliminary Results

M. Ilyas

Astronomy and Atmospheric Research Unit,
University of Science Malaysia, 11800 Penang, Malaysia

In the 1980's a series of studies involving ozone soundings, surface ozone and ultraviolet radiation was undertaken at Penang. Under a re-organized and intensified atmospheric research programme, new physical infrastructure has been established to undertake an expanding research programme including atmospheric composition, minor constituents, ultraviolet radiation and other related parameters. An intensive ozone sounding campaign involving weekly/twice weekly flights one of the earliest projects initiated. The inaugural launch was made on 4 January 1994. Preliminary results from available data will be presented with a view to examine data improvements over the previous series as well as other aspects. A brief discussion of the overall new set up in the context of future research programme will also be included.

p084

CHEMILUMINESCENT SENSORS FOR ATMOSPHERE MONITORING AND INDUSTRY

A. Bryuckanov, I. Zykova, V. Chelibanov
OPTEC Company Ltd., St. Petersburg, Russia

The phenomenon of heterogeneous chemiluminescence was discovered in the system: gas-solid (SO₂-two-component chemiluminescent composition on cellulose /S-48/; NO₂-five-component chemiluminescent composition on cellulose /N-50/. The chemiluminescence was registered in visible spectrum under periodical supply of analyzed gas sample into flow reactor with a solid-state sensor. The results of sensors test given in the table shows that the sensors can be used in gas analyzers for atmosphere monitoring and industry.

Table

Analyzed gas/ sensor model	Lower detec- table limit µg/m ³	Concentr. range µg/m ³	Service life up to 0.5 h.	Response time sec	Interfering components, not observed			
					SO ₂ µg/m ³	NO ₂ µg/m ³	NH ₃ µg/m ³	O ₃ µg/m ³
SO ₂ / N-48	0.050	0.05-3.00	> 90	< 1	-	< 2	-	1.0
NO ₂ / N-50	0.01	0.01-2.00	> 100	< 1	< 2	-	-	0.25
O ₃ / K-3	0.0005	0.0005 - 1.0000	10 000	0.05	< 3	< 10	< 10	-

p085

A global "telescopic" model of chemically active trace constituents:
Application to the Mauna Loa Observatory Photochemistry Experiment. I. Model description.

Paul Ginoux¹ and Guy Brasseur
National Center for Atmospheric Research, Boulder, Colorado, USA
and

¹ Free University of Brussels (ULB), Belgium

A nested regional-global model of chemically active trace constituents is being developed to allow detailed examination of atmospheric chemistry and dynamics associated with experimental measurement programs. The model uses a variable resolution with a smoothly varying triangular mesh which provides an efficient numerical approach for regional modelling of chemistry. The variable resolution, in effect, allows one to "zoom-in" for high resolution in a specific region, and a progressively larger grid is applied as one moves to the global scale. The distribution of 40 species is computed at each one hour timestep. The chemical mechanism includes 120 reactions, most of them related to non-methane hydrocarbon chemistry. Advection is treated in semi-Lagrangian context with the FE method. Diffusion due to eddies in the PBL is calculated with a non-local parameterization, while convection by deep cumuli is parameterized as a function of the amount of precipitation. The boundary conditions for the chemical species at the surface are given by the biogenic and anthropogenic source emissions. This paper will present a description of the model and a companion paper will examine the application of the model to a specific period of the Mauna Loa Observatory Photochemistry Experiment (MLOPEX II).

p086

A global "telescopic" model of chemically active trace constituents:
Application to the Mauna Loa Observatory Photochemistry Experiment. II. Data comparisons

Paul Ginoux, Elliot Atlas, Brian Ridley and Guy Brasseur
National Center for Atmospheric Research, Boulder, Colorado, USA
and

MLOPEX II and PEM WEST-A Science Teams

A nested regional-global model of chemically active trace constituents is being developed to allow detailed examination of atmospheric chemistry and dynamics associated with experimental measurement programs. The model is described in detail in a companion paper. Here we apply the model to the MLOPEX II measurements during the period associated with Mission 20 of the GTE Pacific Exploratory Mission (PEM-WEST A). A large suite of photochemically related species were measured both aboard the aircraft and at the ground based site at Mauna Loa Observatory. Measurements at both locations included non-methane hydrocarbons, ozone, PAN, nitric acid, NO, NO₂, HNO₃, hydrogen peroxide, and organic peroxides. This paper will examine model predictions in relation to the measurements from both platforms. Application of the independent measurements tests the ability to combine data sets from separate campaigns in the context of a regional chemical model. Detailed source emission inventories from the Hawaiian Islands and from ocean sources allow further examination of the impact of boundary layer/free troposphere exchange processes on the chemistry of the mid-free troposphere near Mauna Loa Observatory.

p087

Impact of Changing Natural Volatile Organic Compound Emissions
on Global Tropospheric Chemistry

Alex Guenther, Guy Brasseur, David Erickson, Sophie Fally, and Erwan Favennec
Atmospheric Chemistry Division, NCAR, Boulder, CO, U.S.A.

Perturbations to future earth climate systems could have a significant impact on global volatile organic compound (VOC) emission rates. Conversely, changes in global VOC emission rates can influence the oxidation potential of the troposphere and ambient concentrations of a number of atmospheric constituents. This may result in further perturbations to global tropospheric chemistry and climate.

A high resolution surface emissions model has been developed to generate estimates of global natural VOC emissions. The model incorporates recent advances in our understanding of the processes controlling natural VOC emissions. Annual global emissions of 420 Tg of isoprene, 130 Tg of monoterpenes and 560 Tg of other volatile organic compounds are estimated for the year 1990. In this study, the sensitivity of global natural VOC emissions to potential changes in CO₂, precipitation, temperature, and land cover is investigated. The results suggest that VOC emissions could change by as much as a factor of two or more. The results of a three-dimensional global tropospheric chemistry and transport model indicate that this could result in significant (>10%) deviations from current concentrations of O₃, OH, CO, H₂O₂, NO_x and PAN over some marine and terrestrial regions. The model also predicts significant (>10%) changes in the global average lifetimes of CO and CH₄.

p088

Atmospheric composition changes due to increased ozone precursor emissions and related radiative forcings on climate

D.A. HAUGLUSTAINE¹, C. GRANIER² AND G.P. BRASSEUR²

¹Service d'Aéronomie du CNRS, Université de Paris VI, Paris, France

²National Center for Atmospheric Research, Boulder, Colorado, USA

A two-dimensional (2-D) model of the troposphere, stratosphere and mesosphere, in which dynamics, radiation and chemistry are treated interactively is used to investigate the atmospheric composition changes and the radiative forcings of climate associated with increased ozone precursor gases emissions (e.g. methane, carbon monoxide, nitrogen oxides, aircraft emissions). Several scenarios of increased emissions are adopted to compare and quantify the sensitivity of tropospheric ozone and other key species to the perturbations. We examine the relative impacts of emissions from natural and from anthropogenic sources. With this climate-chemistry model, particular attention is given to the induced changes in radiative forcings and on the analysis of chemically induced radiative perturbations through ozone mixing ratio increase in the troposphere. The relative importance of the various climate forcings is illustrated and discussed. Our results stress the potentially important role of chemical feedbacks on climate.

p089

Convective transports of chemical tracers in global transport models driven by analyses from the forecast centers.

Natalie Mahowald (Massachusetts Institute of Technology, Cambridge, MA), Philip J. Rasch (National Center for Atmospheric Research, Boulder, CO) and Ronald G. Prinn (Massachusetts Institute of Technology, Cambridge, MA)

The sensitivity of tracer transport to formulation of the moist convection and boundary layer parameterizations in global transport models is investigated by comparing mass fluxes and tracer distributions derived from several different parameterizations. The Hack (1994), Feichter-Crutzen (1990), Emanuel (1991), and Tiedtke (1991) parameterizations of moist convection are considered. The Holtslag-Boville (1992) and a simple adiabatic mixing parameterization for boundary layer transports are also investigated. These parameterizations are initially compared in a one-dimensional model, so that the effects of moist convection and boundary layer processes can be isolated. Then comparisons are made in an "offline" global transport model, in which the winds are read from archived datasets. Results demonstrate that tracer distributions are sensitive to which parameterization is chosen, especially for species with atmospheric lifetimes of less than one year. The resulting distributions are also compared to available observational data in order to evaluate the parameterizations.

p090

Generation of Emission Data for Episodes with high temporal and spatial resolution

R. Friedrich

Institut für Energiewirtschaft und Rationelle Energieanwendung
Universität Stuttgart, Germany

The formation of photooxidants is a highly time- and space dependent nonlinear process. To describe it, complex atmospheric transport and chemical transformation models are necessary. To be able to create reliable results, these models need accurate emission data as input data. The emission data needed are hourly data for a square grid during episodes of two to seven days. The species, that should be covered, are NO, NO₂, CO, NH₃, SO₂ and VOC split into about 30 classes. However, there are no emission data available, that fulfill all these features. So, the necessary emission data have to be calculated with often quite complex algorithms using available information. In the paper, methods to calculate space and time dependent emission data for atmospheric models are presented and results for Europe as a whole and various parts of Europe are shown. E.g. the hourly course of emissions can be estimated by using parameters like outside temperature, wind speed, solar radiation, typical working hours for industrial branches, consumer habits, monthly and daily energy consumption and others. The results are used in different national and international projects on atmospheric research (e.g. EUROTRAC).

p091

Photochemical Reactions On Dust In The Troposphere:
A Three Dimensional Global Model Assessment

Frank J. Dentener

Wageningen University, Air Quality Department, Wageningen, the Netherlands
Gregory R. Carmichael and Yang Zhang
University of Iowa, Ctr. for Global & Regional Environmental Research,
Iowa City, Iowa, USA

Semi-arid and arid areas provide large amounts of dust to the atmosphere, thereby offering a significant reaction surface for trace gases in the lower and middle troposphere. Major source areas for dust are the Sahara and the desert areas in Northern-China and Mongolia.

We assess the importance of heterogeneous reactions on dust by using the Moguntia global three-dimensional (3D) tropospheric photochemistry-transport model. We first calculate size-resolved mineral aerosol concentrations originating from arid regions, and compare these with a host of measurements.

The surface offered by these dust particles serves as a sink for HNO₃, N₂O₅, and HO₂, species which play key roles in determining the oxidizing efficiency of the troposphere. The latter reaction is thought to be catalyzed by reactions with trace metals present in the aerosol. The importance of these reactions are assessed by use of the Moguntia model. We calculate that in large parts of the troposphere heterogeneous reactions on dust can significantly influence the photochemical production of O₃. Major uncertainties in the study will also be discussed.

p092

Parameterization of bi-directional NH_3 fluxes in the modelling of long range transport of NO_x .

A. Sorteberg and Ø. Hov
Departemtet of Geophysics, University of Bergen, Norway.

The current description of dry deposition processes in the long-range transport model for NO_x is empirical and does not give a mechanistic description of the different processes controlling the deposition rates.

By introducing deposition to leaf surfaces and bi-directional NH_3 fluxes from stomata it is possible to give the deposition velocities a meteorological and biological dependence. This is especially important for NH_3 because of large spatial differences in the deposition and the existence of bi-directional fluxes related to an NH_3 'compensation point', defined as the concentration at equilibrium with aqueous NH_4^+ in the sub stomata cavity of leaves.

By running the long-range transport model and comparing the new and the current deposition parameterization, the importance of a mechanistic deposition description in long-range transport modelling is investigated.

p093

Correlations between ozone- NO_x -hydrocarbon chemistry and empirical indicators: NO_y , HCHO, H_2O_2 and HNO_3

Sanford Sillman
AOSS, University of Michigan, Ann Arbor MI 48109-2143, USA

The chemistry of ozone in urban environments shows two distinct regimes, a NO_x -sensitive regime and a hydrocarbon-sensitive regime, depending on precursor concentrations and meteorology. The ability to distinguish between NO_x - and hydrocarbon-sensitive chemistry is important in terms of air quality policy and is also associated with seasonally fluctuating photochemical behavior in the remote troposphere (e.g. Kleinman, 1991). A central problem for urban photochemistry is to identify measureable species that may serve as "indicators" for NO_x -sensitive versus hydrocarbon-sensitive chemistry. This paper discusses model correlations between ozone chemistry and four potential indicators: NO_y , O_3/NO_y , HCHO/ NO_y and H_2O_2/HNO_3 . Correlations with total peroxide concentrations will also be presented. It will be shown that H_2O_2/HNO_3 correlates closely with ozone sensitivity in models for gas-phase chemistry only, but the correlation may not hold if either species is removed through heterogeneous processes (fog or haze). The other species show a less exact correlation with ozone sensitivity but may still be useful as diagnostic tools. Examples of concurrent measurements of indicator species in urban and suburban locations show instances where a consistent indication for either NO_x -sensitive or hydrocarbon-sensitive ozone is found.

p094

Regional aspects of the tropospheric ozone budget

P.J.H. Builtjes, M.G.M. Roemer, G.Boersen and P.J. Esser
TNO Environmental Sciences, The Netherlands

An Eulerian grid model, covering the whole of Europe, with a vertical extent of about 2.5 km, coupled with a global two-dimensional tropospheric model has been used to study the regional budget of O_3 , CO and CH_4 .

The European, regional ozone budget is of importance both for its impact on the radiative forcing and its large spatial inhomogeneities, and due to the elevated ozone concentrations - the harmful effects on ecosystems and human beings. Model calculations including data analysis of concentration measurements indicate that the European precursor emissions of CO, CH_4 , VOC and NO_x , contribute about 30% of the northern hemispheric tropospheric ozone budget.

Vice versa, there are indications that the averaged ground level ozone concentrations over continental Europe are to about 30% determined by the anthropogenic determined concentrations in the free troposphere from sources outside Europe. The measured trend in O_3 , NO_2 , VOC and PAN ground level concentrations has been analyzed using the two dispersion models, pointing out that trends in emissions can to a large extent explain the observed trends.

p095

The Vertical Transport, Transformation and Deposition of Air Pollutants by Convective Clouds

Qin Yu Kong Fanyou Zhao Chunsheng
Department of Geophysics, Peking University
Beijing, 100871, PRC

A convective transport model is developed by joining a set of concentration conservative equations into a two-dimensional, slab-symmetric and fully elastic numerical cloud model. Results of numerical experiments show that an isolated, weak storm is able to pump pollutant gases out PBL, and transport them to the mid-troposphere, whereas a deep, intense thunderstorm can very efficiently transport air pollutants up to the mid and upper troposphere and laterally spread with anvil, forming an extensive concentration surge layer at ten odd kilometers' altitudes. Each type of convective transport results in concentration thunderstorm significantly increases and pollutants enter into clouds on the down shear side at low-level and spread downwind in anvil layer. The pictures of transport fluxes through vertical and side bounds of the cloud columns are given.

A condensed chemical mechanism including gaseous and aqueous reactions is coupled into the cloud model and transformation and deposition effects of pollutants by storms are evaluated.

p096

PARAMETERIZATION OF OZONE AND AEROSOL PARTICLE FLUXES

E. Lamaud, J. Fontan, A. Lopez, A. Druilhet
Laboratoire d'Aérodologie, Université Paul Sabatier, Toulouse, France,

and

A. Labatut, S. Cieslik
Joint Research Centre, Environment Institute, Ispra, Italy

Surface fluxes represent a step in the cycles of minor atmospheric constituents. Their parameterization is an essential tool for understanding which factors govern the overall process and is required for modelling purposes. The present work is devoted to the fluxes of ozone and aerosol particles, which have been measured, together with momentum and heat fluxes, by the eddy-correlation method at three South European sites with different types of vegetal cover: pine forest, dry bare soil, and cultivated beet field. Parameterization has been made against various variables: friction velocity, heat flux, Monin-Obukhov length, mixed layer height, stomatal conductance. It appears from the results that particle deposition is mainly controlled by the friction velocity and mixed layer height, i.e. by purely dynamical effects. The diurnal variation of ozone flux is strongly correlated with that of heat flux, and is almost independent from the type of vegetation, which suggests that stomatal aperture is not the only process governing ozone deposition.

p097

Sensitivity of the tropospheric composition of different atmospheric regions over the Earth surface to anthropogenic influences

Natalia G. Andronova¹ and Igor L. Karol²

¹ Department of Atmospheric Sciences, UIUCampaign, USA

² Main Geophysical Observatory, Russia

In this paper we follow the idea of Thompson *et al* (1990) of existing of photochemically coherent atmospheric regions over the Earth surface. Differences between regions are defined by different content of the trace gases in atmosphere and strength of their external sources and sinks. These differences produce the different systems of interactions among of atmospheric species and different sensitivities of the system variables to external influences. To analyze system's feedbacks and determine how the system's sensitivities are formed we built an image model, which determines the changes in tropospheric concentration of the trace-gas groups for oxygen, nitrogen, hydrogen and carbohydrate. The model includes "water vapor - temperature" feedback, and for the northern continental conditions "wetlands - temperature" feedback is included. The relative influences of greenhouse-gas and stratospheric-ozone changes on trace-gas concentrations in annually averaged conditions are quantitatively determined and compared with similar estimates from comprehensive atmospheric photochemical models. The Cause-and Effect is applied to study structure of the system's interactions. As result the main feedbacks among variables and the main pathways from external influences to internal system's variables, which are responsible for formed system's sensitivities, are shown and evaluated.

p098

Rate Coefficients by Parametric Equations for Modeling Purposes

I. Oref
Department of Chemistry
Technion - Israel Institute of Technology, Haifa 32000, ISRAEL

W.C. Gardiner
Department of Chemistry
University of Texas, Austin, USA

Unimolecular and bimolecular rate coefficients are used in modeling schemes of chemical reactions which are involved in atmospheric and combustion chain reactions. They are functions of pressure and temperature. The high pressure values (Arrhenius parameters) can differ by orders of magnitude from falloff and low pressure values. Use of Arrhenius parameters to model reactions under low and moderate pressures can cause very large errors. Finding the correct rate coefficients require a solution of a master equation with RRKM theory individual energy-dependent rate coefficients. This is an impossible computational task which requires very large computational facilities and financial resources. An alternative way is the use of interpolation formulas with a limited number of parameters. The present work discusses such formulas and reports values of the unimolecular rate coefficient for two sample reactions under a wide range of pressures and temperatures and a variety of weak and strong collision partners. It is shown that very reasonable results are obtained when compared with exact master equation-RRKM theory calculations.

p099

Possible impact of ozone column changes on the growth rates of CH₃Br, CH₃Cl and CH₃CCl₃

S. Bekki and K. Law
Center for Atmospheric Science, Cambridge, U.K.

Global total ozone as recorded by the TOMS instrument during the last 15 years shows an irregular behaviour with a net decrease from 1979 to 1985, a moderate increase from 1986 to 1990 and a drop from 1991 to 1993. Models predict that the ozone column changes should have been accompanied by significant changes in OH radical concentrations in the troposphere. Here we investigate the impact that these changes may have had on source gases (e.g. CH₃Br, CH₃Cl, CH₃CCl₃, ...) which are primarily removed by reaction with OH on short time scales compared to CH₄. A two-dimensional model is used to assess the variations in OH and in the growth rates of these source gases. Attempts are made to compare the calculations with available observations. Possible correlations are discussed.

On the diffusional uptake of trace gases by polar stratospheric clouds

S. Ghosh and J. A. Pyle

Centre for Atmospheric Science, Cambridge University, England

The stratosphere holds a variety of particulates like polar stratospheric clouds (PSCs) and sulphate aerosol which catalyse chemical reactions that cause changes in the composition of the stratosphere, including the redistribution of active chlorine which might lead to ozone destruction. As a result during recent years a lot of effort has been directed towards the quantification of the uptake of trace gases like ClONO_2 , HCl , etc. into these particulates. However, it has been observed that many of the two and three dimensional models consider only the collisional uptake neglecting diffusional contributions altogether.

This paper describes a theoretical approach to estimate the heterogeneous uptake rates for 23 gases on both types of Polar stratospheric clouds (type I and II). It is found that for gases like N_2O_5 , ClONO_2 , and HCl on PSCs, diffusional uptake is important and contributes significantly to the heterogeneous reaction rate. A complete Lennard-Jones calculation is used to accurately compute the trace gas diffusion coefficients.

Evidence for ozone depletion in clouds

D. Möller, K. Acker, W. Wieprecht

Fraunhofer Institute for Atmospheric Environmental Research,
Division Cloud Chemistry (ELC), Berlin, Germany

At the Mt. Brocken Cloud Chemistry Station (Germany) we found a strong indication for ozone depletion within clouds as predicted recently by models (Lelieveld and Crutzen, 1990; Möller and Mauersberger 1992). On the Brocken we often observed a rapid decrease in ozone concentration with passing clouds, where the interstitial ozone concentration could be up to 50 % lower than that before the cloud event. When the cloud blew away the ozone concentration increased again to around its former level. The fall in ozone concentration within clouds was observed to be statistically significant. For the cloud events which were observed, 30 % showed no fall in ozone concentration. For both classes of cloud events we found large differences in the chemical composition of cloud water. We assume that the temporary ozone decrease with passing clouds is not due to local processes but a result of chemical processes during the cloud pathway. Based on the experimental results we conclude that (a) clouds deplete and destroy ozone and (b) that this removal capacity increases with pollution, the results support the different ozone removal pathways hypothesized by models.

The Effect of Clouds on OH and the Oxidation of Atmospheric Trace Gases

M.A.K.Khalil and F.Moraes

Global Change Research Center & Department of Environmental Science and
Eng., Oregon Graduate Institute, P.O.Box 91,000, Portland, Oregon 97391 USA

Clouds block the solar radiation that causes the photolysis of O_3 needed to make $\text{O}(^1\text{D})$, which in turn makes OH. Below the clouds there is very little OH. Above the clouds there is more OH than under clear sky conditions, because clouds reflect solar radiation and increase actinic flux above cloud tops. Clouds, therefore, redistribute actinic flux and OH. The effect of clouds on the oxidation of environmentally important trace gases is to reduce the total annual oxidation. This happens because the density of most trace gases decreases with altitude as the scale height of the atmosphere, or faster, and because the reaction rate constants also slow down because of the decreasing temperatures in the troposphere (or in the case of CO, because of the decrease of atmospheric pressure with altitude). Using our detailed photochemical model for OH we calculate that 30 Tg/yr less CH_4 and 130 Tg/yr less CO are removed from the atmosphere than would be expected without clouds. The role of clouds for methane, therefore, is comparable to the annual emissions from the major anthropogenic sources, namely rice agriculture, cattle, and biomass burning, all are between 50-90 Tg/yr. Acknowledgements: This work was supported in part by grants from NSF and DOE and the resources of the Andarz Co.

p203

H₂O₂, CH₃OOH, and CH₂O as Primary and Secondary Pollutants In Fire Plumes

Meehye Lee and Brian Heikes
GSO/CACS, University of Rhode Island, RI, USA

Daniel Jacob
Earth and Planetary Sciences, Harvard University, USA

Atmospheric measurements of H₂O₂, CH₃OOH, and CH₂O will be presented which are significantly elevated with respect to typical background values. The data come from MLOPEX-I, -II, NASA/GTE/TRACE-A and /PEM-West:A experiments. H₂O₂, CH₃OOH, and CH₂O concentrations in unperturbed conditions will be characterized. Event specific measurements from the above field programs will be presented which are factors of 2-3 greater than the unperturbed values for peroxides (ROOH) and factors of 3-10 higher for CH₂O. Using key chemical and meteorological data from the respective experimental archives and existing photochemical theory, it is proposed that the high ROOH and CH₂O values encountered are the result of direct emission, as well as, secondary production. The significance of a pyrogenic ROOH and CH₂O source on the near field photochemistry of biomass fire impacted air will be described. For example, approximately 1/2 of the odd hydrogen radicals could come from CH₂O photolysis with the photolysis of H₂O₂ and CH₃OOH contributing an additional 1/4, and O₃ contributing the remaining 1/4 (assuming diurnally average photolysis rates for solar equinox at 30 lat. and CH₂O = 5 ppbv, H₂O₂ = 5 ppbv, CH₃OOH = 2 ppbv, and O₃ = 50 ppbv).

p204

ATMOSPHERIC EFFECTS OF H₂O₂ IN SOUTH-EAST CHINA

=20

X. Tang, K. Shao, Q. Sun and M. Wang
Peking University, Beijing, China

H₂O₂ is a chemical reservoir for odd-hydrogen radicals as well as a more direct indicator of odd-hydrogen concentration variation which potentially express the chemical reactivity of the troposphere. These effects are particularly significant in the formation of acid precipitation and aerosol production.

Since 1987, H₂O₂ concentration in ambient air, cloud droplets, rainfall and fogs have been observed at different heights by aircrafts and different mountains and surface areas in southern and central parts of China. The vertical profile and the latitudinal gradient of gaseous H₂O₂; the H₂O₂ concentration variation in cloud, fog and rain water and the relationships among SO₂, SO₄, O₃ and H₂O₂ are calculated and discussed. These results demonstrate that H₂O₂ concentration in air and precipitation reflects the oxidizing potential of the tropospheric air in the studied regions.

p205

Relationship between Peroxide and Ozone Measured over the Equatorial South West Pacific

B. J. Bandy, S. A. Penkett, School of Environmental Sciences
University of East Anglia
Norwich, Norfolk. NR4 7TJ, England

G. Jenkins, P. Hignett, A. Kaye Meteorological Research Flight
DRA
Farnborough
Hants, GU14 6TD, England

Peroxide and ozone profiles have been measured up to an altitude of 6 kilometres over the Equatorial and Tropical Pacific. The ozone concentrations recorded in the boundary layer are typically below 10ppbv and in many cases a negative correlation is observed between ozone and peroxide at altitudes between 2 and 6 kms when the air has an easterly origin over the remote Pacific. In these situations the data shows detailed structure with altitude with a strong positive correlation between peroxide and dew point. In a few cases a positive correlation is observed between peroxide and ozone in circumstances where the dew point declines monotonically up to the top of the profile, and trajectories suggest that the air has its origin from a westerly direction. The data is discussed in relation to the photochemical control of ozone in the troposphere over the remote equatorial oceans.

p206 The occurrence of hydroperoxides in mid altitudes of the lower troposphere: measurements at two mountain field sites

W. Junkermann, P. Pietruk and F. Slemr
Fraunhofer Institut für atmosphärische Umweltforschung, Germany

Peroxides play a significant role in the atmospheric radical chemistry and in the conversion of pollutants into acid precipitation. Organic peroxides are phytotoxic and are suspected to contribute to forest damages observed within the last decade. Consequently, peroxide measurements were performed at two field sites in a remote area (Wank mountain) in the Bavarian Alps, one site at mountain top at 1780 m a.s.l., the other in mid elevation in an area with intense forest damages at 1175 m a.s.l. Measurements were performed for a one year period in 1990/91 using the enzyme fluorimetric technique providing the H₂O₂ concentration and a semi-quantitative signal for the sum of organic peroxides.

The data obtained show a strong dependence of the peroxide concentrations both on local and long range transport processes. Free tropospheric air cloud be observed as well as moderately polluted air from the planetary boundary layer. The H₂O₂ data agree well with results of aircraft ascends and are consistent with model calculations. The results of the organic peroxide measurements are higher than expected especially in the planetary boundary layer and point toward a significant source for organic peroxides in lower elevations. Ozonolysis of naturally produced biogenic emissions seems to be an efficient production process for organic peroxides.

Tropospheric aldehydes in remote and urban areas of Japan

M. Ohta¹ and H. Tsuruta²

1. Yokohama Environmental Research Institute, Japan
2. National Institute of Agro-Environmental Sciences, Japan

Aldehydes such as HCHO and CH₃CHO in the troposphere are one of the precursors of photochemical ozone, and CH₃CHO is one of the sources of PAN. These aldehydes are produced through the oxidation of hydrocarbons, but also emitted directly from automotive exhaust. The behavior of aldehydes in the troposphere has not been made clear due to few measurements in gaseous and aqueous phase. We have measured aldehydes in ambient air and cloud/rain water at the urban area of Yokohama closed to Tokyo since 1987, and at Mt. Norikura (sampling sight is a height of 2,700 m) located in the central part of Japan in summer since 1989. At Mt. Norikura, HCHO and CH₃CHO concentrations in ambient air were below 2 ppbv, and significantly lower than in the urban area. These gases showed a clear diurnal variation with a maximum around noon in the fine days, and which indicates that these aldehydes were produced from hydrocarbons emitted from plants with photochemical reaction. The ratios of CH₃CHO to HCHO were much higher at Mt. Norikura than at Yokohama where the major source is supposed to be automotive exhaust. The fate of aldehydes will be discussed by measurement of cloud/rain water.

Atmospheric Formic and Acetic Acids in Venezuela

E. Sanhueza, L. Figueroa and M. Santana
Atm. Chem. Lab., IVIC, Venezuela

Gas Phase and rain concentrations of HCOOH and CH₃COOH have been measured at various sites in the savannah climatic region, a cloud forest (~1800 m above sea level and ~30 km from the ocean), and a coastal site (Caribbean Sea). Gas phase and rain-water samples were collected using the aqueous scrubber technique and an only wet collector, respectively. Analysis were made by ion exchange chromatography. The gaseous acids show diurnal cycles, with higher mixing ratios during daytime; dry deposition rates (calculated from the nocturnal decrease) of both acids are larger during the rainy season. A strong seasonal variation is also observed, with higher concentrations during the dry season. Very similar levels (<1 ppbv) were observed at the various sites during the rainy season (suggesting a widespread source), whereas a significant difference was recorded during the dry season with: savannah > cloud forest > coast. A good correlation was observed between both acids, as well as with O₃ and CO. HCOOH also correlates with HCHO in rain water. Likely sources, rates of removal processes, and lifetimes will be discussed.

KINETICS OF THE OXIDATION OF SO₂, NO₂⁻ AND N-S OXIDES BY OZONE IN AQUEOUS SOLUTIONS

J. Hahn, G. Lachmann and J.J. Pienaar

Department of Chemistry; Potchefstroom University; 2520 Potchefstroom; South Africa.

Recent international research programs such as SAFARI 92 has shown above average ozone concentrations in the Southern African Troposphere. As part of our general interest in atmospheric chemistry, we have studied the kinetics of oxidation reactions of sulfur(IV)-, nitrogen oxides and nitrogen-sulfur oxides by ozone as a function of the pH and temperature by spectrophotometric techniques. The kinetic results were complemented with ion chromatographic analysis of the products.

The kinetic data showed that the reactions have a first order dependence on the S(IV), NO₂⁻ and N-S concentrations but a more complex dependence on the ozone concentration. The reaction rate increased drastically with an increase in the pH of the reaction medium. The processes are accelerated by the presence of dissolved oxygen. All the processes studied are characterised by low activation enthalpies and large negative activation entropies. The study showed that free radicals formed in the spontaneous decomposition process of ozone in water plays an important role in all the processes studied. The experimental reaction curves could be successfully simulated by a judicious combination of experimental and literature data.

THE NON-METHANE HYDROCARBON INTERCOMPARISON EXPERIMENT

Eric C. Apel and Jack G. Calvert

Atmospheric Chemistry Division, National Center for Atmospheric Research, USA

The ability of laboratories throughout the world to perform high quality ambient measurements of volatile organic compounds is crucial to a global understanding of these important precursors and their role in tropospheric ozone formation. The "Non-Methane Hydrocarbon Intercomparison Experiment" (NOMHICE) has been designed to evaluate analytical techniques currently being used by scientists to measure ambient atmospheric hydrocarbon concentrations. NOMHICE consists of a series of planned experiments designed to identify existing problems in participating scientist's laboratories and to correct them. The various experimental steps (or Tasks) have been scheduled in order of increasing complexity so that problems can be addressed as they arise. Results are briefly reviewed for Tasks 1 and 2 and are presented for Task 3. Task 1 evaluated the ability of participating laboratories to quantify a simple 2 component mixture. Task 2 evaluated the ability of laboratories to identify and quantify compounds in 16 component mixture. Task 3 involved the circulation, to participant laboratories, of a prepared synthetic air mixture containing many potentially important non-methane hydrocarbon ozone precursors. Participants were asked to identify and quantify the components. Further tasks are described which will be carried out in the future.

p211

LANDSCAPE SCALE EMISSION INVENTORY OF INDIVIDUAL BIOGENIC ORGANIC COMPOUNDS IN THREE ECOSYSTEMS IN THE US

Detlev Helmig, Lee F. Klinger, Alex Guenther, Jim Greenberg
and Patrick Zimmerman
National Center for Atmospheric Research
Boulder, CO, 80307, U.S.A.

Individual organic compounds emitted from vegetation were measured using a solid multi-adsorbent cartridge sampling method. Branches were enclosed in teflon bags, purged with clean air and the headspace was sampled on the adsorbent traps. Analysis was performed by thermal desorption. A special custom made thermal desorption inlet system with cryogenic preconcentration and internal standard addition was used with gas chromatography/mass spectrometry analysis. Identification of volatile organic compounds covering the retention index range (DB-1) from approximately 400 to 1500 could be achieved.

Vegetation composition and biomass was surveyed for specific sites in Atlanta, GA; Lac du Flambeau, WI and in Hayden, CO. For each research site the dominant vegetation species, which together accounted for at least 95 % of the leaf biomass were sampled. Identified compounds include isoprene and species of the classes of monoterpenes, sesquiterpenes, carbonyl compounds and alcohols. Combining the analytical data with the ecological survey data and other flux measurements on the leaf and landscape level, flux estimates of individual organic compounds from the different ecosystems investigated are obtained.

p212

Oceanic Emissions of Light Nonmethane Hydrocarbons

C. Plass-Duelmer, R. Koppmann, M. Ratte, and J. Rudolph
Institut für Atmosphärische Chemie, Forschungszentrum Jülich, 52425 Jülich, Germany

Emissions of light nonmethane hydrocarbons from the ocean into the atmosphere are of interest for atmospheric chemistry for both their local impacts on photochemistry and their contribution to global NMHC budgets. Based on limited sets of hydrocarbon measurements in sea water global oceanic emissions between several Mt/a and more than 50 Mt/a have been estimated. Due to the considerable uncertainty of these numbers the available measurements of dissolved C_2-C_4 hydrocarbons in the surface water of the oceans are reviewed. The paper focusses on data obtained by in-situ analysis since other techniques generally yield less reliable results. Emission rates are calculated from the measured concentrations and transfer velocities which are determined using sea-air exchange models and climatological data. Distributions of NMHC emissions are discussed using a global and seasonal grid. Global oceanic emissions of C_2-C_4 hydrocarbons sum up to 2 Mt/a with ethene alone contributing about 40% to the total emission. Including 90% of all calculated emission rates an upper limit for the emissions of light NMHC of 5.5 Mt/a can be given. Thus, the oceanic source of light hydrocarbons is on the low side of previous estimates.

p213

Laboratory experiments on the origin of C2-C3 alkenes in sea water.

M. Ratte, O. Bujok, A. Spitz*, J. Rudolph
Institut für Atmosphärische Chemie, Forschungszentrum Jülich, 52425 Jülich, Germany
* Max-Planck-Institut für Meteorologie, Bundesstr. 55, 20146 Hamburg, Germany

The presence of alkenes in the marine atmosphere is mainly due to oceanic emissions. From our present understanding oceanic alkene emissions are essentially determined by the production in the ocean surface water. We carried out several laboratory experiments in order to investigate the production mechanism of alkenes in sea water. In cultures of the marine diatom *Thalassiosira rotula* increasing alkene concentrations with exposure time were found compared to cell free controls. Alkene production was also observed in cell free natural sea water to which different amounts of dissolved organic carbon (DOC) (fulvic acids from river Kongo) were added and which was exposed to different wavelength bands: Ultraviolet light (320-420 nm) and visible light (420-520 nm and 400-800 nm). The alkene production rates depend linearly on initial DOC-concentration and wavelength. The shorter the wavelength of the irradiation, the more alkenes are produced. The calculated quantum yields (molecules alkene produced per photon absorbed) are in the range of 10^{-9} . These results indicate an alkene production mechanism via photochemical transformation of DOC. Preliminary results show that a photochemical alkene production occurs even if the oxygen concentration in sea water is below 0.1 mg/l. Nevertheless, an additional biological pathway of alkene production cannot definitely be excluded.

p214

Airborne Measurements of Organic Trace Gas Emissions from Savanna Fires in Southern Africa

R. Koppmann, A. Khedim, J. Rudolph
Forschungszentrum Jülich, Institut für Atmosphärische Chemie, 52425 Jülich, Germany

Biomass burning emissions are known to be a considerable source of atmospheric hydrocarbons. During the South African Fire Atmosphere Research Initiative (SAFARI) in September/October 1992, whole air grab samples were collected in stainless steel canisters on board of a DC3 aircraft in the immediate vicinity of prescribed and wild savanna fires as well as outside of the fire plumes between the surface and 12000 feet altitude. The samples were analysed in the laboratory for light and medium molecular weight nonmethane hydrocarbons, halogenated hydrocarbons and aromatics by FID/ECD gas chromatography. Inside the plumes NMHC mixing ratios of some 10 ppb up to 100 ppb were observed.

A comparison of the NMHC mixing ratios with those of CO and CO₂ measured simultaneously are used to calculate emission ratios from the fires. From these data the different types of fires encountered during the campaign can be clearly distinguished. Highest emission ratios were found for small uncontrolled savanna fires, while large open fires showed the lowest emission ratios. The emission ratios found in our measurements are at the lower end of published field and laboratory measurements of biomass burning emissions.

In addition, a GC/MS system was used to identify other organic trace gases emitted from the fires. A large variety of compounds could be identified such as aldehydes, ketones, esters, ethers and furanes. An estimate of the emission ratios calculated on a ppb carbon basis show that the emission ratio of the sum of all organic trace gases is in the same order of magnitude as the emission ratio of carbonmonoxide.

Light Hydrocarbons Measured in Plumes of Savanna Fires in South Africa

G. Helas, M. O. Andreae, G. Schebeske, D. Scharffe, S. Manoe
Max-Planck Institute for Chemistry, Biogeochemistry Department, D - 55020 Mainz,
Germany

R. Koppmann, J. Rudolph
Institute for Chemistry and Dynamics of the Geosphere, Jülich, Germany
A. de Kock, University of Port Elizabeth, R. S. A.
E. Atlas, NCAR, Boulder, CO, U. S. A.

Biomass burning adds significant amounts of hydrocarbons to the atmosphere. These hydrocarbons therefore augment to the ozone formed during the photochemical production in the emitted plumes. In order to investigate this contribution we took airborne samples from the regional background and from biomass burning plumes during the experiment SAFARI 92. We used stainless steel canisters and analyzed the samples for CO₂, CO, CH₄, C₂H₂, C₂H₄, C₂H₆, C₃H₆, and C₃H₈. Our ratio of dCO/dCO₂, given as slope of concentrations of CO on CO₂ was very low, close to 3%, revealing very vigorous burning. The emission ratios given as dX/dCO ranged for CH₄ from 5 to 7.5*10⁻², C₂H₂ from 1.8 to 3.6*10⁻³, C₂H₄ from 1.4 to 2.0*10⁻², C₂H₆ from 2.3 to 4.4*10⁻³, C₃H₆ from 2.8 to 3.9*10⁻³, and C₃H₈ from 4.9 to 12*10⁻⁴. Comparison with literature values most often show similar ranges. The observation of high ozone concentrations downwind of these savanna fire plumes in the southern African area imply that the production of ozone is not limited by hydrocarbons.

Concentrations of C₂-C₅ hydrocarbons over the Baltic Sea and Northern Finland

Tuomas Laurila and Hannele Hakola

Finnish Meteorological Institute, Sahaajankatu 22E, FIN-00810, Helsinki, Finland
e-mail: Tuomas.Laurila@fmi.fi fax: -358-0-7581396 tel: -358-0-75811

Light (C₂-C₅) hydrocarbons are emitted both from anthropogenic and natural sources. In photochemical processes they participate in oxidant formation. Since source profiles from anthropogenic sources (mainly traffic related) are different than those from natural sources (mainly alkenes of biogenic origin) the concentration profiles measured in ambient air carry information on sources. C₂-C₅ hydrocarbons have been analysed from flask samples collected at a small island (59° 47'N, 21° 23'E) on the Baltic Sea regularly since February 1992. This data is presented together with concomitant ozone concentrations. Seasonal cycle of concentrations and their profiles are shown. Comparison of these concentration profiles to those observed in the city of Helsinki show that the air samples collected at the island are photochemically relatively aged although the main species are of anthropogenic origin. Reactivity scaled concentrations of light hydrocarbons are comparable to those reported from samples taken at remote oceanic locations. Typical hydrocarbon profiles in air masses originating from the Northern Atlantic and continental Eurasia are investigated. In January 1994 the measurements of light hydrocarbons were also started on a mountain top station north of the Arctic Circle (67° 58'N, 24° 07'E). A preliminary comparison of concentrations measured at these sites is presented.

Preliminary Research on Isoprene Emission from Plant and Soil

Lu Chun and Miao Hong
Research Center for Eco-Environmental Sciences, Academia Sinica

Isoprene (C₁₀H₁₆) emissions from six typical plant species in North China were studied. Three groups were classified according to their isoprene emission rates (IER): 1) *Q. liaotungensis*, its mean emission rate (MEER) was 1.23 μg/g hr; 2) *P. tabulaeformis*, *L. principis-ruprechtii* and *F. chinensis*; their MEER were within the range from 0.03 to 0.11 μg/g hr; 3) *B. utilis* and *T. mandshurica*; almost no isoprene emission could be detected. There was an obvious diurnal variation of IER of *Q. liaotungensis* with the maximum emission rate (1.92 μg/g hr) at 14:00 and the minimum emission rate (0.00 μg/g hr) at 2:00. Mean daily emission rate (MDER) of isoprene from this species was 0.56 μg/g hr. Illumination and temperature both had obvious effects on IER of *Q. liaotungensis*. The correlation coefficients of illumination-IER and temperature-IER were about 0.87 and 0.78. Factors could be ordered as follows according to the degrees of their impacts on plant IER: illumination, ambient temperature, leaf temperature, altitude, leaf shape and humidity.

Isoprene (C₁₀H₁₆) emissions and adsorption from and by soil were also observed. The results of research on influences of soil on isoprene have showed that soil had both abilities to emit and adsorb isoprene. Increasing soil moisture could promote adsorption process of isoprene in soil. However, increasing soil organic matter would lead to improvement of isoprene emission process in soil. These phenomena were possibly related to soil microorganisms and physical and chemical properties of soil.

Above results have exhibited that in a soil-plant-air system mass exchange process of isoprene did happen not only between plant and air, but also between soil and air. Functions of soil in such a process should not be ignored. Perhaps this conclusion is meaningful in leading to a new way to solve the contradiction between high isoprene emission rates from plants and low isoprene concentration in ambient air. More attention should be paid to research work in this field in the future.

Terpenic emissions from *Quercus ilex* and *Pinus pinea* at Castelporzlano (Italy)

J.L. Fugit, B. Clement, M.L. Riba, L. Torres*

*Laboratoire Chimie-Energie et Environnement
Ecole Nationale Supérieure de Chimie de Toulouse - France

and J. Kesselmeier** and L. Schaefer**

**Max Planck Institut für Chemie - Abteilung Biogeochemie
Mainz - Germany

Natural alkenes such as isoprene and monoterpenes emitted by vegetal species play an important role in the formation of atmospheric oxidants and aerosols. The measurements of emission rates and fluxes for biogenic compounds was carried out via the enclosure method in a natural forest composed of 30 years old *Quercus ilex* and *Pinus pinea*. The method consists in measuring the emission of the foliage of a branch enclosed in the teflon cuvet. The principal compounds emitted by *Quercus ilex* are α and β-pinene, sabinene, myrcene, limonene, camphene and traces of isoprene, never exceeding 1 ppbV. The observation that *Quercus ilex* emits much less isoprene than monoterpenes is an unexpected result, contrary to the accepted ideas on the emissions by oak trees. The emission rate profiles show maximum values in the middle of the day and minimum values during the night. The maximum values of emission rates for *Quercus ilex* are of the order of 30 to 35 μg⁻¹.h⁻¹ for the principal monoterpenes as a whole. The data corresponding to the terpenic emission rates provide evidence for the known process called "midday depression". The principal monoterpenes emitted by *Pinus pinea* are β-trans-ocimene, limonene, 1,8 cineole, myrcene, α-pinene, sabinene and β-pinene. The diurnal profile of *Pinus pinea* emissions rates exhibit the same shape as those of *Quercus ilex*, showing in particular the "midday depression" phenomenon. The maximum values of emission rates for *Pinus pinea* are of the order of 4 μg⁻¹.h⁻¹ for the principal monoterpenes as a whole.

Hydrocarbons and their derivatives in volcanic gases:
origin and composition

V.G. Povarov

Chemical Institute of St. Petersburg University, Organic Chemistry
branch, 191804, St. Petersburg, Russia

Volcanic gases emitted into Earth's atmosphere contain a rich variety of organic compounds; among them hydrocarbons of various classes and their derivatives including compounds containing F and Cl have been detected (Stolber et al., 1971). As much as the role of above-mentioned substances in atmospheric chemistry universally acknowledged, the problem of their origin in volcanic gases and gases-analogous composition emitted along deep faults in seismically active zones of Earth deserves interest. The "pyrogenic" hypothesis of formation of organic compounds in the course of the rise of magma through sedimentary rocks which has been advanced earlier (e.g. Symonds et al., 1988) doesn't agree well with data on geological structure of volcanoes.

The present communication examines the problem of origin of the organic component of volcanic gas from thermodynamic point of view. A general mechanism is proposed for the formation of hydrocarbons and their derivatives in magmatic fluid resulting from processes of fractionated gas exchange in the system gas-magma.

Taking volcanoes of the Kurilo-Kamchatka arc as an example it is shown that taking account of this phenomenon in describing processes of magma degassing allows to predict correctly hydrocarbons content in volcanic gas basing on its gross composition.

The developed approach can be applied to describing the global process of degassing of the upper Earth mantle.

References

- Stolber R.E. et al., Geol. Soc. Amer. Bull., 82 (1971) 2269-2302.
Symonds R.B. et al., Nature, 334 (1988) 415-418

Atmospheric Volatile Organic Compounds Containing Nitrogen, Oxygen, Sulfur, and Halogens: Identification, Quantitation, and Sources

Jim Greenberg, Detlev Helmig, Pat Zimmerman, and Elliot Atlas
National Center for Atmospheric Research, Boulder, CO, USA 80307-3000

Volatile organic trace gases, including nitrogen, oxygen, sulfur, and halogen containing-species (NOSH-VOCs), are emitted to the atmosphere from biomass burning, human activities, and natural processes. NOSH-VOCs are also formed in the atmosphere from the chemical processing of other trace gases. Although measurements of many individual NOSH-VOCs have been reported, techniques used are limited by sampling, detection, identification, or quantitation of individual constituents. Consequently, an unknown fraction of NOSH-VOCs is potentially unidentified and not quantified. For example, NOSH-VOCs emitted by vegetation may comprise as much as half of global biogenic emissions.

We have developed a new approach which combines gas chromatography-mass spectrometry (GC-MS) and gas chromatography-atomic emission detection (GC-AED) to characterize individual NOSH-VOCs. GC-AED is used for sensitive detection and quantitation of NOSH-VOCs, classification as O, N, S, and halogen-containing species, and determination of empirical molecular formulae. GC-MS is used to provide structural information required to identify individual NOSH-VOCs. Results from atmospheric and biogenic emission sampling will be presented.

The effect of water vapour on the ozonolysis of simple alkenes
under atmospheric conditions

P. Neeb, O. Horie, S. Limbach, F. Sauer, and G. K. Moortgat
Max-Planck-Institut für Chemie, Division of Atmospheric Chemistry,
D-55020 Mainz, Germany

Ozonolysis of simple alkenes including C_2H_4 , C_3H_6 , $2-C_4H_8$, and C_5H_8 were carried out using a 600 l spherical glass vessel in the 0.5 - 10 ppm concentration ranges, with added water vapour. Products were analyzed by FTIR spectroscopy, HPLC (for peroxides), and ion chromatography (for organic acids). In the case of C_2H_4 , HCOOH and hydroxymethyl hydroperoxide ($HOCH_2OOH$) were found to be characteristic products in the presence of water vapour (2×10^4 ppm), which were completely missing in the absence of water vapour. Also, a significant decrease in the yield of CO was observed with the added water vapour. These results and those of other alkenes will be discussed in terms of the reaction mechanism involving both excited and stabilized Criegee intermediates, and their atmospheric implications will be presented.

Global distribution of NOx emissions from lightning.

Laura Gallardo

Department of Meteorology, Stockholm University, Sweden

Lightning is a very important source of NOx in the free troposphere and thereby also potentially important for the budget of tropospheric ozone. Current estimates of the magnitude and distribution of this source are very uncertain. Price and Rind (1992) proposed a simple parameterization to simulate global lightning activity distribution, which relates the lightning frequency to the updraft intensity, and thereby to the cloud top height of Cb-clouds. Different lightning emission scenarios based on this parameterization using statistics on cloud top heights and maximum updraft velocities from a general circulation model (ECHAM) are studied. This parameterization is implemented in a global 3-D tropospheric chemistry model (MOGUNTIA). The proportion between lightning emission from marine and continental convection and its relevance for the reactive nitrogen balance in remote areas is discussed. Also, the vertical distribution of the lightning source is considered, in particular the relative importance of cloud-to-cloud and cloud-to-ground discharges for the input of reactive nitrogen oxides to the free troposphere.

Measurement and analysis of reactive nitrogen species
in the rural troposphere of Southeast United States

D. -S. Kim*

Dept. of Environ. Engineering, Kunsan National Univ., Kunsan 573-360, KOREA

V. P. Aneja

Dept. of MEAS, North Carolina St. Univ., Raleigh, NC 27695-8208, USA

Ambient concentrations of reactive nitrogen compounds as well as total NO_y were measured during June and early July 1992 at a rural site (Candor, N.C.), in the central Piedmont region of N.C. The measurements of NO_y species were made in an effort to provide a comprehensive understanding of nitrogen chemistry and to investigate the total nitrogen budget at the site. NO_y , NO_2 and NO showed diurnal variations with maxima in the morning. Products of photochemical oxidants such as HNO_3 and PAN, as well as O_3 showed diurnal variation with maxima in the afternoon and minima at night. NO_x was the major species to total NO_y (~45%). The ratio of HNO_3/NO_y was 0.21; it was comparable to the ratios from other rural continental sites in U.S.A. Linear regression of O_3 with $(\text{NO}_y - \text{NO}_x)/\text{NO}_y$ yielded $[\text{O}_3] = 25.8 [(\text{NO}_y - \text{NO}_x)/\text{NO}_y] + 27$, ($r^2 = 0.58$). The regression intercept is interpreted as the O_3 background (27 ppbv) and the slope suggests that 8.6 molecules of O_3 are formed per molecule of NO_x oxidized products (when 3 ppbv of the average NO_y is used). Large NO_y and NO_x/NO_y ratio were found when winds came from continental side; it suggests that synoptic meteorological conditions and transport of source nitrogen species are important in the distribution of NO_y and its relationship with photochemical oxidants.

CHARACTERIZATION OF NITROGEN OXIDE FLUXES
FROM AGRICULTURAL SOILS IN NORTH CAROLINA, U.S.A.

Viney P. Aneja, Wayne R. Rubarge, Vinod K. Saxena
Benny D. Hulbrook, Lee Sullivan and Thomas Moore
Department of Marine, Earth and Atmospheric Sciences
North Carolina State University
Raleigh, NC 27695-8208, U.S.A.

T. Pierce and C. Geron
U.S. Environmental Protection Agency
Research Triangle Park, N.C. 27711, U.S.A.

Abstract

Soil flux measurements of NO_x and NO_y were made during Fall, 1993 and Winter/Summer, 1994 at an agriculturally-managed location in the Coastal Plain of North Carolina. The soil type (Typic Paleudult) is representative of nearly a third of NC. Samples were collected from 6am to 6pm for one month time periods in each season. Additionally, samples were collected over at least two 24-36 hour periods during each of these sampling times to obtain a diurnal profile. These measurements were accomplished using a well-stirred dynamic chamber technique (all internal surfaces made of Teflon). Ambient air was pumped through the chamber at a 9 liter per minute flow rate to reach steady-state (~30 minutes) and then collected in Teflon bags (volume ~10 liter). The collection period was typically ~5 minutes. The samples in the bags were then immediately analyzed for NO , NO_2 and NO_y on-site. These subsequent analyses of the nitrogen species concentrations were carried out using a LMA-3 Luminol-based NO_2 analyzer (Scintrex Ltd.) and a TECO 42S chemiluminescent high sensitivity NO analyzer (Thermo Environmental Instruments Inc.). The instruments were calibrated periodically using multiple dilution with a mixture of 0.019 ppmv NO in N_2 and a mixture of 0.131 ppmv of NO_2 in N_2 . The hourly NO and NO_2 fluxes ranged from 0 to 250 $\text{ng m}^{-2}\text{s}^{-1}$ and <0 to 50 $\text{ng m}^{-2}\text{s}^{-1}$ respectively. Overall average NO flux increased with both level of applied nitrogen fertilizer and temperature.

Vertical distribution of nitric oxide production and consumption in soil cores

J. Rudolph and R. Conrad

Max-Planck-Institut für Terrestrische Mikrobiologie, Marburg, Germany

The flux of NO at the soil-atmosphere interface was modeled by measurements of NO concentration profiles in a column with homogenized soil. The model predicted the NO flux, which was measured in the headspace of the soil core, within 65%. The vertical profiles of NO concentrations could be described by an exponential function. Applying Fick's 2nd law of diffusion we could model the vertical distribution of net NO production and net NO consumption. Depending on whether the NO concentration in the atmosphere was lower or higher than a particular NO concentration, i.e. the compensation point, NO production or consumption dominated. Highest rates of net NO production or consumption were localized at the soil surface. Fertilization with nitrate resulted in increased net NO production and consumption rates in the top soil layer, which was consistent with increased NO fluxes at the soil-atmosphere interface.

An Optimized Method for Airborne Peroxyacetyl Nitrate (PAN) Measurements

W. Schrimpf, K. P. Müller, F.J. Johnen, K. Lienaerts, J. Rudolph

Institut für Atmosphärische Chemie, Forschungszentrum Jülich, 52425 Jülich, Germany

Due to the role of PAN in the photochemical reaction cycles in the troposphere the knowledge of its distribution is of considerable interest for the understanding of the chemistry of the atmosphere. In this presentation we describe a gas chromatographic method for PAN measurement in the background atmosphere, which has been adapted to the special requirements of aircraft based field campaigns. The instrument is installed in a 1,21 m high 19inch rack with a total weight of 50 kg and a power consumption of 750 VA. The instrument is equipped with a commercial liquid injector and a valve system for injection of gaseous samples. The gas inlet system allows automatic injection of samples with defined and constant mass, independent from ambient pressure variations. For calibration we used two different methods: Liquid PAN calibration samples and a permeation device for gaseous calibration samples. Both methods have a reproducibility better than 90 % and agree within an error of less than 15 %. An optimal selectivity of the gas chromatographic separation is obtained by a combination of two short megabore capillary columns of different polarity. The flow rates are 15 ml/min, column temperature 26°C. For detection an electron capture detector operated at 30°C is used. To allow a reliable control of these relatively low temperatures the instrument is equipped with peltier cooling. To avoid baseline or signal drifts from pressure variations in the aircraft cabin an electronic back pressure control is integrated into the instrument. The lower limit of detection is better than 15 ppt, the time needed for one measurement is less than three minutes. Test flights conducted in November 1993 demonstrated the suitability of the instrument for airborne PAN measurements.

Seasonal variation of CO background levels in Venezuela

E. Sanhueza and E. Fernández
Atm. Chem. Lab., IVIC, Venezuela

Using a gas reduction detector, CO was measured in a transect of ~180 km from the coast (Caribbean Ocean) to the central part of the savannah climatic region of Venezuela. Samples were collected at the surface around noontime. Sporadic high levels in polluted plumes were excluded from the averages. No season variation was observed at the coastal site (samples were only collected when air was coming from the ocean) with an average concentration of about 75 ppbv. A large season variation was observed at the savannah sites, with dry season concentrations ranging between 95 and 116 ppbv, and 55 to 75 ppbv during the wet season. At the top of a cloud forest (~1800 m above sea level) located 30 km from the coast, nighttime concentrations (when, due to radiative inversions in the surrounding valleys, the site is not affected by local pollution) are similar to the daytime levels observed in the savannah region. Higher regional CO levels during the dry season are likely due to biomass burning sources. A good correlation between daytime CO and O₃ concentrations suggests a photochemical source of O₃ during the burning season.

OH Radicals-Initiated Photooxidation of Isoprene:
An Estimate of Global CO Production

Akira Miyoshi,^{a#} Shiro Hatakeyama,^b Takashi Imamura^a and Nobuaki Washida^a

^aAtmospheric Environment Division

^bGlobal Environment Division

National Institute for Environmental Studies
16-2, Onogawa, Tsukuba, Ibaraki, 305 Japan

OH radical-initiated photooxidation of isoprene has been investigated experimentally by a 6-m³ photochemical reaction chamber equipped with a long path length FTIR spectrometer. In the presence of NO_x, major primary reaction products were methyl vinyl ketone, methacrolein, and formaldehyde. Their yield were in quantitative agreement with previous measurements. In the absence of NO_x, the reaction mechanism was found to be quite different from that in the presence of NO_x and major reaction products appeared in the infrared spectra were attributed to organic hydroperoxides. The ultimate yield of CO was experimentally determined to be 52 % on the carbon number basis in the presence of NO_x, and 23 % in the absence of NO_x. The CO yield in the real atmosphere was evaluated as 39 % on the carbon number basis and global annual CO production from isoprene was estimated to be 133 Tg C yr⁻¹. Together with a previous estimated of the CO production from terpenes, global CO production from natural hydrocarbons was evaluated to be 229 Tg C yr⁻¹.

#Present address: Department of Reaction Chemistry, The University of Tokyo, 7-3-1 Hongo, Bunkyo-ku, Tokyo 113 Japan.

Measurement of Atmospheric Carbon monoxide
for Environmental Impact Assessment

A. Ramani

Department of Geography, Andhra University, Visakhapatnam, India

Carbon monoxide is of interest as an air contaminant because of its known toxic properties, and also due to its green house effect. Exhaust from the motor vehicles plays a major role. The carbon monoxide produced at the earth's surface migrates by diffusion and eddy currents to the troposphere and stratosphere where it is oxidised to carbon dioxide, which is responsible for 52% of total green house effect. Natural background levels of carbon monoxide are low ranging from 0.01 to 0.9 mg/m³ or 0.01 to 0.8 ppm. Measurements of percentage emission of carbon monoxide have been carried out in Visakhapatnam using carbon monoxide detector tube, and the results reveal that the percentage emission of diesel vehicles (0.015%) is comparatively lesser than that of petrol vehicles (0.033%). The emissions of below one year old vehicle is 0.0 to 0.005 and the emission of five years and above vehicles varies between 0.010 to 0.100. The approximate emission of carbon monoxide for different vehicles per year is observed to be 14,000 tonnes in case of two and three wheelers, 2,300 tonnes by cars and 2,500 tonnes by heavy vehicles. A detailed study is being carried out to measure carbon monoxide emission for industries and motor vehicles of different categories in the city of Visakhapatnam.

A POSSIBLE IMPACT OF STRATOSPHERIC OZONE DEPLETION ON TROPOSPHERIC
TRACE GASES REMOVED FROM THE ATMOSPHERE BY HYDROXYL

L. N. Yurganov (Arctic and Antarctic Research Institute, 38 Bering Street, 199397, St.-Petersburg, Russia)

Carbon monoxide total column abundance was measured in Northern and Southern hemispheres by IR spectroscopical technique. These data (as well as results for CO and CH₄ obtained by other authors) correlated with total ozone measurements. Since 1982 a slowing down of methane increase and in the same time a decrease of carbon monoxide content in spring months were observed. These gases have a common chemical sink in the troposphere: a reaction with radical OH. A possible increase of concentrations of this tropospheric radical can be associated with total column ozone diminution observed in both hemispheres during the last decade and with concurrent increase of UV radiation. The impact of total ozone variations on tropospheric methane and other greenhouse gases (if it is real) has to be taken into account in climate warming simulations.

Transport, turn-over times and effective sink rates of natural sulfur compounds in the remote Arctic Planetary Boundary Layer during the International Arctic Ocean Expedition 1991 (IAOE-91)

E.D. Nilsson, C. Leck, E.K. Bigg, C. Persson
Department of Meteorology, Stockholm University

Large parts of the atmosphere, particularly the northern hemisphere, are under strong influence from anthropogenic emissions of SO₂ (sulfur dioxide) from the use of fossil fuels. Therefore the questions regarding indirect climate control by the biogenic produced DMS (dimethyl sulfide) through the production of CCN (cloud condensation nuclei), suggested by Charlson et al. (1987), are best studied in remote regions. During the IAOE-91, lasting from August to October in the ice-covered Arctic ocean 3-dimensional trajectories showed that air from the Atlantic sector cleaned by the wet removal processes during its transport dominated during the summer while subsiding aged air dominated in the autumn. These unperturbed air masses differ from the polluted air causing arctic haze and known to be transported from the Eurasian continent during winter and spring. The permanent pack-ice offered a unique opportunity to study transport, sinks and sources for substances having an origin in the surrounding biologically productive seas. Measurements of DMS, SO₂, aerosol nss-SO₄²⁻ (non-seasalt-sulfate), aerosol MSA⁻ (methanesulfonate), CN (condensation nuclei) and CCN in combination with transport times from the marine sources, calculated from a large number of trajectories and ice-cover information, have allowed a Lagrangian non-steady state estimation of turn-over times, i.e. 2.5 days for DMS, to be made. Since the pack-ice north of the marginal ice zone compose a negligible source of atmospheric DMS, the effective sink rate of DMS could be estimated. The reliability of the method was tested by calculating the half-life of radon, using the transport time from crustal sources, which was calculated to within 9% of its true value of 3.8 days.

Measurements of oceanic and atmospheric dimethylsulfide, sulfur dioxide, biogenic sulfur and seasalt aerosols during the International Arctic Ocean Expedition 1991 (IAOE-91).

Cecilia Persson and Caroline Leck
Department of Meteorology, Stockholm University, Sweden

IAOE-91, lasting from August to October 1991 provided a unique opportunity to study the natural tropospheric sulfur cycle under conditions of limited anthropogenic influence. Here we report on chemistry measurements that represent a substantial addition to the Northern Hemispheric high latitude (78-90°N) data base. The study covered sampling in open ocean areas, along the ice edge as well as over the pack ice. Chlorophyll *a*, *Phaeocystis pouchetii* and DMS (dimethylsulfide) in the central Arctic Ocean surface mixed layer ranged from 0.33-8.6, 0.33-3.3 µg/L and 0.03-12 nmol/L respectively. Marine boundary layer concentrations of DMS, SO₂ (sulfur dioxide), MSA⁻ (methanesulfonate), nss-SO₄²⁻ (non-seasalt sulfate) and NH₄⁺ (ammonium) ranged from 0.05-17, 0.04-1.7, 0.002-1.4, 0.03-6.9 and 0.03-3.9 nmol/m³ respectively. A three stage cascade impactor (upper size cuts of 0.5, 1.6, 6.5 µm in particle diameter) was used for chemical identification of the above compounds as well as sodium, chloride and nitrate for the size resolved aerosol. Aqueous phase DMS and Chlorophyll *a*, together with atmospheric DMS, MSA⁻, SO₂ and nss-SO₄²⁻, representing airmasses unperturbed by anthropogenic emissions, exhibited a marked seasonal progression. The highest values were found in the open water along the ice edge, in the beginning of August and the lowest values were found in the pack ice in late September. The flux of DMS was calculated to be 0-19 µmol/m²day (mean 0.6 µmol/m²day). In the pack ice region local DMS emissions were negligible compared with long range advection from the bordering seas, except during ice melting in August. Detailed information on airmass origins from trajectory analyses was indispensable for the interpretation of the data.

MODEL-CALCULATED PARTICULATE SULPHATE IN THE ARCTIC.

Trond Iversen, Institute of Geophysics, University of Oslo, Norway
Leonor Tarrason, The Norwegian Meteorological Institute, Oslo, Norway.

A multilayer Eulerian long-range transport model covering major parts of the Northern Hemisphere has been applied to estimate concentrations of Arctic-wide distribution of particulate sulphate. Based on six-hourly meteorological data from ECMWF for the year 1988, the model calculates its own precipitation and diabatic processes, and estimates air concentrations and depositions of anthropogenic oxidized sulphur as well as DMS from the Atlantic Ocean. As is well supported by results from several measurement campaigns, the concentration levels and temporal variance are model-estimated to having a clear seasonal cycle with a winter-spring maximum. Results for several atmospheric levels will be shown and put into the context of large scale atmospheric flows. The main cause of the seasonal variations is the annual variability in these flow patterns. It is hypothesized that the increased contents of sulphate may cause increased cloudiness during the season when the sun is below the arctic horizon. This may in turn increase the infrared absorptivity, and thus disturb the radiation balance so as to decrease the rate of cooling of the lowermost 1-2000 m. As the sun rises above the horizon the increased cloudiness may increase the albedo, as has been anticipated at lower latitudes (IPCC, 1992). However, since the natural arctic albedo is very large, simultaneously imported black carbon probably more than counteracts this slight increase.

Biogenic sulfur and aerosol composition in the Atlantic and Southern Oceans

C N Hewitt¹, B Davison², R M Harrison², M Schwikowski³, U Baltensperger³, C O'Dowd⁴ and M Smith⁴

¹ Institute of Environmental and Biological Sciences
Lancaster University
Lancaster LA1 4YQ UK

² Institute of Public and Environmental Health
University of Birmingham
Birmingham
B15 2TT UK

³ Paul Scherrer Institut
CH-5232 Villigen PSI
Switzerland

⁴ Department of Pure and Applied Physics
UMIST
PO Box 88
Manchester M60 1QD UK

The concentrations of dimethyl sulfide in air were obtained during a cruise between the UK and the Antarctic in the period October 1992 - January 1993 using a method of sampling and analysis optimised to avoid interferences from oxidants. In Equatorial regions (30°N to 30°S) the atmospheric DMS concentration ranged from 3 to 46 ng (S) m⁻³ with an average of 18 ng (S) m⁻³. In the polar waters and regions south of the Falkland Islands concentrations from 3 to 714 ng (S) m⁻³ were observed with a mean concentration of 73 ng (S) m⁻³. The concentrations of a range of DMS oxidation products were also obtained. No clear relationships between reactant and product concentrations were seen. Information on particle number density, Fuchs surface area and the thermal volatility characteristics of the ambient aerosol was obtained, but again no clear relationship with sulfur concentrations was observed. New particle formation during the daytime was seen on a few occasions but it is not clear that this is solely due to DMS oxidation processes. In polar air, the accumulation mode non-sea salt sulfate was found to be in the form of unneutralized sulfuric acid but further north, in maritime air, substantial neutralization by ammonia, probably of marine biogenic origin, occurs.

p235

Dimethylsulfide, aerosols and condensation nuclei over the Atlantic Ocean

B.C. Nguyen, J.P. Putaud, N. Mihalopoulos
 Centre des Faibles Radioactivités, Laboratoire mixte C.N.R.S.-C.E.A.
 91198 Gif-sur-Yvette France

Biological activity of phytoplankton and zooplankton in surface seawater releases about 15 to 40 Tg S/yr of dimethyl sulfide (DMS) into the atmosphere. This gas rapidly oxidizes in the atmosphere to give methane sulfonic acid (MSA) and sulfur dioxide (SO₂) which subsequently reacts to form H₂SO₄. These aerosols (MSA, SO₄⁼) nuclei can act as cloud condensation nuclei (CCN) influencing albedo and therefore, the Earth's climate. Concentration of DMS in seawater was measured during September and October 1991 and during December 1993 and January 1994 in the northern tropical Atlantic ocean in order to estimate the sea-air flux of DMS and to assess the role of DMS in condensation nuclei (CN) production. Atmospheric concentrations of DMS, SO₂, MSA, non sea-salt sulfates (nss SO₄⁼) and CN were also measured during September and October 1991. The division of data into subsets according to continental tracer information by Radon 222 allowed us to show that SO₂ and nss SO₄⁼ concentrations correlated with DMS concentrations in unpolluted air masses. MSA and nss SO₄⁼ were found to be mainly concentrated in particles with diameters <0.6 μm. Daily mean nss SO₄⁼ in the <0.6 μm diameter range and CN concentration were correlated (R = 0.91), which suggests that H₂SO₄ is an important CN precursor. Atmospheric DMS and CN number daily mean concentrations also correlated (R = 0.82). However, the CN population was strongly influenced by continental input less than 500 km downwind of Africa whereas DMS seemed to be able to affect the CN number concentration at about 1500 km from this continent

p236

Seasonal Variations and Origin of Methanesulfonic Acid, SO₄⁼, and SO₂ at Two Marine and One Midcontinental Sites in Canada

Shao-Meng Li, L.A. Barrie, D. Toom, and H. Dryfhout
 Atmospheric Environment Service, Downsview, Ontario, M3H 5T4, Canada

Daily mean atmospheric concentrations of MSA and SO₄⁼ in aerosols and SO₂ at two coastal sites on the Atlantic Ocean and Pacific Ocean and at one midcontinental site in Canada during April 1992 to April 1993 are presented. At the site on the Atlantic coast, Kejimikujik National Park (44°22'N, 65°12'W), Nova Scotia, MSA concentrations usually fall between those at the other sites. A strong seasonal variability is evident in the MSA concentrations, with consistently low winter values of <0.01 μg m⁻³, and more variable spring and summer values in the range of 0.01-0.13 μg m⁻³. At the Pacific Coast site of Saturna Island (48°47'N, 123°08'W), British Columbia, MSA concentration is highest, ranging between 0.001 to 0.2 μg m⁻³, with a mean value of 0.06 μg m⁻³, but with a less pronounced seasonal MSA cycle as at Kejimikujik, reflecting the difference in regional emissions of precursor gases between the two coastal sites. The mid-continental site at the Experimental Lake Area (49°39'N, 93°43'W), Ontario, was selected for its remoteness from marine sources and proximity to potential terrestrial wetland sources. MSA concentrations are generally lower than those at the two coastal sites, about 1/3 of that found at Kejimikujik and a less well defined seasonal variation pattern. In this paper, the relative contribution of anthropogenic, sea salt, and biogenic sulfur to aerosol SO₄⁼ will be discussed. The ratio of MSA/SO₄⁼ in biogenic emissions will be explored using principal component analysis and trajectory sector analysis.

p237

Relative contribution of natural and anthropogenic sources to the aerosol non-sea-salt sulfate at Ny Ålesund, Spitsbergen

W. Maenhaut, G. Ducastel, K. Beyaert (Inst. for Nuclear Sciences, Gent, Belgium) and
 J.E. Hanssen (NILU, Lillestrøm, Norway)

Marine biogenic emissions of dimethylsulfide (DMS) are the major source of atmospheric sulfur and non-sea-salt (nss) sulfate in various oceanic regions. In order to estimate the contribution from this source in the Norwegian Arctic, aerosol samples were continuously collected from April 1991 until September 1993 at the Zeppelin background station in Ny Ålesund. The aerosol was separated in two size fractions of >2.5 μm (impaction stage) and <2.5 μm (filter), and the samples were collected according to a 2-2-3 day schedule. All filter samples were analyzed for methanesulfonate (MSA), sulfate, some other ionic species, and up to 40 elements, including several anthropogenic metals. In addition, selected impaction substrates were analyzed for MSA. The atmospheric MSA levels were highest in the period May-August, with values typically between 10 and 200 ng/m³. From October to March, the MSA concentrations were generally between 0.5 and 4 ng/m³ only. Nss sulfate, on the other hand, showed a quite different pattern, with highest levels in March-April (1-3 μg/m³) and lowest levels from June through September (20-400 ng/m³). MSA was essentially associated with the fine size fraction. The (MSA/nss sulfate) ratio varied very dramatically over the year, from 0.001-0.004 in December-March to 0.05-0.5 in June-July. The marine biogenic and anthropogenic sulfate contributions to the nss sulfate were resolved by multiple linear regression analysis, using MSA as indicator for biogenic DMS and metallic pollution elements as indicators for the anthropogenic sulfate. It was concluded that the marine DMS source contributes about one third of the atmospheric nss sulfate during summer.

p238

Concentrations of Aerosol Methanesulfonate, Non Sea-Salt Sulfate and Ammonium at Three Sites in the Southern Ocean.

R.W. Gillett and G.P. Ayers
 Division of Atmospheric Research, CSIRO, Australia

In order to assess the effect of latitudinal gradients on dimethyl sulfide emissions, and temperature and ultra violet insolation on dimethyl sulfide oxidation, concentration of methanesulfonate, non sea-salt sulfate and ammonium have been measured at the Cape Grim Baseline Station (40.7° S, 144.7° E), Macquarie Island (54.5° S, 158.9° E) and Mawson (67.6° S, 62.9° E) from 1989 until mid 1994. Results of these measurements show a clear annual cycle in methanesulfonate, non sea-salt sulfate and ammonium with concentrations increasing during the southern summer and decreasing during the southern winter. These cycles correspond to those for dimethyl sulfide gas concentrations those already observed at Cape Grim. Differences in the aerosol cycles at the three sites provide some perspectives on the way in which dimethyl sulfide oxidation differs with latitude.

Sulfuric acid particles in the wintertime Antarctic atmosphere

Kikuo Okada and Teruo Aoki
 Meteorological Research Institute
 Tsukuba, Ibaraki 305, Japan

Individual aerosol particles of $>0.3 \mu\text{m}$ radius were collected using an impactor at Asuka Station ($71^\circ 31'34'' \text{S}$, $24^\circ 08'17'' \text{E}$), Antarctica, in the austral winter of 1988. Sulfuric acid particles were found to be dominant in the submicrometer size range. On the basis of electron microscopic examination using the energy-dispersive X-ray (EDX) analyses, approximately 50 % of the particles were determined to be originally sea salt. These sulfuric acid particles would be formed through the modification of sea-salt particles probably by biogenic sulfur gases during transport from the marine atmosphere to the Antarctic atmosphere. Also, sulfuric acid particles without sea-salt inclusions were collected in a south wind.

Emission of biogenic sulfur gases from some Chinese and Japanese soils

Z. Yang
 Institute of Soil Science, Chinese Academy of Sciences, China
 K. Kanda, H. Tsuruta and K. Minami
 National Institute of Agro-environmental Sciences, Japan

Emission of volatile sulfur gases from waterlogged paddy soils and upland soils of Chinese and Japanese were studied in the laboratory. Emission of Hydrogen sulfide (H_2S), carbonyl sulfide (COS), methyl mercaptan (CH_3SH), dimethyl sulfide (DMS), carbon disulfide (CS_2) and dimethyl disulfide (DMDS) were detected. Emission of sulfur gases from paddy soil was more than that from upland, and emission from Chinese paddy soil was more than from Japanese. At same soil, emission of sulfur gases when applied both organic manure and chemical fertilizer was higher than when only organic manure or only chemical fertilizer. On an anaerobic condition, detected biogenic sulfur gas values were far more than on aerobic condition, H_2S was most obvious. Results also have shown that, at higher temperature, oxidized rate of reduce sulfur gases was higher than at lower temperature. It may be related with the distribution of acid rain in China. It is believed that previous results have probably been estimated too low values of emission of volatile sulfur gases from soil-plant system, actual values may be far higher than present estimation.

Transport of anthropogenic sulfur from East Asia to the sea near Japan and its reaction with sea salt particles

Shigeru Tanaka and Hisashi Ishikawa
 Faculty of Science and Technology, Keio University, Japan

Recently, a lot of anthropogenic sulfur has been emitted in East Asia countries with their industrialization. The emitted anthropogenic sulfur has been transported from East Asia to the sea near Japan by the westerly wind. Most of anthropogenic sulfur transported might not be neutralized over the sea for lack of ammonia. Therefore, it is considered that the transported sulfur reacts with sea salt particles (NaCl) and hydrogen chloride is generated in the marine atmosphere. In this study, the atmospheric observation was carried out at remote islands (Okinawa, Tushima and Oki) near Japan and on the route of research vessel, from 1991 to 1994, in order to understand the process of this reaction for the generating hydrogen chloride. As the results of the observation, it was found that the amount of chlorine loss in sea salt particles was strongly correlated with acidity of aerosols. The concentration variation of hydrogen chloride in the atmosphere at Oki was high in day time and low in night time. This fact suggested that the process of hydrogen chloride generated from sea salt particles also depended on the solar radiation.

p242 An emission of marine biogenic sulfur from enclosed coastal sea and coastal area in Japan to the atmosphere

Shigeru Tanaka and Reiji Tahara
 Faculty of Science and Technology, Keio University, Japan
 Kenji Matsunaga
 Solar Terrestrial Environmental Laboratory, Nagoya University, Japan

Dimethyl sulfide (DMS) is considered to a major biogenic sulfur in the marine atmosphere and to play an important role in the global sulfur budget. Many investigations on DMS have been carried out in different marine regions. In this study, concentrations of DMS in both of the atmosphere and sea water were measured especially in enclosed coastal sea (Seto Inland Sea) and coastal area (Saku Island) in Japan, from 1991 to 1994, in order to estimate an emission amount of biogenic sulfur from these areas. As the results, mean concentration of DMS in sea water in Seto Inland Sea was $1340 \text{ ng}/\ell$ in summer and $753 \text{ ng}/\ell$ in winter. An annual DMS emission from Seto Inland sea was calculated to $4.7 \text{ GgS}/\text{y}$ by using the data of DMS concentration measured in this study. This value was less than 1 % of total man made sulfur emission in Japan ($570 \text{ GgS}/\text{y}$). Therefore, it can be mentioned that biogenic sulfur emission from enclosed coastal sea and coastal area is very low compared with man made sulfur emission in Japan.

The Origin of Sulfur dioxide and Sulfate in
the Atmosphere of the North Pacific

Donald C. Thornton, Byron W. Blomquist and Alan R. Bandy
Chemistry Department
Drexel University
Philadelphia, PA 19104

Robert W. Talbot
Institute for the Study of Earth, Oceans and Space
University of New Hampshire
Durham, NH

Our recent studies of the chemistry of sulfur in the atmosphere of the North Pacific Ocean revealed that six months after the eruption of Pinatubo, the stratosphere still contained substantial quantities of sulfur dioxide. Often sulfur dioxide was almost as abundant as sulfate. At northern latitudes transport from the stratosphere to the troposphere was an important contribution to the sulfur dioxide loading of the upper troposphere.

In the mid-latitude troposphere both anthropogenic and stratospherically derived sulfur dioxide were important. Anthropogenic sources became increasingly more important at lower latitudes. Sulfate loadings were comparable to sulfur dioxide loadings in all cases. Anthropogenic sulfur dioxide emitted in the coastal regions of China and Japan remained below about 3 km and was likely removed by dry deposition to the ocean surface. Our data indicate that dimethyl sulfide was not an important precursor of free tropospheric sulfur dioxide.

Most of the sulfur dioxide in the marine boundary layer was brought into the boundary layer by entrainment from the free troposphere. If all the dimethyl sulfide in the boundary were converted to sulfur dioxide it would have made a small contribution to the total sulfur dioxide loading. There was no correlation between sulfur dioxide and dimethyl sulfide in the marine boundary layer suggesting that the oxidation of dimethyl sulfide in the remote marine boundary layer produces little sulfur dioxide.

p244 A model study on the seasonal variation of MSA to n.s.s.sulfate molar ratio
in the marine atmosphere

S.Koga¹ and H.Tanaka²

¹National Institute for Resources and Environment

²Institute for Hydrospheric-Atmospheric Sciences

Recently, the seasonal variation has been observed in MSA to n.s.s.sulfate molar ratio. The cause is still in controversy. The purpose here is to investigate the cause of the seasonal variation. The authors conducted several calculations with the use of a box model under conditions at mid-latitude (40° S). In this model, concentration of NO_x is assumed to be 40pptv. The model calculation shows that while diurnally averaged OH concentration is a factor of 8 smaller in winter (Jun.) than in summer (Dec.), diurnally averaged NO₃ concentration is a factor of 5 larger in winter (Jun.) than in summer (Dec.). Furthermore, the addition reaction rate of DMS with OH in winter is at most 1.4 times as fast as that in summer. Therefore, the oxidation of DMS in winter mainly goes on through the reaction of DMS with NO₃. Consequently, the ratio of MSA to SO₂ production rate is smaller in winter than in summer. One of the reasons for the variation of MSA to n.s.s.sulfate molar ratio is that in winter the reaction of DMS with NO₃ is predominant oxidation pathway rather than that of DMS with OH. The reaction with NO₃ seems to be important for the oxidation of DMS at middle and high latitudes in winter.

Production rates, uptake rate constants and compensation concentrations of OCS in
various soils

S. Lehmann and R. Conrad

Max-Planck-Institut für terrestrische Mikrobiologie, Marburg, Germany

Release and uptake of OCS were measured at 25°C in soil samples which were flushed with a constant flow rate of either air or nitrogen. A cryogenic trapping technique with liquefied argon (-186°C) was used to collect gas samples for analysis in a gas chromatograph equipped with a flame photometric detector. The dependence of net OCS fluxes on gas flow rates and OCS concentrations could be described by a model of simultaneous OCS production and OCS uptake. By using this model, rate constants (*k*) of OCS uptake and OCS compensation concentrations (*m_c*) could be determined as function of the soil type and the incubation conditions. Four different soils were examined. Under aerobic conditions, OCS production (*P*) and uptake were observed in all the soils used. However, the release rates of OCS and the OCS compensation concentrations were small (*P*: 0.33 - 114.1 ngS h⁻¹ gdw⁻¹, *m_c*: 0.83 - 165.85 ngS l⁻¹). The soils showed a larger potential for uptake than for production of OCS. OCS uptake was dependent on temperature (optimum 24°C) which indicated a microbial process. Under anaerobic conditions, OCS uptake could be demonstrated only in one soil.

Formation of COS and methyl thioformate in the oxidation of DMS

I. Barnes, K.H. Becker and J. Patroescu

Bergische Universität - Gesamthochschule Wuppertal, Wuppertal, Germany

The possible climatic implications of the chemistry of DMS for the marine troposphere and COS for the stratosphere are well documented. Studies in this laboratory on the OH initiated degradation of DMS under NO_x-free conditions in large volume reaction chambers using FTIR in situ analysis show that COS is a minor product of the photooxidation. COS accounts for ~0.8 % S in the reaction system. The presence of NO_x in the system reduces the yield of COS. If the yield of 0.8 % S is valid for marine atmospheric conditions, where the NO_x levels are low, then the oxidation of DMS would represent a sizable, as yet unconsidered, source of COS in the atmosphere. Also under NO_x-free conditions methyl thioformate (MTF: CH₃SCHO) has been observed as a product of the DMS oxidation with a yield of ~20 % S. Again, the presence of NO_x reduces the yield of MTF.

Possible mechanisms for the formation of MTF and COS and the influence of NO_x on their formation will be presented and the atmospheric implications for DMS and COS chemistry will be discussed.

Aqueous-Phase Oxidation of S(IV) by CH₃OOH at pH 1-2

H. Hara, S. Nakasato*, and S. Hatakeyama**
 The Inst. Public Health, Aoyama Gakuin Univ.*,
 Nat. Inst. Environ. Studies**

Second-order rate constant was determined for the reaction between sulfite (S(IV)) and methylhydroperoxide (CH₃OOH) over the pH range 1.0-2.0 at 23 C because of its potentially effective process for sulfuric acid formation in the atmosphere. Absorbance of S(IV) at 258 nm was traced by using stopped-flow spectrophotometer. The time profile was analyzed under the pseudo-first order kinetics to evaluate first-order rate constant. This rate constant was obtained for different concentrations of CH₃OOH for three pH values, from which second-order rate constant was determined: $(1.30 \pm 0.05) \times 10^4 \text{ mole}^{-1} \text{ dm}^3 \text{ s}^{-1}$, $(1.31 \pm 0.05) \times 10^4 \text{ mole}^{-1} \text{ dm}^3 \text{ s}^{-1}$, $(1.05 \pm 0.02) \times 10^4 \text{ mole}^{-1} \text{ dm}^3 \text{ s}^{-1}$ for pH 1.0. These values were in good agreement with those derived from second-order reaction rate law.

ESR Studies of the Peroxide Oxidation of aqueous Sulphite

W. G. Filby¹ and W. H. Kalus²

¹Kernforschungszentrum, Karlsruhe

²Bundesforschungszentrum für Ernährung, Karlsruhe, Germany

ESR spectra of free radicals involved in the oxidation of aqueous sulphite solutions have been observed for the cases of hydrogen (I) and di-tert-butyl peroxides (II) and tert-butyl hydroperoxide (III). Spectral parameters indicate that the radical can invariably be assigned the structure SO₃. For the most studied case (III) the reaction is not catalysed by trace metals or light and probably involves the mono-sulphite anion as the reactive species. The formation of the radical can be partially or completely suppressed by stoichiometric amounts of form- or acetaldehyde respectively. Aromatic aldehydes are much less potent. The reaction, which was carried in a flow system, was not noticeably affected by the presence of dissolved oxygen. Trapping experiments indicated that the OH radical is probably not involved and that sulphite radicals do not attack aromatics. The oxidation of sulphite by III is probably several orders of magnitude greater than its complexation by formaldehyde at pH 2.7 and 6.6. Some possible consequences of these reactions in atmospheric processes will be discussed.

Stomatal absorption of sulphur dioxide by pine needles

T. Vesala, K. Hämeri, T. Ahonen, M. Kulmala, P. Aalto, P. Hari*
 University of Helsinki, Department of Physics
 P.O. Box 9, FIN-00014 University of Helsinki, Finland
 *University of Helsinki, Department of Forest Ecology
 P.O. Box 24, FIN-00014 University of Helsinki, Finland

We have studied dry deposition of sulphur dioxide on Scots pine needles both experimentally and theoretically. The measurements were carried out in a cylindrical flow chamber (diameter of 14 cm and length of 23 cm) which contained one normally photosynthesising twig having dry needle surfaces. The drop of the sulphur dioxide concentration in the chamber was detected and the empty chamber did not absorb significant amount of this pollutant. The twig was also dried in order to close stomata and in this case the measurement did not show practically any deposition indicating stomatal transport mechanism for sulphur dioxide. The experimental results were interpreted by a numerical model to deduce an average pore size of stomata. The model solves the steady state diffusion equation for a single stoma. We have also estimated the corrections resulting from the effects of convective flow and stomatal interference (merging concentration fields of adjacent stomata). The average pore size was found to be 4 microns indicating that stomata might be open to different degrees. In addition, the microscopic analysis revealed that some stomatal antechambers were wax-filled.

THE STUDY OF SULPHUR DIOXIDE POLLUTION

S. Madhuri

Urban air contains various pollutants and sulphur dioxide remains one of the major atmospheric pollutant. Severe respiratory and pulmonary problems are observed where SO₂ concentrations in the atmosphere exceeds 150-200 µg/m³. To determine the content of SO₂ in the atmosphere in the city of Visakhapatnam, regular surveys were conducted with the help of high volume ambient air sampler. The SO₂ concentrations of 160 µg/m³ to 390 µg/m³ were observed in industrial areas. In residential zones the concentrations were in between 30 µg/m³ and 120 µg/m³ and at traffic junctions the concentrations were more than 200 µg/m³. The reasons for higher concentrations of SO₂ in premonsoon and minimum during the monsoon are discussed. Correlation was made between meteorological parameters and SO₂ concentrations.

Sulphur in the Siberian atmosphere

A. Ryaboshapko, S. Gromov, and S. Paramonov
Institute of Global Climate and Ecology, Moscow, Russia

A significant part of anthropogenic sulphur emitted into the atmosphere of European industrial regions is transported to the Asian part of Russia. From the other hand there are a lot of anthropogenic sulphur sources in Siberia itself, and emissions here tend to rise. By 1990s the total sulphur emission here was 3.4 Tg/year. The emission field is very uneven. Only one point source of sulphur dioxide provides annual emission of 1.1 Tg sulphur. So, Siberia can be not only the sink but also the source of atmospheric sulphur for the North-western Pacific region. Generalization of monitoring data for last years shows that about 8 Tg of sulphur are removed from the atmosphere over Siberia annually. Main part of this sulphur is removed by wet deposition. The highest sulphur concentrations in air and precipitation are characteristic for industrialized areas of South-western Siberia. At the same time unpredictable high concentrations of excess sulphur in precipitation are observed over Pacific coast areas. The lowest sulphur concentrations can be found in the Northeastern region of Siberia. Seasonal and long-term variations of atmospheric sulphur in Siberia are discussed.

Modelling the global dynamics of soot and sulphate aerosol

W. F. Cooke, F. Raes and J. J. N. Wilson
Environment Institute CEC, Italy

Aerosol particles have a twofold effect on the radiative balance of the earth, by scattering or absorbing light, and by acting as cloud condensation nuclei (CCN) and thus influencing the radiative properties of and lifetimes of clouds. It is recognised that the accumulation mode (0.1 - 1.0 μm) is both the most optically active and the 'source reservoir' from which CCN are formed, and furthermore that the accumulation mode is predominantly formed by the gas-to-particle conversion of gaseous precursors.

Two major components of the accumulation mode aerosol are sulphate and soot. Their precursors have common sources in anthropogenic emissions and biomass burning, although sulphate is additionally formed from natural emissions of DMS and volcanic emissions of sulphur compounds. However, whereas the formation of accumulation mode sulphate aerosol from its gaseous precursors has an as yet uncertain timescale and is strongly influenced by micro-meteorological conditions, soot aerosol is formed over relatively short timescales within the plume, but undergoes physical transformation in the atmosphere. Thus in both cases, the microphysical aerosol dynamics and the larger scale meteorological dynamics are closely coupled. We have developed models for both sulphate aerosol dynamics and soot aerosol, and have implemented them in a global transport model. In this paper, we will present results of our most recent studies with the models.

Tropospheric Aerosols—Their Characteristics of Radiative and Climatic Effects

Yang Jianliang and Wang Mingxing
Institute of Atmospheric Physics, Chinese Academy of Sciences, Beijing 100029, China

Aerosols have radiative effects on solar radiation and terrestrial radiation because of their scattering and absorbing, and therefore impact earth's climate. Unlike the greenhouse gases such as CO_2 , CH_4 , NO_x etc., which are fairly uniform over the global, aerosol distribution (physical and chemical properties) has a much larger temporal and spatial variation. The global climate forcing by aerosols therefore is difficult to exactly estimate. The radiative and climatic effect due to aerosols depends on local aerosol concentrations, size distributions, chemical compositions, optical properties, surface albedo, zenith angles and cloud cover. In this paper practical tropospheric aerosols measured in natural background, rural and industrialized areas are introduced into a radiation transfer model. Finite difference method, which has been proved to be of high accuracy, is used in the model to calculate radiation intensity and flux. Vertically inhomogeneous atmospheres is treated and the calculations are made for different aerosol optical depth and varied physical-chemical properties related to their special source areas, such as in urban areas, in north China, over ocean and over desert. Active atmospheric constituents including water vapor, carbon dioxide, ozone and clouds are also considered. Short-wave and infrared radiative and climatic effects of these aerosols are analyzed.

Physio-Chemical Measurement to Investigate Regional Cloud-Climate Feedback Mechanisms

V.K. Saxena, J.D. Grovenstein and K.L. Burns
North Carolina State University, USA

A critical survey of the existing evidence reveals that the trends in the average global temperature of the Earth-Troposphere system and in global precipitation patterns are mitigated by several natural and anthropogenic differences between the northern versus southern hemisphere. In contrast, climatic changes on a regional scale have been more convincing during the last two decades. A case in point is the frequency of droughts experienced in the Southeast. In situ cloud measurements were taken during 39 individual cloud events between June and October 1993, in Mount Mitchell State Park, North Carolina (home of the highest peak, 6,684 ft. or 2,017m MSL in the eastern United States; Mt. Mitchell is a designated *United Nations Biosphere Reserve*). Cloud reflectivity was simultaneously monitored by the satellite-based Advanced Very High Resolution Radiometer (AVHRR). Clouds with *contrasting microphysical and radiative characteristics* are formed at the site when air masses of marine, continental, and highly polluted origins arrive. Cloud droplet size spectra were obtained and used to determine total droplet concentrations, average droplet radii and cloud liquid water content. Cloud water samples were collected and analyzed for pH and chemical composition. Computation of back trajectories for these cloud events are accomplished by utilizing a hybrid Eulerian-Lagrangian computer model. Clouds formed by polluted air masses had pH as low as 2.4 and by marine air masses as high as 4.75. The latter were found to be least reflective.

p256

Chemical composition of aerosols on a transect from the Sahara to the Gulf of Guinea and the influence on the element concentrations in rain water

L. Herrmann*, K. Stahr* and A. Bationo⁺

*Institute of Soil Science and Site Ecology, University of Hohenheim, Stuttgart, Germany
⁺IFDC/ICRISAT Centre Sahélien, Sadoré, Niger

The chemical composition of aerosols and rain water was investigated on six measurement sites in 1992 on a north-south transect reaching from the border of the Sahara (Ouallam/Niger) to the Gulf of Guinea (Houeto/Bénin). The investigations were conducted in order to estimate the element input, especially of plant relevant nutrients, into the soil. The total element deposition with aerosols and rain water decreases from the north to the south. Aerosols which are transported with the 'Harmattan' in the dry season as well as with convective storms in the rainy season are mainly composed by soil born minerals. On the southern sites plant ashes caused by bush fires contribute to the increase of water soluble element fractions in the aerosols. A close correlation between the amount of transported/deposited aerosols and the element concentrations in the rain water could be found. On all sites the concentrations were high at the beginning of the rainy season and decreased with the ongoing rains. The southern sites were influenced by marine aerosols as well, leading to higher concentrations of Na, Mg and Cl in the rain water.

p257

Effects of Aerosols from Biomass Burning: A Model Study*

Joyce E. Penner, Catherine Lioussé, Charles R. Molenkamp,

John J. Walton, Ingrid Schult^a, and Hélène Cachier^b

Global Climate Research Division, Lawrence Livermore National Laboratory
P.O. Box 808, L-262, Livermore, CA 94551 USA

^aMax-Planck-Institute for Meteorology, Bundesstr. 55, 2000 Hamburg 13 (F.R. Germany)

^bCentre des Faibles Radioactivités, CNRS-CEA, av de la Terrasse, 91198-Gif sur Yvette (France)

We have developed or obtained emissions inventories for the amount of smoke produced from wood fuel burning, agricultural burning, savannah burning, and deforestation. These emissions are used together with our global aerosol model to study the distribution of aerosols from biomass burning. Our aerosol model has been linked to the Hamburg Climate Model, called ECHAM3, as well as to the NCAR Community Climate Model, CCM1. The accuracy of the inventories and the model formulation is tested by comparing the model's simulations of soot or black carbon with observations. The sensitivity of the predicted concentrations is tested by varying the aerosol removal rates by deposition and by precipitation scavenging. Finally, the climate forcing by aerosols from biomass burning is contrasted with that from anthropogenic sulfate aerosols.

*This work was performed under the auspices of the U.S. Department of Energy by the Lawrence Livermore National Laboratory under Contract No. W-7405-Eng-48.

p258

Regional aerosol composition in the eastern Transvaal, South Africa, and impact of biomass burning

W. Maenhaut, I. Salma, J. Cafmeyer (Inst. for Nuclear Sciences, Gent, Belgium),
H.J. Annegarn (Johannesburg, South Africa) and M.O. Andreae (Mainz, Germany)

As part of the Southern African Fire-Atmosphere Research Initiative (SAFARI-92), size-fractionated aerosol samples were collected during September-October 1992 at three ground-based sites in the eastern Transvaal, i.e., at two sites (40 km apart) within the Kruger National Park (KNP) and at a third site on the Transvaal Highveld (150 km SWW of the KNP sites). In addition, aerosol collections were made near prescribed fires in the KNP. The samples were analyzed for particle mass, black carbon, and up to 40 elements. The aerosol concentrations, compositions and time trends at the two KNP sites were quite similar, thus suggesting that regionally representative samples were collected. Receptor modeling calculations, using both absolute principal component analysis and chemical mass balance, indicated that the KNP coarse particle mass (CPM) was essentially attributable to mineral dust and sea-salt, with average relative apportionments of 75% and 25%, respectively. At the Highveld site, mineral dust and sea-salt contributed in a 99/1 ratio to the CPM. The fine size fraction at all three sites was highly influenced by biomass burning products. The pyrogenic component was particularly enriched in black carbon, the halogens (Cl, Br, I), K, Zn and Rb, and it was responsible for about 60% of the mean modeled fine particle mass (FPM). The time trends of CPM, FPM, coarse mineral dust, fine biomass products and fine sulfur at the Highveld site were fairly parallel to those at the two KNP sites. This suggests that the boundary layer air composition of the Highveld and the Lowveld were to some extent coupled by mesoscale meteorology and atmospheric circulation.

p259

Large scale aircraft measurements of biomass burning aerosols in the Amazon basin

F. Gerab(*), P. Artaxo(*) and A. Setzer (**).

(*) Instituto de Física, Universidade de São Paulo, Brazil,

(**) Departamento de Meteorologia, INPE - Instituto de Pesquisas Espaciais, Brazil

In order to assess the large scale distribution of aerosol particles in the Amazon basin during the biomass burning season, aerosols have been sampled during the dry season using aircraft. Two different small two engine aeroplanes from INPE and FUNCEME were used. The flights covered almost all different ecosystems in the Amazon region, including regions with very high frequency of primary forest burning. Aerosols were collected in Nuclepore and Teflon filters, and also cascade impactors were used to measure size distribution. Real time soot carbon determination was performed with Aethalometers. TSI CNC and PMS FSSP probes measured the number of particles. The aerosol samples were analysed by PIXE for elemental composition. Individual particle analysis was performed using Nuclear Microprobe. Very high aerosol concentrations up to 350 µg/m³ were observed. Sulphur, potassium, phosphorus and zinc were the elements associated with biomass burning plumes. Vertical profiles of soot carbon and total particle concentrations were performed in several regions, pointing to a maximum concentration at about 1500m high. These large scale aerosol concentration results allow a comparison with results from three ground based aerosol monitoring stations in the Amazon to obtain information about the long range transport of biomass burning emissions in the Amazon basin.

Trace elements and ionic components in aerosols from direct emissions from biomass burning in the Amazon basin

M. A. Yamasoe(*), P. Artaxo(*), A. H. Miguel(**) and A. G. Allen(**)
Instituto de Física (*), Instituto de Química (**), Universidade de Sao Paulo, Brazil,

Biomass burning emits particulate matter and trace gases that can affect the global atmosphere. The processes involved in vegetation fires, emphasising the flaming and smouldering stages of combustion were studied. We present here results of several sampling campaigns in primary forest sites as well as savannah sites. Fine and coarse aerosol samples were collected using SFU and the elemental concentrations for Si, P, S, Cl, K, Ca, Ti, Fe, Cu, Zn and Br were measured by PIXE. The ionic constituents: K^+ , NH_4^+ , NO_3^- , PO_4^{3-} , Cl^- , SO_4^{2-} , Na^+ , Mg^{2+} , Ca^{2+} , CH_3COO^- , $HCOO^-$ and $C_2O_4^{2-}$, were determined using a Dionex 400 Ion Chromatography system. The comparison between bulk PIXE and IC analyse provided the ratios of soluble to insoluble elements for K, Cl, S, P, Na, Mg and Ca. Large differences in composition were observed between primary forest and savannah emissions. Emissions of Cl and organic acids were observed as unexpected high.

Aerosol Size Distribution and Water Content Measurements During MAGE/ASTEX

Y. Kim^{1,3}, H. Sievering^{2,3}, J. Boatman³, D. Wellman³, and A. Pszenny^{4,5}

Liquid water associated with accumulation-mode aerosols is a strong determinant of their scattering and extinction coefficients. The water content of marine accumulation-mode aerosols has rarely been measured *in situ*, however. We measured size distributions of marine aerosols with PMS ASASP-100X and FSSP-100 optical particle spectrometers aboard NOAA ship *Malcolm Baldrige* as part of the IGAC Marine Aerosol and Gas Exchange (MAGE) Activity's contribution to the Atlantic Stratocumulus Transition Experiment (ASTEX) in June 1992 in the eastern subtropical North Atlantic. Measured distributions were corrected using optical size calibration data based on chemical composition of particles sampled simultaneously with collocated cascade impactors. Corrected distributions were approximated with one or two lognormal functions depending on air mass characteristics. For clean air, $<3 \mu m$ diameter aerosols typically were bimodal, consisting of an accumulation mode and the small end of the sea-salt mode. For polluted air, however, size distributions were dominated by $<1 \mu m$ diameter aerosols in a single mode with high number concentrations. Accumulation mode water content was estimated by differencing series of alternating ambient and dried (heated) air aerosol size distribution measurements. Average accumulation mode aerosol water mass fraction was 0.31, in good agreement with an empirical aerosol growth model estimate.

1. CIRES, Univ. of Colorado, Boulder, CO, 80309 (USA)
2. Center for Environmental Sciences, Univ. of Colorado, Denver, CO, 80217 (USA)
3. Aerosol Research Section, NOAA/ARL - R/E/ARx1, Boulder, CO, 80303 (USA)
4. Ocean Chemistry Division, NOAA/AOML, Miami, FL, 33149 (USA)
5. Now at: IGAC Core Project Office, MIT Bldg. 24-409, Cambridge, MA, 02139 (USA)

J.R. Anderson and P.R. Buseck
Arizona State University, Tempe, Arizona, USA

The individual-particle chemistry and size distributions of mineral particles in samples from the North Atlantic (AEROCE stations on Bermuda and Barbados) and the equatorial Pacific (FeLINE-II) contain information about their history of transport and processing by clouds. Within a single sample, a specific mineral type (e.g., quartz), may have considerable variability with regard to both the degree of aggregation and the soluble salt species with which it is aggregated. For instance, some Saharan dust samples collected on Barbados exhibit only minor aggregation of silicate minerals, whereas in others silicate-containing aggregates are abundant. Although the bulk-sample size distributions may be relatively simple, the size distributions of the separate particle types are typically diverse and more complex than that of the bulk sample. One possible mechanism for the observed features is variable distance of transport in the free troposphere before mixing into the marine boundary layer. When combined with fractionation due to different size distributions of specific particle types, this variable transport history makes it possible for the bulk-aerosol composition to gradually change. The chemical diversity of aggregates must reflect on the diversity of processes occurring within the clouds which form the aggregates. The resulting variability in mineral-particle aggregates should strongly affect the ability of the mineral particles to act as cloud condensation nuclei.

Aerosol dynamics in the equatorial Pacific

Antony D. Clarke
Department of Oceanography, University of Hawaii, Hawaii

For more than a decade the presumed pathway in the conversion of DMS to aerosol sulfate has included SO_2 as a primary intermediate. Recent data has indicated that the lack of variability in SO_2 concentrations in response to changes in DMS is inconsistent with that presumption (Huebert et al., 1993). In July of 1994 a joint experiment on Christmas Island ($2^\circ N$, $157^\circ W$), a clean marine site with significant oceanic DMS emissions, is planned in order to test this hypothesis and other issues related to the source transformation and evolution of aerosol sulfate in the marine boundary layer. Gas phase sulfur species (A. Bandy, Drexel), aerosol chemistry (B. Huebert, U. of Hawaii) and aerosol size distributions and concentrations (A. Clarke, U. of Hawaii) will be collected concurrently over a several week period along with extensive meteorological observations. We will report on the preliminary observations of the aerosol nuclei variability during this experiment including ultrafine condensation nuclei, cloud condensation nuclei, larger condensation nuclei and variations in the size distribution as they relate to this study.

New ways of looking at atmospheric trace element data

R. Arimoto, R. A. Duce¹, K. A. Rahn, and T. M. Church²Center for Atmospheric Chemistry Studies, University of Rhode Island, USA
¹Departments of Oceanography and Meteorology, Texas A & M University, USA
²College of Marine Studies, University of Delaware, USA

As part of the Atmosphere-Ocean Chemistry Experiment (AEROCE), the concentrations of trace elements were determined for aerosol particle samples collected over the North Atlantic Ocean at Bermuda, Barbados, Ireland, and Tenerife. Major components of the marine aerosol population were sea salt, mineral dust, and a suite of trace elements enriched above the concentrations expected from salt or dust. Here we present three new methods for examining the relationships among the trace elements and for assessing their sources. The first method makes use of a normalized fraction of two indicator elements,

$$f(\text{Al}_n) = \text{Al}_n / (\text{Al}_n + \text{Na}_n),$$

where $f(\text{Al}_n)$ is the normalized fraction and the subscript n denotes division of each datum by an average value. This approach allows one to evaluate the relative contributions to a substance from two sources, in this example, dust (represented by Al) vs. sea salt (represented by Na). The second method is graphical and uses elemental ratios plotted on a log-log scale. Through the strategic choice of normalizing elements it is possible to characterize the composition of seawater, crustal and pollution sources. The last method combines aerosol and precipitation data to calculate normalized scavenging ratios,

$$\text{SR}_N = (X/Y)_{\text{Rain}} / (X/Y)_{\text{Air}},$$

where SR_N is the normalized scavenging ratio, X is the element of interest, Y is the normalizing element, and the subscripts *Rain* and *Air* refer to the medium analyzed. When averaged over the proper time scales, SR_N may provide some information on the vertical distributions of the trace elements and on scavenging processes.

Aircraft measurement of aerosol concentration and size-distribution over the western Pacific Ocean

Y. Zaizen, M. Ikegami, Y. Tsutsumi, Y. Makino and K. Okada
Meteorological Research Institute, Nagamine 1-1, Tsukuba, Ibaraki, Japan

Aircraft observation was carried out at an altitude of 4km from Japan to south of Philippine during the period from 19 to 30 January 1993. Aerosol number concentration and its size distribution were measured with three CNCs (TSI Model 3025, 3020 and 3760). Each CNC has different detection size limits; that is, 50% detection radii of CNC 3025, 3020 and 3760, are 2nm, 4nm and 7nm, respectively. Using these CNCs, measurement of the size distribution of fine particles was made. An OPC (Dan Industry model PM730NS-15P) was also used to measure the size distribution of large particles ($r > 0.15 \mu\text{m}$). Small differences in the concentrations were observed with three CNCs in the relation to absolute number concentration of fine particles ($r > 2\text{nm}$), indicating that number proportion of ultra fine particles ($2 < r < 7\text{nm}$) was generally small in the total fine particles ($r > 2\text{nm}$). The observation area was clearly separated into dry- and wet-region in the scale of several hundred km to more than 1000 km. In the wet region, fine particle concentrations showed large variability ($50\text{--}2000 \text{ cm}^{-3}$) on the contrast of those in the dry region ($300\text{--}600 \text{ cm}^{-3}$). High concentrations of the ultra-fine particles were sometimes detected just above the stratocumulus clouds. It is supposed that the new particle formation from gaseous species occurred in the vicinity of clouds in the mixing layer. The results of the Pacific Atmospheric Chemistry Experiment from Melbourne to Japan will also be reported.

Large-scale transport of chemical elements in aerosols over the east coast of Asia

A.N. Medvedev⁺, M. Uematsu^{*}, G.M. Kolesov[#], V.V. Anikiev⁺
⁺ Division of Geochemistry and Ecological problems, POI, Russia;
^{*} Department of Marine Sciences and Technology, HTU, Japan;
[#] V.I. Vernadsky IG & AC, Russia

The long-range transport of aerosol from continents affects the marine atmosphere and oceans. Mineral aerosols from the Asian continent are significant source for the non-biogenic deep-sea sediments in the North Pacific. With this atmospheric transport, pollution aerosol is also expected to be carried from the east coast region of Asia to the western and the central North Pacific. In order to characterize this transport and its effect to the global environment, we have collected the aerosol samples concurrently from Sapporo (43.1° N, 141.3° E), Japan and Vladivostok (43.1° N, 131.9° E), Russia since the fall of 1989. To get a first insight into the data factor analysis was applied. It has been obtained that mineral dust is a common factor for majority of elements over Vladivostok and Sapporo. Local element sources in Vladivostok's atmosphere do not influence element concentrations over Sapporo.

Numerical modeling of transformation of Kosa (yellow sand) in polluted air over China

P.C.S. Lee
Japan Weather Association, Nagoya, Japan.
T. Kitada
Toyohashi University of Technology, Toyohashi, Japan.

It is speculated that Kosa aerosols mitigate acid rain downwind of Kosa sources. A 0-D multi-phase/species equilibrium model including Ca^{2+} , and CO_3^{2-} related constituents is developed based on that of Pilinis and Seinfeld (1987) to investigate the modification of Kosa when advected over Beijing. The urban case results are: (1) In-air H_2SO_4 always resided entirely in the aerosol phase. The aerosol sulfate adhered to Na , and Ca in roughly 50:50 proportion. (2) Deliquescence rh was approximately 70%, and further wetting was rapid. (3) In the presence of abundant Na^+ within the aerosol, majority of the ammonia stayed in the gas phase. (4) With increase of water content, NO_3^- favored the aerosol phase. The rural case results are: (1) H_2SO_4 always resided in the aerosol phase. (2) Deliquescence rh was also approximately 70%, but wetting was slow. (3) Despite of the rather high $\text{NH}_3(g)$ concentration in the air, transport from gas to aerosol was not strong. Thus it shows: (1) Sulfate always resides entirely in the aerosol phase independent of the ambient air quality and rh. (2) In the presence of abundant Na^+ or Ca^{2+} , $\text{NH}_3(g)$ is released. (3) At lower pH levels slower transport of HNO_3 to NO_3^- results. (4) Polluted air accelerates cloud formation during the passing of Kosa. Hence, Kosa mitigates acid rain acidity due (1) to higher dry deposition rate, i.e. larger gravitational settling velocity, (2) to decreased SO_4^{2-} to Ca^{2+} ratio, and (3) to more frequent and intensive wash-out.

Marine and urban aerosols observed by an Aircraft

M. Yamato¹, H. Tanaka², K. Ohta², and K. Matsumoto²¹Gunma University, Maebashi, ²IHAS, Nagoya University, Nagoya, Japan

Aircraft measurements of aerosols were performed over the North Pacific Ocean from mainland of Japan to Hachijyojima which is located at 270 km from mainland in August 10, 1992. Particle chemical composition was analyzed by Ca, BaCl₂, and Nitron thin film method using an electron microscope. Particle concentrations larger than 0.15 μ m radius in five size ranges are monitored with a laser particle counter. It was found that H₂SO₄ particles are basic aerosol in the marine boundary layer (0.3, 0.6 km altitude) and free marine atmosphere (3.0 km altitude). They are cloud condensation nuclei which are formed partially from DMS emitted by marine biota and partially from anthropogenic sulfur. Ammoniated sulfate particles, mineral dust particles and soot particles are transported from the land to the Pacific Ocean. A brownish haze layer was formed at about 0.8 km altitude over the industrial region of Nagoya area. The dominant composition of the layer is soot (coagurated carbon-black particles). Some of them were coated with the solution of soluble materials and can work as cloud condensation nuclei (CCN). NO₃⁻ was combined with pre-existing coarse particles. Heterogeneous chemical reaction process is prevail in anthropogenically perturbed atmosphere.

Asian yellow dust particles observed in Japan

M. Yamato¹, H. Tanaka², Y. Ishizaka², K. Arai³,
Y. Iwasaka⁴, and M. Nagatani⁴¹Gunma University, ²IHAS, Nagoya University, ³Nagasaki University,
⁴STE, Nagoya University, Japan

Asian yellow dust (Kosa) particles were advected to Japan on April 1 1993. At the time, visibility decreased significantly. Radiation intensities, temperature, relative humidity were monitored in Nagasaki. In Nagoya, particles were collected by an impactor and observed with a transmission electron microscope. Size discriminated particle concentrations were measured by a laser particle counter in two places. Dust particle radius ranges up to 2 μ m and has bi-modal size distribution. Assuming that the dust particles are elliptical, a scatter diagram showing the relation between the half length of major axis ($a(\mu$ m)) and the half length of minor axis ($b(\mu$ m)) is plotted. γ defined as $\gamma = b/a$ ranges from 0.3 to unity for the most of the dust particles. Coarse particle concentration decreased after the passage of dust rich airmass advected from Asian continent. On the contrary, the concentrations of particles smaller than 0.15 μ m in radius increased and recovered gradually, indicating that fine particles might have coagurated with dust particles. In the Kosa event, dust particles would interact with "pre-existing" urban aerosols.

Sea-salt component on Asian dust-storm particles

N. Niimura¹), K. Okada²), X.-B. Fan³), K. Kai¹), K. Arai⁴) and G.-Y. Shi³)¹) University of Tsukuba, Tsukuba, Ibaraki 305, Japan²) Meteorological Research Institute, Tsukuba, Ibaraki 305, Japan³) Institute of Atmospheric Physics, Beijing 100029, China⁴) Nagasaki University, Nagasaki 852, Japan

Individual aerosol particles were collected on electron microscopic grids in Beijing (China) and Nagasaki (Japan) during the spring of 1991. Dust-storm particles were examined with an electron microscope and an energy-dispersive X-ray (EDX) analyzer. Asian dust-storm particles mixed internally with sea salt were detected in the samples collected in Nagasaki. Number proportion of the mixed dust particles in all the dust particles ranged from 20 % to 100 %. Brownian coagulation and impaction by differential sedimentation cannot explain the formation of the mixed particles in the radius range of 1-2 μ m during the transport time. Most plausible mechanism is considered to be following cloud processes. Coalescence of cloud droplets formed individually on the dust and sea-salt particles in clouds will occur and the internally mixed dust could be formed upon the evaporation of the cloud droplets. Moreover, the Cl/Na weight ratios in most of the dust particles showed low values less than 1. These results imply the importance in chemical modification of dust-storm particles through cloud processes.

Deposition and inflow sources of non-seasalt sulfate in Shimane Prefecture, Japan

M. Nakao, F. Tanaka, K. Yamaguchi, T. Tatano, H. Wakuri

Shimane Prefectural Institute of Public Health and Environmental Science

H. Mukai

The National Institute for Environmental Studies

H. Hara

The Institute of Public Health

Atmospheric sulfur dioxide and non-seasalt(nss-) sulfates were determined at Oki Islands in order to discuss the sulfur balance in the prefectural area where sulfur deposition is larger than sulfur species emissions in the area. Oki islands are located in Japan Sea, where these concentration levels are one or two orders lower in magnitude than those at rural sites in the Main Islands of Japan. A number of high concentration episodes of sulfur species were observed both in cold and warm seasons, though in fewer cases in warm season. The concentration variations were discussed in terms of transport from major sources surrounding the prefecture by applying back-trajectory analysis. Cold season episodes were found to be associated frequently with trajectories passing potential emission sources in Asian Continent. Sulfur species were interpreted to be transported by strong northwesterly seasonal wind over the Japan Sea. High concentrations in warm season were attributed to sulfur species from active volcanoes, Sakurajima in particular, in Kyusyu, one of the Main Islands of Japan.

ABSTRACT

Gobi Dust Storms and Forestation in China

Farn Parungo
Air Resources Laboratory, NOAA, U.S.A.

Eolian transport of Gobi dust was investigated. During dust storms, dust samples were collected at 10 stations near and downwind of the Gobi Desert. Particle concentrations, size distributions, and chemical compositions at each station were analyzed in relation to air trajectories and satellite imageries. A large dust plume could extend thousands of miles, and dust loading of a plume could exceed a hundred megatons. The falling dust along the path reduces visibility, deteriorates air quality, and causes damages. In past decades, the Chinese planted hundred millions of trees across the northern arid lands to reduce dust. Preliminary data indicate a negative trend in dust storms since 1960. Possible side effects of forestation on surface temperature and precipitation appear to be statistically insignificant in this period. The long-term impact on radiation budget, cloud microphysics, and climate will be discussed.

Scavenging processes of particles by using natural radionuclide

M. Uematsu
School of Engineering, Hokkaido Tokai University, Japan

Atmospheric ^7Be (53.3 day half-life) is thought to be useful as a tracer of submicron particles from stratospheric and upper troposphere. These particles are mainly removed by wet deposition.

In Japan, there are over a dozen regional monitoring networks of environmental radionuclides around nuclear power plants. Several networks have reports of total deposition flux and atmospheric concentration of ^7Be with meteorological data, although their purpose is monitoring the artificial radionuclides.

A seasonal variation was observed at the network of the mid-latitude, with high atmospheric concentrations in spring and fall. Total deposition fluxes were high in winter. On the basis of on atmospheric concentrations, total deposition fluxes, precipitation amounts, and frequencies of precipitation, a significant liner relationship was found between total deposition fluxes of ^7Be and duration of precipitation, not precipitation amount. The results suggest that the efficiency of wet scavenging is rather low for submicron particles compared with large particles.

Variation of tropospheric aerosol extinction profile and optical thickness over Tsukuba, Japan, observed by the NIES lidar

Yasuhiro Sasano¹, Tamio Takamura² and Tadahiro Hayasaka³

¹National Institute for Environmental Studies, Tsukuba, Japan

²The National Defense Academy, Yokosuka, Japan

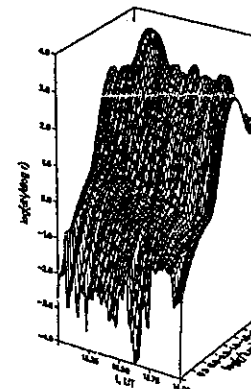
³Center for Atmospheric and Oceanic Studies, Tohoku Univ., Sendai, Japan

A Mie scattering lidar has been routinely operated to obtain aerosol vertical profiles in clear-sky conditions since 1984. The purposes of the measurements are to provide representative aerosol profiles over Japan as functions of month and season and to study their variations. Basic assumptions are that the aerosol optical properties are horizontally homogeneous and that the extinction to backscattering ratio is constant over the region of interest. In the present study, we have assumed the value of extinction to backscattering ratio as 30, 50 and 70, to derive profiles of extinction and backscattering coefficients from the lidar data as a function of extinction to backscattering ratio. The extinction and backscattering coefficient profiles are summarized as monthly, seasonal, and yearly means. The total optical thickness, defined as an integral of extinction coefficient over the altitude region from the ground level to 10 km, shows a clear seasonal change with the maximum in spring (March, April and May). Lidar data are supplemented with aureolemeter and sunphotometer data to infer size distribution and refractive indices of aerosols.

The distribution of aerosols as function of altitude in the atmosphere

R. Jaenicke and V. Dreiling
Institute for Physics of the Atmosphere, University Mainz/Germany

In order to investigate the Arctic Haze the atmospheric aerosol has been investigated with an aircraft with as a set of six continuously recorded aerosol parameters. In an algorithm, these parameters are transposed into aerosol size distributions covering the radius range from a few nanometers up to several ten micrometers. Additional tracers like ozone, nitric oxides, and sulfur dioxide have been recorded. Measurements have been carried out in Summer 1993 and Spring/Summer 1994 in campaigns of 80 flight hours in the Arctic from Sredny (Arctic Ocean) to Resolute (Canada) across the North Pole and over Northern Siberia in an altitude range up to 8000 m. A vast area could be surveyed. These measurements reveal an extremely detailed picture of the atmospheric aerosol with rapidly changing characteristics. Horizontal and vertical structures are very prominent, showing layers at all levels. Gas-to-particle conversion as well as removal could be seen, depending on trace gases present, the transport mechanism and the geographical source region.



Sedimentation and Subsequent Deposition of the Mt. Pinatubo Aerosol over Antarctica

V. K. Saxena and John Anderson
North Carolina State University, USA

Recent discoveries of climate signatures in the antarctic ice sheet of major volcanic events over the past 2 centuries have been well documented. The eruption of Mt. Pinatubo (15.1N, 120.4E) during June 12-16, 1991, injected an estimated 20-30 megatonnes of sulfur dioxide (SO₂) gas and crustal material well into the stratosphere. The SO₂ rapidly converted to sulfuric acid (H₂SO₄/H₂O) aerosol through homogeneous and heterogeneous reactions and got incorporated into the Junge layer where it lingers to this day between 15-25 km. Over time, the Pinatubo aerosol will coagulate and settle into the lower stratosphere and upper troposphere where removal mechanisms will then deposit the larger particles on the Antarctic surface leading to an eventual climate signature. This study focuses on stratospheric settling of the Pinatubo aerosol and subsequent deposition onto the Antarctic surface. The aerosol characteristics such as mass concentration M($\mu\text{g m}^{-3}$), number density N(cm^{-3}), surface area concentration S($\mu\text{m}^2 \text{cm}^{-3}$), and effective radius Re(μm) are inferred from the Stratospheric Aerosol and Gas Experiment (SAGE) II measurements using a modified randomization search technique (RMST) between 15-30 km in the radii range between 0.1 μm to 0.8 μm in 0.1 μm increments. The temporal span of measurements covers September 23-30 and November 13-23, 1991. Preliminary results indicate sedimentation in the presence of vertical and horizontal transport. Bimodal distributions were prevalent between 20-25 km in November with the large mode radii decreasing with an increase in altitude indicating the sedimentation of larger particles. 'Ground truth' measurements at Palmer Station, Antarctica are in progress to measure the deposition fluxes of the Pinatubo aerosol onto the surface. These will be compared with the estimates derived from the SAGE II measurements.

Stratospheric aerosol lidar measurements from Mount Pinatubo at Camaguey, Cuba.

Juan Carlos Antuña
Camaguey Meteorological Center, INSMET, Cuba

Lidar measurements of stratospheric aerosols made at Camaguey, Cuba, 21 N, six months after Mount Pinatubo eruption, show a very large increase in the stratospheric aerosols burden. Peak scattering ratios greater than 20 have been observed in early January 1992. In the same month integrated backscattering between 16 and 33 km show a maximum value bigger than 0.005 1/sr. The course of those parameters as such as the height of peaks and of the layer base between January 1992 and November 1993 are shown.

Precipitation chemistry in India: Dusty atmosphere and alkaline rain

L.T. Khemani¹, G.A. Momin¹, P.D. Safai¹, L. Granat² and H. Rodhe²

¹Indian Institute of Tropical Meteorology, Dr. Homi Bhabha Road, Pashan, Pune 41108
India

²Department of Meteorology, Stockholm University, Sweden

We report on rain chemistry measurements in western India at semi-urban, coastal and high elevation (1300 m) sites with focus on sampling techniques. Large differences were found in base cation concentration between bulk and wet-only collectors even with daily sampling and cleaning of collection equipment. Results from the wet only collectors showed that non-seasalt base cations were giving an excess of bicarbonate over hydrogen ion. Components giving the high alkalinity to the rainwater may have a rather short residence time in the atmosphere which could limit the spatial representativity of stations in these areas.

Estimates of CCN spectra from hygroscopic growth factors and aerosol particle size distributions

B. Svenningsson and H.-C. Hansson
Dept. of Nuclear Physics, Lund University, Sweden

The number of Cloud Condensation Nuclei (CCN) as a function of supersaturation can be calculated from a combination of hygroscopic growth factors and aerosol particle size distributions. There are instruments available that directly measure the CCN spectra, but calculating it as described below gives some additional information e.g. dry particle size and solubility of the CCN.

Hygroscopic growth spectra are measured in terms of diameter change with increasing relative humidity and normally they show two groups of particles with different hygroscopic growth. A comparison of these hygroscopic growth factors with those for pure salt gives the relative amounts of salt in the particles and the minimum size for particles that contain enough salt to be activated at a given supersaturation. The particle size distribution is separated into two distributions according to the fractionation of the particles in the two hygroscopic groups. The number of CCN for a given supersaturation is obtained by integrating these two size distributions from the minimum activated size for each group.

The estimated CCN spectra show that the CCN active at low supersaturations (<0.4%) are dominated by the more-hygroscopic particles. With increasing supersaturation the less-hygroscopic particles become more important as CCN. This means that the effect of soot on the light absorption in cloud depends on the peak supersaturation, since soot probably is most abundant in the less-hygroscopic particles. It means also that the less-hygroscopic particles, and the chemical compounds that they contain, contribute very little to the cloud liquid phase chemistry when the peak supersaturation is low.

Potential Acid-Reducing Capacity of Aerosol Particles and Its
Dependence on Particle-Size over Northern China

Y. Gao, R. A. Duce¹, R. Arimoto, and M. Y. Zhou²

Center for Atmospheric Chemistry Studies, University of Rhode Island, USA

¹ Departments of Oceanography and Meteorology, Texas A & M University, USA

² State Oceanic Administration, P. R. China

Atmospheric dust and anthropogenic sulfate aerosol particles originating from China are two major contributors to atmospheric aerosols in the Northern Hemisphere. In addition to their effects on climate change, their influence on regional air quality in terms of acidification still remains a central concern in Asia. With the projected increase in the emission rate of SO₂ in China, large-scale acidification of rain should be expected, especially in Northern China. However, most of the areas currently affected by acid rain are to the south of the Huai River and the Qin Mountain Chain; these are considered Southern China. One hypothesis that may explain this geographical pattern of acid rain is that a higher acid-reducing capacity of the atmosphere exists over Northern China due to the presence of Asian dust. In order to address this question, we conducted a field experiment to measure aerosol acidity at Beijing, China where the atmospheric concentrations of dust and sulfate are high. We investigated the geographical distributions of dust particles and anthropogenic sulfate, and our analyses also focused on the relationships among trace elements and selected nitrogen and sulfur containing aerosol species. Results from this experiment provide preliminary evidence to support the above hypothesis, suggesting a potential role of heterogeneous interaction between dust particles and anthropogenic sulfate in reducing acidic precipitation.

RESEARCH INTO THE CHEMICAL CONTENT OF AEROSOLS AND GASES
IN THE ATMOSPHERE OVER THE NORTH ATLANTIC, BALTIC,
MEDITERRANEAN AND BLACK SEAS

Medinets V.I.

Ministry for Environmental Protection, Ukrainian Scientific Centre of the Ecology
of Sea (UkrSCES), Odessa, Ukraine

The results of research into the chemical content of aerosols and gases in the marine atmosphere of the North Atlantic and the adjacent seas carried out on the research vessels of the UkrSCES in 1987-93 are discussed. The experimental data on the spatial distribution of the SO₂, NO₂, Na, NH₄, NO₃, SO₄ concentrations and the radionuclides of natural origin Rn-222 (tracer of continental air masses) and Be-7 (indicator of vertical movements of atmosphere) are presented. The anthropogenic inputs of sulphur and nitrogen compounds into their total content in marine atmosphere are estimated. They amount to 25-40, 70-85 and 92-95% for the North Atlantic, the Mediterranean Sea and the Black Sea correspondingly. The influence of air masses from continents transport on the formation of fields of concentration of the substances under research is shown. Life times of aerosol and gas compounds in marine atmosphere are estimated. The programme of marine atmospheric chemistry research being carried out now in the Black Sea region is briefly described. It is suggested to go on with this work in the framework of the NARE project or to create a new international IGAK project for research into the marine atmospheric chemistry in the intercontinental seas.

High abundance of oxalic, malonic and succinic acids in the the remote marine aerosol
samples

Kimitaka Kawamura and Futoshi Sakaguchi

Department of Chemistry, Tokyo Metropolitan University, Tokyo, Japan

A homologous series of low molecular weight dicarboxylic acids (C2-C10) have been detected in the remote marine aerosol samples collected from Pacific Ocean (34°N-15°S, 140°E-150°W) by using a capillary gas chromatography (GC) and GC-mass spectrometer. The molecular distributions of diacids showed a predominance of oxalic acid (C2), which comprised 40-70% of total diacid concentrations (10 - 248 ng/m³). The second most abundant diacid was malonic (C3) or succinic (C4) acid. The diacids with more carbon numbers were generally less abundant. Higher concentrations were observed in the western North Pacific whereas lower concentrations were in the central Pacific. The diacid-carbon accounted for 1-16 % of the total aerosol carbon. The highest value was observed in the low latitudes of central Pacific. Interestingly, relative abundance of oxalic acid was higher in the equatorial and central Pacific. The molecular distributions of the dicarboxylic acids suggested that they are most likely produced in the atmosphere by photochemical reactions of both anthropogenic and biogenic organic compounds. During the atmospheric transport, oxalic acid (C2) seemed to be accumulated in the remote marine aerosols as a result of a preferential production by the photochemical oxidation of longer chain diacids and other organic compounds.

Seasonal changes of dicarboxylic acids and related polar compounds in the Arctic aerosol
samples

K. Kawamura¹, H. Kasukabe¹ and L. A. Barrie²

¹ Department of Chemistry, Tokyo Metropolitan University, Japan and ² Atmospheric
Environment Service, Environment Canada, Canada

Normal saturated dicarboxylic acids (C2-C11) and unsaturated diacids (maleic, fumaric, methylmaleic, phthalic acids) were determined in the Arctic aerosol samples weekly collected in Alert (82.5°N, 62.3°W) 1987-1988 by capillary gas chromatography (GC) and GC-mass spectrometry employing dibutyl ester derivatization. ω-Oxocarboxylic acids (C2-C5, C9), pyruvic acid and α-dicarbonyls (methylglyoxal and glyoxal) were also detected in the aerosols. Oxalic (C2) acid was generally found as a dominant diacid species (1.8-70 ng/m³, av. 14±12 ng/m³) followed by malonic (C3; 0.05-19 ng/m³, av. 2.5±3.3 ng/m³) and succinic (C4; 0.51-18 ng/m³, av. 3.8±3.5 ng/m³) acids throughout seasons. Total concentrations of dicarboxylic acids showed seasonal variation (4.3-97 ng/m³, av. 25±20 ng/m³), with two maxima both in September to October and in March to April. The autumn peak was suggested to be caused by enhanced contributions from both biogenic and anthropogenic sources followed by photochemical reactions, because this was consistent with higher concentrations of n-alkanes from terrestrial plant waxes and of soil-derived aluminum in the autumn aerosol samples. On the other hand, the spring peak was observed during the period of "Arctic Sunrise", suggesting that diacids in the spring aerosols were secondarily produced by photochemical oxidation of organic pollutants carried into the Arctic.

Interactions between aerosol particles, cloud droplets and ice crystals at the high-alpine site Jungfraujoch

M. Schwikowski, U. Baltensperger and H.W. Gäggeler
Paul Scherrer Institute, CH-5232 Villigen PSI, Switzerland

In-cloud scavenging experiments were conducted at the high-alpine observatory Jungfraujoch, Switzerland (3450 m asl) to study the interactions between aerosol particles, cloud droplets and ice crystals. The aerosol phase was characterized by number concentration, size distribution and chemical composition, the cloud phase by liquid water content, size distribution and chemical composition, and the ice phase by ice water content, chemical composition and morphology. The concentration of chemical trace species in ice crystals was found to be governed by the prevailing scavenging mechanism. This can be pure nucleation scavenging, impaction scavenging of aerosol particles, diffusion scavenging of gases, and the accretion of supercooled cloud droplets (riming). A chemical fractionation between cloud droplets and ice crystals is observed, with NH_4^+ and SO_4^{2-} predominant in cloud droplets whereas ice crystals are enriched in NO_3^- (from gaseous HNO_3) and Ca^{2+} (Ca^{2+} rich soil particles serve as ice nuclei). This indicates that the physical and chemical properties of the aerosol particles like size and composition are responsible for the observed chemical fractionation.

Historical and future trends of lead and cadmium air concentrations and total depositions over Europe

J. Alcamo¹, L. Bozó², J. Bartnicki³ and J.M. Pacyna⁴
¹RIVM Environmental Forecasting Division, The Netherlands
²Institute for Atmospheric Physics, Hungary
³IBM Bergen Environmental Sciences and Solutions Center, Norway
⁴Norwegian Institute for Air Research, Norway

Lead and cadmium are emitted to the atmosphere first of all as volatile gases. Within a few minutes or hours the emitted gases condense into or adhere onto fine particles which can be transported hundreds or more kilometres from their sources before gradually being removed from the atmosphere. Air concentration and total deposition of aerosols containing lead and cadmium were estimated by means of a long-range atmospheric transport model (TRACE) computations over Europe. Both historical (1955-1985) and future (1985-2015) trends based on three different emission scenarios were analyzed. Cumulative depositions for both 30 years periods were also calculated. It was found that air concentration and total deposition of lead decreased significantly in Europe (mostly over the western part of it) due to the decrease of lead content of gasoline as well as to the introduction of unleaded fuel. The emission of cadmium also decreased in all European countries during the last decades. The air concentration and rate of cadmium deposition computed by TRACE model are greater over central-eastern Europe as compared to the western part of the continent.

Chemical Composition of Small Particles and Annual Behaviour of Ozone Concentrations in the Eastern Highlands of Zimbabwe, Africa

W.Kosmus, R. Wippel* and S.B.Jonnalagadda**
*Institute for Analytical Chemistry, University of Graz, Austria
**Chemistry Department, University of Zimbabwe

With passive samplers ozone was monitored in the eastern highlands at ground level of Zimbabwe during 1991 and 1992, partially 1993. With the dependence of the zenith angle of the sun ozone levels increase during August, with a first maximum in October. As during the dry season grass burning is common, the atmosphere contains high concentrations of fine particles. To get an idea how these particles could influence the atmospheric chemistry, we collected these particles in September 1993. With a laser-microprobe-mass-analyser we studied the chemical composition of each individual particle, altogether 800. About 85% of the particles with a diameter around 2µm are of biogenic origin, containing mainly Na, K, NO_3 , SO_4 , PO_4 and carbon, but through condensation reactions they are highly loaded with salt of marine origin. About 15% of the particles show the typical composition of soil erosion, namely Al, Si, Fe, Ti and Ca. As several parameters change at the same time, e.g. dry season with increased biomass burning, it is hard to explain the ozone behaviour by only one parameter. It is obvious that grass fires first decrease the ozone levels by the oxidation of nitrogen oxides to nitrate. In the following days the ozone levels increase to such an level, which is appropriate to the seasonal climatic conditions. After heavy rain showers, when the particles are removed, the ozone increases according to the strength of the sun radiation. Therefore we presume a higher impact of climatic factors to the ozone levels rather than atmospheric chemistry by particles.

J.Cainey, G.Ayers and M.Hooper

Division of Atmospheric Research, CSIRO, Australia.
Centre for Environmental Science, Monash University, Australia.

A micro orifice uniform deposition impactor (MOUDI) was installed at Cape Grim, Tasmania (40°40'56", 144°41'18"), in September 1993, to monitor the size distributed chemical composition of cloud condensation nuclei.

The MOUDI consists of twelve stages, with cut offs from particle radius of 9 to 0.028µm. It was installed with a heated inlet to bring ambient air to a relative humidity to less than 50%. Sampling criteria were set for a minimum volume of 100m³ of baseline air, that is air originating from the remote southern ocean, arriving at Cape Grim in the sector 190° to 280° and having a CN concentration of less than 600Ncm⁻³.

Each of the twelve stages were analysed, using ion chromatography, for cations (sodium, ammonium, calcium, potassium and magnesium), anions (chloride, bromide, nitrate, sulfate and oxalate) and methane sulfonic acid.

The results indicated that sea salt predominated at the larger size ranges and that the non sea salt sulfate maximum occurred at a lower size range. Methanesulfonate showed a bimodal distribution, suggesting that particle surface area influences the uptake of methane sulfonate.

The MOUDI results, taken in conjunction with concurrent measurements of CCN number/size distribution, give an insight into the relative importance of sea salt, sulfur species and possibly other compounds, such as organic carbon, in climate modification.

The chemistry and size distribution of aerosol measured at Baring Head, New Zealand

M.J. Harvey*, I.S. Boyd*, D.J. Wylie, A.G. Allen & A.L. Dick

*National Institute of Water & Atmospheric Research Ltd., Lower Hutt, New Zealand

With the aim of providing data on air quality and background atmospheric composition, measurements of aerosol chemistry started at Baring Head (41°S) in 1991. Few previous measurements are available for New Zealand. Differences between aerosol in onshore and offshore winds have been examined. Composition of major ions and methanesulphonic acid (MSA) has been determined by ion chromatography from samples collected by a single stage cascade impactor with size cuts at either 0.5 or 7.2 μm . The chemistry measurements are accompanied by occasional sizing measurements from an optical particle counter (PMS ASASP-100X). During onshore winds, marine background aerosol is supplemented with aerosol from the surf zone. Offshore winds contain a significant marine component with the addition of crustal and anthropogenic aerosol from the greater Wellington region. The onshore concentration of sodium and chloride is typically 8 to 10 $\mu\text{g m}^{-3}$, two to four times greater than in offshore winds. 30 to 40% of the sea salt is found in particles $>7 \mu\text{m}$, which fall out fairly rapidly with passage inland. Of other components measured, sulphate concentrations are largest in onshore winds ($\sim 1.5 \mu\text{g m}^{-3}$) and nitrate concentrations, due to anthropogenic influences, are largest in offshore winds ($\sim 0.5 \mu\text{g m}^{-3}$). MSA shows a distinct seasonal cycle with mid-summer maximum as a result of the seasonality in the strength of its biogenic source. Comparisons will be made between these measurements and a data series collected at Leigh (36°S) on the north-east coast.

Physicochemical properties of Arctic aerosols

M. Yamato¹, H. Tanaka², K. Tsuboki³, R. Kimura³, T. Endou⁴, Y. Asuma⁴, A. Yamashita⁵, H. Toritani⁶, M. Calvez⁷, and R. Gillis⁷

¹Gunma University, ²IHAS, Nagoya University, ³ORI, University of Tokyo, ⁴University of Hokkaido, ⁵Osaka University of Education, ⁶The Defense Academy, Japan, ⁷Atmospheric Environment Service, Canada

As a part of the Influence of the Arctic on mid-latitude Weather and Climate Program, Arctic aerosol particles were observed in August 1992, September 1993, and January 1994 in Resolute (74° N), Cambridge Bay (69° N) and Inuvik (68° N) in Northwest Territories, Canada. Aerosol particles were examined with electron microscope. The radii of the secondary particles at Resolute in August in 1992 range from 0.01 to smaller than 1 μm with mode being smaller than 0.1 μm . The particles is generally smaller than those in mid-latitude troposphere. This reflects the difference in aerosol growth process. Nitrate was combined with mineral dust particles of local origin. There is no significant difference between Resolute and Cambridge Bay aerosols. These aerosols have an homogeneous distribution in space in the Arctic regions. The present results suggest that the Canadian Arctic atmosphere is relatively "clean" atmosphere during the period in summer season. The laser particle counter data and the seasonal trend of the properties of the Arctic aerosols will be presented.

Wet Deposition in Remote Regions: Implications for Environmental Processes

J. N. Galloway & W. C. Keene
University of Virginia
Charlottesville VA, USA

G. E. Likens
Institute of Ecosystem Studies
Millbrook NY, USA

The natural atmosphere is a major link among ecosystems. Emissions from one system are deposited to downwind ecosystems, often at rates significant enough to affect ecosystem processes. Unfortunately, there are few long-term estimates of atmospheric deposition in remote regions to examine atmospheric:biospheric links over scales of space and time.

For the past fifteen years, we have measured the composition of wet deposition to remote ecosystems under the auspices of several programs: Western Atlantic Ocean Experiment; Atmosphere/Ocean Chemistry Experiment and the Global Precipitation Chemistry Project. In this paper we use data from several remote locations (Amsterdam Island, Indian Ocean; Bermuda and Barbados, North Atlantic Ocean; Torres del Paine, Chile; Katherine, Australia; Lijiang, China) to address the following questions.

1. What are the temporal and spatial variabilities of the rates and composition of wet deposition to remote marine and terrestrial ecosystems?
2. What are the linkages between ecosystem processes and atmospheric deposition in the remote world?
3. To what extent do atmospheric models accurately reflect the wet deposition of S and N species in remote regions?
4. How do the composition and the variability of wet deposition rates in remote regions compare to those in populated regions?

The Model Simulations on the Amount of Soluble Mass During Cloud Droplet Formation

M. Kulmala, P. Korhonen, T. Vesala and S. Clegg*

University of Helsinki, Department of Physics
P.O. Box 9, FIN-00014 University of Helsinki, Finland

*University of East Anglia, School of Environmental Sciences, Norwich
NR4 7TJ, U.K.

According to various measurements the amount of cloud droplets is considerably increased in polluted areas. Conventionally this has been assumed to be caused by the increase in the total amount of aerosol particles, which also has an effect on the amount of Cloud Condensation Nucleus (CCN) available. However, Kulmala et al. (J. Geophys. Res., Vol. 98, D12, pp. 22949-22958, 1993) have recently suggested that also the condensation of nitric acid (HNO_3) could allow bigger fraction of the initial aerosol particle distribution to act as CCN. In this work we have studied the development of the amount of soluble mass (NH_4^+ and NO_3^- ions) during the formation and growth of cloud droplets by using an air parcel model. According to our simulations, considerable amount of HNO_3 condenses on the droplets in the very early stages of the development of cloud droplets, which increases significantly the amount of NO_3^- ions in the droplets. When the concentration of HNO_3 vapour corresponds to that in the polluted areas, the formation and growth of cloud droplets become easier.

A Model Calculation of Sulfate and Nitrate Deposition in Japan

N. Katatani¹⁾, Y. Sasaki²⁾, N. Murao³⁾, S. Okamoto⁴⁾ and K. Kobayashi⁵⁾¹⁾Yamanashi Univ. ²⁾Fujitsu F.I.P. Corp. ³⁾Hokkaido Univ. ⁴⁾Tokyo Univ. of Inf. Sci., ⁵⁾Japan Environ. Management Assoc. for Industry.

Acid deposition is one of the most important environmental problems in east Asia. It is necessary to clarify the source-receptor relationship for effective countermeasures based on the international cooperation. For these objectives, model calculations are useful. Many models have been already proposed to predict acid deposition, however, few studies are concerning nitrates deposition because of its complexity in chemical and physical processes compared to that of sulfates.

The authors have developed a numerical model to predict the concentration and deposition amount of sulfur oxides. The description of the model and the results of validation studies are reported in our previous papers. In this report, the results of application of our model to nitrogen oxides are shown. After that, the results of trial calculations are shown to estimate the region-by-region and/or nation-by-nation source contribution ratio to the deposition of both sulfur oxides and nitrogen oxides in Japan.

From the results, it is shown that the overseas transport of pollutants have certain contribution to the acid deposition in Japan, especially in the area along Sea of Japan. On the contrary, the contribution of domestic emission is not negligible especially concerning volcano emissions.

p294 Increase of radiation dose due to acid precipitation

K. Okamoto and S. Tanimoto

Toyo Gakuen University, Hiregasaki, Nagareyama, Chiba, Japan

Emission of sulphur and nitrogen oxides into the atmosphere gives rise to acid precipitation and its effects are usually interpreted in terms of lake acidification, forest destruction and so on, but it also increases radiation doses of the public. It is well known that leaching rates of metals are increased by acidification. In the case of radioactive nuclides such as uranium or thorium and their decay products also their leaching rates as well as transfer rates to plants are increased. Radiation doses of the public are increased either by intake of these plants directly or of meat or milk of animals who eat such plants. Dependences of leaching and transfer rates of natural and man-made radioactive nuclides on pH are investigated and they are found to be inversely proportional to nth power of pH, where n is around 5. Therefore the increase of radiation dose due to this effect is fairly large, and should be considered in certain cases.

Influence of the growth mechanism of a snow particle on its acidification

T. Takahashi*, T. Endoh**, K. Muramoto***, T. Nakagawa*** and I. Noguchi****

*Hokkaido Univ. of Educ., **Hokkaido Univ.,

Kanazawa Univ., *Hokkaido Inst. of Environ. Sci.

A snow particle grows by deposition from the vapor phase or riming in cloud. In this paper, we throw light on the difference of snow acidification by these growth mechanisms. Snow samples collected at intervals of about 1 hr at the suburb and the center of Sapporo, Japan were chemically analyzed. The shape of a snow particle, the snowfall intensity and so on were continuously observed. Simultaneously, the data from a dopplar radar were collected.

Whether rimed or not, the samples collected at the suburb had a pH between 4.0 to 4.5. In vapor deposition, the concentration of NO_3^- was relatively high. HNO_3 vapor was most likely adsorbed on the surface of a snow particle because of the less concentration of NH_4^+ . Cl^- also contributed to the acidification of the particle. On the other hand, rimed snow particles included many amounts of SO_4^{2-} . The samples at the center of the city were less acidic at the start of a snowfall because of relatively high concentration of nss- Ca^{2+} .

RELATIONSHIP BETWEEN THE ATMOSPHERIC PARTICULATE FRACTION AND THE IONIC CONTENT OF PRECIPITATION.

H. Casado¹, D. Encinas¹ and J.P. Lacaux²¹ Dpto. Física Aplicada II. Facultad de Farmacia, Vitoria (Spain)² Laboratoire d'Aérologie, 65300-Lannemezan (France).

In the cattle-raising and forest region of Olaeta (Spanish Basque Country), we have studied during the period April 88 and April 91, the relationship among the ionic content of the atmospheric particulate fraction and the ionic content in the rainwater.

The atmospheric particulate fraction is dominated by the SO_4^{2-} and NH_4^+ ions with $4.6 \mu\text{g m}^{-3}$ each of them.

The precipitation is characterized by abnormal high concentrations of the Cl^- ion with $173.4 \mu\text{eq l}^{-1}$ (relation $\text{Cl}^-/\text{Na}^+ = 3$), following in importance the NH_4^+ and Ca^{2+} ions with 95.9 and $91.0 \mu\text{eq l}^{-1}$, respectively. The mean concentration of H^+ is $47.9 \mu\text{eq l}^{-1}$ (pH=4.3).

The contribution of the soluble particulate fraction in a hand and of the gases in the other to the ionic concentrations registered in the precipitation, differs widely from some ions to some others, being the contribution of the HCl gas the most important one. Approximately the 95% of the Cl^- ion of the precipitation, proceed from the gas phase.

The scavenging relation, is very marked by the Cl^- ion ($W = 40000$), because this ion is found in the atmosphere mainly in gaseous form. The minor scavenging relation are present for the SO_4^{2-} and NH_4^+ ions ($W = 1100$ y 700 , respectively) due, probably, because these species are found forming part of the smaller particles of the aerosol.

S and N wet deposition at two rural sites of the western Maracaibo Lake Basin, Venezuela.

J. Morales *, C. Bifano and A. Escalona**
 *Lab. de Química Ambiental. LUZ. Venezuela
 ** Instituto de Geoquímica .UCV. Venezuela

Event rains were collected during one year at Catatumbo and La Esperanza sites. Volume-weighted average (VWA) acid pHs were found at both sites: La Esperanza VWA-pH= 4.23 (3.4-6.2) and Catatumbo VWA-pH= 4.64 (3.0-6.3). In general, the monthly trends of wet deposition of ions show two peaks. The first peak occurs at the early rainy season (April-May); and the second one occurs at the end of the rainy period (October-November). It was found that the wet deposition of hydronium and sulphate show the same seasonal cycle. The annual depositions of S (SO_4) were $638.5 \text{ mg-S m}^{-2}$ (La Esperanza) and $1483.1 \text{ mg-S m}^{-2}$ (Catatumbo), levels which are considered to be dangerous to aquatic ecosystems. The annual depositions of N (NO_3 and NH_4) were $563.6 \text{ mg-N m}^{-2}$ (La Esperanza) and $1396.5 \text{ mg-N m}^{-2}$ (Catatumbo); and the ammonium deposition accounts for ~ 67% of the total nitrogen wet deposition.

Assessment of the sulphur and nitrogen wet deposition and rain acidity over the Central Caribbean Region. Evidence for natural fluctuations and anthropogenic perturbations

C.M. López Cabrera
 Meteorology Institute, Sciences Academy, Cuba

The Caribbean Region is located between a Northern continental area which confronts present problems of acid deposition and another Southern area considered likely to have the same problem for the rapid increase of its emissions (Rodhe et al., 1988). Cuba, for being an island and its location, is the right place for monitoring the acidification expansion in the tropical zone. An evaluation of sulphur, nitrogen and hydrogen wet deposition in Cuba in the period 1981-1992 is presented, from rain samples collected monthly which excludes dry deposition, obtained in eight regional stations of the Meteorological Institute. Measurements have revealed acid rain problem signs and higher values of deposition and anomalies in the sulphur trend. The atmospheric budget of this element for the country has show that a considerable part of it, comes from external sources out of the country. Evidences suggest that this behavior is related to changes in the natural and anthropogenic emissions and to the climatic variability, especially for ENSO event influence.

A 90-year precipitation chemistry record from the Chongce Ice Cap in West Kunlun Mountains, China

Kumiko Goto-Azuma
 Nagaoka Institute of Snow and Ice Studies,
 Suyoshi, Nagaoka, Niigata 940, Japan

Masayoshi Nakawo
 Institute for Hydrospheric-Atmospheric Sciences,
 Nagoya University, Chikusa-ku, Nagoya 464-01, Japan

Han Jiankang
 Lanzhou Institute of Glaciology and Geocryology,
 Academia Sinica, Lanzhou, China

A 32 m deep ice core was retrieved on the Chongce Ice Cap in West Kunlun Mountains, China to reconstruct the past environment and precipitation chemistry around the area. The altitude of the ice coring site was 6100 m a.s.l.. The core was analyzed for stable isotope ratio of oxygen, electrical conductivity, major anions, major cations and solid particles. The seasonal variations of stable isotope ratio, electrical conductivity, solid particle concentrations and ionic concentrations in the past snow seemed to be preserved in the core, although relatively heavy surface melting takes place at the ice coring site during the summer. Combined measurements of different components enabled us to identify most of the annual layers, even when the seasonal variation of each component was obscured by the summer melting.

The core was roughly dated by counting annual layers. We could trace the past snow chemistry back to the 1890's. Throughout the last 90 years, the predominant impurity in snow on the Chongce Ice Cap was calcium. Major portions of chloride, nitrate and sulfate were suggested to be of salt origin, not of acid origin. Nitrate and sulfate concentrations did not show any increasing trends in the past 90 years. This might be explained in terms of the high altitude of the coring site where the lower tropospheric pollution cannot reach. To draw a firm conclusion, we are now analyzing a new ice core excavated in 1992, which suffered less melting than the 1987 core and is expected to cover at least several hundred years.

Acid Deposition of Sulfur in Asia

Richard Arndt and Gregory R. Carmichael
 Department of Chemical & Biochemical Engineering
 Center for Global & Regional Environmental Research
 University of Iowa, Iowa City, IA USA

The long range transport of SO_2 and sulfate in Asia is analyzed through the use of multidimensional models. The future air quality of this region can be expected to be heavily influenced by consideration of Asia's population and its trends, its growing economy, and the associated systems of energy consumption and production. These factors combined with a major fuel shift in the region to the use of indigenous coal, will result in increased emissions of pollutants into the environment. By the year 2010 the emissions from Asia are projected to exceed the combined emissions from Europe and North America !!! Similar growth in emissions are projected for NO_x .

Potential impacts resulting from present (and future increases in) emissions are being evaluated through the use of multi-dimensional air pollution models. Presented in this paper will be current results of the seasonal cycle and annual deposition patterns of sulfur in Asia. Calculated sulfur distribution and deposition patterns in the region from Pakistan to Japan and from Mongolia to Indonesia will be presented and compared with available observational data. Results will be presented in relation to new critical load estimates for Asia. Preliminary results from a new 40 station background network of SO_2 passive samplers will also be presented.

p301

Rainwater Composition and Acidity at the Hong Kong BAPMoN site, Yuen Ng Fan

G.P. Ayers¹ and K.K. Yeung²

1. Division of atmospheric Research, CSIRO, Australia
2. Royal Observatory, Hong Kong

Rainwater composition determined at the Hong Kong BAPMoN site since February 1988 is analysed in terms of data quality, then investigated for evidence of acid-base components contributed by anthropogenic emission sources. Rainwater composition at the site exhibits clear evidence of enhanced acidity resulting from anthropogenically-derived sulfuric and nitric acids, at levels consistent with expectations based on estimated regional emission fluxes of acid precursors.

The annual wet deposition fluxes of mineral acidity at the site are at levels that have caused concern in acid-sensitive environments in Europe and North America, indicating the need for ongoing work on wet and dry deposition in the region, as well as studies on the sensitivity of regional ecosystems to acidification resulting from atmospheric deposition.

p302

On Acid Precipitation of Shanghai

Zhang Chao

(East China Normal University, 200062, Shanghai China)

The pH value of Precipitation of Shanghai District becomes lower since 1983. The yearly mean pH values of 1983 to 1986 are all less than 5.6, ranging from 5.12 to 5.23. The mean pH value of acid precipitation is 5.09, ranging from 4.65 to 5.44. The area of acid precipitation is gradually extending. Before 1983, the acid precipitation mainly happened in the southwest of Shanghai, Shanghai County, Shongjiang County, and Qingpu County. After 1983, the acid precipitation takes the urban area as centre, including the southwest and the southeast district, Chuansha County, Fengxian County, Naihui County and etc. In urban areas, the frequency of acid precipitation is highest, reaching to 50%-90%, the acidity of precipitation is also highest, pH values of precipitation are all less than 5.0. The acid precipitation of Shanghai District is obviously seasonal in suburbs, pH values are higher in winter, while lower in spring, summer and autumn. The seasonal variation of acid precipitation in urban districts is not obvious, the acid precipitation distributes in 12 months of a year. The dust in the atmosphere of Shanghai district produces an obvious cushion effect to the acid precipitation. With the dust in the atmosphere decreasing, the acidity of precipitation is increasing. There is close relation between the rainfall and the acidity of precipitation, when the dust pollution is not serious, the frequency of acid precipitation becomes higher with the increase of rainfall. The result of regression analysis indicates that the acid precipitation of Shanghai district is mainly controlled by the ions SO_4^{2-} , Ca^{2+} , HCO_3^- . Ions Ca^{2+} , HCO_3^- mainly come from soils and the SO_4^{2-} , Ca^{2+} in rain water have good connectedness with the pH value of precipitation. The SO_4^{2-} in rain water also has good connectedness with alkaline metal ions and NH_4^+ , which shows that the SO_4^{2-} in rain water mainly exists in the form of sulphate. The acid precipitation of Shanghai district is mainly controlled by local pollution.

p303 The Acidification of Atmospheric Aerosol Related to Relative Humidity and Its Contribution to the Acid Precipitation

Yang Jianliang and Wang Mingxing

Institute of Atmospheric Physics, Chinese Academy of Sciences, Beijing 100029, China

The sulphate aerosol has attracted much attention as it can not only bring about serious problem of acid deposition, but also cause radiative and climatic perturbation. In this paper, theoretical investigation of the effect of relative humidity on the oxidation of $\text{S}(\text{+4})$ to sulfuric acid on aerosol particles through aerosol films has been studied. Experiment and measurement results about the acidification of atmospheric aerosol in polluted atmosphere related to different air humidity are then given out. The studies show that the water content in aerosol particle is a necessary and important condition for the successful oxidation of SO_2 to sulphate (SO_4^{2-}). The relative humidity can greatly change the water content of aerosol particles, and therefore will affect the degree of aerosol acidification resulting from the deposition of SO_2 oxidation products, *i.e.* sulfuric acid (H^+), on particles. It is found that $\text{r.h.}=30\%$ and $\text{r.h.}=70\%$ are two critical values for aerosol growth. The experiment and measurement results clearly show that under the same condition, 'dry' particle, which is defined as in $\text{r.h.}\leq 30\%$, and 'wet' particle, which in $\text{r.h.}\geq 70\%$, will undertake different degree of acidification. According to this finding, we can easily explain why the aerosol in southwestern China where the relative humidity is usually above 80% contains much more sulfuric acid than the aerosol in North China does where the usual relative humidity is about 30%. Furthermore, the phenomenon of the distribution of acid rain in China, Japan, and even in whole world can then also be explained.

p304 Variation of sulphate and nitrate concentration in precipitation in Jakarta Indonesia and their roles in acidification :1983-1992

Nurlaini and Mahmud

Atmospheric Research & Development Center, LAPAN Indonesia

Precipitation chemistry data from the National Institute of Meteorology and Geophysics (BMG) were collected from 1983 until 1992 in a location in Jakarta Indonesia. That data were used to investigate the variation of sulphate and nitrate and their roles in acidification. Beside that in this paper will be presented too about gases SO_2 , NO_2 in the same location and then will be tried to look relationship between that gases with pH. From 106 monthly rain water pH data in ten years there were 63 pH data (59%) was below 5.60; maximum and minimum pH were 6.65 and 4.24.

p305 Washout of alkaline components during the convective showers at Pune, India

Medha S. Naik, G.A.Momin, P.S.P.Rao, P.D.Safai,
A.G.Pillai and L.T.Khemani
Indian Institute of Tropical Meteorology, Pune 411008, India

Rain water is, by and large, alkaline in nature in India. High levels of Ca^{2+} and Mg^{2+} in atmospheric aerosols which are alkaline in nature are responsible for maintaining the pH of rain water in alkaline range. In order to understand the role of individual ion in neutralizing the acidic effects, 73 rain water samples of equal volume were collected sequentially from 4 convective showers at Pune ($18^{\circ}32'N$, $73^{\circ}51'E$ 559 m amsl) during southwest monsoon season of 1990 and analysed for major ionic components.

In all the showers, the concentrations of SO_4^{2-} , Na^+ , K^+ , Ca^{2+} and Mg^{2+} showed negative correlation coefficient with accumulated rainfall. However, H ion concentration showed positive correlation with accumulated rainfall. This suggests that increase in H ion concentration is due to decrease in alkaline components such as Ca^{2+} , K^+ and Mg^{2+} in subsequent rain water samples during the shower. High concentrations of Ca^{2+} , K^+ and Mg^{2+} in initial samples are responsible for maintaining the pH of rain water in alkaline range.

p306 Chemical composition of wet and dry deposition at Delhi, north India

R.K.Kapoor, S.Tiwari and R.N.Chatterjee
Indian Institute of Tropical Meteorology, Pune

Wet and dry deposition samples were collected at Delhi during the period April 1990 to March 1991. Samples were analysed for major cations (NH_4 , Na, K, Ca and Mg) and anions (Cl , NO_3 and SO_4) in addition to their pH measurements. Majority of the samples have been found to be either neutral or alkaline in character, as a result of neutralisation, primarily caused by alkaline properties of the soil oriented elements (K, Ca and Mg) which have been found to be present in higher concentrations as compared to the concentrations of anthropogenic elements (SO_4 and NO_3).

Cross correlations between the concentrations of different ionic species have also been determined. Details of the results will be discussed.

p307

Acid Rain Analysis

P. Suneetha
Department of Geography, Andhra University, Visakhapatnam, India

Large quantities of oxides of sulphur and nitrogen are being emitted into the atmosphere and they react with large quantities of water vapour to form acids like sulphuric acid, sulphurous acid, nitric acid and nitrous acid, which then return to the earth's surface as rain water and dew or may remain in the atmosphere in clouds and fog. Industrial areas with pH value of rain below or close to the critical value had been recorded in some cities of India. Visakhapatnam, an industrial town of South India has been chosen for the present analysis of acid rain. Samples of the first rain were collected during monsoon season and tested for acidity. The pH values of the rain water varied between 5 and 6. To get accurate concentrations of pollutants in the air, dew and fog were intercepted during winter season and the samples were tested for acidity. The analysis of samples collected from commercial centres indicated the pH value of 5.6 and 6.0 whereas the samples from residential areas have shown the pH values in between 6.0 to 7.0. Samples from industrial zone have shown the pH values varying between 5.0 and 6.0. The concentrations of SO_2 and NO_x in different areas of Visakhapatnam city in different seasons are also discussed.

p308

Some observations from the statistical analyses of major ion concentrations in precipitation in an industrial-coastal environment

A. Narayana Swamy
Department of Geophysics, Andhra University, Visakhapatnam, India

With increase in industrialization and urbanization as well as increase in the use of fossil fuels, the atmospheric environment is contaminated through release of waste gases. A major portion of these impurities may fall back on the surface of the earth as dry fall out and with precipitation. In the coastal regions, the oceanic spray may contribute significantly to some of the major ion concentrations in the precipitation. In the present study 207 bulk precipitation samples on daily basis were collected at a sampling site in Visakhapatnam city located on the east coast of India adjoining Bay of Bengal which is being subjected for rapid urbanisation and industrialization during the last three/four decades. In addition 130 wet precipitation samples were collected during 25 rains/storms at different time intervals. All the samples were analysed for conductivity, total hardness, chloride, bicarbonate, sulphate, calcium, magnesium and sodium. Statistical analyses of the above data has been carried out to study the nature of deposition of major ions during different seasons, months, rains with varying magnitudes and rainstorms. Studies on frequency distribution and principal component analyses were made to establish relationships between various ions and delineation of their sources. The results are discussed in the paper.

AUTHOR INDEX

-A-

Aalto, P. p250
 Abrahamsen, G. p021
 Acker, K. p201
 Aduna, J. B. p023
 Aggarwal, M. p080
 Ahonen, T. p250
 Akimoto, H. 3.01, 3.13, 4.04, p044
 Alberto, M. C. p023
 Alcamo, J. p286
 Alexandrov, G. A. p033
 Allen, A.G. p260, p289
 Alyea, F. N. 2.10
 Ambus, P. p039
 Amdt, R. p300
 Ancellet, G. p071, p072
 Anderson, B. p063, p068
 Anderson, J. p277
 Anderson, J. R. p263
 Andreae, M. O. 2.14, 3.09, 4.10, p215, p258
 Andreae, T. W. 4.10
 Andres, R. J. 1.09
 Andronova, N. G. p097
 Aneja, V. P. p223, p224
 Anikiev, V. V. p267
 Annegarn, H. 4.10, p258
 Antuña, J. C. p278
 Aoki, Tadao p034
 Aoki, Teruo p034, p239
 Aoki, S. 2.23
 Apel, E. C. p210
 Arah, J. R. M. 1.17, p039
 Arao, K. p270, p271
 Arimoto, R. 3.08, p066, p265, p281
 Artaxo, P. 4.11, p259, p260
 Asuma, Y. p290
 Atherton, C. S. p058
 Atlas, E. p086, p220
 Ayers, G. P. 4.01, 4.08, 4.11, p238, p288, p301

-B-

Baart, A. C. p003
 Bakken, L. R. p020, p021
 Baltensperger, U. p234, p285
 Bandow, H. 4.04
 Bandy, A. R. 3.10, 4.07, p243
 Bandy, B. J. p205

Banic, C. M. p053, p055
 Barnes, I. p246
 Barrie, L. A. 2.25, p044, p236, p284
 Barrick, J. p063
 Bartnicki, J. p286
 Bates, T. S. 2.27, 4.13
 Bationo, A. p256
 Becker, K. H. p246
 Beekmann, M. p071, p072
 Beer, F. 4.10
 Bekki, S. 1.11, p099
 Benkovitz, C. M. 4.09, p005
 Berdowski, J. J. M. p001
 Bertman, S. 2.01
 Beverland, I. 1.17
 Beyaert, K. p237
 Bifano, C. p297
 Bigg, E. K. 3.16, p231
 Blake, D. p063
 Blake, D. R. 2.06
 Blomquist, B. W. 3.10, 4.07, p243
 Boatman, J. p261
 Boersen, G. p094
 Bonasoni, P. p015, p073
 Borchers, R. 1.22
 Borrell, P. 2.20
 Bottenheim, J. W. 2.25
 Bouwman, A.F. p001
 Boyd, I. S. p077, p289
 Boz6, L. p286
 Bradshaw, J. p063
 Brasseur, G. P. 2.12, 2.13, 2.15, 3.06, p070, p085, p086, p087, p088
 Broadgate, W. J. 2.26
 Bronson, K. p023
 Browell, E. V. p060, p063, p068
 Brunke, E. -G. p078
 Bryuckanov, A. p084
 Buhr, M. 2.02
 Bultjes, P. J. H. p003, p094
 Bujok, O. p213
 Burns, K. L. p255
 Buseck, P. R. p263
 Butler, C. F. p068
 Butterbach, K. p038

-C-

Cachier, H. 4.10, p257
 Cabrera, C. M. L. p298
 Cafmeyer, J. p258

Cainey, J.	p288	Delmas, R.	2.15, 3.17
Calvert, J. G.	p210	De Muer, D.	p072
Calvez, M.	p290	Dentener, F. J.	p091
Canadell, P.	1.07	De Serves, C.	2.18
Cao, Mei-qui	1.18	Des Rosiers, J.	1.07
Cárdenas, L.	3.04	Diab, R. D.	p078
Carmichael, G. R.	2.04, p091, p300	Dick, A. L.	4.08, p289
Casado, H.	p296	Dignon, J.	1.06, p005
Chalita, S.	1.03	Dreiling, V.	p276
Chambers, S.	p076	Druilhet, A.	p096
Chameides, W. L.	2.09	Drummond, J. R.	p070
Chao, Zhong	p302	Dryfhout, H.	p236
Chapin, F.	1.07	Ducastel, G.	p237
Chatterjee, R. N.	p306	Duce, R. A.	3.08, p066, p265, p281
Chelibanov, V.	p084	Dzhora, A.	1.20
Chen, D. Z.	p025		
Chen, G.	p063	-E-	
Chen, Limin.	1.24, p045	Elbert, W.	4.10
Chen, Zong Liang	p027, p028	Ellermann, T.	p046
Chiariello, N.	1.07	Encinas, D.	p296
Christensen, S.	p039	Endoh(Endou), T.	p290, p295
Chuang, C. C.	4.12	Erickson, D. J., III	1.05, p087
Chun, Lu	p217	Escalona, A.	p297
Church, T. M.	p265	Esser, P. J.	p094
Ciais, P.	1.05	Evangelisti, F.	p073
Cieslik, S.	p096		
Clark, N. J.	p076	-F-	
Clarke, A. D.	4.02, p264	Fabian, P.	1.22
		Fally, S.	p087
Clayton, H.	p039	Fan, X. -B.	p271
Clegg, S.	p292	Favennec, E.	p087
Clément, B.	p218	Fehsenfeld, F. C.	2.01, 2.02, p052
Collins, J.	p063	Feichter, J.	3.07
Colombo, T.	p015, p073	Feng, Zongwei	p018
Combrink, J.	p078	Fenn, M. A.	p068
Conrad, R.	p225, p245	Fernández	p227
Cooke, W. F.	p253	Field, C.	1.07
Covert, D.	4.16	Figuerola, L.	p208
Covert, D. C.	3.16	Filby, W. G.	p248
Covert, D. S.	4.13	Finlayson-Pitts, B. J.	2.11
Crawford, J.	p063	Fishman, J.	2.17, p068
Crutzen, P.	1.01	Flocke, S.	4.15
Cunnold, D. M.	2.10	Fontan, J.	p096
		Fowler, D.	1.17
-D-		Francey, R.	1.21
Damski, J.	2.21	Fraser, P. B.	1.21, 1.23, 2.10
Daum, P.	p055	Fredeen, A.	1.07
Davison, B.	p234	Fridman, Sh. D.	1.14
Davidson, K. A.	p004, p051	Friedrich, R.	p090
Daviodov, S. P.	1.13	Fugit, J. L.	p218
Davis, D. D.	2.03, p062, p063	Fukabori, M.	p034

Fung, I.	1.09	Harrison, R. M.	p234
Fushimi, K.	p014	Hartley, D. E.	2.10
		Harvey, M. J.	p077, p289
-G-		Hastings, S. J.	p010
Gäggeler, H. W.	p285	Hatakeyama, S.	3.13, 4.04, p228, p247
Gallardo, L.	p222	Hauglustaine, D.	1.03, 2.13, p088
Galle, B.	1.17, p039	Hayasaka, T.	p275
Galloway, J. N.	3.03, p291	Heintzenberg, J.	3.16
Gao, Y.	p281	Heikes, B.	p063, p064, p203
Gardiner, W. C.	p098	Helas, G.	4.10, p215
Gasche, R.	p038	Helmig, D.	p211, p220
Gerab, F.	4.11, p259	Hemminger, J. C.	2.11
Geron, C.	p224	Herrmann, L.	p256
Ghosh, S.	p100	Hess, P. G.	4.15
Gille, J. C.	p070	Hewitt, C. N.	p234
Gillet, R.	4.11, p238	Hignett, P.	p205
Gillis, R.	p290	Hingane, L. S.	p037
Ginoux, P.	p085, p086	Hirose, T.	p040, p041
Ginzburg, M.	2.21	Hirota, M.	p014
Giovanelli, G.	p015, p073	Hjorth, J.	3.11, 4.05
Goldan, P.	2.02, p052	Hoell, J.	2.03
Goto-Azuma, K.	p299	Holbrook, B. D.	p224
Graedel, T. E.	1.02, p005	Holland, E.	1.07, p017
Granat, L.	3.12, p279	Hong, Miao	p217
Granier, C.	2.13, 3.06, p088	Honrath, R. E.	p056
Grant, W. B.	p068	Hooper, M.	p288
Gras, J. L.	4.06	Hopkins, D.	p002
Gray, L.	p071	Horie, O.	p221
Grechko, E. I.	1.20	Hov, Ø.	p092
Greenberg, J.	p211, p220	Hudson, R. D.	2.16
Gregory, G. L.	p062, p068	Huebert, B.	4.07
Griffith, D. W. T.	1.17, p039	Hungate, B.	1.07
Gromov, S.	p252	Hussain Wani, A.	p016
Gröne, T.	4.05		
Grovenstein, J. D.	p255	-I-	
Guenther, A.	p087, p211	Ibusuki, T.	p049
		Ieda, M.	2.05
-H-		Iida, T.	p035
Hacker, J. H.	p076	Ikebe, Y.	p035
Hahn, J.	p209	Ikegami, M.	p266
Hakola, H.	p216	Ilyas, M.	p083
Hallberg, A.	4.14	Imai, K.	4.04
Hämeri, K.	p250	Imamura, T.	p228
Han, Jiankang	p299	Inoue, G.	2.22, p009, p031, p032
Hansson, J. E.	p237	Inoue, H. Y.	1.10
Hansson, H. -C.	4.16, p280	Isaac, G.	p055
Hao, Wei Min	1.08	Isaki, R.	p047, p048
Hara, H.	4.03, p247, p272	Ishi-i, K.	p013
Harazono, Y.	p011, p030	Ishikawa, H.	p241
Hargreaves, K. J.	1.17	Ishizaka, Y.	4.04, p270
Hari, P.	p250	Iversen, T.	p233

Ivey, J. 4.08
 Iwasaka, Y. 4.04, p270
 Iwatsuki, T. p042
 Izumi, K. 2.22, p009, p031

-J-
 Jackson, R. 1.07
 Jacob, D. p203
 Jaenicke, R. p276
 Jenkins, G. p205
 Jiafa, L. p020
 Johansson, C. 2.29
 Johnen, F. J. p043, p226
 Johnson, J. E. 2.27
 Jonnalagadda, S. B. p287
 Junkermann, W. p206

-K-
 Kai, K. p271
 Kalus, W. H. p248
 Kanakidou, M. 2.28
 Kanda, K. p022, p040, p240
 Kapoor, R. K. p306
 Kapustin, V. 4.13
 Karelin, D. V. p010
 Karasudani, T. p013
 Karol, I. L. p097
 Kasibhatla, P. S. 2.08, 2.09
 Kasibhatla, P. p057
 Kasukabe, H. p284
 Katatani, N. p293
 Kawakami, S. 2.05, p061, p062
 Kawamura, K. 4.17, p283, p284
 Kaye, A. p205
 Keene, W. C. p291
 Kegami, M. p067

Keller, M. 3.05
 Kelly, K. C. 2.27
 Kercher, J. R. 1.06
 Kesselmeier, J. p218
 Khalil, M. A. K. 1.19, p202
 Khattatov, V. 2.22, p009, p031, p032
 Khedim, A. p214
 Khemani, L. T. p279, p305
 Kim, D. -S. p223
 Kim, Y. p261
 Kimura, R. p290
 Kiss, Gy. p012
 Kitada, T. p065, p268
 Kjellström, E. 3.07

Kleinman, L. p055
 Klemedtsson, L. 1.17, p039
 Klinger, L. F. p211
 Kobayashi, K. p293
 Koch, G. 1.07
 Koga, S. p244
 Koike, M. 2.05, p061, p062
 Kokorin, A. O. p019
 Kolesov, G. M. p267
 Komala, Ninong 2.19
 Kondo, Y. 2.05, p061, p062, p063, p065

Kong, Fanyou p095
 Koppmann, R. 2.24, p043, p212, p214, p215
 Kopylov, Y. 2.22, p009, p031, p032
 Korhonen, P. p292
 Kosmus, W. p287
 Kulmala, M. p250, p292
 Kulshrestha, U. C. p006
 Kumar, N. p006
 Kumari, K. M. p006
 Kuster, W. (B.) 2.02, p052
 Kutsuna, S. p049
 Kyrö, E. 2.21

-L-
 Lacaux, J. P. 2.15
 Labatut, A. p096
 Lacaux, J. P. p296
 Lachmann, G. p209
 Lal, S. p081, p082
 Lamaud, E. p096
 Langenfels, R. 1.21
 Lansford, H. p002
 Lantin, R. S. p023, p024
 Lasse, K. R. 1.12
 Laurila, T. p075, p216
 Laux, J. M. 2.11
 Law, K. S. 1.11, p059, p099
 Leitch, W. R. p053, p055
 Le Canut, P. 4.10
 Leck, C. 3.16, p231, p232
 Lee, J. p055
 Lee, Meehye p064, p203
 Lee, P. C. S. p268
 Lee, Yin-Nan p053, p054, p055
 Lehmann, S. p245
 Lelieveld, J. 3.07
 Le Treut, H. 1.03
 Levin, I. 1.21

Levy, H., II 2.08, 2.09
 Li, Arthur p004, p051
 Li, Debo p027
 Li, Shao-Meng p053, p236
 Lienaerts, K. p226
 Likens, G. E. p291
 Limbach, S. p221
 Lind, A. M. p039
 Liousse, C. p257
 Liss, P. S. 2.26, 3.02
 Liu, P. S. K. p053
 Liu, S. C. 2.03
 Lopez, A. p096
 Lowe, D. C. 1.12
 Lu, Chun p217
 Luo, Y. 1.07

-M-
 Maag, M. p039
 Machida, T. 2.22, p009, p031, p032
 MacPherson, I. p055
 Madhuri, S. p251
 Madronich, S. 4.15
 Maenhaut, W. 4.10, p237, p258
 Mahmud p304
 Mahowald, N. p089
 Maiss, M. 1.21
 Makide, Y. 1.24, p045
 Makino, Y. 2.07, p067, p266
 Maksyutov, S. 2.22, p009, p031, p032
 Malm, W. C. p249
 Manning, M. R. 1.12
 Manoe, S. p215
 Marland, G. 1.09
 Marshall, S. 4.13
 Martins, J. V. 4.11
 Martinsson, B. 4.16
 Mase, J. p035
 Matsui, I. p032
 Matsueda, H. 1.10
 Matsumoto, K. p269
 Matsunaga, K. p242
 McNamara, D. P. 2.16
 Medinets, V. I. p282
 Medvedev, A. N. p267
 Meixner, F. X. p079
 Mégie, G. 3.06
 Merrill, J. T. p061, p062, p063
 Mészáros, E. p012
 Miao, Hong p217

Middleton, P. p002
 Miguel, A. H. 4.11, p260
 Mihalopoulos, N. p235
 Müller, B. R. 2.10
 Minami, K. 1.15, p022, p240
 Mitsumoto, S. 2.22, p009, p031
 Miyata, A. p011, p030
 Miyoshi, A. p228
 Molenkamp, C. R. p257
 Möller, D. p201
 Molnár, A. p012
 Momin, G. A. p279, p305
 Mooney, H. 1.07
 Moore, T. p224
 Moortgat, G. K. p221
 Moraes, F. p202
 Morales, J. p296
 Moriizumi, J. p035
 Moxim, W. J. 2.08
 Mukai, H. 3.13, 4.04, p272
 Müller, J. F. 1.03, 2.13, 3.06
 Müller, K. P. p226
 Murano, K. 3.13, 4.04
 Muramatsu, H. p074
 Muramoto, K. p295
 Murao, N. p293
 Murata, A. p014

-N-
 Nagamine, K. p035
 Nagatani, M. p270
 Naik, M. S. p305
 Naja, M. p081, p082
 Nakagawa, T. p295
 Nakajima, H. 2.05
 Nakao (Nakawo), M. 4.03, p272, p299
 Nakasato, S. p247
 Nakhutin, A. I. 1.14
 Nazarov, I. M. p019
 Neavyn, R. 2.11
 Neeb, P. p221
 Nemesure, S. 4.09
 Nemoto, K. p014
 Neue, H. U. p023, p024
 Newell, R. 2.03
 Nguyen, B. C. p235
 Nichol, S. E. p077
 Nielsen, O. J. p046
 Niimura, N. p271
 Niki, H. p055

Nikolaev, V.	p009, p032	Prospero, J. M.	3.08, p066
Nilsson, E. D.	3.16, p231	Pszenny, A.	p261
Ninong, Komala	2.19	Purvaja, G. R.	p036
Nisbet, E.	1.11	Putaud, J. P.	p235
Noguchi, I.	p295	Pyle, J. A.	p059, p100
Noone, K. J.	4.14		
Norton, R. N.	2.01	-Q-	
Nurlaini	p304	Qin, Yu	p095
		Quinn, P. K.	4.13
-O-			
O'Dowd, C.	p234	-R-	
Oechel, W. C.	p011	Raes, F.	4.05, p253
Ogawa, T.	2.19	Rahn, K. A.	p265
Ogren, J. A.	4.14	Ramesh, R.	p036
Ohta, K.	p269	Ramani, A.	p229
Ohta, M.	p207	Rao, P. S. P.	p305
Okada, K.	p239, p266, p271	Rapsomanikis, S.	3.09
Okamoto, S.	p293, p294	Rasch, P. J.	2.12, p089
Olivier, J. G. J.	p001	Ratte, M.	p212, p213
Oram, D. E.	1.23	Ravegnani, F.	p073
Oref, I.	p098	Rasmussen, R. A.	1.19
		Rennenberg, H.	p023
-P-		Riba, M. L.	p218
Pacyna, J.	p005, p286	Ridley, B.	p086
Pan L.	p070	Robarge, W. R.	p224
Papen, H.	p023, p025, p038	Roberts, J.	2.01
Paramonov, S.	p252	Rodhe, H.	3.07, 3.12, p279
Parrish, D. D.	2.01	Rocha, V. C.	p050
Parungo, F.	p273	Roemer, M. G. M.	p003, p094
Patroescu, J.	p246	Romero, J.	3.04
Patra, P. K.	p081	Rondón, A.	2.18, 2.29, 3.04
Pearson, H.	1.07	Rong, X.	p029
Penkett, S. A.	1.23, 2.26, p205	Rowland, F. S.	2.06
Penner, J. E.	1.06, 4.12, p058, p257	Rowland, S.	p063
Persson, C.	3.16, p231, p232	Ryaboshapko, A.	p252
Peterson, M. C.	p056	Rudolph, J.	2.24, p043, p212, p213, p214, p215, p225, p226
Phadnis, M.	2.04	Rummukainen, M.	p075
Pham, M.	1.03, 3.06		
Pickering, K. E.	2.16, p069	-S-	
Pienaar, J. J.	p209	Sachse, G. W.	p062, p063
Pierce, T.	p224	Safai, P. D.	p279, p305
Pietruk, P.	p206	Sakaguchi, F.	p283
Pilewskie, P.	4.02	Sala, O.	1.07
Pillai, A. G.	p305	Salma, I.	4.10, p258
Plass-Dülmer, Ch.	2.24, p212	Saltelli, A.	3.11
Polissar, A. V.	p249	Sandholm, S.	p063
Porter, J. N.	4.02	Sanhueza, E.	2.29, 3.04, p208, p227
Postnov, A.	2.22, p009, p031, p032	Santana, M.	p208
Povarov, V. G.	p219	Sasaki, Y.	p293
Prather, M. J.	1.04		
Prinn, R. G.	2.10, p089		

Sasano, Y.	p275	Sullivan, L.	p224
Sato, H.	p047, p048	Sun, Q.	p204
Sauer, F.	p221	Suncetha, P.	p307
Savoie, D. L.	3.08, p066	Sunwoo, Young	2.04
Saxena, V. K.	p224, p255, p277	Sugiyama, Y.	1.10
Saxena, A.	p006	Suksomsankh, K.	3.12
Schaefer, L.	p218	Svenningsson, B.	4.16, p280
Scharffe, D.	p215	Swamy, A. N.	p308
Schebeske, G.	p215	Swap, R.	4.10
Scholtz, M. T.	p004, p005, p051	Swietlicki, E.	4.16
Schrimpf, W.	p226		
Schult, I.	p257	-T-	
Schwartz, S. E.	4.09	Taalas, P.	2.21
Schwikowski, M.	p234, p285	Tabucanon, M.	3.12
Scott, A.	p039	Tafari, V.	2.21
Sehested, J.	p046	Tahara, R.	p242
Sehested, K.	p046	Takahashi, T.	p295
Seiler, W.	p023	Takamura, T.	p275
Semiletov, I. P.	1.13	Takeuchi, M.	p047
Sempéré, R.	4.17	Talbot, R.	p063, p243
Setzer, A.	p259	Tanaka, F.	4.03, p272
Shangguan, Xingjian	1.16, p025, p026	Tanaka, H.	4.04, p244, p269, p270, p290
Shao, K.	p204	Tanaka, S.	4.04, p241, p242
Shao, Ke Sheng	p027	Tang, X.	p204
Shen, R. X.	p025	Tanimoto, S.	p294
Shi, G. -Y.	p271	Tao, W. -K.	p069
Shmeter, S.	p009	Tarrasón, L.	p005, p233
Sievering, H.	p261	Tatano, T.	4.03, p272
Sillman, S.	2.08, p058, p093	Tavares, T. M.	p050
Simachaya, S.	3.12	Taylor, K. E.	4.12
Simmonds, P. G.	2.10	Thompson, A. M.	2.16, 2.17, p069
Singh, H. B.	2.28, p061, p062, p063	Thornton, D. C.	3.10, p243
Sirois, A.	2.25	Tindale, N. W.	p262
Sitaula, B. K.	p020, p021	Tiwari, S.	p306
Skiba, U.	1.17	Toelg, M.	p025
Slama, C.	p051	Tohjima, Y.	2.22, p009, p031, p032
Slamet, S.	2.19	Tominaga, T.	1.24, p045
Slemr, F.	p206	Toom, D.	p044, p236
Smith, K. A.	1.17, p039	Toritani, H.	p290
Smith, M.	p234	Torres, L.	p218
Smith, M. D.	p070	Townsend, A. R.	p017
Sokolic, F.	p078	Trainer, M.	2.01, 2.02, p052
Sorteberg, A.	p092	Tsuboki, K.	p290
Spitzzy, A.	p213	Tsunogai, S.	3.15
Springston, S.	p055	Tsuruta, H.	4.04, p022, p040, p041, p207, p240
Srivastava, S. S.	p006	Tsutsumi, Y.	2.07, p067, p266
Stahr, K.	p256		
Steele, P.	1.21	-U-	
Su, W. H.	p029	Ueda, H.	p013
Subbaraya, B. H.	p081, p082		
Sueper, D.	2.02		

Uematsu, M.	p267, p274	Wippel, R.	p287
Utiyama, M.	p009	Wylie, D.	4.07, p289
-V-		-X-	
Valero, F.	4.02	Xie, X. L.	p026, p026
Van Dingenen, R.	4.05	Xu, Qun	3.14
Van der Maas, C.W.M.	p001		
Varshney, C. K.	p080	-Y-	
Vaughan, G.	p071	Yagi, K.	p022, p040
Veldkamp, E.	p017	Yamaguchi, K.	4.03, p272
Venkataramani, S.	p081	Yamanouchi, T.	2.23
Venning, S.	p076	Yamamoto, H.	3.15
Vesala, T.	p250, p292	Yamamoto, T.	p065
Vinnichenko, N.	2.22, p009, p031, p032	Yamashita, A.	p290
Vögt, R.	2.11	Yamasoe, M. A.	4.11, p260
Voldner, E. C.	p004, p005, p051	Yamato, M.	4.04, p269, p270, p290
Vorobyev, V. A.	1.14	Yang, Jianliang	p254, p303
Voropaev, Yu. V.	1.13	Yang, Z.	p240
Vouritis, G.	p011	Yang, Zhang	2.04, p091
-W-		Yang, Wen-Xiang	p008
Wade, T.	4.07	Yao, Heng	p027, p028
Wagener, R.	4.09	Yeung, K. K.	p301
Wakita, H.	p032	Yienger, J.	2.09
Wakuri, H.	4.03, p272	Yokouchi, Y.	p044
Walford, P. M.	4.08	Yoshida, N.	p042
Walters, S.	2.12	Yoshimoto, M.	p011
Walton, J. J.	1.06, p 058, p257	Young, Sunwoo	2.04
Wani, A. H.	p016	Yurganov, L. N.	p230
Wang, Bujun	p027	-Z-	
Wang, M.	p204	Zaizen, Y.	2.07, p067, p266
Wang, Mingxing	1.16, p025, p026, p254,	Zamolodchikov, D.G.	p010
	p303	Zenker, T.	4.10
Wang, Xiaoke	p018	Zhang, Chao	p302
Wang, Y. S.	p025	Zhang, Yang	2.04, p091
Wang, W. D.	p025, p026	Zhao, Chunsheng	p095
Ward, D. E.	1.08	Zhao, Dianwu	3.03
Washida, N.	p228	Zhao, Xianliang	p053, p054, p055
Wassmann, R.	p023, p024, p025	Zhou, M. Y.	p281
Watanabe, I.	4.04	Zhuang, L.	4.07
Watanabe, S.	3.15	Zhuang, Ya-hui	1.18, p016, p028
Wei, Min Hao	1.08	Ziereis, H.	p061, p062
Weiss, R. F.	2.10	Zimmerman, P.	2.15, p211, p220
Welling, M.	1.17	Zimov, S. A.	1.13
Wellman, D.	p261	Zykova, I.	p084
Wiebe, H. A.	p053		
Wiedensohler, A.	3.16, 4.16		
Wienhold, F.	1.17, 4.10		
Wieprecht, W.	p201		
Wild, O.	p059		
Wilson, J. J. N.	p253		